

BERICHTE

aus dem Fachbereich Geowissenschaften
der Universität Bremen

No. 285

Krastel, S. , G. Wefer,
A. Anasetti, R. Andreula, G.L. Arnold, A. Beck, V. Bender, M. Bergenthal,
K. Bogus, G. Bozzano, C. Chiessi, J. Collins, S. Dekeyzer , V. Diekamp,
Y. Domnia, R. Düßmann, F.D. Esteban, N. Fekete, C. Fink, M. Formolo,
T. Freudenthal, G. Greif, T. Hanebuth, S. Henkel, C. Hilgenfeld, H.-J. Hohnberg,
T. Huppertz, S. Kasten, T. Klein, H.-O. Könnecker, B. Kokisch, M. Lange,
H. Lantzsch, K. Lindhorst, M. Meyer, S. Mill, H. Müller, O. Mund,
W.-T. Ochsenhirt, B. Preu, A. Raeke, S. Razik, J. Renken, N. Riedinger, U. Rosiak,
J.E. Sawicka, W. Schmidt, T. Schwenk, C. Seiter, M. Strasser, J. Tomasini,
T. Truscheit, R. Violante, A. Vossmeier, D. Winkelmann

**REPORT AND PRELIMINARY RESULTS OF RV METEOR CRUISE M78/3.
SEDIMENT TRANSPORT OFF URUGUAY AND ARGENTINA:
FROM THE SHELF TO THE DEEP SEA.
19.05.2009 – 06.07.2009, Montevideo (Uruguay) – Montevideo (Uruguay).**



The "Berichte aus dem Fachbereich Geowissenschaften" are produced at irregular intervals by the Department of Geosciences, Bremen University and by MARUM.

They serve for the publication of cruise reports, PhD-theses, experimental works, and scientific contributions made by members of the department.

Reports can be ordered from:

Monika Bachur

DFG-Forschungszentrum MARUM

Universität Bremen

Postfach 330 440

D 28334 BREMEN

Phone: (49) 421 218-65516

Fax: (49) 421 218-65515

e-mail: MBachur@uni-bremen.de

Citation:

Krastel, S., G. Wefer and cruise participants

Report and preliminary results of RV METEOR Cruise M78/3. Sediment transport off Uruguay and Argentina:

From the shelf to the deep sea. 19.05.2009 – 06.07.2009, Montevideo (Uruguay) – Montevideo (Uruguay).

Berichte, Fachbereich Geowissenschaften, Universität Bremen, No. 285, 79 pages. Bremen, 2012.

ISSN 0931-0800

METEOR-Berichte 78-3

***Sediment transport off Uruguay and Argentina:
From the shelf to the deep sea***

Cruise No. 78, Leg 3

19.05.2009 – 06.07.2009, Montevideo (Uruguay) – Montevideo (Uruguay)



Sebastian Krastel, Gerold Wefer

A. Anasetti, R. Andreula, G.L. Arnold, A. Beck, V. Bender, M. Bergenthal, K. Bogus, G. Bozzano, C. Chiessi, J. Collins, S. Dekeyzer, V. Diekamp, Y. Domnia, R. Düßmann, F.D. Esteban, N. Fekete, C. Fink, M. Formolo, T. Freudenthal, G. Greif, T. Hanebuth, S. Henkel, C. Hilgenfeld, H.-J. Hohnberg, T. Huppertz, S. Kasten, T. Klein, H.-O. Könnecker, B. Kokisch, M. Lange, H. Lantzsich, K. Lindhorst, M. Meyer, S. Mill, H. Müller, O. Mund, W.-T. Ochsenhirt, B. Preu, A. Raeke, S. Razik, J. Renken, N. Riedinger, U. Rosiak, J.E. Sawicka, W. Schmidt, T. Schwenk, C. Seiter, M. Strasser, J. Tomasini, T. Truscheit, R. Violante, A. Vossmeier, D. Winkelmann

Contents

1. Summary	3
2. Participants	4
3. Research Program	5
4. Narrative of the Cruise	8
5. Preliminary Results	12
5.1. Hydroacoustics	12
5.1.1. Bathymetric mapping	12
5.1.2. Sediment echo sounding	14
5.2. High resolution multichannel seismic profiling	21
5.2.1. Introduction	22
5.2.2. System components	23
5.2.3. First results of seismic survey	29
5.3. Sediment Sampling	35
5.3.1. Introduction	35
5.3.2. Methods	35
5.3.3. Sedimentology: Initial shipboard results	45
5.4. Physical Properties Studies	48
5.4.1. Introduction	48
5.4.2. Methods	49
5.4.3. Preliminary shipboard results	52
5.5. Sediment and Pore Water Geochemistry	58
5.5.1. Objectives	58
5.5.2. Methods	59
5.5.3. Shipboard Results	60
5.6. Water column and dinoflagellate studies	64
5.6.1. Introduction	64
5.6.2. CTD profiling	65
5.6.3. Water sampling	66
5.6.4. In-situ pumps	67
5.6.5. Sediment samples	68
6. Ship's Meteorological Station	69
6.1. Weather conditions during Leg M78/3a	69
7. Station List M78/3	72
8. Data and Sample Storage and Availability	77
9. Acknowledgements	77
Appendix	80
Core plot summary legend	80
Core descriptions	81
Physical and geotechnical properties	125

1. Summary

The waters off Uruguay and Northern Argentina offer the possibility to study sediment transport processes from ‘source-to-sink’ in a relatively small area. Quickly accumulated sediments are potentially unstable and might be transported downslope in canyons and/or on the open slope. Strong contour currents result in along-slope sediment transport. Within the scope of Meteor-Cruise M78/3 we investigated sediment transport and depositional patterns by means of hydroacoustic and seismic mapping as well as geological sampling with conventional coring tools and the new MARUM seafloor drill rig (MeBo). Geotechnical investigations were carried out with the aim to analyze the controlling parameters for the destabilization of the slope and the succeeding failure of a sediment body.

Various types of sediment instabilities have been imaged in geophysical and core data, documenting particularly the continental slope offshore Uruguay to be locus of frequent submarine landslides. Apart from individual landslides, however, gravitational downslope sediment transport along the continental slope is restricted to the prominent Mar del Plata Canyon and smaller canyons identified in the bathymetric data. In contrast, many morphological features reveal that sediment transport is predominantly controlled by strong contour bottom currents. This suggests a significant impact of the western boundary currents on the overall architectural evolution of the margin. The investigations are related to projects of the DFG Research Center / Excellence Cluster ‘The Ocean in the Earth System’, University of Bremen, as well as the Excellence Cluster ‘The Future Ocean’, University of Kiel.

Zusammenfassung

Das Seegebiet vor Uruguay und Nord-Argentinien bietet in idealer Weise die Möglichkeit, zahlreiche Transport- und Sedimentationsprozesse im „source-to-sink“-Schema auf engem Raum zu untersuchen. Hangabwärts findet Sedimenttransport in Canyons und in Form von Rutschungen statt. Starke Randströmungen führen zudem zu ausgeprägter hangparalleler Verlagerung. Im Rahmen der Meteor-Fahrt M78/3 haben wir Sedimenttransport und Ablagerungsmuster mittels hydroakustischer und seismischer Kartierungen sowie geologischer Probennahme untersucht werden, wobei sowohl konventionelle Beprobungs-Systeme und des am Marum entwickelte Meeresboden-Bohrgerät MeBo eingesetzt wurden. Geotechnische Analysen sollen die für die Destabilisierung und nachfolgende Abscherung von Sedimentkörpern verantwortlichen Mechanismen aufklären.

Unterschiedliche Arten von Sediment-Instabilitäten konnten mittels geophysikalischer Daten und geologischer Beprobung nachgewiesen werden. Insbesondere am Kontinentalhang vor Uruguay treten regelmäßig submarine Rutschungen auf. Abgesehen von diesen Rutschungen ist der gravitative Sedimenttransport auf den großen Mar del Plata Canyon und einige kleinere Canyons beschränkt. Im Gegensatz dazu deutet eine Vielzahl morphologischer Strukturen darauf hin, dass der Sedimenttransport insbesondere durch starke Kontur-Ströme kontrolliert wird. Dies weist auf einen signifikanten Einfluss der westlichen Randströmung auf die Entwicklung des Kontinentalhanges hin. Die Untersuchungen werden im Rahmen von Projekten des DFG-Forschungszentrum / Exzellenzcluster ‘The Ocean in the Earth System’, Universität Bremen und des Exzellenzcluster ‘The Future Ocean’, Universität Kiel durchgeführt.

2. Participants

Leg M78/3a, Montevideo – Montevideo, 19.05.2009 - 13.06.2009

Name	Discipline	Institution
Krastel, Sebastian, Prof. Dr.	Chief Scientist	IFM-GEOMAR
Anasetti, Andrea	Seismics	IFM-GEOMAR
Bozzane, Graciella, Dr.	Sedimentology	SHN
Chiessi, Cristiano Mazur, Dr.	Marine Geology	INPE
Domnia, Yana	Seismics	Marum/GeoB
Fekete, Noemi, Dr.	Seismics	Marum/GeoB
Fink, Christina	Micropaleontology	Marum/GeoB
Formolo, Michael J., Dr.	Biogeochemistry	MPI
Greif, Gabi	Micropaleontology	Marum/GeoB
Hanebuth, Till, Dr.	Sedimentology	Marum/GeoB
Henkel, Susann	Geochemistry	AWI
Hilgenfeld, Christian	Geophysics	Marum/GeoB
Huppertz, Tammo	Sedimentology	Marum/GeoB
Kasten, Sabine, Dr.	Geochemistry	AWI
Kokisch, Brit	Sedimentology	Marum/GeoB
Lantzsich, Hendrik	Sedimentology	Marum/GeoB
Lindhorst, Katja	Seismics	IFM-GEOMAR
Meyer, Mathias	Seismics	IFM-GEOMAR
Mill, Simon	Deck Technician	Marum/GeoB
Müller, Hendrik	Geophysics	Marum/GeoB
Preu, Benedict	Seismics	Marum/GeoB
Raeke, Andreas	Meteorology	DWD
Riedinger, Natascha, Dr.	Biogeochemistry	MPI
Schwenk, Tilmann, Dr.	Seismics	Marum/GeoB
Strasser, Michael, Dr.	Geotechnics	Marum/GeoB
Tomasini, Juan	Geochemistry	ANCAP
Truscheit, Thorsten	Meteorology	DWD
Violante, Roberto, Dr.	Sedimentology	SHN
Voßmeyer, Antje	Biogeochemistry	UA
Winkelmann, Daniel, Dr.	Sedimentology	IFM-GEOMAR

Leg M78/3b, Montevideo – Montevideo, 17.6.2009 – 6.7.2009

Name	Discipline	Institution
Wefer, Gerold, Prof. Dr.	Chief Scientist	Marum/GeoB
Andreula, Roberto	Geotechnics	Marum/GeoB
Arnold, Gail L., Dr.	Biogeochemistry	MPI
Beck, Andreas	Meteorology	DWD
Bender, Vera Barbara	Sedimentology	Marum/GeoB
Bergenthal, Markus	MeBo	Marum/GeoB
Bogus, Kara	Micropaleontology	Marum/GeoB
Collins, James	Geology	Marum/GeoB
Dekeyzer, Stefanie	Micropaleontology	Marum/GeoB
Diekamp, Volker	Geolab	Marum/GeoB
Düßmann, Ralf	MeBo	Marum/GeoB
Esteban, Frederico Damian	Hydroacoustics	UBA

Freudenthal, Tim, Dr.	MeBo	Marum/GeoB
Henkel, Susann	Geochemistry	AWI
Hohnberg, Hans-Jürgen	Piston coring	Marum/GeoB
Klar, Steffen	MeBo	Marum/GeoB
Klein, Thorsten	MeBo	Marum/GeoB
Könnecker, Hans-Otto	MeBo	PRAKLA
Lange, Matthias	Geotechnics	Marum/GeoB
Mund, Oliver	Deck Technician	Marum/GeoB
Ochsenhirt, Wolf-Thilo	Meteorology	DWD
Preu, Benedict	Hydroacoustics	Marum/GeoB
Razik, Sebastian Lukas	Geomagnetics	Marum/GeoB
Renken, Jens	MeBo	Marum/GeoB
Riedinger, Natascha, Dr.	Biogeochemistry	MPI
Rosiak, Uwe	MeBo	Marum/GeoB
Sawicka, Joanna E.	Biogeochemistry	MPI
Schmidt, Werner	MeBo	Marum/GeoB
Seiter, Christian	MeBo	Marum/GeoB
Tomasini, Juan	Geochemistry	ANCAP

ANCAP	Administración Nacional de Combustibles Alcohol y Portland, Exploración y Producción, Montevideo, Uruguay
AWI	Alfred-Wegener-Institut für Polar- und Meeresforschung, Bremerhaven
DWD	Deutscher Wetterdienst – Seewetteramt, Hamburg
IFM-GEOMAR	Leibniz Institute of Marine Sciences (IFM-GEOMAR), Kiel
INPE	Center for Earth System Science, National Institute for Space Research, Sao Jose dos Campos SP
Marum/GeoB	Marum and Fachbereich Geowissenschaften, Universität Bremen
MPI	Max Planck Institute for Marine Microbiology, Bremen
Prakla	Prakla Bohrtechnik GmbH, Peine
SHN	Servicio Hidrografía Naval, Ciudad Autónoma de Buenos Aires
UA	Center for Geomicrobiology, Aarhus University,
UBA	University of Buenos Aires

3. Research Program

About 90% of the sediments generated by weathering and erosion on land get finally deposited at the ocean margins. The redistribution of sediments from terrigenous sources to marine sinks is one of the most important processes shaping the surface morphology of Earth. The processes distributing the sediments on land are relatively well understood but there is an urgent need for detailed investigations of submarine transport and sedimentation processes. The type of sediment transport at continental margins is variable and includes turbidity currents as well as different types of mass wasting events, e.g. slumps, translational slides, and debris flows. The pattern is further complicated by slope-parallel sediment transport, which is driven by contour currents. Submarine mass wasting in this context represents an important sediment transport process, but also a major geohazard due to the increasing numbers of offshore constructions on the shelf and

the continental slope as well as densely populated coastal areas. The interacting processes of sediment redistribution, sediment partitioning, and sediment diagenesis at the ocean margin off Uruguay and Northern Argentina was investigated during Meteor-Cruise M78/3.

The ocean margin in the working area (Fig. 1) is characterized by a high amount of fluvial input by the Rio de la Plata and other rivers. The continental slope is relatively wide and shows average slope gradients between 1° and 2.5° but locally higher slope gradients may occur ($>5^\circ$). The transition to the continental rise with low slope gradients is found in $\sim 3000\text{m}$ water depth. The working area is located in a highly dynamic oceanographic regime. Cold Antarctic water masses of the northward flowing Falkland/Malvinas current meet warm water masses of the southward flowing Brazil current in the working area.

Sediments deposited on the slope are relatively unstable due to high water contents and high sediment accumulation rates. The continental slope in the working area is therefore characterized by sediment instabilities and various types of sediment transport processes. Geochemical investigations demonstrated that the highly dynamic sedimentation processes in space and time significantly influences early diagenetic and bio-geochemical processes in this region, thereby also influencing geochemical and rock-magnetic parameters.

Previous studies in the working area gave sufficient background information to carry out process-orientated investigations in selected areas (Fig. 1). The sediment transport processes and the depositional patterns were investigated from the coast to the deep sea by means of hydroacoustic and seismic mapping as well as geological sampling. Geotechnical analyses were carried out at selected locations.

During Cruise M78/3 the following specific questions were analyzed:

- Which principal differences in sediment transport pattern can be identified in the working area?
- What is the relevance of sediment transport parallel and perpendicular to the coast for the distribution of sediments delivered by the Rio de la Plata?
- What are the component-specific residence times of sediments in the shelf system? Where, when and what type of sediment is preferentially transported across the shelf edge?
- What types of sediment transport processes occur along the continental slope? What is the relevance of the different processes? Which factors and processes control the sediment transport patterns?
- Which mechanisms are responsible for the destabilization of the slope and the resulting detachment of a sediment body?
- Are geochemical, mineralogical, and rock-magnetic sediment properties preserved in older sediment sequences and are they suitable indicators for pronounced changes in sedimentation and for a reconstruction of the sedimentary history?
- Which biogeochemical processes control the mobilization and reduction of iron and manganese hydroxides in greater sediment depths?
- What is the relationship between oceanographic conditions and the lateral and vertical distribution of selected coccolithophores, acantharia and dinoflagellates?

The different kinds of technical equipment used during M78/3/ required a large amount of space and personnel. Therefore, Leg M78/3 was subdivided into two parts. Seismic and hydroacoustic data as well as geological samples with conventional tools were collected during the first leg (M78/3a, Montevideo – Montevideo, 19.05.2009 - 13.06.2009). The second leg (M78/3b,

Montevideo – Montevideo, 17.6.2009 – 6.7.2009) was used to collect up to 50m-long cores with the MeBo for geotechnical, sedimentological and geo-chemical analyses. Water samples were taken during both legs.

Despite numerous problems (logistics, bad weather conditions, see narrative of the cruise for details), sufficient data were collected to address most of the questions. A very valuable data- and sample set of short and long sediment cores in combination with seismic and hydroacoustic data will allow to reconstruct sediment transport processes from ‘source-to-sink’ in the M78/3 working area.

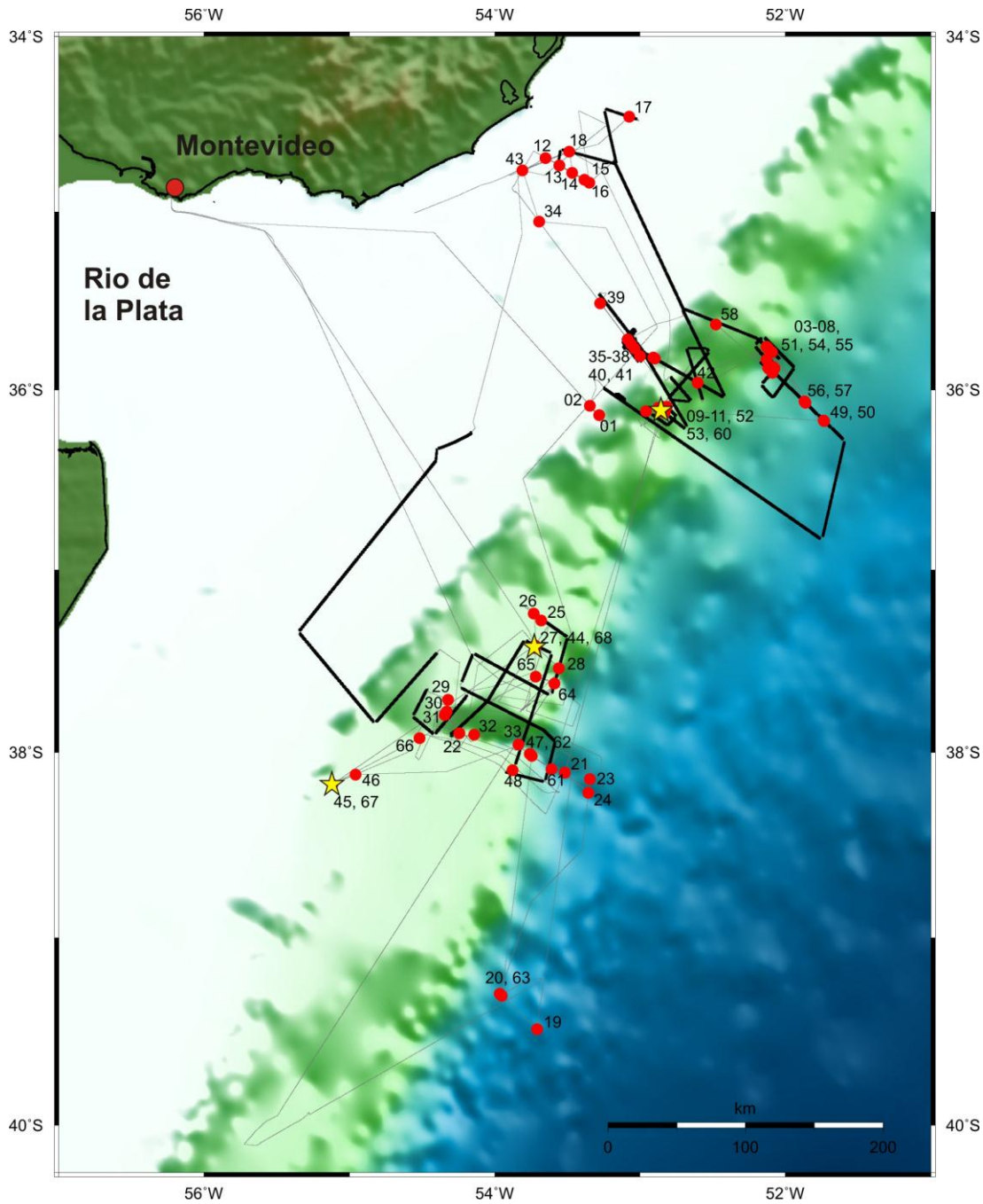


Fig. 1: Cruise track of Cruise M78/3. Thick black lines show location of seismic profiles. Red dots represent stations with station numbers. MeBo stations are marked as yellow stars. GeoB138 is prefix of all stations.

4. Narrative of the Cruise

The main group of the scientific party of Meteor-Cruise M78/3a arrived in Montevideo on May 18th. It was originally planned to embark in Rio de Janeiro but due to problems with immigration authorities in Brazil it was decided to embark in Montevideo instead. All container handling, however, was done by the crew of RV Meteor in Rio. Due to some delay during port operations in Rio, RV Meteor arrived in Montevideo on May 19th in the morning. In total we lost about 2.5 working days as a result of the delay in Rio and the additional port call in Montevideo. We left the port of Montevideo on May 19th at 3:00h pm local time under blue skies and a light breeze. The morning in the port was used to set up the equipment, which was very quick due to the great support of the crew.

The scientific crew of Meteor-Cruise M78/3a included 18 scientists from the DFG Research Center and Cluster of Excellence 'The Ocean in the Earth System' at Bremen with scientists from Bremen University, the Max Planck Institute for Marine Micro-Biology, and the Alfred-Wegener-Institute for Polar and Marine Research, 5 scientists from the Leibniz-Institute of Marine Sciences (IFM-GEOMAR) and the Cluster of Excellence 'The Future Ocean' (Kiel), two scientists from Servicio Hidrografía Naval in Buenos Aires, one scientist each from Administracion Nacional de Combustibles Alcohol y Portland (ANCAP), Montevideo, Uruguay, Aarhus University, Denmark, and the National Institute for Space Research in Sao Jose dos Campos, Brazil, as well as two technicians from the German Weather Service.

The scientific program started with switching on the hydroacoustic systems of RV Meteor as soon as we left the 3 mile zone. We were heading to the outer shelf in order to take first geological samples. Several small sediment lenses were identified at the outer shelf. Seaward of the shelf break a 300-500 m deep terrace like feature shows thick sediment accumulations and seems to act as depositional center. The first core (GeoB13801) was taken at this terrace. The 9.5m long gravity core shows an interlayering of undisturbed and redeposited sediments indicating significant sediment transport across the shelf break. Core GeoB13802 was taken at the edge of an isolated sediment lens at the outer shelf. The 3.5m-long core mainly contains glauconite sand with indications of at least three major storm events.

Seismic profiling started in the evening of May 20th at the continental margin off Uruguay using two streamer systems and a small airgun. The slope is characterized by numerous small to medium sized landslides and several features formed by strong contour currents. Based on the seismic data a small area with slid sediments and canyons was chosen for a detailed mapping and coring campaign. Daytime was used for coring while additional acoustic measurements were collected during night. We identified a blocky debrite, several small faults, which might act as future failure planes, and sedimentary features formed by bottom currents. Core 13805 is located directly beneath a headwall and first analyses indicate that we managed to core the glide plain of a debrite. Work in this area lasted until May 23rd in the evening (Cores 13803-13808) and was followed by a seismic survey of the upper slope off Uruguay until May 25th in the morning. The following day was used for a coring transect across another morphological step in ~1200m water depth identified in the bathymetry. The new data show that this step is not a simple headwall but formed by a complex interplay between gravitational and current induced sediment redeposition. The cored sediments are strongly consolidated. Varying sediment thickness landward of the morphological step will allow investigating, if differential loading resulted in a destabilization of the slope.

Work on the shelf off Uruguay started on May 26th. Main target was a mud belt north of the mouth of the Rio de la Plata. Mud belts offer the possibility to sample a continuous sedimentary shelf record of the current sea level high stand. Detailed mapping of the mud belt started in the afternoon with the hydroacoustic systems of RV Meteor and the novel electromagnetic sea floor profiler 'GEM Shark', which was developed at Bremen University. Unfortunately the 'GEM Shark' was lost at an unknown underwater barrier in 45m water depth. Usually it is possible to recover the sledge with a rescue rope but this rope broke during rescue operations. Dredging for the 'GEM Shark' was also not successful, hence the instrument is lost. The night was used for additional hydroacoustic mapping. Based on the results, a coring profile with giant box corer and gravity corer was collected on May 27th. It was possible to recover a 10m-long gravity core from the center of the mud belt (Core 13813). Seismic and acoustic profiling was continued during night time and additional cores were collected the next day. An 11.5m-long gravity corer at the northern part of the mud belt (Core 13817) shows laminated sediments in its lower part. Investigations after the cruise will show whether the laminated sediments are of marine or lakustrine origin. Pore water data show extremely high concentrations of dissolved iron in the laminated sediments. The biogeochemical processes being responsible for the high iron content will be analyzed in detail in the future.

May 29th and 30th was used to collect a long seismic profile to the south along the 70m contour between 36°00'S and 37°15'S. Main objective was to search for incised valleys, which would represent a direct connection between canyons on the slope and rivers on land during times of sea-level-low stands. We did not find clear indications for incised valleys; therefore we concluded that canyons on the slope including the deeply incised Mar del Plata Canyon originated at an upper slope location. The night was used for a bathymetric profile along the axis of the Mar del Plata Canyon and was followed by a short transit to the southernmost location of our cruise at 39°30'S, 53°43'W (Stations 13819 and 13820). These cores were mainly taken for geochemical analyses. Ikaite was recovered during previous cruises at these locations. Small amounts of ikaite were recovered again and the ~10m-long cores offer most promising possibilities for investigating diagenetic processes especially at the sulphate-methane transition zone. The water column was sampled with CTD/rosette water sample and insitu pumps at this location.

On the way back to the distal Mar del Plata Canyon the wind was increasing up to force 8-9. Station work on June 1st was stopped because it was not possible to keep the vessel on position due to strong currents and winds. Therefore we continued bathymetric mapping of the Mar del Plata Canyon. The canyon originates at ~900m water depth, is deeply incised (more than 1000m) and runs relatively straight up to 3500m water depth. Slightly decreasing winds on June 3rd allowed recovering three gravity cores of the distal part of the canyon. Several sandy turbidites and small debrites were identified in the cores. A combined analysis of these cores and cores from the proximal part of the canyon will allow reconstructing canyon activity through time. Increasing winds forced us to stop the coring program again and also prohibited the deployment of the seismic system. Hence the night was used for additional bathymetric profiling of the canyon.

A short period with wind forces less than 6 in the morning of June 4th allowed deploying the seismic system. Seismic profiling was continued until June 6th in the morning despite increasing winds up to force 9 again. Contouritic deposits north of the Mar del Plata Canyon were the main

target of the seismic survey. The new data show that the contouritic deposits are more complicated than previously assumed and build out of individual sedimentary bodies separated by small gullies. The new seismic net is dense enough for a reconstruction of the sedimentary history of this area. June 6th was used for collecting 4 gravity cores of the contourites (13825-13828). The cores are characterized by an interlayering of sandy and clayey layers and are partly laminated, hence indicating changing current intensities.

Additional seismic profiles of the head region of the Mar del Plata Canyon were collected during the night. The data prove an upper slope origin of the canyon. June 7th was used for coring the thalweg of the canyon (Cores 13829-13833). The upper part of the thalweg could only be cored with a box corer, which recovered coarse grained sediments including large rock fragments. Two gravity corers further downslope are characterized by fine grained sediments and numerous turbidites. These two cores completed our work in the southern working area.

After one day of transit we continued the work on the shelf north of the mouth of the Rio de la Plata. Due to much better weather conditions, it was now possible to take cores with vibro corer and giant box corer on the shelf on June 9th and 10th. Seismic data collected during night time shows a complex pattern of erosion and deposition on the shelf. June 11th was used for collecting cores of the uppermost slope in order to reconstruct sediment transport from the shelf across the shelf edge. Two gravity cores were taken on terraces in 240m and 280m water depth. One additional core was taken from a contourite in 1500m water depth. This contourite was mapped with the seismic system until June 12th early morning. Two vibro corer stations in close proximity to the mud belt off Uruguay and some surface water samples in the outflow area of the Rio de la Plata concluded the scientific program of Meteor-Cruise M78/3. At 19:00h on June 12th we started our short transit to Montevideo, where we arrived on June 13th at 08:30h.

The first group of M78/3b scientist was already waiting at the pier during arrival of RV Meteor in Montevideo. A smooth continuation of the cruise during Leg M78/3b was guaranteed by three scientists staying onboard for both legs and an intensive exchange of data and ideas during the port call in Montevideo. The departure of M78/3b, however, was delayed due to logistical problems with the MeBo containers.

The MeBo-system (MeBo: Abbreviation of Meeresboden-Bohrgerät, the German expression for sea floor drill rig) was shipped within six 20'containers from Bremen and Bremerhaven to Montevideo. The containers were scheduled for arriving in Montevideo on June 4th, more than a week before starting installation of the equipment on the deck of RV METEOR on June 14th. However, the containers were disembarked on June 2nd in Buenos Aires instead of in Montevideo and it was not before the morning of June 18th that the containers stood ready for unloading on the pier next to RV Meteor. With optimal support of the Meteor crew and of the agent for the harbor logistics we managed to set up the complicated system within two days. After a successful harbor test of the drill rig and its launch and recovery system RV Meteor left the harbor at June 19th at 09:00 pm local time, two and a half days later than initially planned.

The scientific crew included 25 scientists and technicians from the DFG Research Center and Cluster of Excellence "The Ocean in the Earth System" with scientists from the University of Bremen, the Max Planck Institute for Marine Microbiology and the Alfred-Wegener-Institute for Polar and Marine Research, an engineer from the drill rig manufacturer Prakla Bohrtechnik, a technician and a meteorologist from the German Weather Service and one scientist each from

Administracion Nacional de Combustibles Alcohol y Portland and the University of Buenos Aires.

After arriving the next evening in the first investigation area characterized by contourite deposits – this area was identified as a promising site for drilling with MeBo during the first leg – we started the scientific program with water sampling for dinoflagellate studies, sea floor mapping with Parasound und multibeam echo sounder and a first test of an experimental sediment sampling tool for piston sampling to be used in combination with a pressure core barrel for the MeBo. In the morning of June 21st the MeBo was deployed on the Contourite site. This deployment had to be stopped after drilling the first barrel due to an electric fault. Although the weather conditions deteriorated during the deployment, we managed thanks to the experienced decks crew to recover the drill rig safely. The deployment and recovery of this 10-tonnes device from a moving platform requires fairly calm conditions (not more than 2 m swell). The weather conditions thus had a major impact on cruise planning during this leg.

Since the Contourite Area was already intensively investigated during leg M78/3a by conventional geological tools and hydroacoustics we decided not to wait on calmer conditions for a second MeBo deployment at this site but to steam to the next investigation area located south of the Mar del Plata Canyon. After deployment of the experimental piston corer, gravity corer, multicorer and CPT the weather conditions allowed a MeBo deployment at the afternoon of June 22nd. This site is located at the confluence of the Malvinas and Brazil current and was proposed for a deep drilling site (NAM1) for the drill ship Joides Resolution within the Integrated Ocean Drilling Program (IODP). Results of the MeBo drilling will help to evaluate the suitability of this site for deep drilling in order to reconstruct the history of the Malvinas-Brazil-confluence zone. After 19 hours deployment and 21.5 m drilling depth a strengthening of the wind forced us to finish the deployment and to recover the MeBo. Core recovery rates varied between 50 and 100% depending on the sediment composition and the selected drill bit and core catcher.

After two unsuccessful deployments of the gravity corer at selected sites on the way (the vessel was not able to keep station due to adverse directions of wind waves and currents) a successful sampling, probing and mapping program including water sampling, CPT, gravity corer, experimental piston corer and hydroacoustics was conducted in the northern scarp and drift working area between June 24th and June 27th. Calming of the sea conditions allowed the next MeBo deployment in this area. After a 24 hours deployment reaching 36 m drilling depth the MeBo was recovered in the early afternoon of June 28th. The recovered cores confirmed the interpretation of seismic investigations showing a large older consolidated sediment body covered by a sediment cap consisting of young and soft muds.

An intense low-pressure system forced us to escape towards the south afterwards. On the way three gravity cores were successfully recovered at about 38°/39°S in 3600 to 3700 m water depth in an area known for the occurrence of Ikait-minerals. We were able to recover samples of this diagenetic formed Hexahydrate-Carbonate. The investigation of the minerals as well as the adjacent sediments and pore water profiles will give further insights into the diagenetic formation conditions of this mineral, that is also found at the base of glaciers in high latitudes. Intensification of the storm inhibited a continuation of the station program until the early morning of July 2nd.

After taking three gravity cores in a prominent Canyon system, additional water sampling and a further test deployment of the experimental piston corer we returned to the NAM1 site in order to continue the MeBo drilling at this site. A 29 hours deployment until midnight of July, 3rd / 4th resulted in a drilling depth down to 50.5 m below sea floor. Immediately after recovery, the drill rig was prepared for the next deployment at the contourite site. Within 12 hours drilling time on July, 4th a drilling depth of 20 m was reached and pure fine sands were recovered. The research program was concluded with complementary hydroacoustic mapping on the way back to Montevideo. After arrival at the harbor of Montevideo in the morning of July, 6th the entire scientific equipment and the recovered samples were unloaded and shipped within ten 20' containers back to Bremen.

Despite of the delay at the start of both expedition's legs and despite of the changing and partly inappropriate weather conditions during the southern hemisphere winter we were able to conduct a comprehensive sampling and mapping program. During Meteor-Cruise M78/3 more than 1050 nm of seismic profiles were collected off Uruguay and Argentina, mostly in exceptional quality. 380m of gravity cores were recovered and ~130m of sediments were drilled with MeBo at 61 stations. MeBo worked reliably and the operational speed of the system could be accelerated considerably. Core recovery rates up to 90 – 100 % were reached especially in cohesive sediments. The combined new data set of both legs will allow to reconstruct the sediment transport processes at the continental margin of Uruguay and Northern Argentina.

5. Preliminary Results

5.1. Hydroacoustics

5.1.1. Bathymetric mapping

(T. Schwenk, B. Preu and Shipboard Scientific Party)

Technical description

During Cruise M78/3 the hull-mounted Kongsberg Simrad systems EM120 and EM710 were used for bathymetric mapping. The deep water system EM120 was operated continuously during all seismic surveys but also on transit routes in a 24 hour schedule. The shallow water systems EM 710 was switched on during profiling in shelf areas.

The EM120 system allows an accurate bathymetric mapping down to full ocean depth. Basic components of the system are two linear transducer arrays in a Mills cross configuration with separate units for transmitting and receiving. The nominal sonar frequency is 12 kHz with an angular coverage sector of up to 150° and 191 beams per ping. The emission cone is 150° wide across track, and 1° along track direction. The reception is obtained from 191 beams, with widths of 2° across track and 20° along track. Thus, the actual footprint of each beam has a dimension of 1° by 2°. The achievable swath width on a flat bottom will normally be up to six times the water depth dependent of the roughness of the seafloor. The angular coverage sector and beam pointing angles may be set to vary automatically with depth according to achievable coverage. This maximizes the number of usable beams. The beam spacing is normally equidistant, but an equiangular mode is also available. For depth measurements, 191 isolated depth values are obtained perpendicular to the track for each ping. Using the detected two-way-travel-time and the beam angle known for each beam, and taking into account the ray bending due to refraction in the water column due to sound speed variations, depths are calculated for each beam. A combination of amplitude (for the central beams) and phase (slant beams) is used to provide a

measurement accuracy practically independent of the beam pointing angle. Beside the depth values, the EM120 provides also backscatter information and pseudo-sidescan images (1024 pixel).

The EM 710 multibeam echo sounder is a high to very high resolution seabed mapping system. The minimum acquisition depth is from less than 3 m below its transducers, and the maximum acquisition depth is specified down to 2000 m. However, during the cruise it turned out that the quality of the data degrades in water depths deeper than 600 m. The across-track coverage (swath width) can reach 5.5 times the water depth. During the cruise, the swath width was adjusted manually to get the best compromise between coverage and data quality with changing water depth and sea state. The EM 710 operates at sonar frequencies in the 70 to 100 kHz range. The transmit fan is divided into three sectors to maximize range capability but also to suppress interference from multiples of strong bottom echoes. The sectors are transmitted sequentially within each ping, and uses distinct frequencies or waveforms. The along-track beamwidth of the system installed on RV Meteor is 1 degree. A ping rate of up to 25 per second is possible. The transmit fan is electronically stabilized for roll, pitch and yaw. The EM 710 on R/V Meteor has a reception beamwidth of 1 degree as well. The number of beams is 256 or 400 (high resolution mode). The beamspacing may be set to equiangular or equidistant. The receive beams are electronically roll stabilized. A combination of phase and amplitude bottom detection algorithms is used in order to provide soundings with the best possible accuracy. Additionally, an integrated seabed acoustical imaging capability is included as standard. A real time display window for water column backscatter is also available.

Processing and imaging of the data was done in two ways: For quick overview maps, the raw data were loaded into the Fledermaus Professional Suite for gridding and display. Later, the data were processed with the open source MultiBeam software, including interactive editing and gridding, and also loaded into Fledermaus for displaying. Final maps were produced by use of Fledermaus or GMT (Generic mapping Tools). Due to bad weather conditions, part of the data are quite noisy and even time-consuming processing could not remove all artifacts. For the EM710 data it turned out that for high variations in roll, pitch and heave the corrections of the used motion sensor were not sufficient enough to gather reasonable data and processing of these data was not successful. Therefore only EM120 data are presented here.

Preliminary results

Bathymetric maps were produced for the two main studies offshore Uruguay (Fig. 2) and offshore Argentina around the Mar del Plata Canyon (Fig. 3).

The bathymetric map collected offshore Uruguay (Fig. 2) span depths from 500 m down to 3000 m water depths. Main morphological features are incisions into the sediment across and along slope. The main canyon structure in the centre of the study area is characterized by a relief of ~ 300 m and a width of up to 3 km. The scarp in southwest has a height of around 100 m and runs nearly contour parallel, suggesting a contouritic development (labeled drift and scarp area on Fig. 2). In the northeastern study area, two scarps are visible running subparallel to the contours (labeled northern slide area on Fig. 2). A small U-shaped headwall has been formed at their junction point. The process building these structures is not fully understood yet, but it seems that down-slope and along-slope processes strongly interact in this area.

The main features visible in the data of the southern study area (Fig. 3) are the Mar del Plata Canyon and a smaller canyon structure northwards, both deeply incised in a terrace on the Argentine slope. The canyon head is located in a depth of around 1000 m, the canyon mouth in a depth of 3800 m. In between, the canyon shows over a length of 90 km a slight sinuosity and reaches a maximum relief of 1800 m. The width increases from 2000 m at the head to 8000 m at the mouth. On the northern flank a prominent terrace with an area of 7x14 km shows up, 500-600 m above the canyon thalweg. The smaller canyon is characterized by a length of just 15 km; it starts in a depth of 1300 m and terminates at 3000 m water depths. The maximum relief reaches 1700 m by a width of 5000 m. Beside the both canyon structures, smaller incisions, which are not orientated downslope, can be identified.

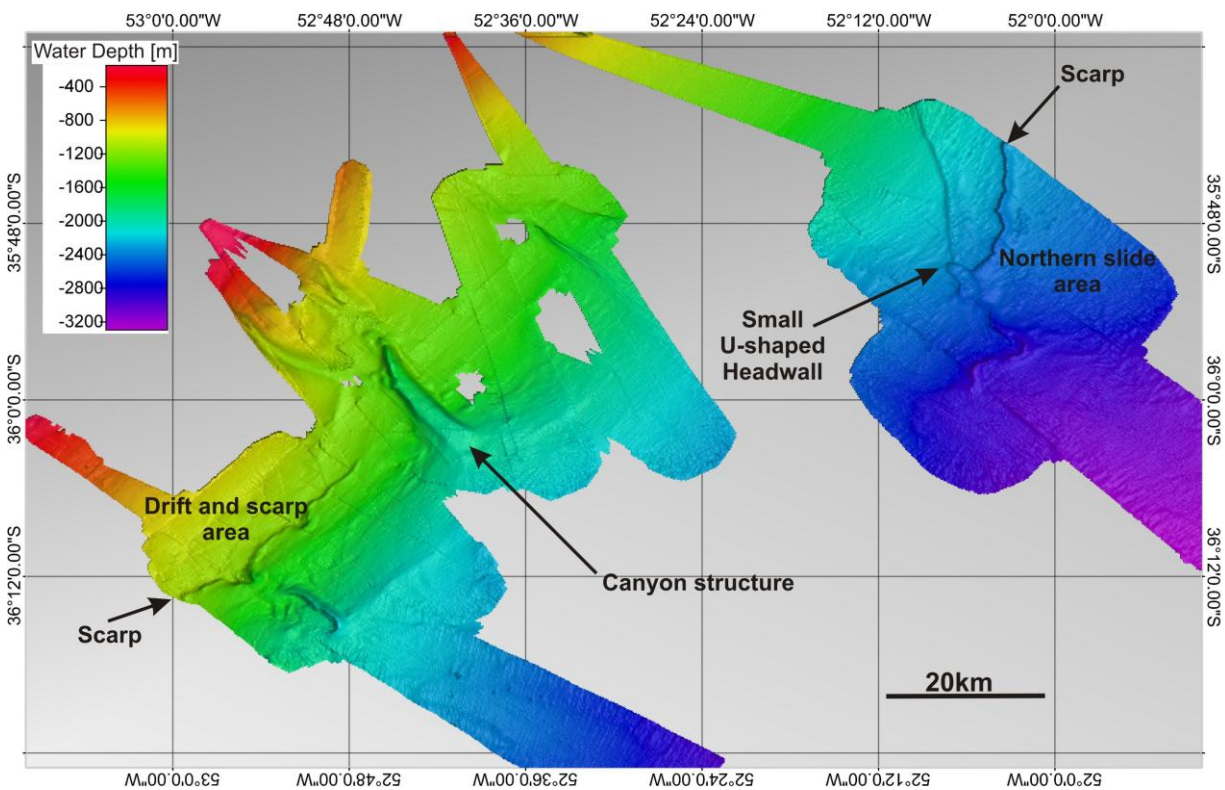


Fig. 2: EM120 multibeam map of the northern study area located offshore Uruguay.

5.1.2. Sediment echo sounding

(B. Preu, T. Schwenk, S. Krastel and Shipboard Scientific Party)

During the whole M78-3 cruise the hull-mounted sediment echo sounder system Parasound was used in a 24 hour watch mode. The system was mainly used to image sediment depositional processes and sediment suspension clouds in the water column. The system was especially used to identify promising coring locations. The system worked most of the cruise stable. Unfortunately, during the last weeks of M78/3a and the first week of M87/3b a data transfer error occurred regularly, which produced data gaps of 20 minutes. These major breaks could be fixed with a program update sent by the Atlas Hydrographics support.

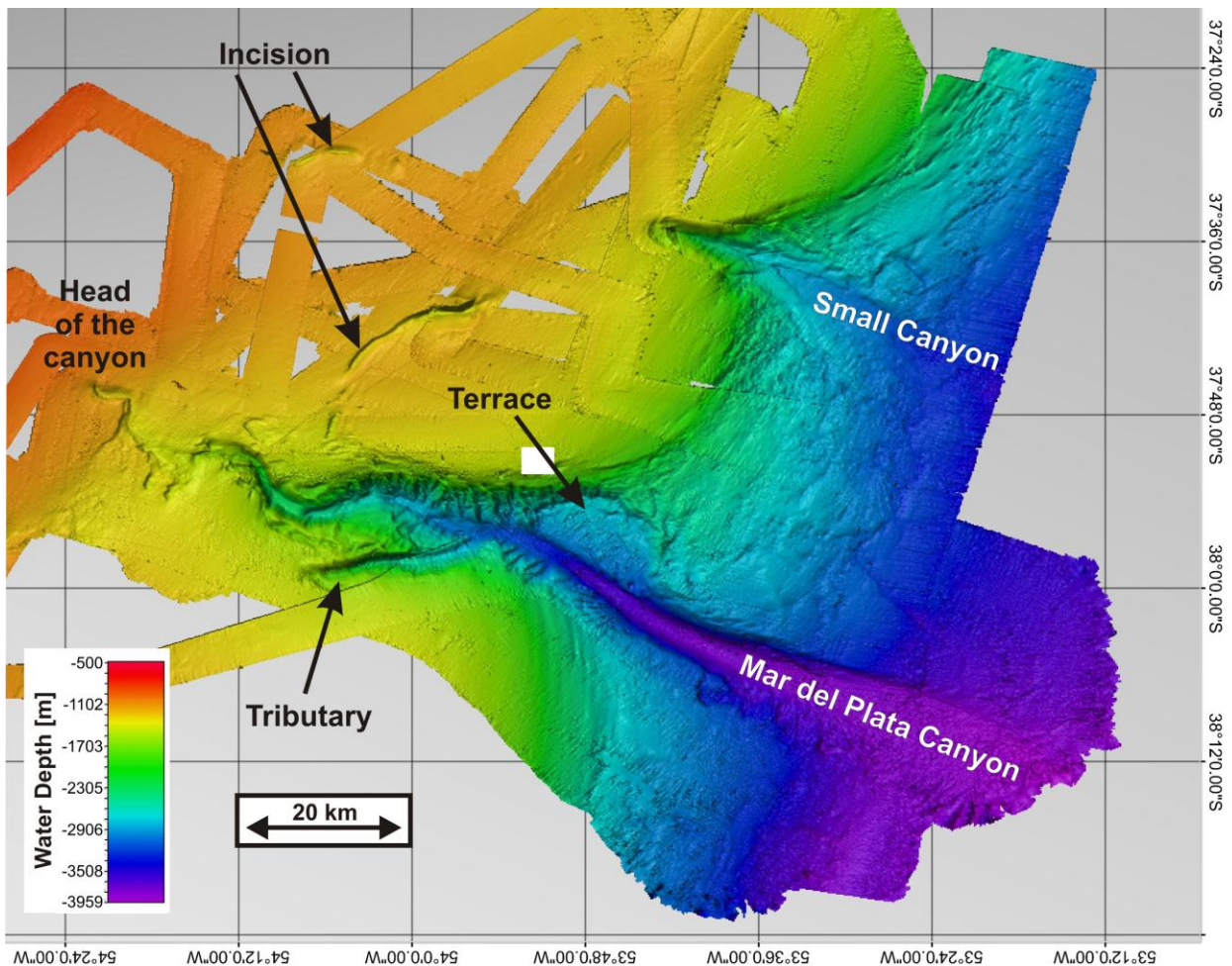


Figure 3: Bathymetric map of the Mar del Plata Canyon and its surrounding area.

System description

Since March 2006 the new Parasound system P70 is installed on RV Meteor. The system uses the parametric effect, which occurs when very high (finite) amplitude sound waves are generated. If two waves of similar frequencies are generated simultaneously, also the sum and the difference of the two primary frequencies are emitted. For the Parasound System, 18 kHz is one fixed primary frequency, which distributes energy within a beam of 4.5° for a transducer of ~ 1 m length. The second primary frequency can be varied between 18.5 and 24 kHz, resulting in difference frequencies from 0.5 to 6.0 kHz. This signal travels within the narrow 18 kHz beam, which is much narrower than e.g. a 4 kHz signal, emitted from the same transducer directly (30°). Therefore, a higher lateral resolution can be achieved, and imaging of small scale structures on the sea floor is superior to conventional systems. As another consequence, the signal bandwidth is also increased, and much shorter signals can be generated with improved vertical resolution. However, due to the very narrow beam, it is necessary to control beam direction to compensate the ship's movement and to send the energy vertically downwards. The system treats three signals separately: the primary high frequency signal (18 kHz; PHF), the secondary low frequency signal (selectable 0.5 to 6.0 kHz; SLF) and the secondary high frequency (selectable 36.5 to 42 kHz; SHF). All three signals are recorded separately. Alternatively, also exclusively a low frequency signal (PLF; 3 or 12 kHz) can be emitted at much lower energy levels, where sound emission energy levels have to be limited (e.g. for mammal protection).

The Parasound system uses minimum three different computer systems. Two of them control realtime signal generation and data acquisition through a Linux and a Windows XP system. The third PC is available for the operator. This Operator-PC hosts the Hydromap Database Server, the Hydromap Control Software and the ParaStore 3 Software. The Hydromap Control Software is responsible for all systems settings and for communication with the realtime computers. This system was updated during the port time between leg M78/3a and M78/3b. This software change done by a technician of Atlas Hydrographics resulted in a significant increase in received amplitudes and followed by that it was even possible to produce reliable data during station work. For visualization, online processing and storage, the ParaStore Software Package is used. Data can be stored in the Parasound own ASD format, but also in the more common PS3 or SEG-Y Format. Several windows can be opened to display different signals (PHF, SLF, SHF) with different scaling and/or processing parameters. This allows optimizing windows for specific purposes, as e.g. imaging of the upper 20m of sediments to select optimal coring locations, to choose a full penetration plot, which also allows coverage of the topography, or to study the complete water column.

The system can be used in the single pulse mode, when a single pulse is emitted and the water column and sediment response are recorded before the next pulse is sent, or in the pulse train mode, by which the two-way travel time of the signal through the water column until the first return is used to emit more signal at regular intervals. Then, the signal density can be increased by as much as a factor of 16, if the time interval between pings and water depths allow. Since this mode did not work properly during cruise M78/3, most of the data were collected using the single pulse modus. To adapt the ping rate of both modes for half of the cruise the automatic depth detection by using the PHF was used. Hence the system failed frequently during bad weather operations. Therefore the system depth was set manually afterwards resulting in much more continuous images.

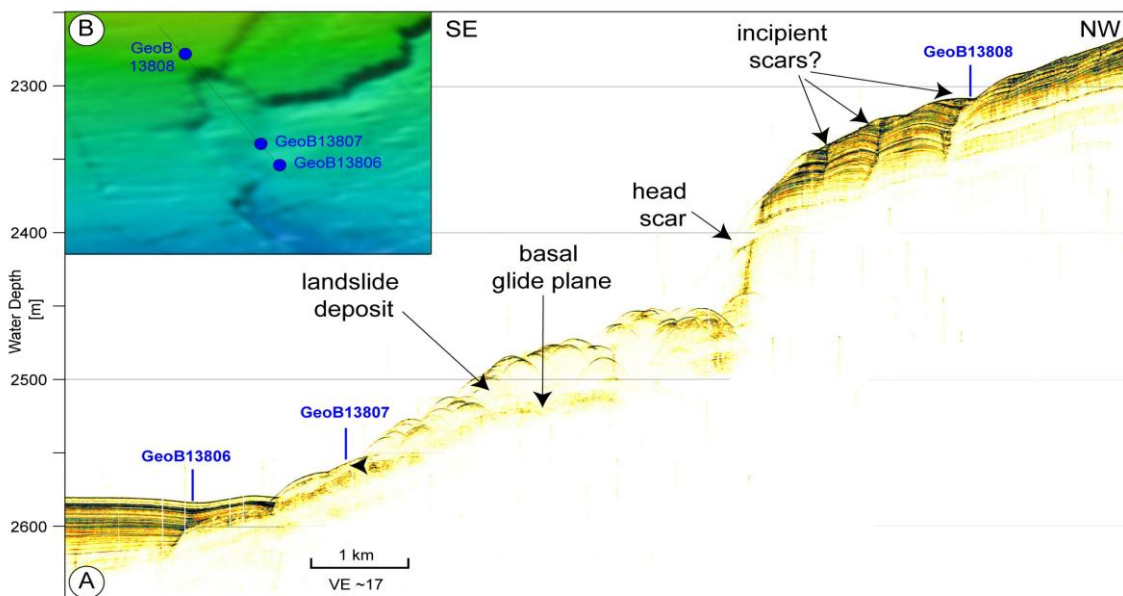


Fig. 4: A: Sediment echo sounder data crossing a small amphitheater-like incision interpreted as landslide scarp. Landslide deposits are imaged as chaotic to transparent facies beneath the headwall. Small faults above the headwall are interpreted as possible incipient scarps. B: Location of profile crossing the amphitheater-like incision

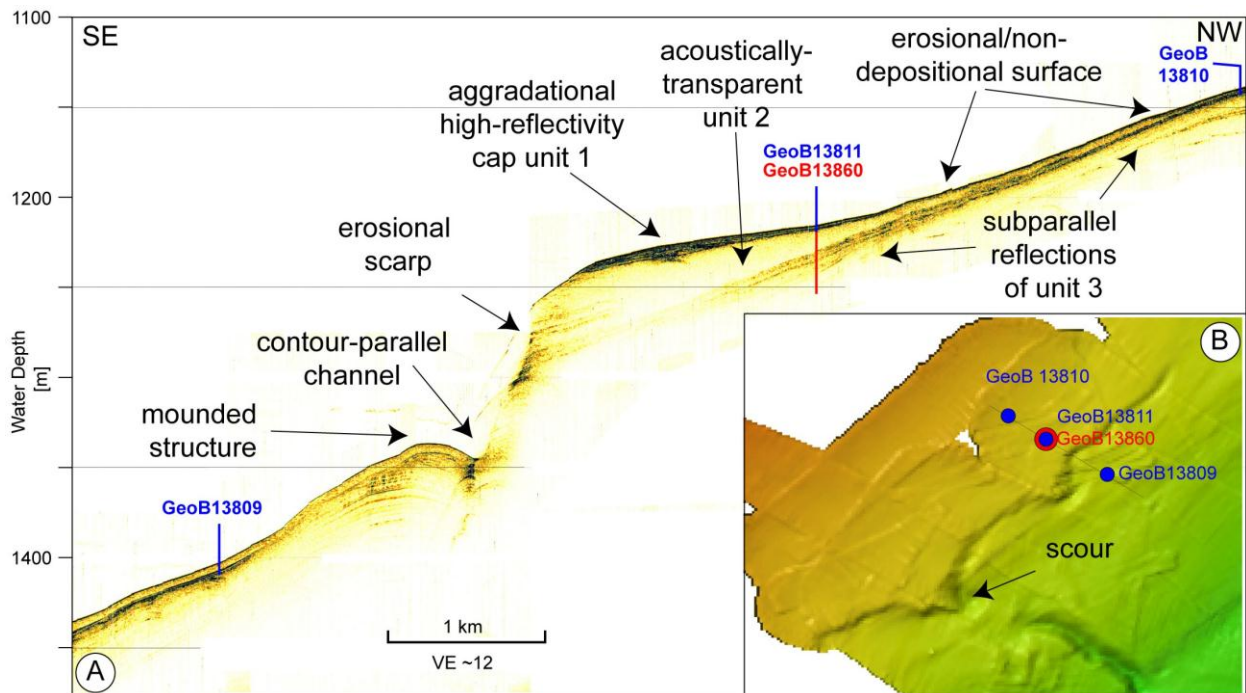


Fig. 5: A: Sediment echo sounder profile crossing an up to 100 m-high erosional scarp. At the foot of the scarp a 5-10 meter deep contour-parallel depression and mounded structure at its seaward side suggest that the scarp focuses contour currents resulting in an alongslope channel. A prominent aggradational cap is found upslope of the scarp. This cap was target of the 35.5 m long MeBo-core GeoB13860 B: Location of the profile crossing the scarp.

Preliminary results:

Parasound data were recorded along all seismic profiles and across all stations. A few examples are shown in the following.

A Parasound profile crossing a morphological step at the Northern Slide area (see Fig. 2 for location) clearly shows landslide deposits beneath the morphological step (Fig. 4). The headwall is about 100m high and shows a slope angle of $\sim 10^\circ$, while the average slope angles landward and seaward of the scarp are $\sim 1.5^\circ$. Landslide deposits characterized by a chaotic-to-transparent acoustic facies with hummocky surface expressions are found directly beneath the headwall. These deposits are up to 60m thick. Towards the south-east and more distal part, the landslide body is thinner and less chaotically structured, possibly indicating a transition from landslide to debris-flow deposits. No hemipelagic drape can be identified on the Parasound profiles.

Another pronounced morphological scarp is found in the so called drift and scarp area off Uruguay (see Fig. 2 for location). A Parasound profile (Fig. 5) crossing this feature clearly shows the erosional character of the morphological step, which is interpreted as erosional scarp. A thin (~ 5 m) transparent layer is found directly beneath the scarp but the very smooth surface and the low amplitude of the upper reflector of this unit does not support the interpretation of this layer as landslide deposit. This layer is the result of very homogenous sediments recovered in Core GeoB13809. A prominent aggradational cap with very strong surface reflector is found upslope of the scarp. The cap can be divided into an upper unit characterized by very strong reflectors (Unit 1 in Fig. 5) and a lower acoustically transparent unit (Unit 2 in Fig. 5). The cap is deposited on top of Unit 3, which is characterized by continuous subparallel reflections of

medium amplitude. The landward part of the sedimentary cap shows an erosional/non depositional surface. The sedimentary cap was target of a MeBo-site. A 35m-long core with almost complete recovery was drilled at this location (marked as station GeoB13860 on Fig 5).

A Parasound profile crossing a mud belt on the inner shelf off Uruguay is shown on Fig. 6. A nearly 30 m deep depression has been found and studied by several crossing Parasound Profiles and coring stations. The Parasound data reveal a complex pattern of units of different acoustic facies beneath and beside the depression. Directly beneath the depression a well layered unit has been deposited, which settles on top of a nearly transparent unit. This transparent unit is separated by an erosional unconformity from the lower units, which are characterized by parallel layering and transparency, respectively. The whole feature is interpreted to represent the paleo-valley of the Rio de la Plata, refilled by different sediments with respect to sea-level rise. Several cores were taken along this profile (Fig. 6) in order to characterize the sedimentological composition of the individual units.

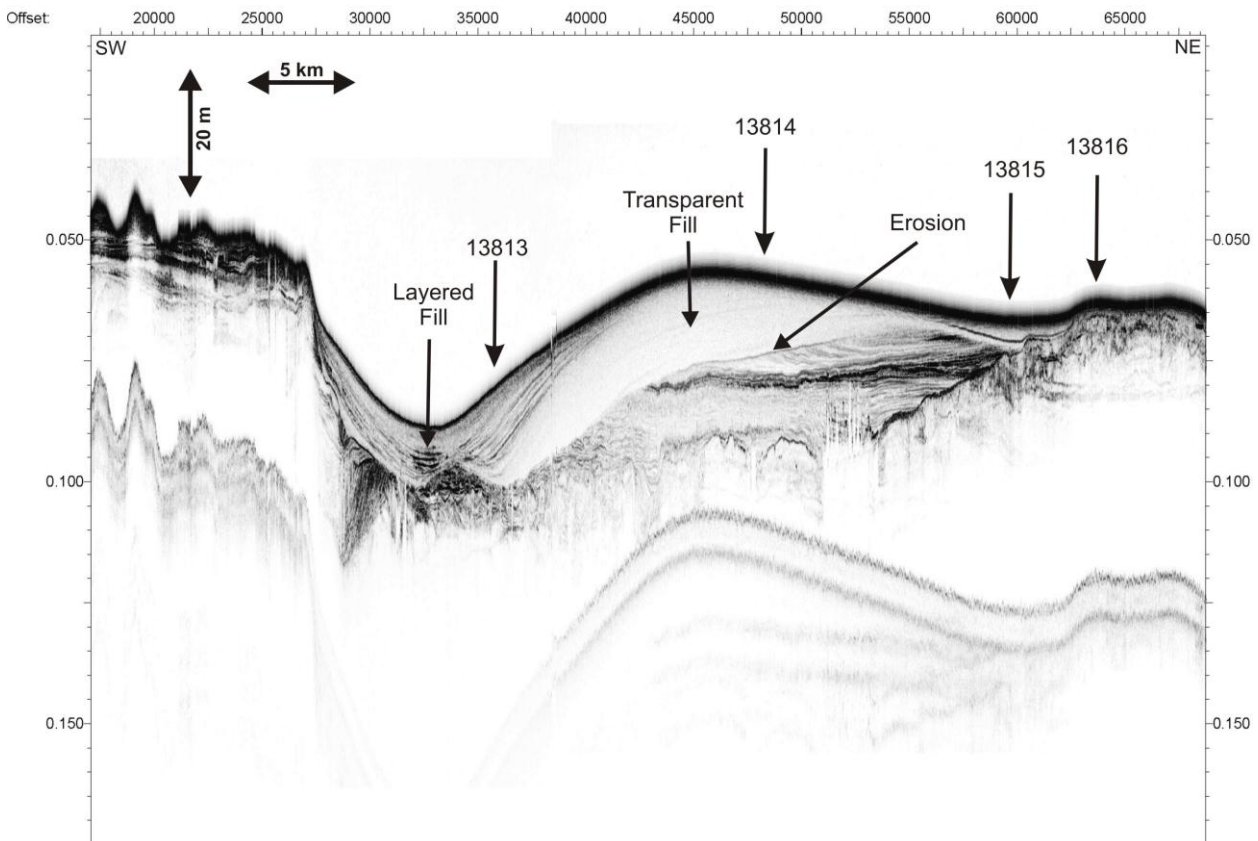


Fig. 6: Parasound Profile from the inner shelf offshore Uruguay. Positions of cores are indicated by arrows. See Fig. 19 for location of profile.

Parasound data from Profile 09-099 show the crest of the contouritic deposits north of the Mar del Plata Canyon. Clearly visible are the different deposition units characterized by different seismic facies. These units are separated by strong unconformities or prominent conformities. Two unconformities have a clear erosional character. Especially one of the lower units shows the geometry of a plastered drift. In general, the data reveal that sedimentation differs from unit to unit and show pure aggrading, prograding or depression filling, which suggest that the current regime controlling the deposition has been changed significantly in time and space.

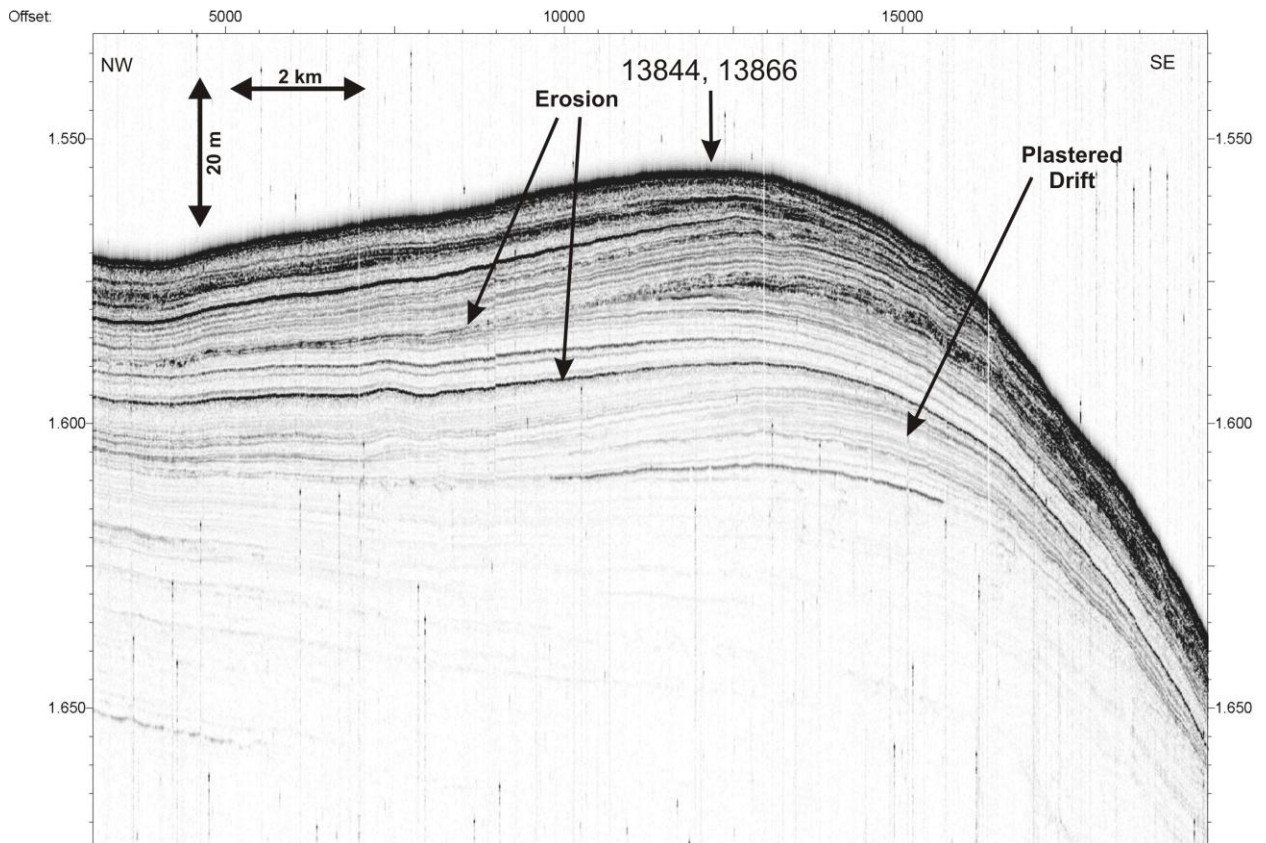


Fig. 7: Parasound Profile crossing the crest of the contourite depositional system north of the Mar del Plata Canyon. The location of the contourite MeBo site is shown as arrow. See Fig. 22 for location of profile.

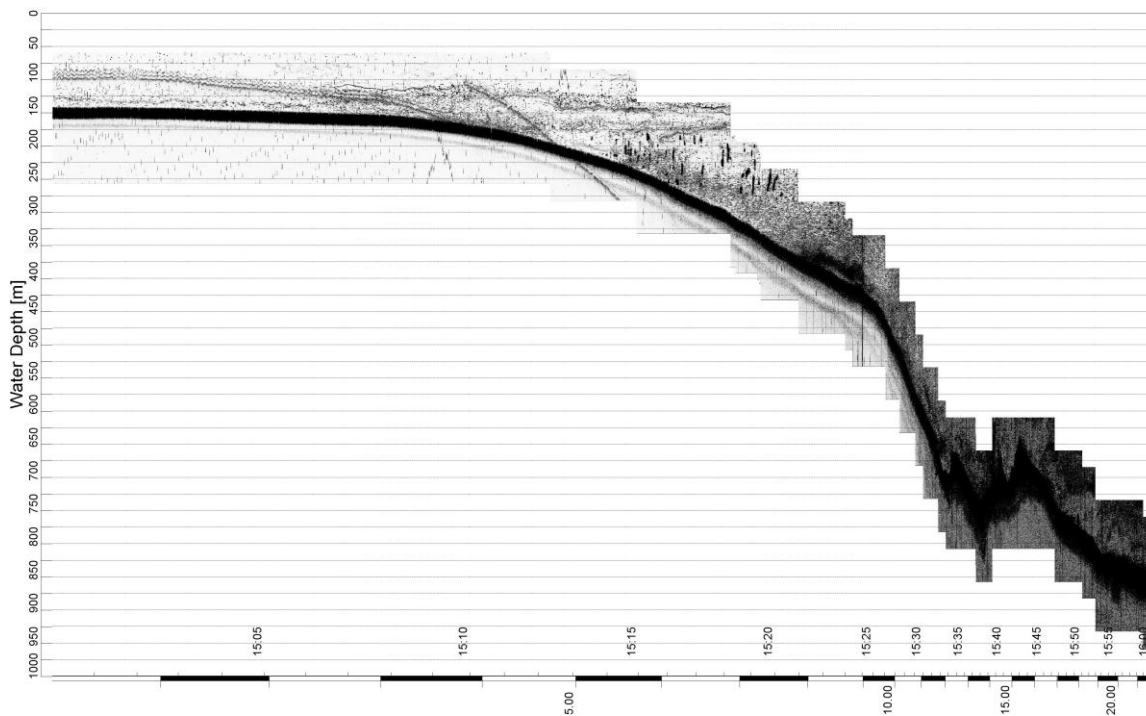


Fig. 8: PHF image acquired during M78/3 during the transit to GeoB13844 at the Uruguayan slope probably imaging current induced sediment transport in the water column

The PHF signal of the Parasound system was used to map reflections in the water column. A special focus was the determination of signals close to the seafloor in areas of current induced sedimentary bodies and current anomalies. Fig. 8 exemplarily shows a profile across the Uruguayan shelf break and slope. Several acoustic anomalies with high amplitudes could be observed in the water column along the whole profile.

5.1.3. Advanced Doppler Current Profiler (ADCP)

(B. Preu, T. Schwenk, and Shipboard Scientific Party)

For comparing the results of the PHF (18 kHz) of the Parasound, current velocity and direction were measured using an Advanced Doppler Current Profiler. These parameters are calculated by using the Doppler shift produced by particles passing four narrow acoustic beams submitted by the ADCP.

The RD Instruments ADCP permanently installed on the ship's hull operates with a frequency of 75 kHz measuring current velocity and direction. The system was configured to collect data in 16 m steps up to depth of 960 m in narrow band mode. The incoming data were corrected for the ships movement using the ship's GPS navigation and gyre system. Additionally to the raw data two different smoothed data sets were recorded averaging over an interval of 1 and 5 minutes. Data stored in these averages were also filtered for data points with more than 50% reliability. This allowed fast visualizing and quality control of the recorded data on board.

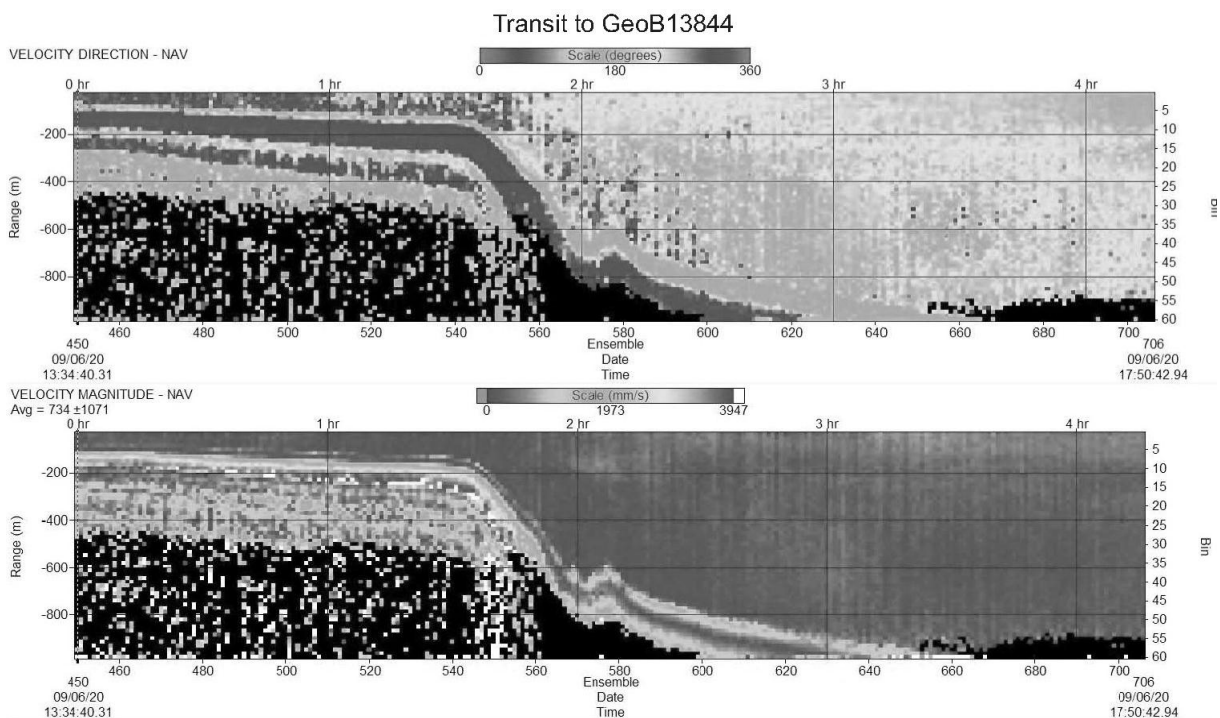


Figure 9: ADCP data of the transit to station GeoB13844: Upper part shows the current direction; the lower part shows current velocity.

Additionally the non permanent installed 38 kHz RD Instruments ADCP was used. The instrument also acquired data in narrow band mode. The maximum target depth was set to 2000 m in 20 m steps. The collected values were averaged over an interval of 1 and 5 minutes. Data

were collected during M78/3a until technical problems appeared. These problems could not be solved on board and thus, the system could not be used during M78/3b.

ADCP data were collected along most profiles, on stations and during transit times. Of main interest were areas, where the PHF of the Parasound showed strong reflections in the water column. One example of an ADCP profile is shown in Fig 9.

5.2. High resolution multichannel seismic profiling

(S. Krastel, T. Schwenk, A. Anasetti, Y. Domnina, N. Fekete, K. Lindhorst, M. Meyer, B. Preu)

i) analogue streamer (Uni-Bremen)

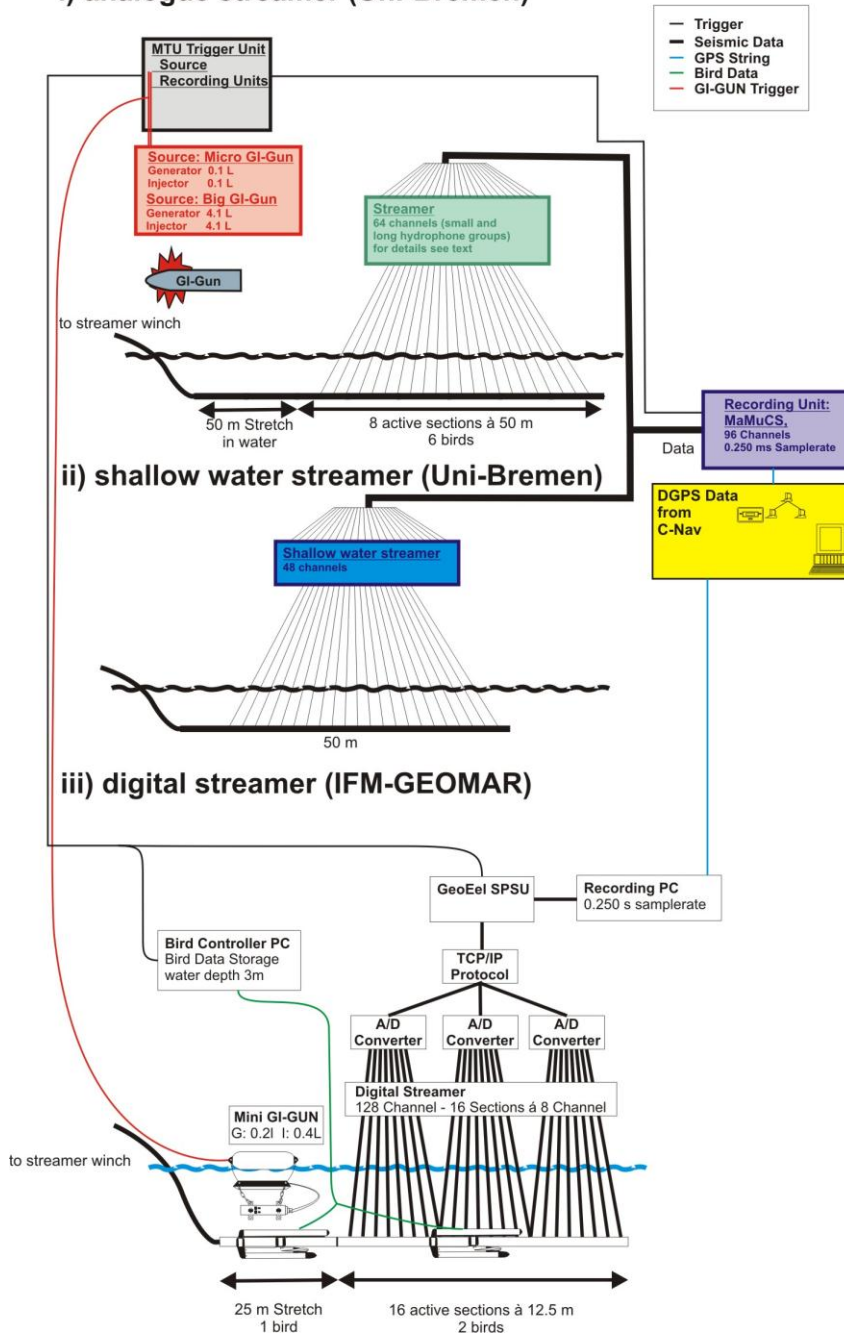


Fig. 10: Seismic system setup during R/V Meteor- Cruise M78/3.

5.2.1.Introduction

During Cruise M78/3a equipment of Bremen University and IFM-GEOMAR (Kiel) was used to acquire high-resolution multichannel seismic data. The aim was to resolve small scale sedimentary structures and closely spaced layers on a meter scale, which can usually not be resolved by means of conventional seismic systems. During the cruise, the following sources were used: i) a Mini-GI gun shot in true GI Gun-mode (Generator Volume: 0.2l, Injector Volume: 0.4l); ii) a Micro-GI gun (Generator Volume: 0.1l, Injector Volume: 0.1l), and iii) a 4.1 l GI gun (Generator Volume: 4.1l, Injector Volume: 1.7l). Data were recorded with three different streamer systems: i) a 400m-long 64-channel analogue streamer of Bremen University with up to 13 hydrophones per group; ii) a 200m-long 128-channel digital streamer of IFM-GEOMAR with 2 hydrophones per group, and iii) a 50m-long 48 channel shallow water streamer with single hydrophones per group. The 200m-long 128-channel digital streamer was the main tool for the continental slope. It was originally planned to tow the 400m-long 64-channel analogue streamer parallel to this streamer but strong winds and currents did not allow to deploy both streamer system at the same time. The 50m-long 48-channel shallow water streamer was used for all profiles on the shelf. Fig. 10 gives an outline of the system setup as it was used during R/V Meteor Cruise M78/3a. Tab. 1 lists the individual setting for each profile.

Table. 1: Source and receiver settings for individual profiles.

Profile	Source, mode, shooting rate (s)	Digital streamer (IFM-GEOMAR)	Shallow water streamer (Uni-Bremen)	Analogue streamer (Uni-Bremen)
09-069 - 09-071	Micro GI Gun (0.1L) and GI Gun (4.1L), 7-16s	Only deployed for the first part of profile	Not deployed	400m, 64 channels
09-072 - 09-079	Mini GI-GUN 0.2, true GI, 5.5s	213m, 120 channels	Not deployed	Not deployed
09-080 - 09-089	Mini GI-GUN 0.2, true GI, 2.5-5.5s	200m, 112 channels	Not deployed	Not deployed
09-090 - 09-093	Mini GI-GUN 0.2, true GI, 2.5s	Not deployed	50m, 48 channels	Not deployed
09-094 - 09-096	Mini GI-GUN 0.2, true GI, 2.5s	225m, 128 channels	50m, 48 channels	Not deployed
09-097 - 09-100	Mini GI-GUN 0.2, true GI, 4.5-6s	225m, 128 channels	Not deployed	Not deployed
09-101 - 09-110	Mini GI-GUN 0.2, true GI, 4.5-6s	213m, 120 channels	Not deployed	Not deployed
09-111 - 09-118	Mini GI-GUN 0.2, true GI, 2.5s	Not deployed	50m, 48 channels	Not deployed
09-119 - 09-124	Mini GI-GUN 0.2, true GI, 4.5s	213m, 120 channels	Not deployed	Not deployed

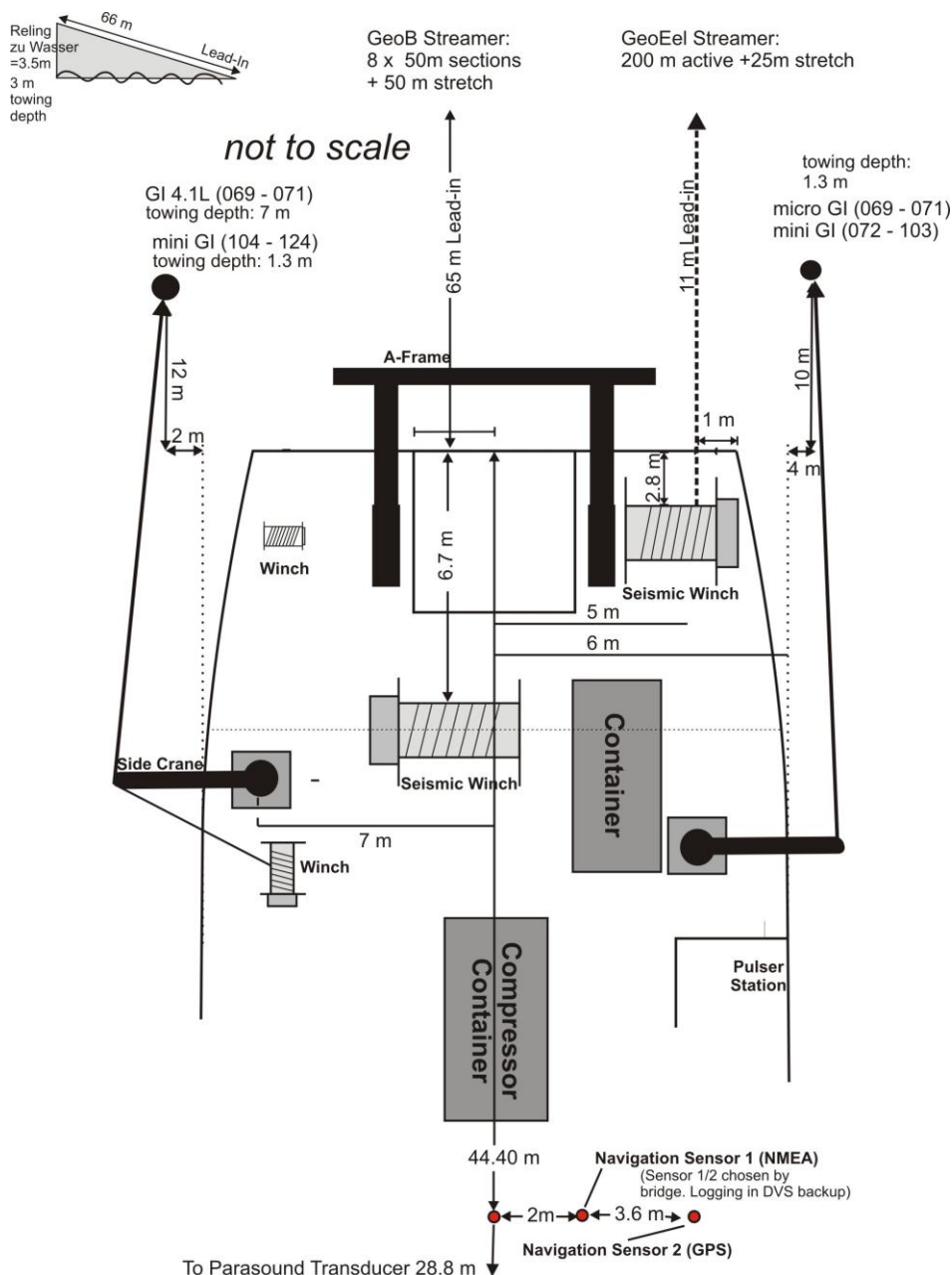


Fig. 11: Deck and seismic gun setting during Cruise M78/3a.

5.2.2. System components

Seismic sources

During seismic surveying, three different guns were used (see Tab. 1 for individual settings). The main source was a Mini-GI Gun, which was shot in true GI-mode (Generator 0.2l, Injector 0.4l). The GI-Gun was towed from the port side crane appx. 10 m behind the ship's stern for profiles 09-072 – 09-103 and from the starboard crane appx. 12 m behind the ship's stern for profiles 09-104 – 09-124 (Fig. 11). The Mini-GI-gun was connected to a bow with the GI-Gun hanging on two chains 30 cm beneath. An elongated buoy, which stabilized the guns in a horizontal position at a water depth of ~1.3m, was connected to the bow by two rope loops. The Injector of the Mini-GI gun was triggered with a delay of 20 ms with respect to the Generator signal, which basically eliminated the bubble signal. For the first three profiles (09-069 - 09-071) a 4.1l GI Gun and a Micro-GI gun (0.11) were shot in an alternating mode. The 4.1l GI-gun was towed in

~7m water depth. The Micro-GI gun was towed in the same configuration as described above for the Mini-GI Gun. The shooting rate was adjusted to the water depth (see Tab. 1). The guns were shot at 150 bar. The guns worked very reliable during the entire cruise except for some problems with the large gun during the first survey.

Streamer-systems

Three different streamer systems were used during the cruise: i) a 400m-long 64-channel analogue streamer (Syntron) of Bremen University, ii) a 200m-long 128-channel digital streamer (Geometrics GeoEel) of IFM-GEOMAR, and iii) a 50m-long 48-channel analogue shallow water streamer of Bremen University. At the beginning of the cruise, we tried to deploy the 400m-long 64-channel streamer and the 200m-long 128-channel streamer simultaneously. Due to the relatively small distance between the streamers and strong currents, this approach was stopped after the streamers were entangled already on the first profile. Most of the time only the 200m-long 128-channel digital streamer was deployed. The shallow water streamer was used for profiling on the shelf. The streamer setup for individual profiles is listed in Tab. 1. The 400m-long Bremen streamer was towed beneath the A-Frame of RV Meteor, while the 200m IFM-GEOMAR streamer was towed on the port side. The 50m shallow water streamer was deployed by hand beneath the A-frame (Figs. 11, 12).

The Bremen streamer consists of a lead-in (65m in water), a 50m-long stretch section and 8 active sections of 50m length each. A 20m-long Meteor rope with a buoy at the end was connected to the tail swivel. A 30m-long deck cable connected the streamer to the recording system. Active 50m-sections are subdivided in 8 hydrophone groups. Each of the 6.25m long hydrophone groups is again subdivided into 5 subgroups of different length (Fig. 13). A programming module distributes the subgroups of 4 hydrophone groups, i.e. a total of 20 groups, to 4 channels. For all profiles every second 6.25m hydrophone subgroup was completely used with all 13 hydrophones, whereas the two additional channels were reduced in length to 2.2m and 3.3m, respectively (Fig. 13). Locations of individual hydrophone groups are given in Tab. 2. For the entire cruise output channels 1 to 64 were directly connected to the MaMuCS recording system, independent of the hydrophone group length (see below). Depth control of the streamer was achieved by five DigiBird Remote Units. The designated streamer depth was 3m (see below).

The Bremen shallow water streamer was used for the profiles on the shelf. It is a 50m-long 48-channel analogue streamer. Each channel consists of one single hydrophone in order to prevent any distortion of the signal at low incident angles. The streamer is towed by a combined lead-in/two cable. The distance to the first channel was 35 m. Recording of the 48 channels were done by the MaMuCS recording system.

The Geometrics GeoEel digital streamer of IFM-GEOMAR consists of an 80m-long tow cable (11m in water), a 25m-long stretch section and 16 active sections of 12.5m each (Fig. 14). A small buoy was attached by a 20m long Meteor rope to the tail swivel. A 60m-long deck cable connected the streamer to the SPSU (Streamer Power Supply Unit). Active 12.5m sections are divided in 8 channels. Each channel consists of two hydrophones; channel distance is 1.56m. One AD digitizer module belongs to each active section. These AD digitizer module are small Linux computers. Communication between the AD digitizer modules and the recording system in the lab is via TCP/IP. A repeater was located between the deck cable and the tow cable. The

SPSU manages the power supply and communication between the recording system and the AD digitizer modules. The recording system is described below. Three birds were attached to the streamer (see below). Designated streamer depth was 3m.

Only minor problems occurred with the streamer during the cruise. The leakage sensor indicated a few leakages during seismic profiling. These sections were taken out of the streamer for careful inspection; hence individual profiles are not recorded with all 16 sections (see Tab. 1).

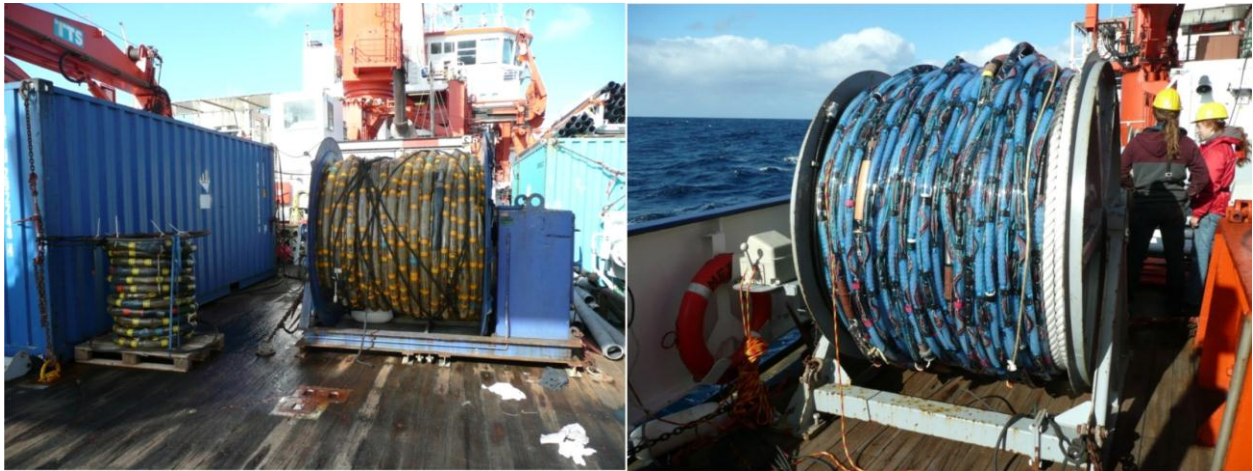


Fig. 12: Picture of the streamer systems used during Cruise M78/3a. Left: Bremen shallow water streamer (at the container) and 400m-long 64-channel streamer. Right: Kiel 200m-long 128-channel streamer.

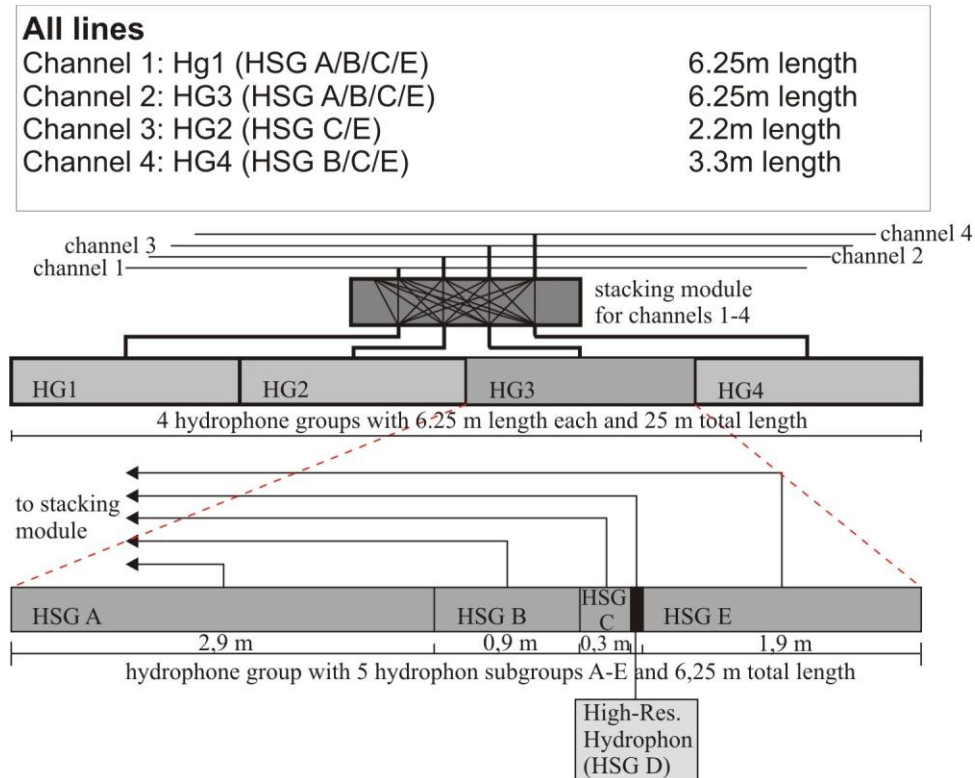
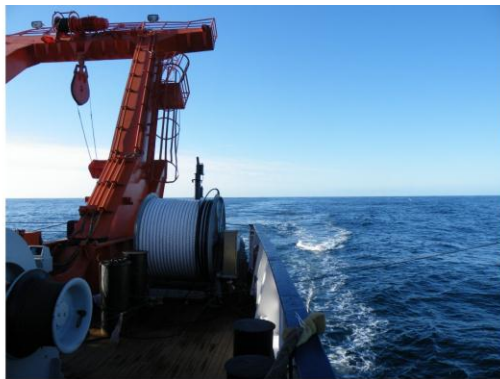


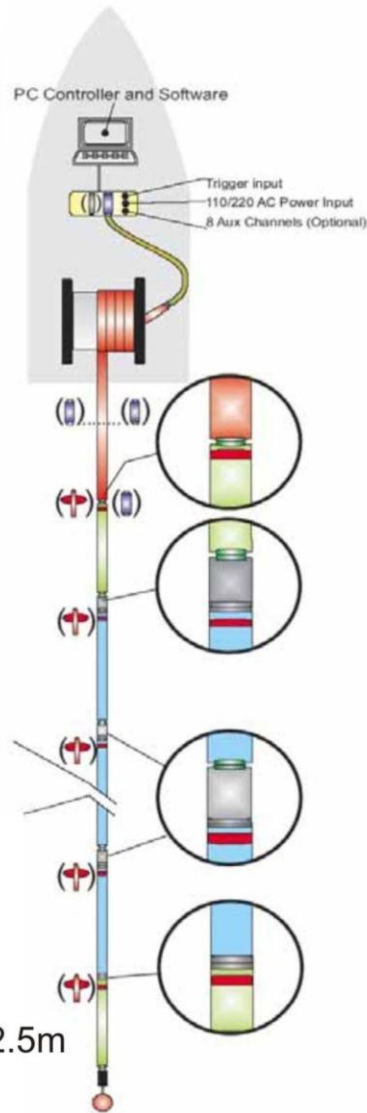
Fig. 13: Configuration of the Bremen Streamer as used during Cruise M78/3a.

Table 2: Channel assignment and midpoint distances of hydrophone groups of the Bremen deep water streamer during cruise M78/3a.

Segment of 25 m length	Hydrophone Group No.	Channel No. In Section	Midpoint Distance
A (0-25 m)	1	1	3.1 m
A	2	3	11.3 m
A	3	2	15.6 m
A	4	4	23.3 m
B (25-50 m)	1	5	28.1 m
B	2	7	36.3 m
B	3	6	40.6 m
B	4	8	48.3 m



- Components:**
- Streamer Power Supply Unit (SPSU)
 - Deck Cable
 - Tow Cable
 - Repeater Module
 - Stretch Section
 - A/D Digitizer Module
 - Bird
 - 8-channel Active Section
 - Digital Connector Pair
 - Analog/Digital Combo Connector Pair
 - Bird Coil
 - Tail Swivel
 - Tail Buoy
 - Optional



Configuration M78/3a

- 60m deck cable
- 80m Tow Cable
- 25m Stretch
- 16 active sections (8channels) a 12.5m
- 2 Birds
- Tail buoy

Fig. 14: Configuration of the Kiel Streamer as used during Cruise M78/3a.

Bird Controller

Three Oyo Geospace Bird Remote Units (RUs) were deployed at the Kiel Streamer. The locations of the birds are listed in Tab 3. All RUs have adjustable wings. The RUs are controlled by a bird controller in the seismic lab. Controller and RUs communicate via communication coils nested within the streamer. A twisted pair wire within the deck cable connects controller and coils.

Each shot trigger started the bird scan of diving depth, wing angle and heading data. The current location of the streamer can be displayed as a depth profile on a monitor and stored on the controller PC. Before the streamer was deployed, each RU was programmed in the seismic lab to keep an operating depth of 3 m. The RUs thus forced the streamer to the chosen depth by adjusting the wing angles accordingly. Possible depth variations of the streamer could be checked later during preliminary data processing and depth control appeared to be successful. The birds worked very reliable during the cruise.

A similar bird system was used for the Bremen streamer. Up to five DigiBird Remote Units were available for the Bremen Streamer and could be configured using the bird controlling unit. The communication between birds and bird controller did not work very well. Especially for the more distal birds no data could be recorded due to the communication failures. Nevertheless, the birds worked reliable and kept the streamer in the designated depth.

Table 3: Bird Positions for the Kiel Streamer during Cruise M78/3a

Profile	Distance behind stern		
	Bird 20376	Bird 20399	Bird 2045
09-072 - 09-079	33 m	170 m	233 m
09-080 - 09-093	33 m	158 m	220 m
09-094 – 09-124	33 m	158 m	233 m

Data acquisition systems

Data of the Bremen streamer systems were recorded with a MaMuCS-System (Marine Multi Channel Seismic Acquisition System), which was developed at Bremen University. It consists of a Pentium IV based PC (3 GHz, 1GB RAM, Windows XP) with three NI6052E 16bit AD-converters. Each ADC is connected to a 32 channel multiplexer (NI- SCXI1102-C) with onboard preamplification and anti-alias filter. The system therefore provides a maximum of 96 channels at maximum sampling rate of 10 kHz per channel. Sample rate can be increased dynamically if number of channels is reduced.

The acquisition software is also a custom development and provides nearly continuous recording of the 96 channels with data storage in demultiplexed SEG-Y (floating-point IEEE) to hard disk. The software allows online quality control by displaying shot gathers and an online profile plot using brute channel stacks of arbitrary channels. The online profile can additionally be printed immediately to an attached windows printer and/or stored in SEG-Y format. The acquisition system worked very reliable during the cruise.

Data were recorded at 4 kHz. The delay was adjusted to the water depth. The MaMuCS-PC was also used for logging the ship's GPS data and also for distribution the GPS data to other PCs via the network.

Data of the Kiel Streamer were recorded with acquisition software provided by Geometrics. The analogue signal was digitized with 4 kHz. The data were recorded as multiplexed SEG-D. One file was generated per shot. Data were recorded with delay but the delay is not written to the header. The delay was adjusted to the water depth. The acquisition laptop allowed online quality control by displaying shot gathers, a noise window, and the frequency spectrum of each shot. The cycle time of the shots is displayed as well. The software also allows online NMO-Correction and stacking of data for displaying stacked sections. Several logfiles list parameters such as shot time and shot position. Data were converted to SEG-Y file while being at sea.

Trigger unit

A custom trigger unit, the so called SchwaBox was used during Cruise M78/3a. The box generates triggers (TTL) at arbitrary combinations for controlling seismic sources, acquisitions systems, and bird controllers (Fig. 10). The box was also connected to a gun amplifier unit. The trigger scheme was adjusted to the water depth during the survey. This trigger system worked very reliable during the entire cruise.

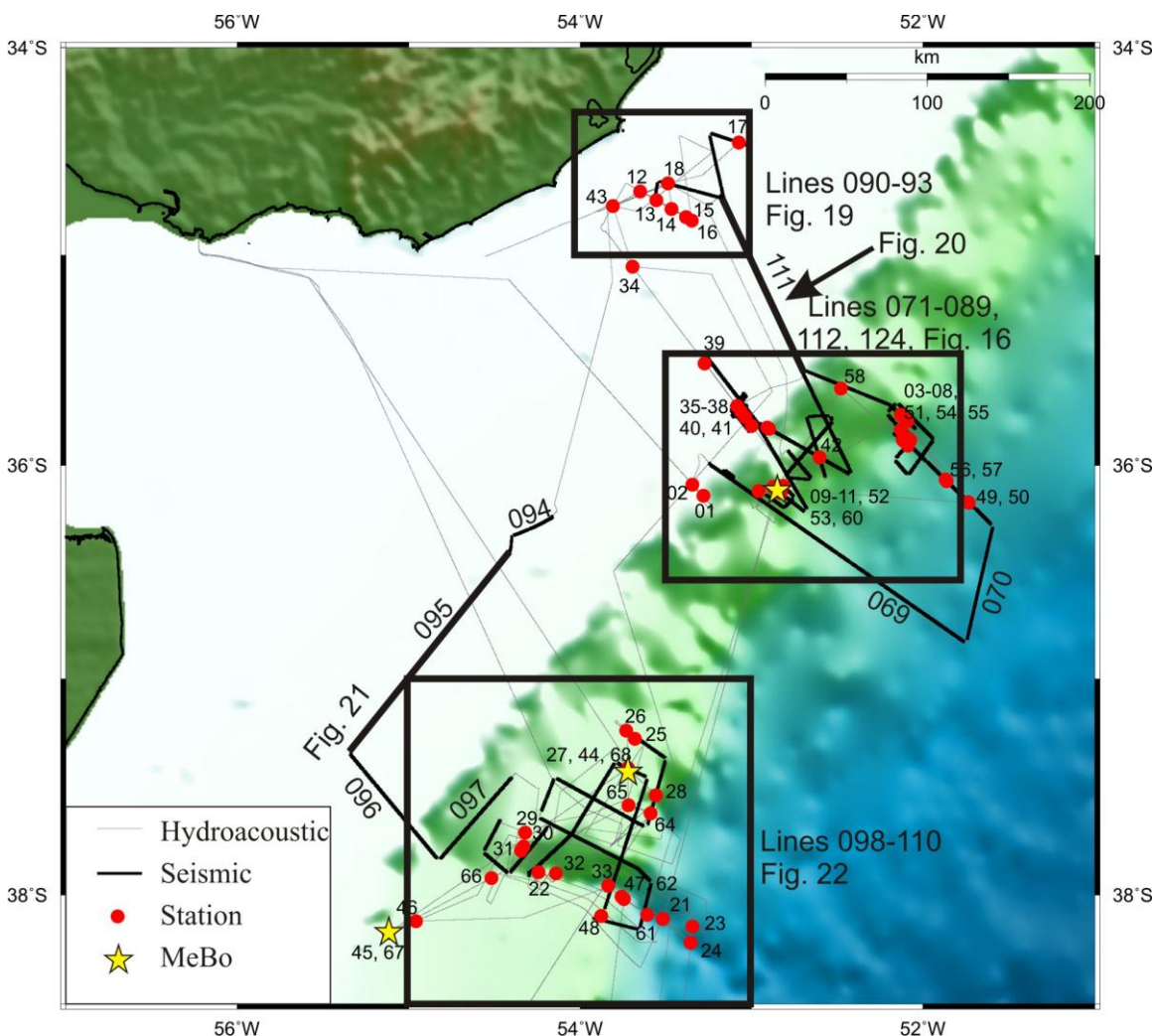


Fig. 15: Overview map showing locations of seismic profiles and stations of Cruise M78/3.

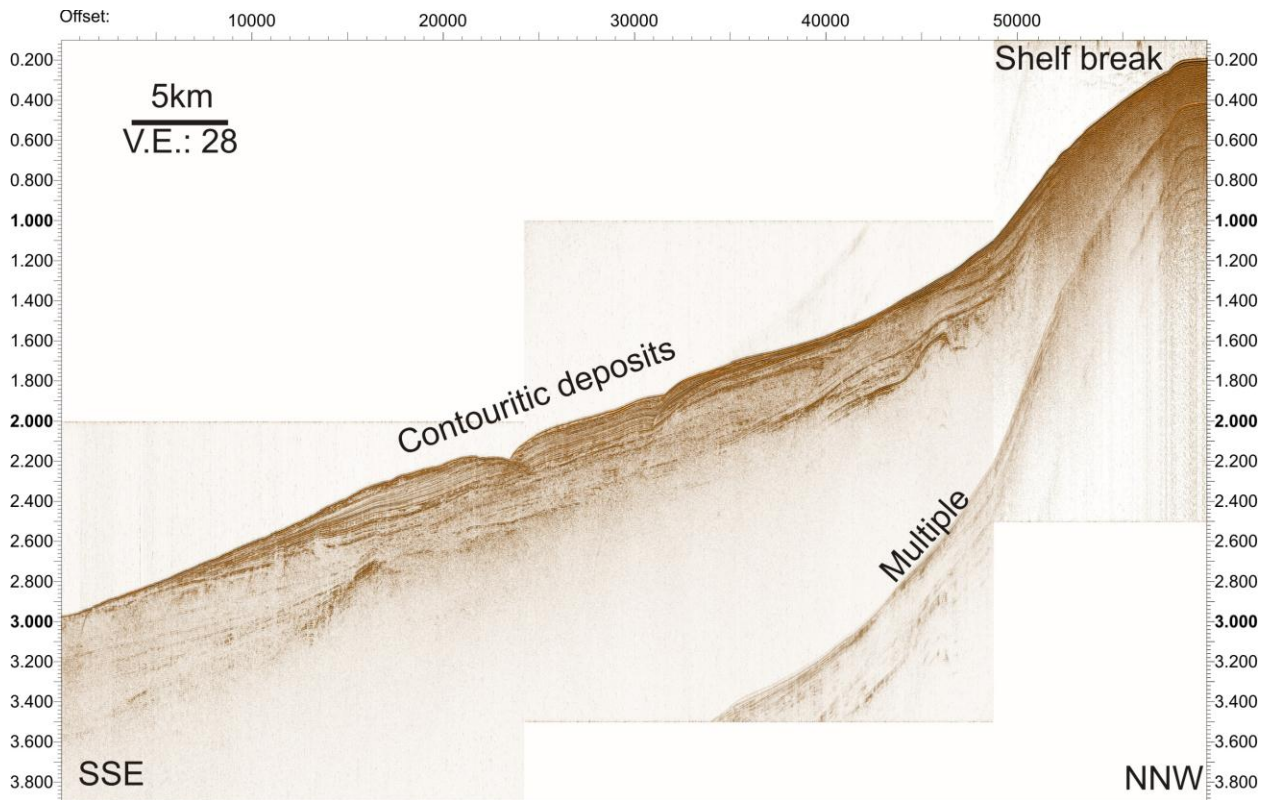


Fig. 17: Seismic Line 09-082 off Uruguay. For location of profile see Fig. 16.

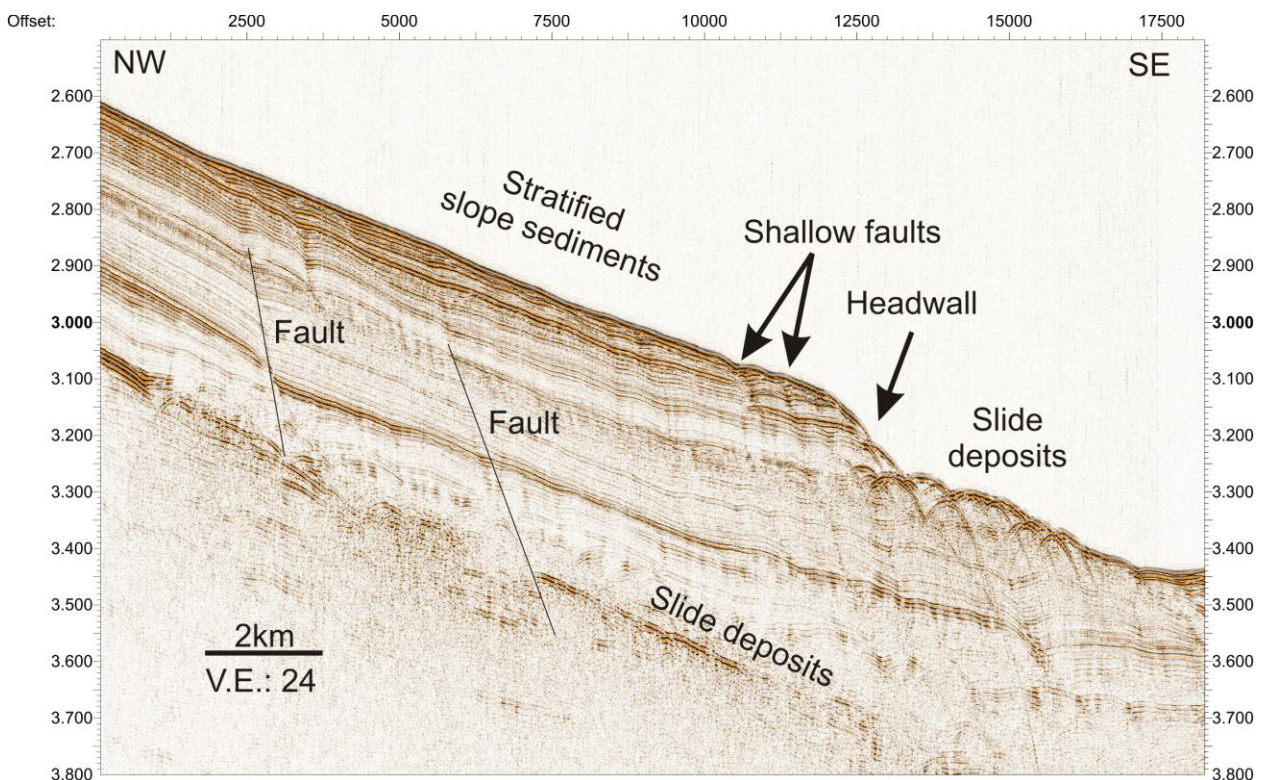


Fig. 18: Seismic Line 09-072 crossing a headwall in the Northern slide area. For location of profile see Fig. 16.

The seismic profile shown on Fig. 18 crosses the so called northern slide area (see Figs. 2 and 16 for location). A pronounced headwall is visible in ~2300 m water depth; headwall height is ~100m. The area downslope of this scarp is characterized by a chaotic to transparent seismic

facies typical for slide deposits. The base of the slide deposits is difficult to identify on the unmigrated data but preliminary interpretation allows tracing the base reflector to undisturbed sediments upslope of the headwall. The area upslope of the headwall is characterized by well stratified sediments with some indication for faulting. Shallow faults traceable to ~100m sub-bottom depth are located immediately upslope of the headwall. These faults might indicate creeping of the sediments and may represent incipient future slope failures. The faults differ from deeper reaching faults further upslope. The shallow reaching faults are only identified in close vicinity to headwall scarps. A hummocky chaotic seismic facies at greater sub bottom depth most likely represent deposits of older mass wasting events.

A second area surveyed off Uruguay was the inner and outer shelf (Figs. 15 and 19). A typical example of a profile running from the inner to the outer shelf is shown on Fig 19. Water depth increases from less than 50 m on the inner shelf to more than 150 m at the outer shelf. The modern shelf break is not imaged on the profile but the seismic data might show former shelf breaks, which would mean that sediment accumulation resulted in a seaward shift of the shelf break. The entire profiles show a complex patten of erosive and depositional unconformities, strong variations in amplitude, and significant lateral variations in sediment accumulation rate. Relatively low amplitude reflectors with increased continuity were found at the SSE-part of the profile.

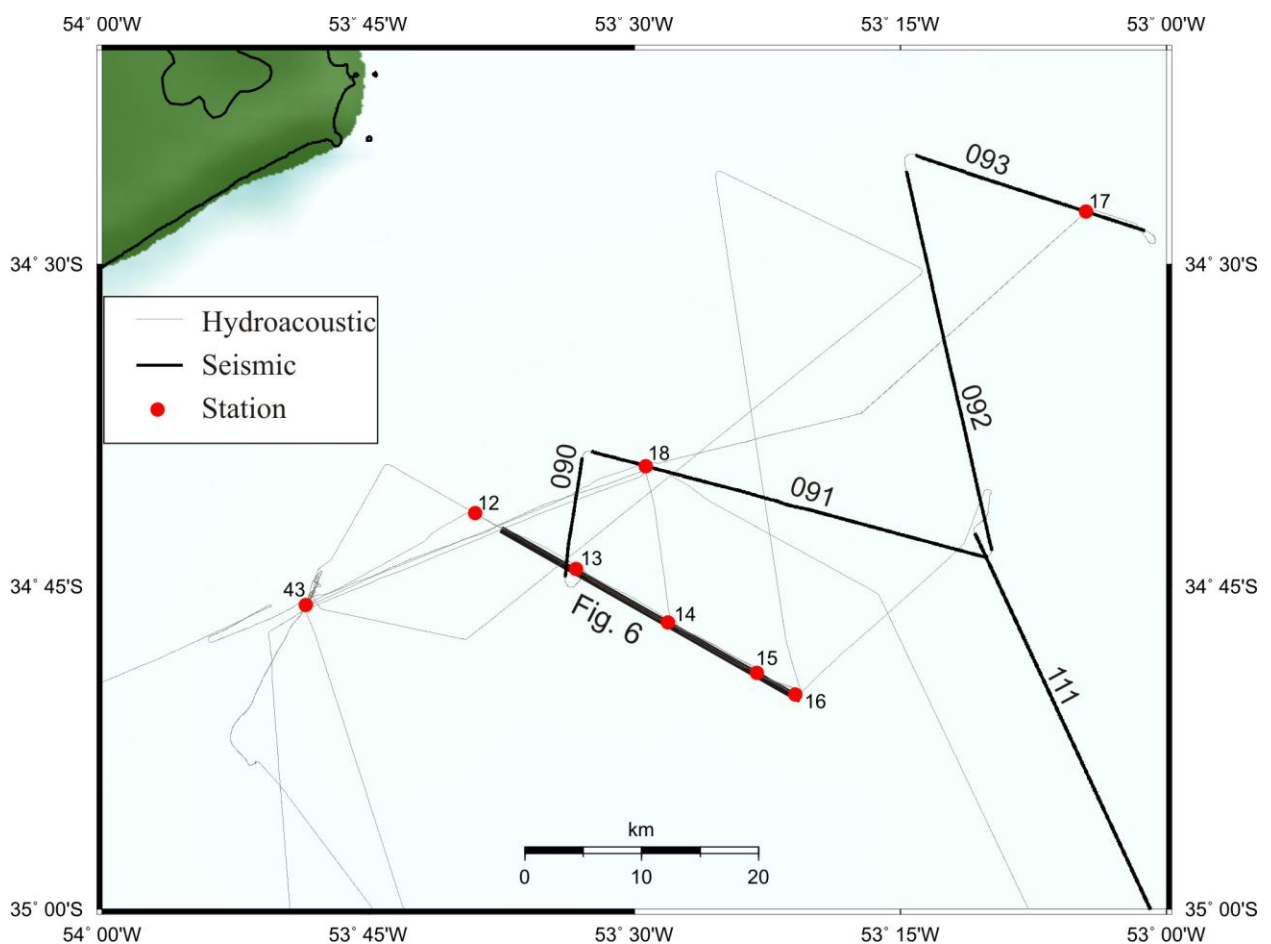


Fig. 19: Map showing locations of seismic profiles and stations of Cruise M78/3at the inner shelf off Uruguay. See Fig 15 for location of map.

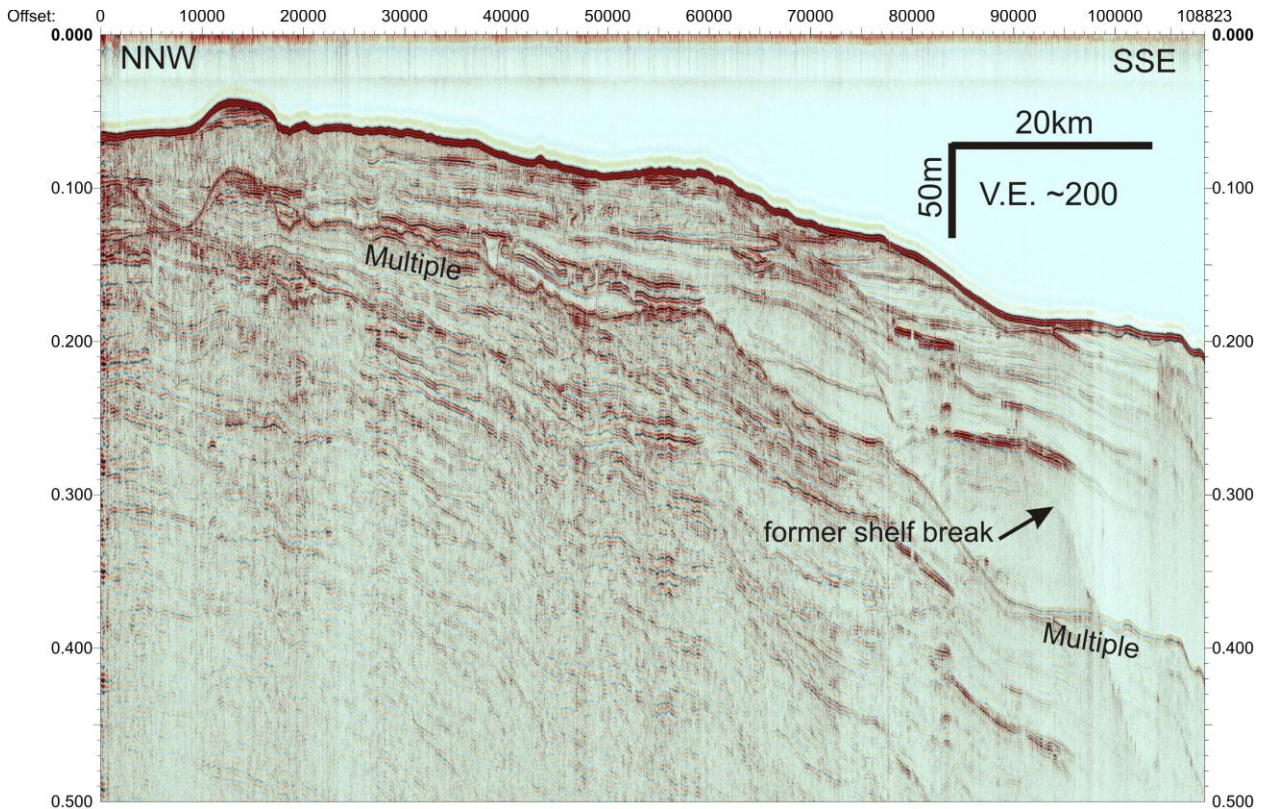


Fig. 20: Seismic Line 09-111 crossing the inner and outer shelf off Uruguay. See Fig. 15 for location of profile.

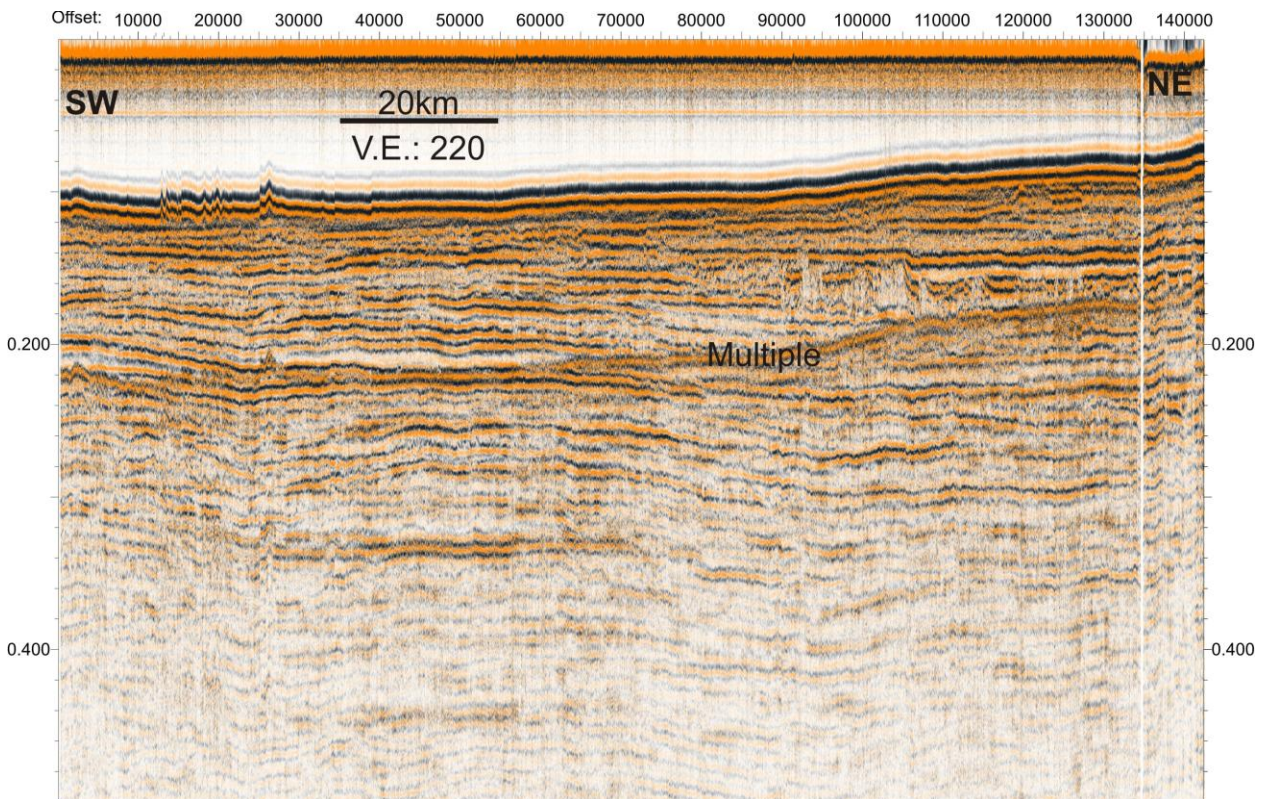


Fig 21: Seismic Profile 09-095 crossing the shelf area off the mouth of the Rio de la Plata. See Fig. 15 for location of profile.

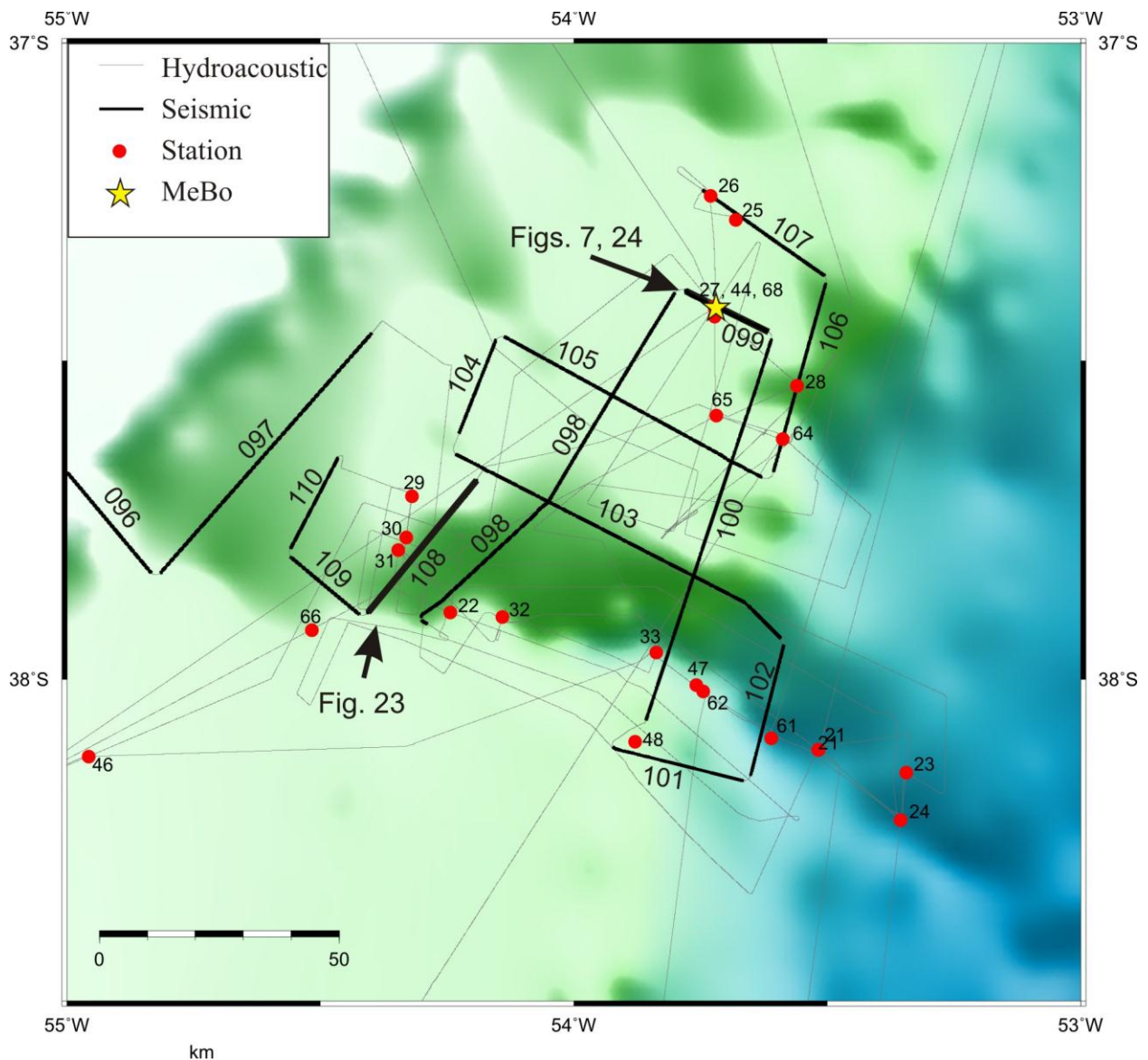


Fig. 22: Map showing locations of seismic profiles and stations of Cruise M78/3 around the Mar del Plata Canyon. See Fig 15 for location of map.

On the way to the working area off Argentina, a long seismic profile was collected on the shelf in water depth around 70m parallel to the shelf break (Fig. 21). The main objective of this profile was to identify potential filled incised valleys, which might have formed through erosion of the Rio de la Plata on an exposed shelf during periods of low sea level. In addition we wanted to investigate if the sediment load of the Rio de la Plata is directly feeding the submarine Mar del Plata Canyon during periods of low sea level. Numerous unconformities on the profile (Fig. 21) clearly document the importance of sea level fluctuations during the evolution of the shelf but no incised valley was found on the entire profile. We also investigated the area directly above the current head of the Mar del Plata Canyon between the shelf break and water depths of ~1000 m but no indication of a buried upward continuation was found. Hence the Mar del Plata canyon does have a mid slope origin and was never connected to the shelf.

The Mar del Plata Canyon and a contouritic system north of the canyon were surveyed in detail with the seismic system during Cruise M78/3a (Fig. 22). Profile 09-108 (Fig. 23) crosses the canyon in its upper part, where the incision depth is ~150 m. The canyon is located in an area

of extremely complex sedimentary structures, which are probably formed by the interaction of canyon processes and strong bottom currents. These features are not studied in detail yet. However, it is worth to mention that an area slightly NE of the present day canyons shows a transparent seismic facies, which is tentatively interpreted as a former buried canyon. Levee structures on both sides support the interpretation as former canyon. This interpretation implies that the Mar del Plata Canyon changed its course in the past. The deeper part of the seismic section images well stratified sediments suggesting a different oceanographic and sedimentary setting than today. The sediments NW of the canyon show a slightly wedge shaped pattern probably resulting from sediment redeposition due to contour currents.

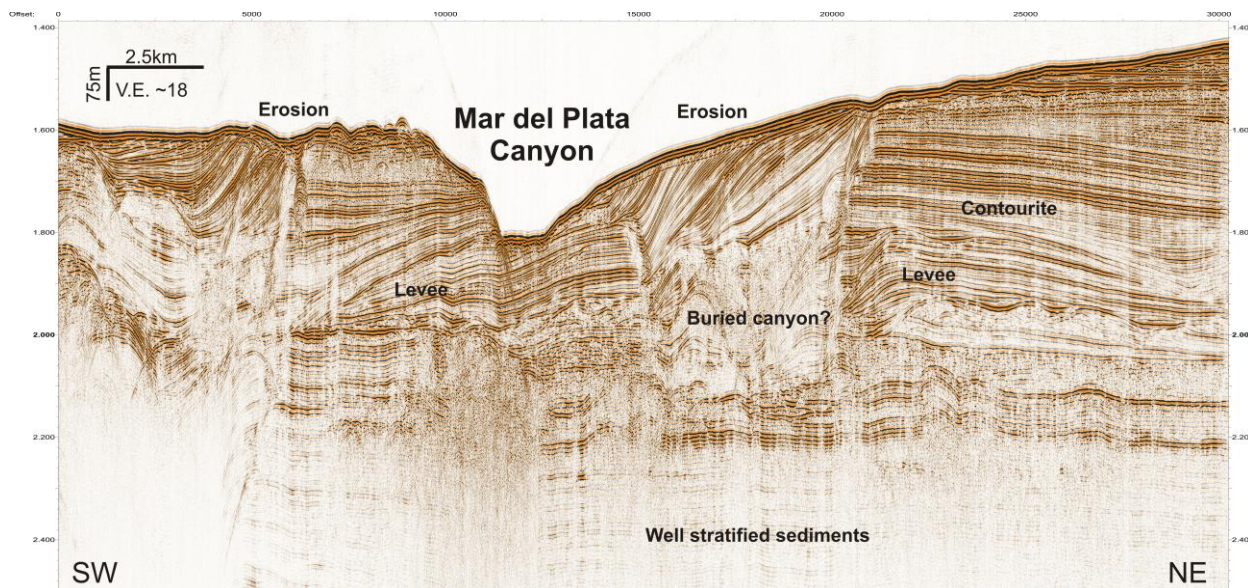


Fig 23: Migrated Profile 09-108 crossing the upper part of the Mar del Plata Canyon. See Fig. 22 for location of the profile.

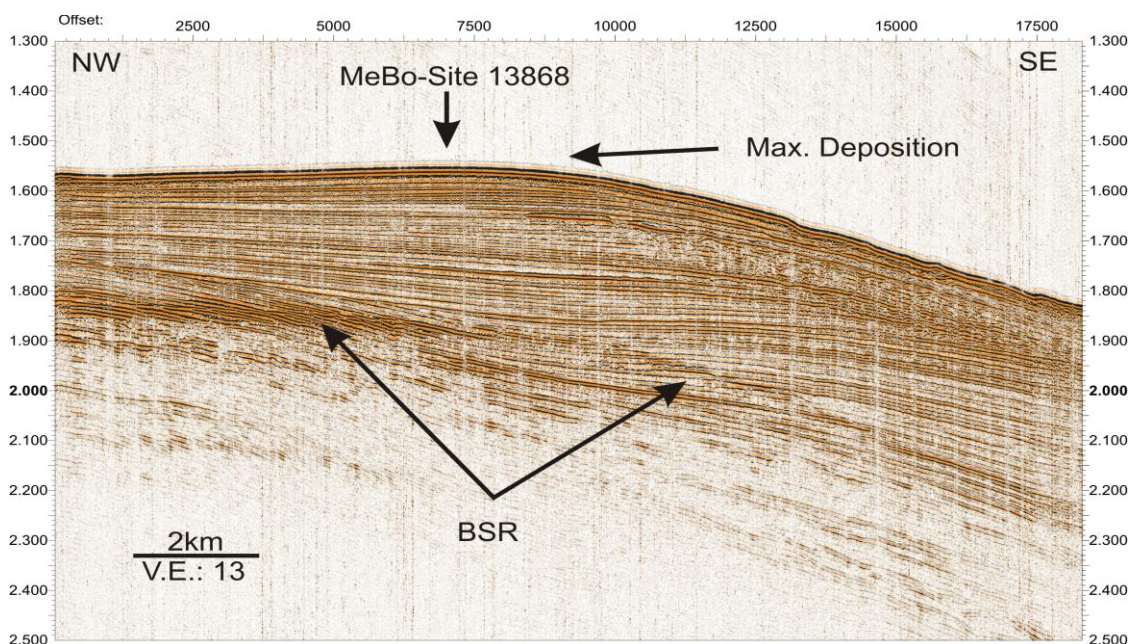


Fig. 24: Seismic Profile 09-099 crossing a contouritic system north of the Mar del Plata Canyon. See Fig. 22 for location of profile.

Contouritic patterns are clearly imaged in the entire region north of the Mar del Plata canyon. A typical example is shown on Fig. 24. Sediment accumulation rates vary significantly along the profile. The wedge shaped pattern is very typical for contouritic deposits. A location close to the area with the highest accumulation rates was chosen as one of the MeBo sites during the campaign. Drilling depth at this location was 21.50 m. Another important feature is the clear bottom simulating reflector (BSR), which is widespread in the entire survey area.

5.3. Sediment Sampling

5.3.1. Introduction

(T.J.J. Hanebuth, V. Bender, T. Freudenthal)

During cruise M78/3 different contrasting environmental settings have been targeted, although adjacently located to each other. The current-dominated coarse-grained continental shelf, locally protected mud deposits in shallow waters, the like-wise current-controlled upper to lower portions of the continental slope (canyon systems, gravity mass movement, contourites), and hemipelagic muds from the continental rise were cored during operations. Therefore, we have used a wide range of sampling tools: Multicorer (*Multilot*), Giant Box Corer (*Großkastengreifer*), and Grab Sampler (*Backengreifer*) for sampling of the uppermost seafloor sediments, as well as Gravity Corer (*Schwerelot*), Vibrocorer (*Vibrolot*), and the sea floor drill rig MeBo (Meeresboden-Bohrgerät) for deeper penetration.

In total, we have cored at 50 stations including 3 MeBo stations. We recovered ~380m sediments with gravity and vibro corer, while 132 m sediments were drilled with MeBo. In addition, prototype tests of a pressure core barrel were carried out at 5 stations. The detailed station list is given in the appendix. The individual systems and first shipboard results are summarized in the following.

5.3.2. Methods

The Multicorer (Multilot)

(T.J.J. Hanebuth, V. Bender, G. Bozzano, C. Chiessi, T. Huppertz, B. Kockisch, H. Lantzsch, S. Mill, J. Tomasini, R. Violante, D. Winkelmann)

During cruise M78/3, the Multicorer (MUC) was used to retrieve undisturbed sediments (up to 50 cm) and bottom-water samples. The samples were taken in a set of 12 60-cm long plastic tubes, divided into 8 larger (L; 10 cm in diameter) and 4 smaller (S; 6 cm in diameter) tubes. The MUC was used at 7 stations (Tab. 4). After retrieval, the overlying water, and the sediment was sampled. For lithological core description, one of these cores was cut into two halves. The following standard scheme was applied for Multicorer sampling:

Large tubes (L):

1. Cut into 1 cm slices for organic purposes
2. Cut into 1 cm slices for planktonic and benthic foraminifer studies
3. Cut into 1 cm slices for planktonic and benthic foraminifer studies
4. Cut along-core in two half pieces for detail description
5. Cut into 1 cm slices for paleontological purposes
6. Surface sampling for paleontological purposes

Small tubes (S):

1. Cut into 1 cm slices for geomagnetic investigations
2. For geochemical/RFA purposes
3. Frozen for organic purposes
4. Frozen as archive core

Table 4: List of Multicorer stations.

GeoB #	Ship's #	Date 2009	Time (UTC)	Latitude	Longitude	Water depth [m]	Recovery Remarks
13801-1	346	20.05.09	15:25	36° 08.50' S	53° 16.98' W	243,9	7xL, 3xS, 35 cm
13803-1	351	22.05.09	15:30	35° 52.67' S	52° 7.17' W	2465,6	7xL, 3xS, 21 cm
13804-2	362	24.05.09	01:19	35° 54.26' S	52° 5.43' W	2593	7xL, 2xS, 23 cm
13809-2	368	26.05.09	00:22	36° 07.67' S	52° 49.90' W	1397,8	7xL, 1xS, 36 cm
13819-4	396	31.05.09	21:40	39° 29.44' S	53° 42.56' W	4273	5xL, 2xS, 31 cm
13845-2	461	22.06.09	10:34	38° 10.42' S	55° 07.07' W	550	6xL, 4xS, 30 cm
13846-1	467	23.06.09	15:15	38° 07.21' S	54° 57.44' W	637	6xL, 4xS, 20 cm

The Giant Box Corer (Großkastengreifer)

(T.J.J. Hanebuth, G. Bozzano, C. Chiessi, T. Huppertz, B. Kockisch, H. Lantsch, S. Mill, J. Tomasini, Roberto Violante, Daniel Winkelmann)

The Giant Box Corer (GBC) was used in areas, where we expected coarse-grained surface covers. This was the case in shelf settings and on the continental slope where strong currents influence deposition. The Giant Box Corer was applied at 20 stations (Tab. 5). The over-standing water was removed after retrieval and the sediment surface was described and photographed. Then, the front wall was opened and the downcore profile was described and photographed. Finally, surface and downcore-profile samples were taken.

Tab. 5: List of Giant Box Corer stations.

GeoB #	Ship's #	Date 2009	Time (UTC)	Latitude	Longitude	Water depth [m]	Recovery Remarks
13802-1	348	20.05.09	17:23	36° 5.30' S	53° 20.72' W	142,1	4xsurface, 2xL, 28 cm
13812-2	374	27.05.09	15:52	34° 41.61' S	53° 38.97' W	32,8	empty
13812-3	375	27.05.09	16:04	34° 41.61' S	53° 38.97' W	33,3	16 cm
13813-1	376	27.05.09	17:02	34° 44.21' S	53° 33.29' W	58	3xsurface, 2xL, 40 cm
13814-1	378	27.05.09	18:09	34° 46.68' S	53° 28.11' W	40,1	3xsurface, 3xL, 32 cm
13815-1	379	27.05.09	18:58	34° 49.04' S	53° 23.08' W	47,3	3xsurface, 4xL, 40 cm
13816-3	381	27.05.09	19:55	34° 50.04' S	53° 20.92' W	44,5	1xsurface, 3xL, 41 cm
13817-3	388	28.05.09	14:01	34° 27.54' S	53° 4.51' W	62,4	3xsurface, 4xL, 49 cm
13818-1	390	28.05.09	18:05	34° 39.41' S	53° 29.36' W	40,1	1xsurface, 2xL, 17 cm
13829-2	418	07.06.09	12:11	37° 42.79' S	54° 19.19' W	950,2	3xsurface, 3xL, 27 cm
13830-1	419	07.06.09	13:49	37° 46.66' S	54° 19.83' W	1261,6	1xsurface, 2xL, 22-25cm
13831-1	420	07.06.09	15:15	37° 47.83' S	54° 20.76' W	1087,8	1xsurface, 2xL, 20 cm
13832-1	421	07.06.09	18:54	37° 54.14' S	54° 8.47' W	2229	1xsurface, 2xL, 30 cm
13833-1	423	08.06.09	01:11	37° 57.45' S	53° 50.21' W	3369,7	3xsurface, 4xL, 41 cm
13834-1	426	09.06.09	09:05	35° 3.27' S	53° 41.74' W	16,2	1xsurface, 2xL, 12-16 cm
13835-1	434	10.06.09	11:52	35° 43.10' S	53° 5.13' W	131	1xsurface, 2xL, 28 cm
13836-1	435	10.06.09	12:33	35° 44.72' S	53° 3.66' W	134,7	1xsurface, 3xL, 32 cm
13837-1	436	10.06.09	13:06	35° 46.18' S	53° 2.31' W	167,5	1xsurface, 3xL, 30 cm
13838-1	437	10.06.09	13:50	35° 48.69' S	52° 59.97' W	148,4	1xsurface, 3xL, 16 cm
13939-2	443	10.06.09	20:12	35° 30.87' S	53° 16.43' W	67,1	1xsurface, 2xL, 18 cm

Generally, the following standard scheme was applied for the Giant Box Corer sampling:

1. 1-3 surface samples
2. 2-4 large tubes (L)

The Gravity Corer (Schwerelot)

(T.J.J. Hanebuth, V. Bender, G. Bozzano, C. Chiessi, J. Collins, T. Huppertz, B. Kockisch, H. Lantzsch, S. Mill, J. Tomasini, R. Violante, G. Wefer, D. Winkelmann)

During the cruise, 57 sediment cores from 46 stations were recovered using a Gravity Corer (GC) with station-individual lengths of 6, 12, 15 m, respectively (Table. 6). The top weight was 1.5 tons. After retrieval, the core liners were cut into 1-m long sections, closed with caps and labelled according to the general GeoB scheme. Afterwards the cores were cut down-core into two halves: one containing the *Work* and the other the *Archive* material. The majority of the cores were opened onboard but due to time constraints, it was not possible to open all cores, especially during Leg M78/3b.

Tab. 6 List of gravity corer stations.

GeoB #	Ship's #	Date 2009	Time (UTC)	Latitude	Longitude	Water depth [m]	Recovery Remarks
13801-2	347	20.05.09	16:10	36° 8.49' S	53° 17.16' W	240,8	955 cm
13803-2	352	22.05.09	18:00	35° 52.65' S	52° 7.19' W	2462,8	321 cm
13804-1	353	22.05.09	20:08	35° 54.30' S	52° 5.42' W	2593,7	608 cm
13805-2	355	23.05.09	00:05	35° 53.02' S	52° 6.79' W	2522,1	196 cm
13806-1	357	23.05.09	14:52	35° 52.82' S	52° 4.61' W	2586,6	944 cm
13807-1	358	23.05.09	17:00	35° 52.29' S	52° 5.15' W	2540,2	476 cm
13808-1	359	23.05.09	18:58	35° 49.85' S	52° 7.76' W	2300,3	467 cm
13808-2	360	23.05.09	20:44	35° 49.85' S	52° 7.76' W	2295,8	-
13808-3	361	23.05.09	22:37	35° 49.85' S	52° 7.76' W	2296,2	182 cm
13809-1	365	25.05.09	19:38	36° 7.67' S	52° 49.90' W	1400,9	942 cm
13810-1	366	25.05.09	21:20	36° 6.04' S	52° 52.49' W	1149,3	124 cm, core bent
13811-1	367	25.05.09	22:39	36° 6.61' S	52° 51.56' W	1210,6	216 cm, core bent
13813-3	383	27.05.09	22:00	34° 44.22' S	53° 33.28' W	56,9	565 cm, overpenetrated
13813-4	384	27.05.09	22:44	34° 44.22' S	53° 33.27' W	57,1	1028 cm
13814-2	382	27.05.09	21:05	34° 46.68' S	53° 28.10' W	39,3	64 cm, core bent
13817-1	386	28.05.09	12:32	34° 27.54' S	53° 4.52' W	63	556 cm, overpenetrated
13817-2	387	28.05.09	13:23	34° 27.55' S	53° 4.52' W	61,9	1111 cm
13819-2	394	31.05.09	15:42	39° 29.44' S	53° 42.56' W	4274,2	792 cm
13820-1	397	01.06.09	03:12	39° 18.06' S	53° 58.03' W	3613,8	966 cm
13821-1	399	01.06.09	14:59	38° 6.58' S	53° 31.07' W	3749,6	565 cm, overpenetrated
13821-2	406	03.06.09	19:55	38° 6.57' S	53° 31.02' W	3761,8	737 cm
13822-1	401	02.06.09	16:03	37° 53.70' S	54° 14.63' W	1384	core bent
13823-1	403	03.06.09	10:06	38° 8.69' S	53° 20.65' W	3783	570 cm, overpenetrated
13823-2	404	03.06.09	12:47	38° 8.68' S	53° 20.64' W	3780	938 cm
13824-1	405	03.06.09	15:36	38° 13.14' S	53° 21.29' W	3821,7	1066 cm
13825-1	409	06.06.09	10:36	37° 16.72' S	53° 40.80' W	1230,6	573 cm, overpenetrated
13825-2	410	06.06.09	11:42	37° 16.72' S	53° 40.80' W	1233,8	749 cm
13826-1	412	06.06.09	14:33	37° 14.44' S	53° 43.83' W	1223,5	475 cm
13827-1	413	06.06.09	17:16	37° 24.92' S	53° 43.32' W	1154,8	581 cm
13827-2	414	06.06.09	18:24	37° 24.93' S	53° 43.33' W	1154,9	631 cm
13828-1	415	06.06.09	21:20	37° 32.39' S	53° 33.54' W	1730,1	494 cm
13829-1	417	07.06.09	11:10	37° 42.79' S	54° 19.19' W	949,4	empty
13832-2	422	07.06.09	20:54	37° 54.15' S	54° 8.44' W	2204,8	560 cm

Tab. 6 continued

GeoB #	Ship's #	Date 2009	Time (UTC)	Latitude	Longitude	Water depth [m]	Recovery Remarks
13833-2	424	08.06.09	03:46	37° 57.45' S	53° 50.21' W	3404,6	805 cm
13835-3	445	11.06.09	09:49	35° 43.11' S	53° 5.14' W	131	435 cm
13840-1	446	11.06.09	11:13	35° 49.21' S	52° 54.56' W	232,3	387 cm
13841-1	447	11.06.09	11:55	35° 49.53' S	52° 53.88' W	285,2	568 cm, overpenetrated
13841-2	448	11.06.09	12:45	35° 49.53' S	52° 53.87' W	285	817 cm
13842-1	449	11.06.09	15:35	35° 57.57' S	52° 36.30' W	1555,4	1002 cm
13845-3	462	22.06.09	11:37	38°10.42' S	55°07.07' W	550	Bag sample, core bent-
13845-9	465	23.06.09	12:30	38°10.42' S	55°07.08' W	550	empty
13846-2	468	23.06.09	16:16	38°07.19' S	54°57.46' W	637	520 cm
13847-1	469	23.06.09	01:18	38°00.50' S	53°45.48' W	3560	empty
13849-1	472	25.06.09	04:10	36°10.41' S	51°43.96' W	3278	1129 cm
13850-1	473	25.06.09	07:35	36°10.28' S	51°44.15' W	3267	820 cm
13851-1	477	25.06.09	17:28	35°46.00' S	52°07.20' W	2213	72 cm
13852-1	480	26.06.09	00:28	36°05.70' S	52°48.984 W	1320	560 cm
13854-1	483	26.06.09	09:46	35°45.54' S	52°07.89' W	2109	552 cm
13855-1	484	26.06.09	12:32	35°47.30' S	52°05.48' W	2277	479 cm
13856-1	486	26.06.09	17:29	36°03.94' S	51°52.25' W	3059	779 cm
13857-1	487	26.06.09	20:27	36°04.31' S	51°51.79' W	3077	802 cm
13861-1	494	28.06.09	00:51	38°05.51' S	53°36.59' W	3715	668 cm
13862-1	496	29.06.09	04:44	38°01.11' S	53°44.70' W	3588	1026 cm
13863-1	498	29.06.09	14:38	39°18.70' S	53°57.16' W	3687	856 cm
13864-1	499	02.07.09	00:25	37°37.43' S	53°35.29' W	2776	748 cm
13864-2	500	02.07.09	02:59	37°37.47' S	53°35.33' W	2757	792 cm
13865-1	501	02.07.09	05:25	37°35.19' S	53°43.10' W	1634	530 cm

Lithological core description and core photography was used to document cores. Colours have been identified following MUNSELL soil colour chart. Special efforts have been made for a detailed description of deposits resulting from gravity-driven processes. In order to gain a better understanding of the mechanism of sedimentation processes, first radiograph slabs of 25 cm length were taken from selected cores. Most cores were not sampled routinely since the internal structures suggest a radiographic analysis prior to sampling strategy. This scheme was followed generally to avoid a blind and destructive sampling of horizons that are of highest significance in terms of understanding their formation process for the associated research projects.

The Vibrocorer (Vibrolot)

(T.J.J. Hanebuth, G. Bozzano, C. Chiessi, T. Huppertz, B. Kockisch, H. Lantsch, S. Mill, J. Tomasini, R. Violante, D. Winkelmann)

A VKG-5 Vibrocorer (VC) was of essential use during this cruise to obtain sub-bottom samples from the coarse-grained shelf areas. The Vibrocorer has a maximum core length of 500 cm and a diameter of 10 cm. Deployed with a 300-m long electricity cable, which is run parallel to the wire by hand, coring in a maximum water depth of 220 m was possible during calm weather conditions.

Once a core was back on deck, the plastic liners were cut into 1 m long sections, closed with caps and labelled according the scheme generally applied to GeoB cores. After cutting the sections into *Work* and *Archive* halves, the *Archive* half was described and photographed similarly as the gravity cores. For some cores, radiographies and an initial sampling were done, as long as internal structures would not have damaged by this.

During the cruise M78/3a, 14 sediment cores from 12 stations were recovered using the Vibrocorer (Table 7).

Tab. 7: List of VibroCorer stations.

GeoB #	Ship's #	Date 2009	Time (UTC)	Latitude	Longitude	Water depth [m]	Recovery Remarks
13802-2	349	20.05.09	18:59	36° 5.30' S	53° 20.72' W	141,6	345 cm
13814-3	430	09.06.09	18:20	34° 46.68' S	53° 28.19' W	39,5	507 cm
13815-2	431	09.06.09	19:22	34° 49.05' S	53° 23.10' W	46,6	507 cm
13816-4	432	09.06.09	20:05	34° 50.06' S	53° 20.93' W	44,5	508 cm
13818-2	428	09.06.09	16:13	34° 39.41' S	53° 29.36' W	40,2	108 cm
13818-3	429	09.06.09	17:11	34° 39.41' S	53° 29.36' W	40,4	271 cm
13818-4	451	12.06.09	15:27	34° 39.41' S	53° 29.36' W	40,6	406 cm
13834-2	427	09.06.09	10:00	35° 3.29' S	53° 41.74' W	16,5	486 cm
13835-2	441	10.06.09	17:21	35° 43.10' S	53° 5.13' W	131,1	506 cm
13836-2	440	10.06.09	16:28	35° 44.72' S	53° 3.66' W	134,6	507 cm
13837-2	439	10.06.09	15:38	35° 46.18' S	53° 2.29' W	140,1	314 cm
13838-2	438	10.06.09	14:32	35° 48.69' S	52° 59.97' W	150,8	508 cm
13839-1	442	10.06.09	19:20	35° 30.87' S	53° 16.43' W	66,8	492 cm
13843-1	452	12.06.09	17:54	34° 45.88' S	53° 48.51' W	37	389 cm

The sea floor drill rig MeBo

(T. Freudenthal, M. Bergenthal, R. Düßmann, S. Klar, T. Klein, H.-O. Könnecker, J. Renken, U. Rosiak, W. Schmidt, C. Seiter)

During Meteor cruise M78/3b, the seafloor drilling rig MeBo was used for getting long sediment cores (Fig. 25). This device is a robotic drill that is deployed on the sea bed and remotely controlled from the vessel (Fig. 26). The complete MeBo-system, including drill, winch, launch and recovery system, control unit, as well as workshop and spare drill tools is shipped within six 20' containers. A steel armoured umbilical with a diameter of 32 mm is used to lower the 10-tons heavy device to the sea bed where four legs are being armed out in order to increase the stability of the rig. Copper wires and fibre optic cables within the umbilical are used for energy supply from the vessel and for communication between the MeBo and the control unit on the deck of the vessel. The maximum deployment depth in the current configuration is 2000 m.

The mast with the feeding system forms the central part of the drill rig (Fig. 26). The drill head provides the required torque and rotary speed for rock drilling and is mounted on a guide carriage that moves up and down the mast with a maximum push force of 4 tons. A water pump provides sea water for flushing the drill string for cooling of the drill bit and for removing the drill cuttings. Core barrels and rods are stored on two magazines on the drill rig. We used wire-line core barrels (HQ) and hard metal drill bit with 55 mm core diameter (push coring) and 63 mm core diameter (rotary drilling). The stroke length was 2.35 m each. With complete loading of the magazines a maximum drilling depth of 70 m can be reached. Station time can reach more than 48 hrs per deployment.

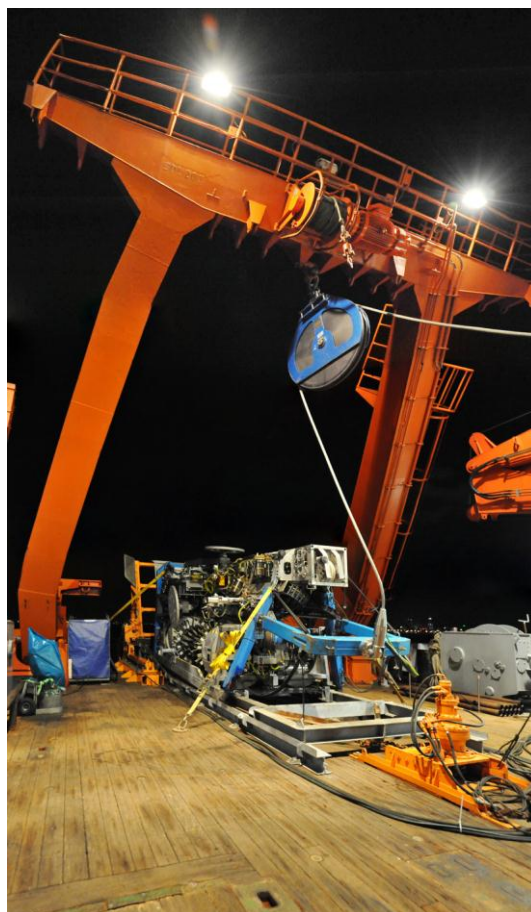


Figure 25: The sea floor drill rig MeBo during deployment (photo: T. Klein, © Marum)

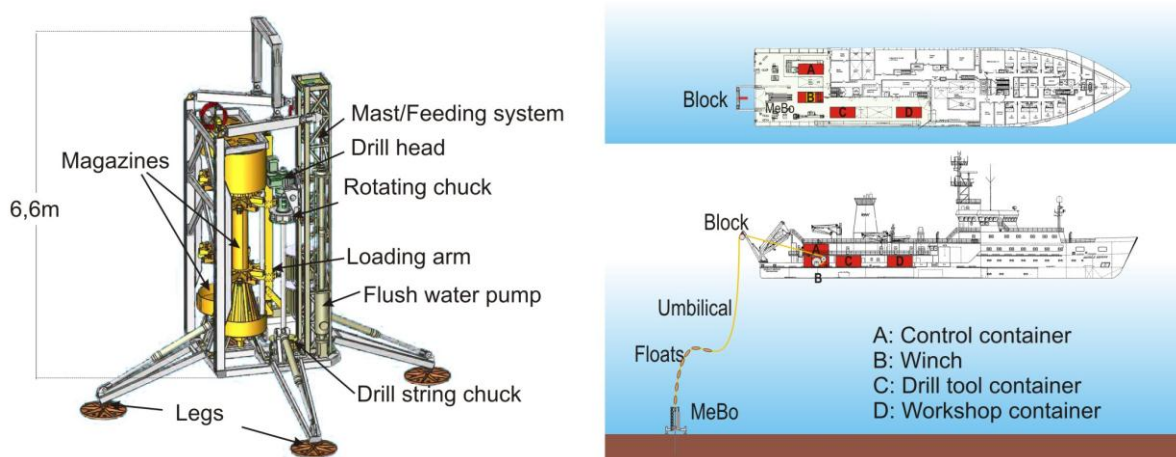


Figure 26: Schematic overview on the MeBo drill rig (left) and its deployment from a research vessel (right)

At three stations, MeBo was deployed to sample long cores from the Argentine/Uruguay continental margin between 36° and 38° S (see Figs. 1, 15 for locations). Stations GeoB13844 and GeoB13868 (same location) were drilled on a contouritic body, where seismic data indicate maximal accumulation rates (see Figs. 7, 24). The main aim was to investigate the temporal evolution of this contourite. Station GeoB13845 was drilled at a proposed IODP site of the IODP-proposal 556-Full (Brazil-Malvinas (Falkland) Confluence: Paleoceanography of a Frontal

Region, Wefer et al) off Northern Argentina. MeBo was deployed at the proposed site NAM-1A where seismic data show well stratified sediments but occasionally include massive slump deposits. The exact site location has been chosen to avoid interbedded slumps and to ensure undisturbed sediments. Station GeoB13860 (drift and scarp area off Uruguay) was drilled on a prominent aggradational cap with a very strong surface reflector. This cap is located immediately upslope of a scarp (see Fig. 5 for location). The main objective of this site is to investigate the stability of contouritic deposits.

Detailed information on deployment of MeBo and recovery of sediments is summarized in the stations list (Table 8).

Table 8: Station list for MeBo deployments.

GeoB ident	Ship ident	Date 2009	Deploy-ment start / duration (hrs:min)	Latitude (°S)	Longitu de (°W)	Water depth [m]	Drill depth (cm)	Reco-very (cm/%)	Remarks
13844-4	458	21.06.	11:55 / 8:02	37°25.07	53°43.56	1150	270	240 89%	pushed down to 2.70 m, then stopped due to techn. Problem
13845-8	464	22.06.	16:20 / 19:15	38°10.40	55°07.11	548	2150	1242 58%	Cored from 2150 to 5050
13845-11	507	02.07.	19:54 / 29:50	38°10.44	55°07.11	547	5050	2424 84%	
13860-1	492	27.06.	11:20 / 25:31	36°06.65	52°51.58	1190	3560	2918 82%	
13868-1	509	04.07.	09:18 / 11:56	37°24.87	53°43.32	1146	2150	727 34%	Same location as GeoB 13844

During MeBo drilling at Leg M78/3b cohesive hemipelagic sediments were sampled as well as sandy contourites. Altogether 132 m sediments were drilled. The average recovery rate was 66% with much better results in cohesive sediments than in sands.

The deployment time of the MeBo was severely affected by the difficult weather conditions. Due to the dimensions of the drill rig (weight: 10 tonnes, seize: comparable to a 20' shipping container) and the high requirements on station keeping during MeBo deployments only the short periods with low wind speed and low wave heights (<2m) were suitable for MeBo deployments. Fig. 27 shows that we were able to use these short time periods with suitable deployment conditions quite effectively thanks to a very precise weather forecast and the technical reliability of the drill rig.

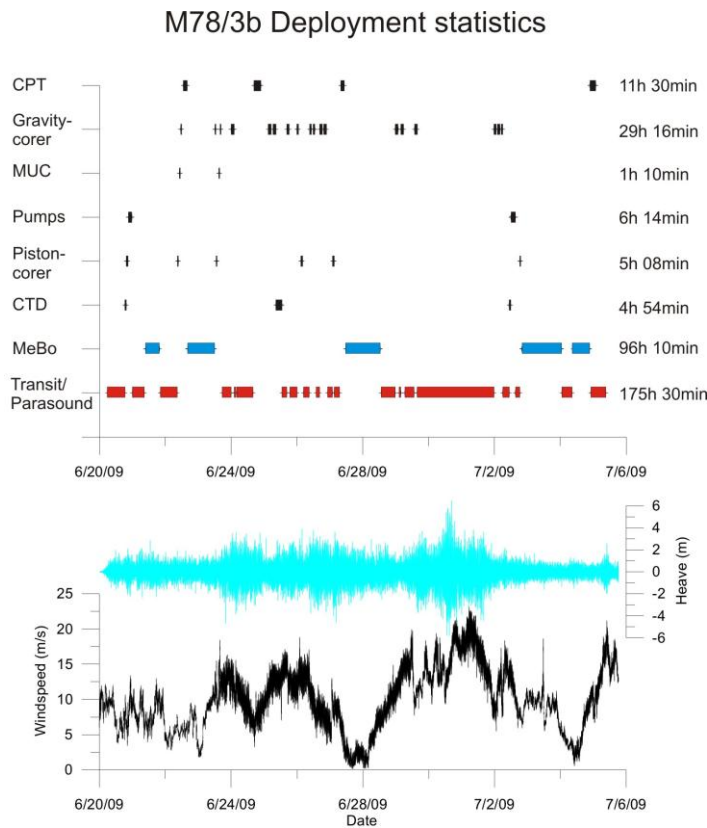


Fig. 27: Deployment times of the MeBo and other devices during research expedition M78/3b in relation to wind speed and ship's heave

Prototype tests of pressure core barrel
(H.J. Hohnberg)

Within the BMBF-Project SUGAR a pressure core barrel is developed for the use with the sea floor drill rig MeBo. This core barrel will be used like as a wire-line inner core barrel when quantitative sampling of gas within the sediments drilled with MeBo is required. The pressure core barrel will consist of (a) a cutting shoe or drill bit cutting the sediment core with the required core diameter, (b) a piston using hydrostatic pressure to force the penetration of the core into the core barrel, (c) a pressure housing and a valve that closes after the coring process in order to keep the in-situ pressure within the core barrel, (d) a core catcher that inhibit loss of sediment before the valve is closed, and (e) a latching device that ensures the correct position of the pressure core barrel within the MeBo drill string and that activates the closing of the valve when the core barrel is hooked up by wire inside the drill string.

The main goal of the prototype tests during M78/3b was the test of the patent pending piston system. This system uses a pressure gradient between the pressure enclosed in the core barrel housing and the ambient pressure in order to control the movement of a piston that forces the sediment core into the core barrel at the same time as the core barrel pushed into the sediment. The piston is locked mechanical until a touch sensor has contact with the sediment at the bottom of the drilled hole during the start of the coring process.



Figure 28: Deployment of the prototype pressure core barrel on RV Meteor

The tests were conducted with a prototype pressure core barrel that was deployed on a ship's wire like a typical gravity core (Fig. 28). This prototype consisted of the pressure housing, the cutting shoe and the core catcher, a pressure resistant inner core barrel (liner), the piston with the touch sensor and the barrel. The pressure core barrel was lowered to the sea bed with a speed of 1.2 ms^{-1} until contact at the sea floor activated the sampling. After a few seconds the pressure core barrel was lifted out of the sediment and recovered. Unfortunately a test of this prototype with the sea floor drill rig MeBo was not possible due to time constraints caused by the difficult weather conditions.

Questions that were investigated during the tests are:

- What is the influence of motion of the sea and heave down speed on the locking of the piston?
- Is the sensitivity of the touch sensor during contact with the sediment sufficient?
- How fast is the piston activated during contact with the sediment?
- How reliable are the handmade CFK breaker plates at different pressure levels and their snapping through behaviour during the activation of the piston?
- How deep is the penetration into the sediment?
- Is the Core length comparable to the penetration depth?
- Is there any obvious core disturbance due to the sampling procedure?
- How reliable is the core catcher?
- Is the stability of the different materials sufficient at different ambient pressure levels?
- What are the dynamic loads during the dynamic unlocking of the piston?

- Does the piston retaining system that shall impede a backward movement of the piston after the coring is completed, work properly?

Table 9: Station list for prototype pressure core barrel.

GeoB ident	Ship ident	Date 2009	Deployment start / duration (hrs:min)	Latitude (°S)	Longitude (°W)	Water depth [m]	Recovery (cm)	Remarks
13844-2	455	20.06.	20:16	37°24.98	53°43.29	1150	30	
13845-1	466	22.06.	03:23	38°10.42	55°07.07	555	190	
13845-10	466	23.06.	13:30	38°10.43	55°07.07	549	83	Geochemical investigation
13853-1	481	26.06.	03:33	36°07.18	52°57.51	973	190	
13858-1	489	27.06.	02:40	35°38.06	52°28.74	1102	150	Geochemical investigation
13867-1	506	02.07.	18:48	38°10.40	55°07.01	548	-	Provisoric cutting shoe

The prototype pressure core barrel was deployed six times during M78/3b (Tab. 9). The motion of the sea (wave heights up to 6-7 m) did not have an influence on the locking of the piston. The touch sensor worked perfectly. The piston is activated during contact with the sea floor on impulse. The vertical movement of the piston is very fast. With the penetration of the sediment into the core barrel all possible water channels are blocked which results in a retarding of the piston movement and a short term generation of under pressure which resulted in a collapsing of the liner in water depth of 900-1000 m. The breaker plates worked down to a water depth of 1500 m. The penetration depth and relation between core length and penetration depth cannot be evaluated yet. The core catcher with blade strength of 0.2 mm was in principle suitable for keeping the sediment inside the core barrel. However, the dynamic load during the activation of the piston caused a damage of blades in some cases. The cutting shoe was damaged during the first and the fourth deployment.

In conclusion it can be stated that the functionality of the pressure core barrel was as expected. Modifications that can improve the functionality are according to the test results:

- An attenuation of the piston speed immediately after its activation will reduce the under pressure that caused the collapsing of the liner.
- By controlling the water pathways the maximum speed of the Piston can be controlled and adjusted to the coring speed
- The position of the core catcher has to be modified in order to prevent damage by the piston
- The liner has to be strengthened in order to fulfil the requirement of a maximum deployment depth of 2000 m
- The water channel at the cutting shoe have to be positioned and dimensioned such that free water flow is ensured during unlocking of the piston
- The piston retaining system requires a slight modification

5.3.3. Sedimentology: Initial shipboard results

(T.J.J. Hanebuth, V. Bender, T. Freudenthal, G. Bozzano, C. Chiessi, V. Diekamp, T. Huppertz, B. Kockisch, H. Lantzsch, S. Mill, J. Tomasini, R. Violante, D. Winkelmann)

Descriptions of all cores opened on board are given in the appendix. In the following we summarize initial results based on coring in different areas.

The Uruguayan Inner Shelf

According to our Parasound lines (see Fig. 6), the inner Uruguayan shelf is dominated by two major features. Firstly, an elongated depression on the modern seafloor possibly represents an ancient fluvial pathway. This depression is starting to be refilled with younger sediments. Secondly, off this depression, a chain of sandy, partly carbonaceous ridges is found, which have formed earlier than the depression fill and under different conditions (calm vs. high-energy water conditions). We have taken a number of cores from both features. The cores from the depression fill show several meters of very monotonous muds suggesting that this material is supplied from the Rio de la Plata river. In addition, one core shows in its lower parts a 5 m package of sand-mud intercalations with lens and cross-bedding structures, clearly evident for a tide-dominated paleo-environment. The cores from the sandy ridge area are composed of well-sorted sands. These findings suggest, that during flooding two main processes have occurred: a) during times of a shallow water cover strong hydrodynamic conditions have led to the built-up of a coast-parallel sand barrier; and b) after drowning by rising sea level was nearly completed, the formation of a sort of mud belt started under the calm conditions of an exceptional and deep seafloor depression sheltering these fines against any current or wave action. However, this interpretation remains very speculative until first radiocarbon dates are available.

Main questions to answer in the context of the project are:

- What can we learn about the interaction between sediment availability, hydrodynamic conditions and sea level during Latest Pleistocene/Holocene times?
- How is the history of terrigenous sediment supply reflecting climatic conditions of the hinterland preserved in the mud depocenter (hopefully in highest resolution)?

The Uruguayan mid to outer shelf

The mid to outer shelf off Uruguay was target for one profile of cores (see Fig. 15 for locations of cores) to get an insight into the abundance and characteristics of sediments deposited since the last glacial sea-level lowstand. We expected only sparse depositional remains due to the intensive current regime. According to the Parasound profiles, a series of locally confined sediment bodies occurs at the outer shelf representing evidence of short-term but high accumulation depositional centres. The sediment cores are composed of a number of different sedimentary facies from massive sands to intercalated or homogenous muds. At a first glance, these facies seem to represent a stratigraphic succession which is preserved as a laterally extending mosaic. The diversity of facies, as result of different hydrodynamic regimes and different sources of material might even suggest that these deposits are younger than formerly expected.

Questions of major interest are:

- When did these deposits form? What were the driving forces of their formation?

- What was the source and what were the mechanisms for material distribution and deposition?
- What can we learn about the temporal and spatial transport pathway of sediment and about timing of sediment storage vs. sediment bypassing?

The terrace off the shelf break (Uruguay)

Just off the shelf break, a terrace-like structure is located in 200-300 m water depth. This terrace is only few km wide and about 20 km long. It hosts a pile of stratified sediments which are hoped to document two independent aspects: a) the history of sediment export from the shelf, which should over large parts be forced by the oceanography/atmospheric system, as well as b) the influence of contour-parallel currents providing lateral sediment transport. We recovered three sediment cores from this terrace. These cores show a succession of contrasting sedimentary facies, dominated by intercalations of muddy and sand horizons. These successions suggest that the spill-outs of sediments from the shelf are not only sensitively recorded on the terrace but even short-lasting high-energy events made an imprint into the deposits. It seems that this succession spans the time interval since the last glacial maximum, but radiocarbon dating is needed to confirm this suggestion. The outstanding advantage of this terrace is that the deposits directly record the shelf export. Commonly, such a documentation is not found on continental margins, because sediments delivered across the shelf break are usually transported in form of turbidity currents to much deeper waters. Furthermore, turbidity currents lead to a reorganization of the material and thereby erasing the original signals of supply dynamics dramatically.

This off-shelf archive will be used to find answers on the following questions:

- How was the shelf system organized in the past, which forces have dominated the sediment transport along the Source-to-Sink pathway?
- How did the oceanographic regime as part of the regional climatic system change through time?
- Can we identify influence and changes of the Brazil-Malvinas Confluence Zone, which is located above this area?

Slope of Uruguay

The acoustic data off Uruguay show widespread mass transport deposits and sediments deposited under strong influence of contour currents. Sampling was concentrated in the so called Drift and Scarp Area and in the Northern Slide area (see Figs 2 and 16 for location). Cores in the Drift and Scarp area were taken across a prominent morphological scarp and an aggradational sedimentary cap immediate upslope of the scarp. The aggradational cap was also target of a MeBo core (see Fig. 5 for location). The MeBo and other cores show an alternating succession between contouritic and mass transport deposits. The widespread occurrence of contourite facies demonstrates the importance of contour currents at this part of the margin.

Main target of the Northern Slide area were individual slide deposits at different water depth. A transect of cores was usually taken from undisturbed sediments above the headwalls, the slide deposits itself, and the most distal part of the slide deposits (see Fig. 4). This strategy shall allow sedimentological and geotechnical investigations of the failed and unfailed sediments as well as dating of individual slide events. Numerous cores show debrite sediments documented by internal deformation and rotational fold structures which indicate thinning, stretching, and shearing of strata in a plastic-mode as it is typical for debris flows.

The cores in this area will mainly be used to investigate the following questions:

- Why, when and where did the sediments fail?
- How stable are the sediments at present times?
- How stable are contouritic deposits

The La Plata Canyon System off Argentina

This canyon system can be divided into three parts, the head region, the canyon course, and the mouth area at the continental foot (Fig. 3). The head region is located in 1.200 m water depth. No direct shelf break connection can be identified. The attempts to receive sediment cores from this location were generally not successful because the seafloor is obviously dominated by coarse-grained materials. However, the spectacular retrieval of broken to well-rounded and surface-scratched rocks of up to ~20 cm in size may indicate that drifting icebergs have been the transport mode to get such erratic material so far to the north and so far offshore. The canyon course is partly narrow and sediments are not visible on the Parasound profiles. Nevertheless, in some places, morphological steps act as barriers for down-canyon delivered materials. Here, packages of stratified deposits are found and profoundly covered with cores. These cores document that major portions of sand enter the canyon but are not essentially transported in the form of turbidity currents. Rather, a direct import of sands from across the side walls might be a common contribution process, which would link the sandy contourite deposits on both sides of the canyon (as sources) and the canyon's depositional processes with each other (as final sink). It must thus be assumed that the canyon acts as efficient trap for laterally (contour-parallel) transported material, suggesting that these sediment cores might provide high-resolution environmental records. However, at this stage, we cannot exclude that some turbidites had their origin on the shelf. Some thin (10-cm thick) debritic beds consisting of old consolidated mud clasts in a normal hemipelagic matrix might hint on local sources such as canyon flank collapses. In the canyon's mouth area the canyon widens abruptly and a rapid deposition of canyon-passing material must be assumed. We took a number of sediment cores from the central fan area as well as from surrounding elevated levels to cover not only the activity along the main course but also get information about eventually over-spilling processes leaving an imprint on such elevated levels. These cores show a long-term normal sedimentation intercalated with series of turbidites. The exclusive occurrence of these turbidite beds in deeper sections of the cores suggests that the canyon was not active during Holocene times. The source area for these turbidites was probably the upper-slope plateau receiving materials either directly from the shelf or from contour-parallel slope currents which are, according to our observations, extremely strong in close distance to the seafloor in any water depth (shelf, upper slope, lower slope).

Major questions to solve in the future are:

- During which time intervals was the canyon system active and what controls its activity?
- Did the source of sediments change through time and how are the contourite deposits and sedimentary processes in the canyon linked with each other?
- How did the oceanographic patterns, such as depths of individual water masses, boundaries between water masses, and current strength change through time?

Mid-slope Contourites off Argentina

Off northern Argentina, thick and wide contourite bodies occur, building up a morphological terrace. These deposits seem to be intersected by the La Plata Canyon and other minor canyon

systems. The retrieved sediment cores show succession of mainly well-sorted sands with surprisingly little cohesiveness. As could be observed during core splitting these sands tend to immediate liquifaction. Such tendency to instability would easily explain a downslope creeping or failure of larger packages on the slope, probably even without the requirement of a major trigger mechanism. The sands are intercalated by units of fine-grained material. These changes seem to have occurred repeatedly in the past pointing to remarkable changes in current strength. It must therefore be assumed, that the current system has significantly slowed down in certain time intervals and switched back to long-term prevailing and stronger current intensity at the end of these intervals. Main issue must be to establish a robust age framework for these cores and slight carbonate content seems to be promising for this challenging issue.

Investigation of this material will help to understand:

- At what time are the contourite bodies accumulating and when are the contourite currents most efficient?
- Where does the material come from and how do the sorting processes along the transport way lead to changes in accumulation styles, i.e., the construction of these contourite bodies?
- What is the effect of an existing canyon on contourite deposition in terms of efficient sediment piracy, changes in sorting when the material is crossing such a cutting structure, and the effect of current transformation from contour-parallel to inside-canyon directions on sedimentation?

5.4. Physical Properties Studies

(M. Strasser, H. Müller, S. Razik, R. Andreula, C. Hilgenfeldt, M. Lange)

5.4.1. Introduction

Measurements of physical properties in marine sediments quantify and contribute to characterize variations in the sediment records, caused by environmental changes, depositional and erosional events, post-depositional diagenesis processes and other geological phenomena. They further help to correlate core lithology and seismic data. In combination with geochemical major elements and pore-water analysis, the magnetic properties of marine sediments are often used as proxy for paleoclimate and paleoceanography, to trace pollutants and to indicate provenance regions, as well as transport and reworking of sediments.

The main objectives for physical properties studies during cruise M78/3 was (i) to measure magnetic susceptibility and porosity of near-surface sediments by electromagnetic in-situ mapping and surface sampling to study input and distribution of terrigenous material from the Rio de la Plata estuary and other current-controlled sedimentation patterns, (ii) to evaluate magnetostratigraphic and diagenetic signals in sediment cores to study processes of sediment deposition and iron-oxide dissolution, and (iii) to assess a detailed geotechnical characterizations of physical properties controlling submarine slope stability conditions to study causes and consequences of submarine landslides of the Uruguayan and Argentine continental margin.

During cruise M78/3, shipboard physical property analyses were restricted to (i) measurements of the magnetic susceptibility on whole round gravity and MeBo cores, (ii) moisture content measurements on samples taken immediately after core splitting, and (iii) undrained shear strength measurements on the working half of selected cores. Further standard physical property measurements, which routinely are performed on ocean drilling legs and

expeditions (Blum, 1997), could not be performed onboard. They will be continued as post-cruise shore-based laboratory program. This includes the complementary bulk and solid-grain density and porosity measurements, gamma-ray attenuation density and compressional wave velocity measurements, as well as high resolution digital image (red, green, blue) line scans of the undisturbed archive halves. For this purpose Geotek Multi Sensor Core Logger (MSCL) will be used at MARUM, University of Bremen. Additionally, 25 whole round (WR) samples up to 20 cm length were cut from cores prior to splitting (Table 10). These WR-samples will be used as “undisturbed” samples for shore-based geotechnical laboratory experiments to assess compressibility, consolidation state, frictional behavior and permeability. Also, for post-cruise rock and paleomagnetic studies oriented cube samples were taken at 5 cm or 10 cm intervals.

During Cruise M78/3 two novel in-situ measurement devices were deployed to assess physical properties at or below the seafloor, under in situ conditions: (1) an electromagnetic sea floor profiler ‘GEM Shark’ and (2) a deep-water cone penetrometer instrument (DW-CPT). The ‘GEM Shark’ maps in high resolution subtle and gradual variations in magnetic susceptibility and electrical conductivity of near surface sediments (0-50 cm), and tracks bottom water salinity and temperature. Magnetic susceptibility is a proxy for fine-grained terrigenous clay/silt content, diagenetically forced magnetite depletion, as well as anthropogenic contaminants. Electric conductivity in first case depends on porosity, the grain-size distribution and salinity of the pore fluid. The DW-CPT measures pressure variations while profiling the sediment and assesses the sediment pore-pressure response after the impact. This provides quantitative in-situ information on in-situ effective stress conditions, permeability of the sediment and its potential to maintain excess pore-pressure with time.

5.4.2. Methods

Magnetic Volume Susceptibility (H. Müller, S. Razik, C. Hilgenfeldt)

Magnetic susceptibility was routinely measured on closed gravity core segments before splitting, beside core GeoB13801-2, that was measured on the archive half’s. Gravity core GeoB 13801-2 was measured at 5 cm spacing at high sensitivity (1×10^{-6} SI). Gravity cores GeoB 13813-4 to 13835-1 and 13846-2 to 13861-1 were measured at 2 cm spacing and high sensitivity. Gravity cores GeoB 13803-2 to 13810-1, 13841-2, 13842-1 and 13862-1 to 13865-1 were measured at 2 cm spacing with lower resolution (10×10^{-6} SI). MeBo cores GeoB 13844-4, 13845-8 and 13860-1 (segment 1 to 5) were sampled at 2 cm spacing at high sensitivity. MeBo cores GeoB 13860-1 (segment 6 to 15) and 13845-11 were measured at 2 cm spacing at the lower sensitivity. In most cases, measurements were performed directly after retrieval of the core or after maximal 12 h storage at 4°C.

The magnetic volume susceptibility κ is defined by the equation $M = \kappa \times H$ with magnetizing field H [$A\ m^{-1}$] and volume magnetization M [$A\ m^{-1}$]. Magnetic volume susceptibility κ is a dimensionless physical quantity that represents the amount to which a material is magnetized by an external magnetic field.

Table 10: List of whole round samples taken onboard for shore-based geotechnical laboratory studies

Core Number	Section	depth in cm below seafloor
-------------	---------	----------------------------

GeoB13808-1	6	447-467
GeoB13808-2	1&2	0-180
GeoB13849-1	4	249-269
	9	644-664
	14	1109-1129
GeoB13854-1	2	73-93
	4	274-294
	6	471-491
GeoB13857-1	1	90-110
	3	290-310
	6	510-530
	8	782-802
GeoB13860-1	2p1	0-20
	4p1	0-20
	5p2	100-120
	8p2	0-20
	12p1	0-20
	15r1	0-20
GeoB13862-1	3	143-163
	7	540-560
	9	839-850
GeoB13864-2	2	107-127
	4	305-325
	7	607-627

For marine sediments, the magnetic susceptibility may vary between an absolute minimum value of around -15×10^{-6} SI (diamagnetic value of pure carbonate or silicate) to a maximum of some 10000×10^{-6} SI for basaltic debris, rich in (titano-) magnetite. In most cases, κ is primarily determined by ferrimagnetic mineral content, while paramagnetic matrix components, such as clays are of minor importance. High magnetic susceptibilities indicate high terrigenous or low carbonate deposition. Low values of magnetic susceptibility can also result from post-depositional reduction of oxic iron minerals. In absence of pervasive diagenesis, magnetic susceptibility can serve for correlation of sedimentary sequences deposited under similar conditions.

For long core measurements a commercial Bartington MS2C susceptibility meter with a 135 mm diameter loop sensor is mounted on a non-magnetic aluminum frame with adjusted core liner guidance. The core segments were manually shifted to the next position using a centimeter scale, fixed to each core segment. Temperature drift of the sensor is corrected by air measurements before and after each segment and at subsequent intervals of 20 to 25 cm during the measurement process. The measured susceptibility signal represents a weighted mean over a down-core interval of about ± 8 cm (50% of the signal related to the sampling point ± 2.5 cm, 90% to ± 6.2 cm). Consequently, sharp susceptibility changes in the sediment column appear smoothed in the κ log and thin layers may not be resolved appropriately by the whole-core susceptibility measurement.

Moisture and Density (MAD) (R. Andreula, M. Strasser)

MAD parameters, including water content, bulk density, grain density, and porosity are determined from wet mass, dry mass, and dry volume measurements of ~ 10 cm³ samples taken

immediately after core-splitting according to ODP and IODP onboard laboratory practices (Blum, 1997). During cruise M78-3 only wet and dry mass were measured onboard. For each gravity and MeBo core section, at least two samples of $\sim 10 \text{ cm}^3$ were taken and placed in a 10 ml glass beaker of predefined mass (i.e. vertical spacing of samples $\sim 50 \text{ cm}$). Care was taken to sample undisturbed parts of the core and to avoid sampling of the drilling fluid in MeBo cores. The wet weight of the samples was measured, and then the samples were dried for at least 24 h in an oven at 105°C . Afterwards, the samples were cooled in a desiccator to room temperature before the dry weight was measured. Sample mass was determined to a precision of 0.01 g using the IFM-GEOMAR-seagoing balance, equipped with two electronic balances and a computer-averaging system to compensate for ship motion. The reference mass was always set within a 5 g margin of the actual sample weight. The samples then were stored and transported to MARUM, University of Bremen, where dry volume measurements will be performed using a helium-displacement penta-pycnometers in the shore-based marine geotechnology laboratory.

Shipboard moisture content has been calculated from the measured wet mass and dry mass as described by Blum (1997). The presented data have been corrected for the mass and volume of evaporated seawater assuming a seawater salinity of 35 ppt. This results in a fluid density of 1.024 g cm^{-3} assuming a salt density of 2.20 g cm^{-3} . The results are presented as moisture content expressed as fraction of the sample's dry weight.

Shear strength (R. Andreula, M. Strasser)

Shipboard undrained shear strength was measured with two independent methods: (1) vane shear tests and (2) cone penetrometer tests. Note that absolute values measured by these two methods may not be directly compared to each other because the two methods are based on different physical principles and, for the cone penetrometer test, empirical calibrations to derive the shear strength were used (Hansbo, 1957; Wood, 1982; 1985; Lu and Bryant, 1997). Also, these measurements generally underestimate the true in-situ undrained peak shear strength, because shipboard measurements by definition take place after disturbance of sediment due to coring and splitting (e.g. Lee et al., 1979). Also, they do not take into account possible anisotropy effects, as all shear strength measurements were performed in the y - z plane.

Vane shear tests in order to determine the undrained shear strength $s_{u(\text{vane-shear})}$ was measured using a Mennerich Geotechnik (Hannover) vane shear apparatus and following the procedures of Boyce (1977) and Blum (1997). For the measurements, a four-bladed vane ($l = 12.5 \text{ mm}$, $h = 6.25 \text{ mm}$, $d = 12.5 \text{ mm}$) was inserted into the split, undisturbed core surface and rotated at a constant rate of $90^\circ \text{ min}^{-1}$ until the sediment failed. The torque T , required to shear the sediment along the vertical and horizontal edges of the vane, is a relatively direct measure of the shear strength. It must be normalized to the vane constant K , which is a function of the vane size and geometry:

$K = \pi \times d^2 \times h / 2 + \pi \times (d^3 / 6)$ for fully inserted vanes.

The here-used vane shear system measures angular deflection of springs that were calibrated for torque. The peak undrained shear strength $s_{u(\text{vane-shear})\text{peak}}$ at failure then equals the maximal torque measurement during the experiment T_{max} , divided by the vane constant K :

$$s_{u(\text{vane-shear})\text{peak}} = T_{\text{max}} / K$$

With ongoing shearing of the sediment after failure the torque decreases with increasing duration t of the experiment and eventually will reach a constant value that, when normalized by

the vane constant K , is a relatively direct measure of the residual shear strength $s_{u(\text{vane-shear})\text{residual}}$ of the sediment:

$$s_{u(\text{vane-shear})\text{residual}} = T_{(t \rightarrow \infty)} / K$$

Due to time constraints during M78-3, onboard vane shear measurements of peak strength only were performed on few selected cores (marked with an asterisk (*) in Fig. 29) and on a maximal vertical resolution of ~50 cm.

Shore-based laboratory testing will include longer-lasting vane shear experiments on all relevant cores. Additionally, laboratory shear experiments (direct shear and ring shear tests) on discrete samples will be performed to reliably calibrate absolute shear strength values from shipboard measurements and to obtain residual strength and rate-dependent frictional properties, respectively.

A Wykeham-Farrance cone penetrometer WF 21600 was used for a first-order estimate of the sediment's stiffness and of the relative downcore trends in undrained shear strength. For the measurement, the metal cone was brought to a point exactly on the split core surface. A manual displacement transducer was then used to measure the distance prior and after the release of the cone (i.e. penetration after free fall of the cone). Precision is 0.1 mm of displacement. The so measured penetration depth of the falling cone (d) can then be translated into sediment strength using empirical calibration factor “cone factor” (k), derived from systematic comparison of fall-cone tests and shear strength experiments (see Hansbo, 1957; Wood, 1985, Lu and Bryant, 1997). The undrained shear strength $s_{u(\text{penetrometer})}$ is calculated as

$$s_{u(\text{penetrometer})} = k \times m \times g / d$$

where the cone factor has been set as $k = 0.85$ for the used 30° cone (Wood, 1985), m is the defined weight of the cone (80.51 g) and g is the gravitational acceleration (set constant as 9.81 m s^{-2} and ignoring variation due to ship motions).

During cruise M78-3 cone penetrometer tests have only been performed on selected cores that have been retrieved with a “submarine landslide” and “slope stability” scientific target (Fig. 29). For those cores, 7 to 10 tests have been performed on each 1 m-core-segment, resulting in a vertical resolution of ~10 to 15 cm.

5.4.3. Preliminary shipboard results

The database of onboard measured physical properties of M78/3 cores consists of magnetic volume susceptibility and water content measured on all cores, as well as undrained shear strength measured with the fall cone penetrometer and vane shear apparatus on selected cores, that have been retrieved with a “submarine landslide” and “slope stability” scientific target. The compiled results are presented in summary Fig. 29, showing mean values for each single core from variable water depths. They are described and briefly discussed in the individual results paragraph below. Individual data plots, presenting all acquired shipboard physical properties of each single core, are presented in the appendix. In this section, data of three showcase core-profiles (GeoB13807-1, GeoB13820-1 and GeoB13828-1) are presented and briefly discussed in the individual sections below.

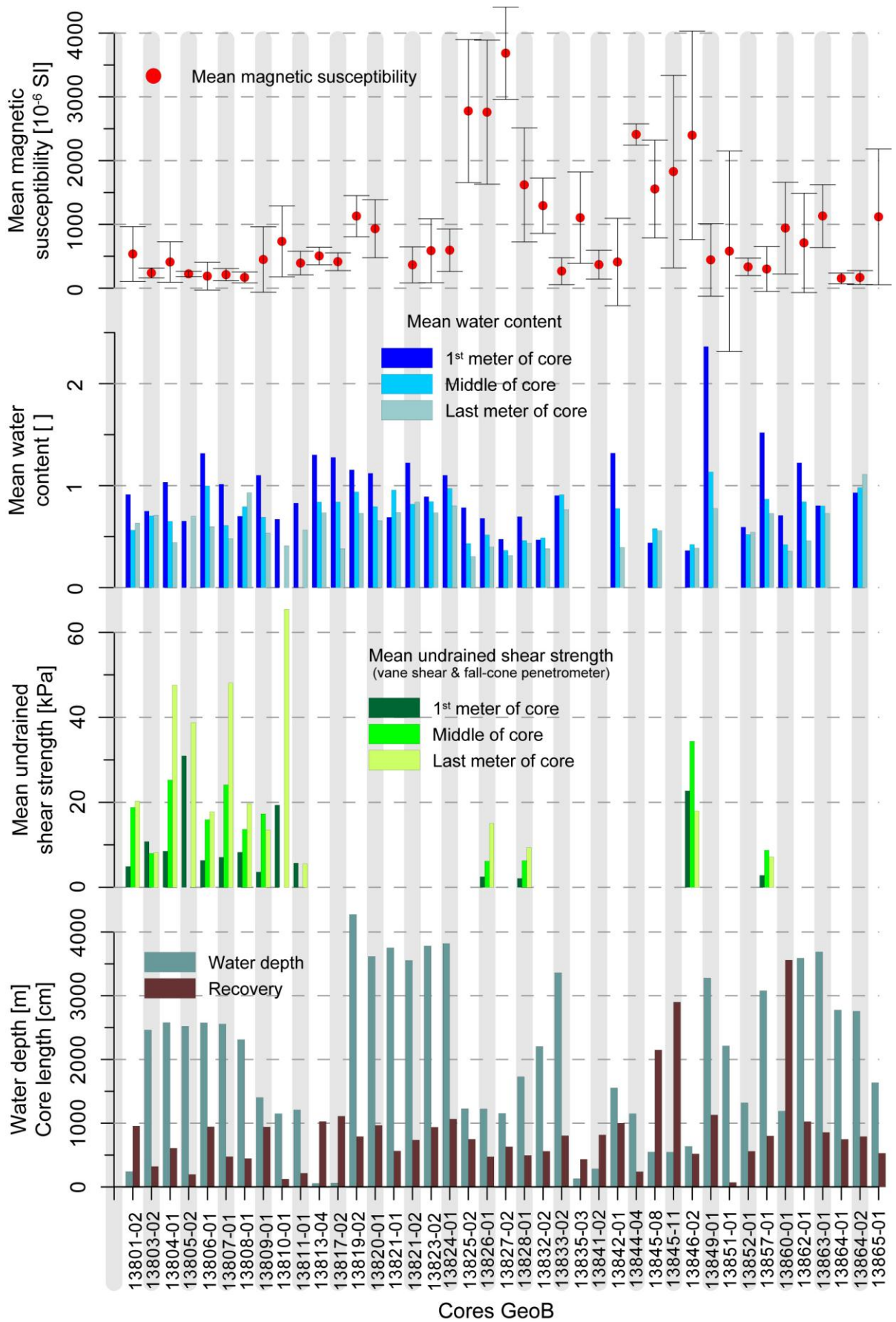


Fig. 29: Compiled results of M78-3 physical properties analysis showing mean values of magnetic volume susceptibility, water content (expressed as fraction of the sample’s dry weight), and undrained shear strength as measured on cores from variable water depths.

Magnetic Susceptibility (H. Müller, S. Razik, C. Hilgenfeldt)

Mean values of magnetic susceptibility measurements on 41 gravity and MeBo cores (upper part of Fig. 29) are in the range of $150\text{--}3700 \times 10^{-6}$ SI. The vertical error bars represent the standard deviations within each core in the range of $\pm 40\text{--}1633 \times 10^{-6}$ SI. The high variability of the magnetic susceptibility signal within each core might be controlled by local diagenetic reduction of primary iron oxides (e.g., titanium magnetite), precipitation of highly magnetic iron sulfides (e.g., greigite or pyrrhotite), carbonate enrichment, or due to stratigraphic changes in sediment provenance, lithology and grain size. For example, the susceptibility minimum between 4.8 and 6.7 m sub-bottom depth in core GeoB13820-01 (Fig. 30) correlates to the enrichment of hydrogen sulfide in the pore water related to the sulfate-methane-transition (SMT) (Garmin et al., 2005). However, variations in core GeoB13828-01 (Fig. 31) might be more dominated by material changes related to turbidite sequences and different lithological units.

From a more general perspective, highest magnetic susceptibility values ($2700\text{--}3700 \times 10^{-6}$ SI) are found in the *contourite* study area off Argentina (37.5° S, 53.7° W) in 1100-1250 m water depth. Here, the magnetic phase is supposed to be related to relatively coarse grained sediments of high specific density. Second largest mean magnetic susceptibility values are found at stations GeoB13845 and 13846 (38° S, 55° W; IODP presite survey). Cores taken within the Mar del Plata Canyon are of median susceptibility values, but are highly variable in the down-core magnetic susceptibility signal (e.g. delineating highly magnetic turbidite sequences). Sediment cores taken on the inner shelf mud-belt off Uruguay have mean susceptibility values of $400\text{--}500 \times 10^{-6}$ SI and standard deviations of $\pm 140 \times 10^{-6}$ SI, where the highest variability is related to highly magnetic lens-like structures in core GeoB13817-2 at sub-bottom depths greater than 6.5 m. The lowest mean magnetic susceptibility values were found in cores taken off Uruguay, where enhanced susceptibility values often correlate with the concentration of dissolved iron in the pore water.

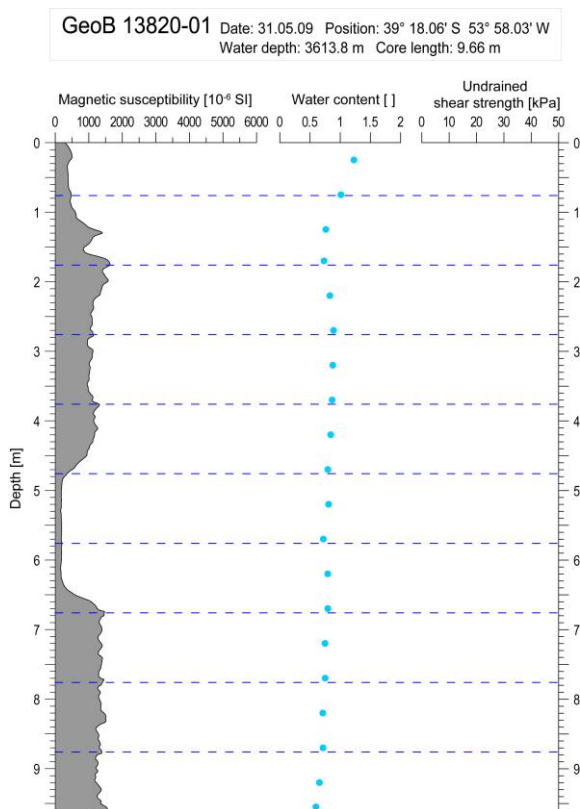


Fig. 30: GeoB13820-01 data plot showing magnetic volume susceptibility and water content (expressed as fraction of the sample's dry weight). Undrained shear strength has not been measured on this core. The core is located on the lower continental margin off Argentina (see Fig. 1 for location)

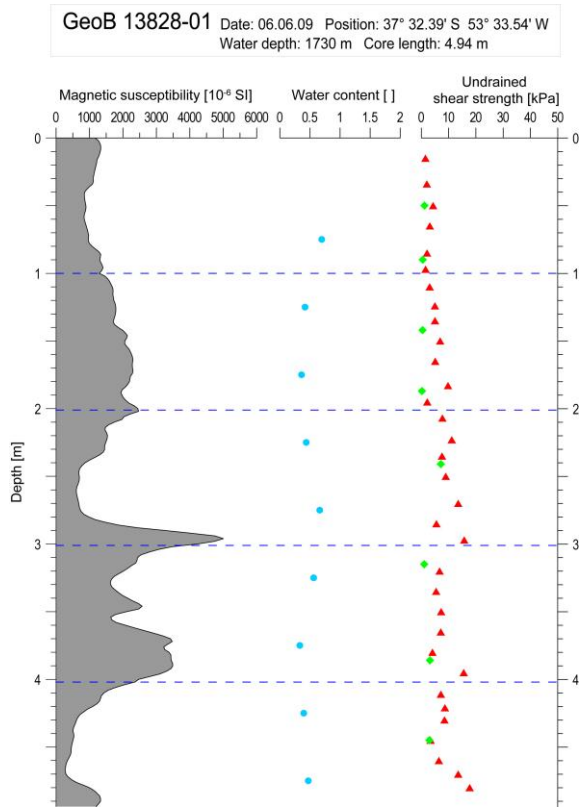


Fig. 31: GeoB13828-01 data plot showing magnetic volume susceptibility, water content (expressed as fraction of the sample’s dry weight) and undrained shear strength both derived from vane shear tests and penetrometer tests (diamonds and triangles, respectively). The core is located in the contourite working area off Argentina (see Fig. 22 for location)

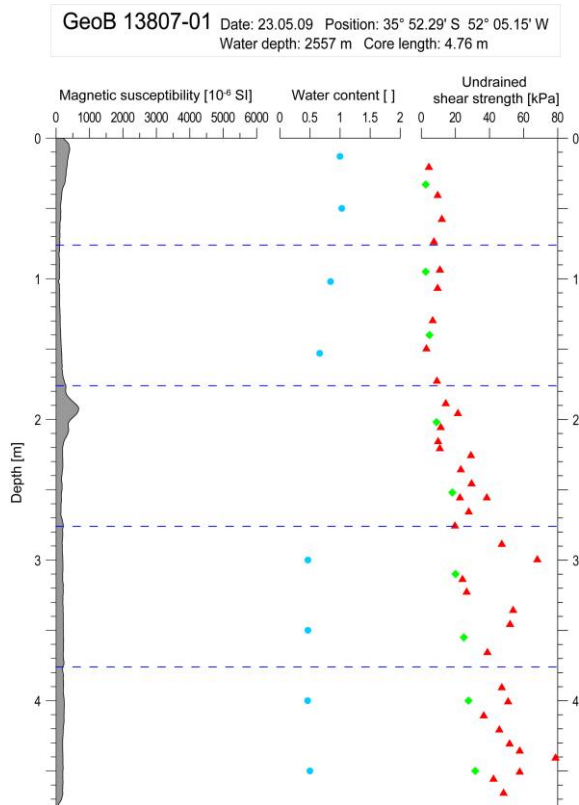


Fig. 32: GeoB13807-01 data plot showing magnetic volume susceptibility, water content (expressed as fraction of the sample’s dry weight) and undrained shear strength, both derived from vane shear tests and penetrometer tests (diamonds and triangles, respectively). The core is located in the Northern Slide area off Uruguay (see Fig. 16 for location).

Moisture content (M. Strasser, R. Andreula)

Moisture content, expressed as fraction of the sample’s dry weight, generally decrease with depth over the first few meters (Figs, 30, 31, 32), mimicking general consolidation trends down-core (i.e. pore space reduction and extrusion of pore water during sediment compaction after

deposition). Absolute values in the uppermost part of the drilled stratigraphic succession (expressed as mean values averaged over the first meter of the core) range between an upper extreme value of 2.36 (in core GeoB13849-1) and a lower extreme value of 0.36 in core GeoB13846-2 (Fig. 29). These extreme values, however, likely represent special under- and over-consolidation conditions of near-surface sediments, likely related to recently deposited mass-transport deposits (e.g. high moisture-content values in core GeoB13849-1) and recent erosion or non-deposition (low water content values in core GeoB13846-2 and also GeoB13845-8), respectively. Ignoring extreme values, water content generally range between 1.3 and 0.6 in the top meter and between 0.35 and 1.0 at the base of the cores. Minimum values have been observed in the deepest section of MeBo core GeoB13860-1 at 34 mbsf. Data from long cores generally show that the prominent decrease of moisture content with depth is restricted to the uppermost few meters and values are rather constant in the deeper stratigraphic sections (Figs, 30, 31, 32). The relatively wide scatter of moisture content and variable gradients of down-section decrease over all M78/3 cores shown in Fig. 29 likely represent the various lithologies, sedimentary regimes and erosional and/or depositional histories in areas ranging from shallow-water shelf systems, mid-slope and canyon regions, to deep-water Argentine Basin environments. The relatively low observed moisture-content values in cores from the “contourite” study area (cores GeoB13825 – GeoB13828; Figs. 29, 31) are in contrast to the visual impression, that these cores were fully water-saturated upon core opening on board. This discrepancy may possibly be explained by the loose packing compactness of sandy contourite deposits (i.e. low effective density) that got disturbed during the sampling procedure of the MAD samples and needs further post-cruise investigation.

Undrained shear strength (M. Strasser, R. Andreula)

Measured undrained shear strength values from vane shear tests range between around 2 kPa and 35 kPa. S_u values derived from cone penetrometer test range around 5 kPa in the shallow subsurface of most cores and 110 kPa in the sticky sediment recovered at the base of core GeoB13810-1. Where both vane shear and cone penetrometer data are available (e.g. core Geo13807-1; Fig. 32), there is a systematic trend that s_u derived from vane shear tests is slightly lower than s_u derived from penetrometer experiments. However, general downcore trends are nicely reproduced. In most cores, undrained shear strength values increase with depth, following up general consolidation trends down core (i.e. the sediment gains strength with compaction). Variable gradients of Δs_u with depth likely represent variable consolidation trends, over and underconsolidation stages due to the various lithologies, sedimentary regimes and erosional and/or depositional histories in areas ranging from shallow-water shelf systems, mid-slope and canyon regions, to deep water Argentine Basin environments. For example the cores from the contourite study area (e.g. core GeoB13828-1, Fig 31) only shows a very subtle increase in shear strength with depth, suggesting that these sediments may be slightly underconsolidated likely due to the high sedimentation rates in such depositional systems. Changes in s_u gradient with depth within one core and/or sudden increase of undrained shear strength with depth likely reflect different stratigraphic intervals or sediment packages. For example, the increase and higher scatter below ~2 mbsf in core GeoB13807-01 (Fig. 32) correlates with a slump deposit observed in visual core description and suggests, that the slumped material is stiffer than background sediment overlying this mass transport deposits.

Further post-cruise shore-based laboratory testing will complement penetrometer and vane shear tests on relevant cores not measured onboard and also will include laboratory shear experiments (direct shear and ring shear tests) on discrete samples to reliably calibrate absolute shear strength values from shipboard measurements and to obtain residual strength and rate-dependent frictional properties, respectively. This data base will eventually reveal the quantitative means for in-depth geotechnical interpretations of consolidation and how it relates to the strength of the sediment, as well as for slope stability calculations, testing different trigger mechanism of submarine landslides in the studied areas.

Electromagnetic sea floor profiler 'GEM Shark' (H. Müller, C. Hilgenfeldt)

The profiler was deployed in ~40 m water depth (Fig. 33; black line) on sediments of relatively high magnetic susceptibility (red line) and porosity (brown line). More sandy sediments dominate the seafloor between 2500 and 7500 m profile length. The Uruguayan mud patch is situated in a morphologic depression with sediments characterized by high susceptibility and porosity. At profile length of ~10000 m, the sled lifted off the seafloor, until further release of the tow-cable enabled bottom-contact. The NW part of the mud patch is characterized by a steep slope in bathymetry and abrupt changes in susceptibility and porosity to lower values, which is typical for sand. A collision with an unknown barrier of relict sediments caused the loss of the system in ~45 m water depth on the shelf.

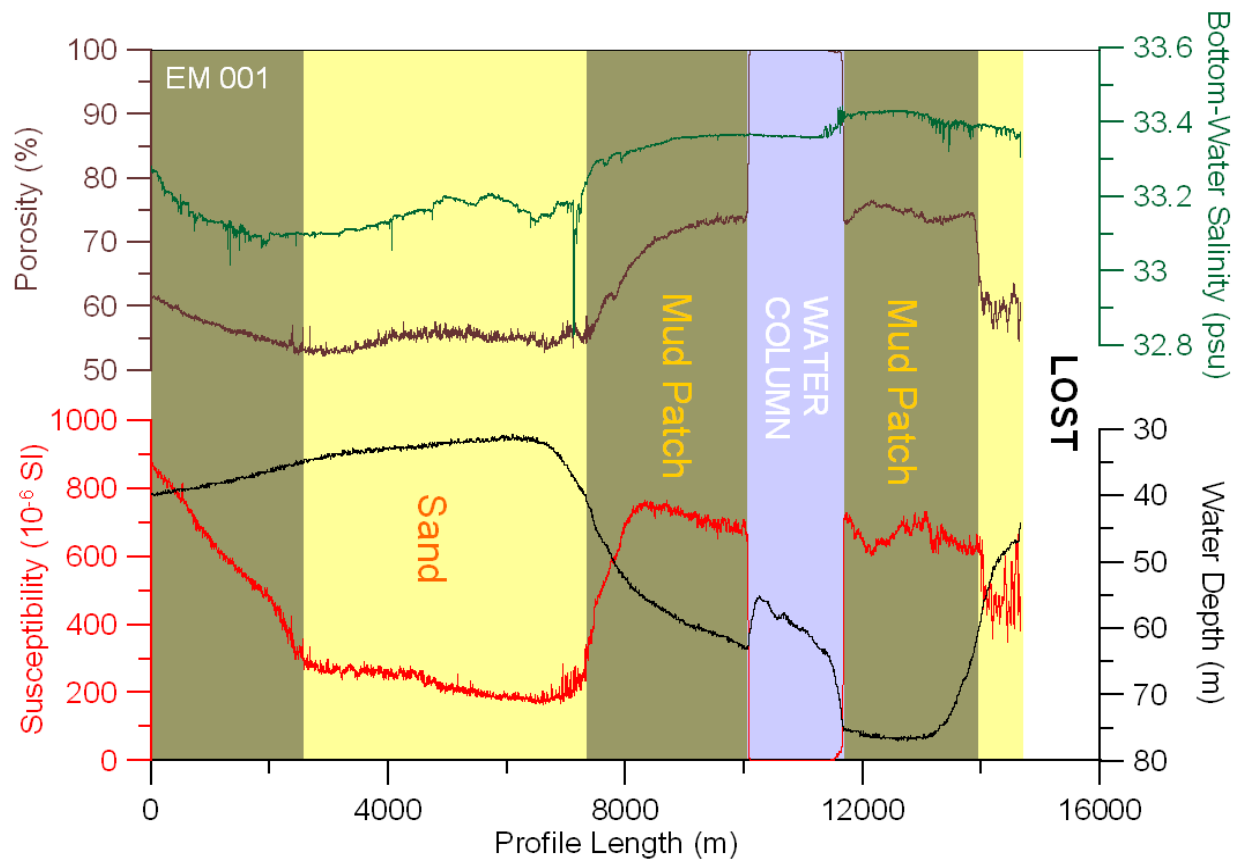


Fig. 33: GEM Shark profile, taken on the shelf off Uruguay (SE-NW profile).

CPT Testing (M. Strasser, M. Lange)

During Cruise M78/3b 10 attempts for DW-CPT tests were carried out. A first 2 h pogo-style survey with 4 deployments (GeoB13845-4, -5, -6 and -7) was carried out during the beginning of Leg M78/3b in the study area of the proposed IODP drill site and MeBo drill site GeoB13845 to test telemetry communication, probe configuration, and sensors. Data reveal that all sensors worked fine and that there was good control of probe penetration and differential pore-pressure readings. Following this initial test survey, the instrument was deployed in the “drift and scarp” study area (see Fig. 2 for location), during two pogo-style surveys at 4 sites (13848-1, -2 and 13859-1, -2) near MeBo drill site GeoB13860. In this area, DW-CPT data acquisition aimed at providing quantitative in-situ information on pore-pressure regime, permeability of the sediment and its potential to maintain excess pore-pressure with time. Such information is crucial to quantify in-situ effective stress and stability condition in order to test the hypothesis if the scarp in this area resulted from slope instability and subsequent mass-wasting processes. Unfortunately, as a result of the very stiff sediment (see also unsuccessful gravity-coring attempts (“bananas”) at sites GeoB13810 and GeoB13811) the first survey failed and the instrument was finally damaged (“CPT-banana”) during the second survey. After some onboard rescue-efforts, the instrument was deployed again twice at the site GeoB13869 at the “contourite” study area. But real-time quality control of the pressure readings showed, that the probe leaked and the penetrating water led to sensor errors.

5.5. Sediment and Pore Water Biogeochemistry

(G.L. Arnold, M.J. Formolo, S. Henkel, S. Kasten, N. Riedinger, J. Sawicka, J. Tomasini, A. Voßmeyer)

5.5.1. Objectives

The main objective of the Geochemistry Group during Cruise M78/3 was to acquire high-resolution profiles of pore water and sediment geochemistry and microbiology to investigate metal- and sulfur-based biogeochemical processes. The summarized objectives are as follows: (1) To address the reliability of iron and manganese minerals as diagnostic recorders of geochemical and biogeochemical processes in marine sediments. Complimentary to these studies will be the geochemical investigations of how iron and sulfate reduction may influence the magnetic signals. (2) To better understand the biogeochemical cycling of trace metals and their isotopic signatures as these metals are subjected to continual burial, diagenesis, and varying redox biogeochemistry. (3) To integrate organic and inorganic geochemical studies to address the potential role of dissolved organic chemicals as mediators of abiotic or biotic iron reduction in deep marine sediments. (4) To determine the spatial variability of organic matter reactivity and how it is controlled by the regional sedimentary processes. (5) To widen our knowledge about the early diagenetic redistribution of phosphorus in iron-rich sediments and the precipitation of vivianite and other authigenic phosphate minerals below the sulfate-methane transition zone. (6) To determine the dependence of hydrostatic pressure on sulfate reduction rates across a transect from the shelf to the continental rise. (7) To investigate microorganisms in different temperature regimes in marine environments and to reveal the influence of changes in bottom water currents on the subsurface biosphere.

5.5.2. Methods

To prevent warming of the sediments on board multicorer (MUC) cores were transferred into a cooling room immediately after recovery and maintained at a temperature of about 4°C. The MUC core was processed directly after recovery. Samples of the supernatant bottom water were taken and prepared for subsequent analyses. Pore water sampling was carried out using Rhizons (Seeberg-Elverfeldt et al., 2005). ^{210}Pb and porosity samples were taken from a parallel core. Gravity cores (GC) were cut into 1 m segments on deck and syringe samples were taken from every cut segment surface for methane analysis. Higher resolution sampling for methane and mineral analyses was carried out within a few hours to days after recovery. Gravity cores were cut lengthwise into two halves and processed. On the working halves pH was determined and pore water sampling using Rhizons was carried out. Solid phase samples and pore water samples were taken in intervals of 20 to 30 cm.

Alkalinity was determined on a 1 mL aliquot of sample by titration with 10, 50 or 100 mM HCl. pH measurements were performed using a Hamilton micro-electrode. The samples were titrated with a digital burette to a pH below 3.9 and both titration volume and final pH were recorded. The alkalinity was calculated using a modified equation from Grasshoff et al. (1999).

Ammonium (NH_4^+) will be analysed in the home-lab of the Alfred Wegner Institute (AWI). 1 mL sub-samples were taken and stored frozen at -20°C.

CH_4 samples were taken as 3cm³ sediment plugs and injected into 20 mL septum vials containing 10 mL of 5M NaCl solution. After closing and subsequent shaking, methane becomes enriched in the headspace of the vial. Concentration and $\delta^{13}\text{C}$ measurements will be made onshore at the Max Planck Institute for Marine Microbiology (MPI).

Dissolved inorganic carbon samples were filtered using the 0.1 - 0.2 micron Rhizons and stored at 4°C in a headspace free Zinsser vial.

Dissolved iron (Fe^{2+}) was detected photometrically (CECIL 2021 photometer) at 565nm. 1 mL of sample was added to 50 μL of Ferrospectral solution to complex the Fe^{2+} for colorimetric measurement. Samples with high concentrations of iron ($> 1\text{mg L}^{-1}$) were pretreated with 10 μL ascorbic acid and diluted with oxygen-free artificial sea-water (1:2 or 1:5) prior to complexation.

Dissolved pore-water sulfur species were collected using Rhizon samplers. Pore waters were immediately fixed using a 2.5% zinc-acetate solution to preserve the sulfate and sulfide. Aliquots of pore water were split for sulfide and sulfate measurements onboard. Sulfide concentrations ($\Sigma\text{H}_2\text{S} = \text{H}_2\text{S} + \text{HS}^- + \text{S}^{2-}$) were measured directly onboard using the methylene blue method of Cline (1969). Pore water for sulfate measurements were diluted 1:50 or 1:100 for measurement onboard using a Sykam solvent delivery system coupled to a Waters 430 Conductivity Detector. Daily standard calibrations using IAPSO were performed and duplicate and triplicate samples were measured when appropriate. When available 4 - 6 mL of pore water were also fixed with a 2.5% zinc-acetate solution for shore-based analysis of stable sulfur and oxygen isotope composition of sulfate and sulfide (MPI).

DNA samples were taken using a sterile 50cc syringe. Samples were stored in a sterile Whirlpack and frozen at -80°C.

E_H and pH were determined by punch-in electrodes (MUC cores: 1-2 cm interval, gravity cores: 25-50 cm interval).

FISH (Fluorescence in situ hybridization) samples were taken using sterile cut-off 3 cm³ syringes. Samples were incubated with 4% Para-formaldehyde at 4°C for 12-24h, washed with PBS, fixed in Ethanol-PBS and stored at -20°C.

Organic/inorganic carbon/solid-phase sulfur and phosphorus species samples were collected from gravity cores and MUC cores for the shore-based analysis, including concentration and stable isotope composition of total organic, inorganic carbon and solid-phase sulfur and phosphorus species. Samples were collected with cut-off 10 or 20 mL syringes or 15 or 50 mL centrifuge tubes. Samples were then frozen at -20°C. Samples for organic analysis were collected in combusted glass jars and stored at 4°C or under oxygen-free conditions and stored at -80°C.

Pore-water zero-valent sulfur concentrations were determined following the protocol of Kamyshny et al. (in prep). Pore-water samples were extracted in an Ar-filled glove bag using rhizones. Aliquots of pore water were partitioned and chemically fixed for polysulfides, thiosulfate, hydrogen sulfide, colloidal sulfur and elemental sulfur. Analysis and quantification using HPLC will be performed at the Center for Geomicrobiology in Århus, Denmark or at the MPI.

Phosphate (PO₄³⁻) was determined photometrically (CECIL 2021 photometer) using the Molybdenum Blue method (Grasshoff et al., 1999). To 1 mL of sample 50 µL of an ammonium molybdate solution was added and spiked with 50 µL of an ascorbic acid solution. The phosphomolybdate complex was reduced to molybdenum blue and measured photometrically at 820 nm wavelength.

Pore water cations (Al, Ba, Ca, Mg, Mn, Fe, Si, P, and S) will be analysed in our home-laboratory at the AWI with ICP-OES. Subsamples of pore water were diluted 1:10 with de-ionized water and acidified with 1% HNO₃ (diluted 65% HNO₃ s.p.).

²¹⁰Pb/amino acids/chlorins samples were collected from MUC cores at 1 cm or 2 cm intervals throughout the top 30 cm for the determination of sedimentation rates at the MPI for Marine Microbiology. These samples will also be used to measure the reactivity of organic matter in surficial sediments throughout the region. Measurements of chlorins will be performed using the method of Schubert et al. (2000) on a Hitachi F-2000 fluorometer. Amino acids will be analysed using the method of Cowie and Hedges (1992) and quantified using an HPLC.

Sulfate reduction rate experiments were performed by using the radiotracer method of Jørgensen (1978). After injection of ³⁵SO₄²⁻ sediment slurries were incubated at 4°C and under a pressure gradient from atmospheric to in situ pressure, or incubated in subcores at 2°C and atmospheric pressure. Analysis of SRR will be performed at the Center for Geomicrobiology using the single step cold chromium reduction of Kallmeyer et al. (2004).

Trace metals samples were stored frozen at -20°C. Trace metals will be extracted using a multi-acid digestion and resin and quantified using a high mass resolution multiple collector-ICPMS (Arnold et al., 2004).

5.5.3. Shipboard Results

Geochemical analyses for selected cores are provided below. These locations highlight the variable pore water geochemistry throughout the working area of Cruise M78/3.

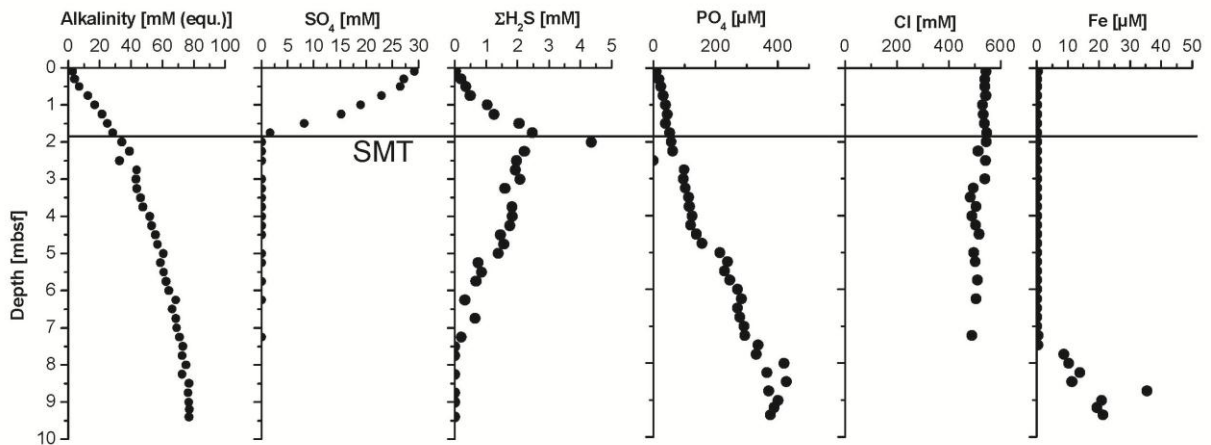
GeoB 13801-2

Figure 33: Pore water geochemistry from site GeoB 13801-2. The core is located beneath the shelf break off Uruguay (see Fig. 16 for location).

The alkalinity profile increases with depth as expected in sediments dominated by microbial respiration of organic matter. The profile gradient becomes less steep at approximately 2 m depth. This gradient change is due to the transition into the methanic zone. The sulfate profile is almost linear except for the approximately uppermost 50 cm. Based on the sulfate profile the present day sulfate-methane transition (SMT) is located at approximately 3 m. The chloride concentrations are near seawater values (approximately 546 mM) throughout the core. These consistent values suggest that there is no active hydrate formation at this location. Phosphate increases with depth in the sediments as a result of diagenetic release under anoxic conditions. The iron concentration increases in the lowermost two meters of the core indicating iron reduction processes in methane bearing sediments.

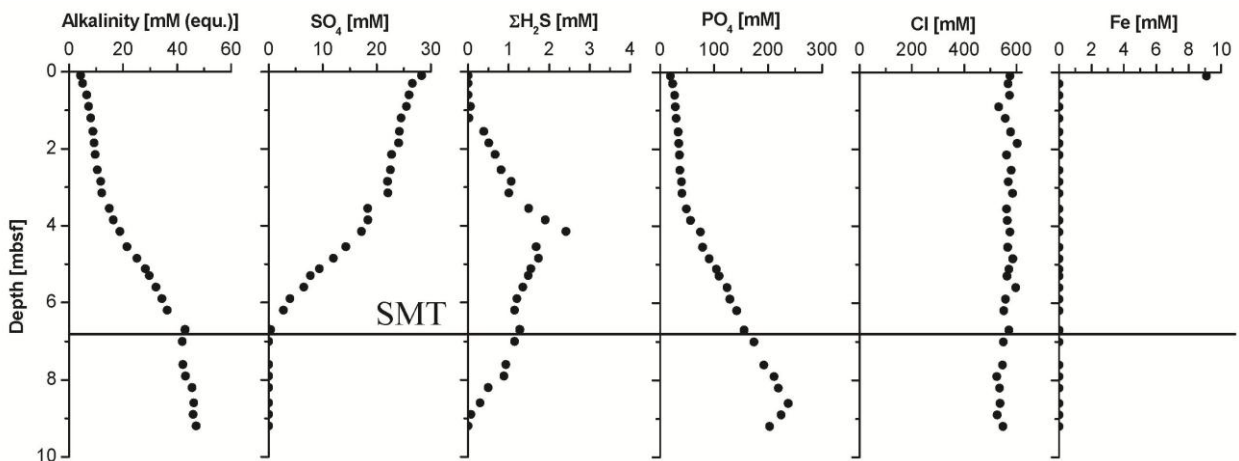
GeoB 13806-1

Figure 34: Pore water geochemistry from site GeoB 13806-1. The core is located in the Northern Slide area off Uruguay (see Fig. 16 for location).

The alkalinity profile shows a small increase in concentration in the upper about 3 m and a higher increase between 3 to 6.5 m, mirroring the shape of the sulfate profile. The profile gradient becomes more linear at approximately 6.5 m depth. This gradient change is due to the transition into the methanic zone. The sulfate profile is a kink-type profile defined by Hensen et

al. (2003). This kink profile suggests a change in the depositional conditions, likely mass movement, and reflects a transient stage as the diffusion-dominated system gradually returns to more steady-state conditions. The sulfide maximum is also decoupled from the zone of sulfate depletion. This offset is potentially due to the variable depositional conditions. Based on the alkalinity and sulfate profiles the present day sulfate-methane transition is located at approximately 6.5 m. The chloride concentrations are near seawater values (approximately 546 mM) throughout the core, similar to station GeoB 13801. Phosphate increases with depth in the sediments as a result of diagenetic release under anoxic conditions. The iron concentration is also only elevated in the shallowest sample indicative of a narrow zone of microbial iron-reduction.

GeoB 13809-1

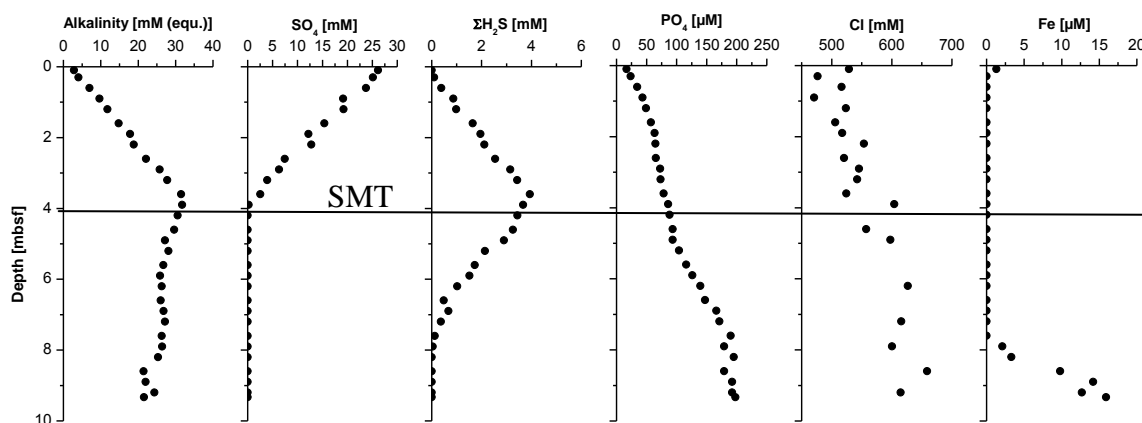


Figure 35: Pore water geochemistry from site GeoB 13809-1. The core is located in the Drift and Scarp area off Uruguay (see Fig. 5 for location).

The alkalinity profile is indicative of the continual remineralization of buried organic matter through microbial processes. The linearity of the alkalinity profile below 3.8 m reflects the transition into the methanic zone. The presence of the linear sulfate profile suggests near steady-state conditions in a diffusion-dominated sedimentary system. The maximum in sulfide corresponds accordingly to the depletion in sulfate. The similar depths in the sulfate and sulfide pore water depletions and maxima also are evidence of a stable sedimentary package that has not been recently, in the last 1000s of years, effected by mass movement. The corresponding sulfate, sulfide, and alkalinity profiles suggest a depth for the sulfate-methane transition at approximately 4 m. While dilutions in chloride are often used as evidence for clathrate formation due to an artifact of the coring procedure, the increasing chloride concentrations in these pore waters may indicate actively forming hydrates (Ussler and Paul, 2001; Haeckel et al., 2004; Torres et al., 2004). Similar enrichments in chloride were observed during ODP Leg 204 at Hydrate Ridge (Haeckel et al., 2004; Torres et al., 2004). The unique iron geochemistry in the region is exemplified in the iron pore water profile. The primary iron peak at the shallowest sediment depth is commonly observed in many marine environments. Due to the high fluxes of detrital iron in this region there is often a secondary iron peak observed at greater depths, always below the sulfidic zone (Riedinger et al., 2005). The produced sulfide cannot titrate and consume the available iron leading to this secondary peak. Phosphate profiles are indicative of reducing

sediments. As the phosphate minerals are buried and diagenetically altered in the anoxic sediments phosphate is liberated to the surrounding pore waters.

GeoB 13845-8

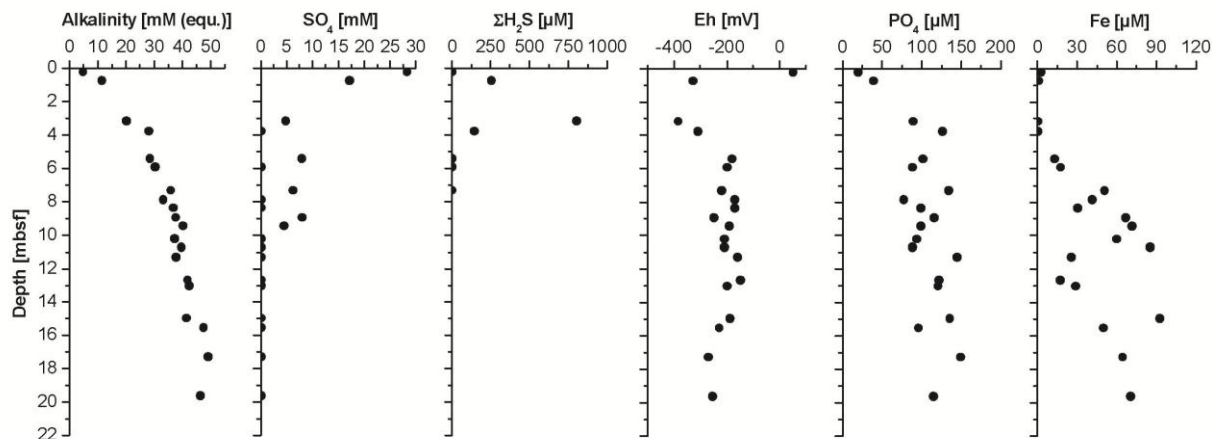


Figure 36: Pore water geochemistry from MeBo site GeoB 13845-8. The site is located at the continental margin off Argentina. See Fig. 15 for location

The alkalinity profile increases with depth and the profile gradient becomes more linear at approximately 15 m depth. The shape of the sulfate profile in the upper few meters suggests a linear decrease to about 3-4 m depth. The sulfate concentrations below this depth indicate contamination due to core retrieving. The maximum in sulfide is at approximately 3.5 m depth. The corresponding sulfate, sulfide, and alkalinity profiles suggest a depth for the sulfate-methane transition at between 3-4 m depth. The iron pore water profile shows an increase in concentration below approximately 6m depth, the scattering is probably due to sampling.

GeoB 13852-1

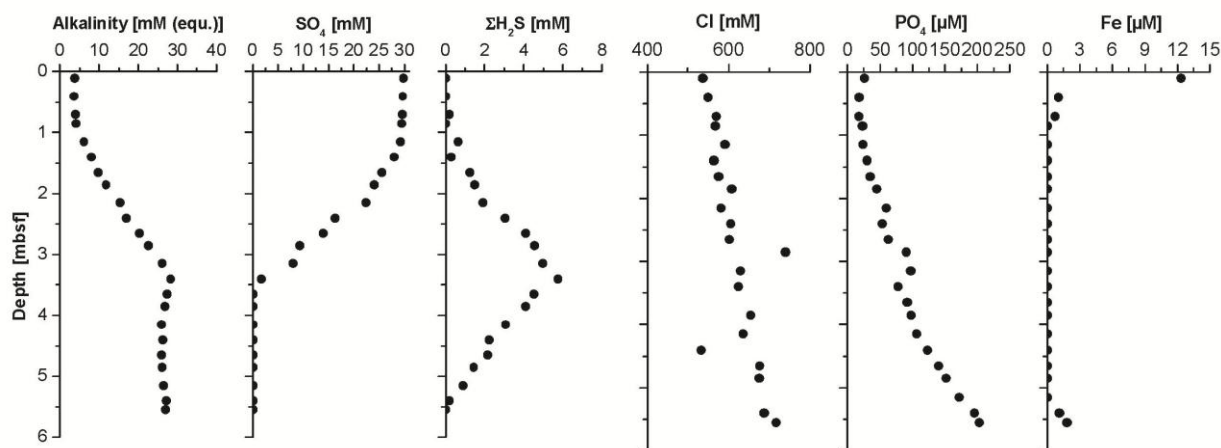


Figure 37: Pore water geochemistry from site GeoB 13852-1. The core is located in the Drift and Scarp area off Uruguay (see Fig. 16 for location).

The alkalinity concentration increases with depth till about 3.5 m depth, except for the first approximately 1 m, where the concentration profile is rather linear. The shape of the alkalinity profile of these upper meters in the sediment column mirrors the kink-profile of sulfate. The

sulfate profile indicates non-steady state conditions for the pore water constituents. The sulfide concentration has a maximum at approximately 3.5 m which corresponds with the depletion in sulfate. The described pore water profiles indicate a sulfate-methane transition zone at about 3.5 m depth. The chloride profile increases with depth, similar to station GeoB 13809, suggesting the formation of hydrates. The phosphate concentration increases with depth, where the shape of the profile is slightly concave. This suggests a release of phosphate to the pore water in the deeper sediments. Iron is depleted in the sulfidic zone. The concentration increases again in the lowermost sediments.

5.6. Water column and dinoflagellate studies

(S. Dekeyzer, K. Bogus, G. Greif, C. Fink)

5.6.1. Introduction

The investigated area has a very complex oceanography. From CTD profiling, we were able to identify some of the major water masses present. Principally, the Brazil-Malvinas Confluence (BMC) area is the region where the two surface currents converge: the southward flowing Brazil Current and the northward flowing Malvinas Current. The subtropical Brazil Current is characterized by relatively warm, saline waters while the subantarctic Malvinas Current is colder and less saline (Gordon, 1989). Simplistically speaking, Antarctic Intermediate Water (AAIW) is the major component of intermediate waters in the working area; it flows northward with the Malvinas Current and then sinks below the subtropical thermocline in the BMC (Piola and Gordon, 1989). Beneath the intermediate waters, the Antarctic deep waters and the North Atlantic Deep Water (NADW) can be distinguished in this area (Peterson, 1992; McDonagh et al, 2002).

Nannofossil assemblages are an important proxy for paleoclimatic and paleoceanographic reconstructions. Furthermore, the stable isotopic and geochemical composition of coccolithophores (and also dinoflagellates) is increasingly being used as indicators for climate and productivity changes. However, the relationship between elemental and isotopic composition of these organisms and the ambient water column is still not well understood and thus requires further investigation.

Dinoflagellates are one of the major groups of the marine phytoplankton (for an overview see e.g. Evitt, 1985; Dale, 1986). These unicellular, biflagellate organisms undergo two different stages during their life cycle: a motile vegetative-thecate stage and a resting cyst stage which can either be calcareous or organic-walled. During this cruise, our main focus was on the calcareous dinoflagellate species *Thoracosphaera heimii*. Since previous research has indicated that this species shows highest abundances around the deep chlorophyll maximum (DCM; e.g. Zonneveld, 2004), we were particularly interested in sampling at and above the DCM. For this reason, water samples from the upper water column, ranging from the surface to 200 m, and in-situ pump samples positioned at and above the DCM were taken. In addition, sediment samples from the upper 3 cm from a multicorer were taken. All samples will be analyzed as to the content of calcareous dinoflagellate cysts, and in particular *T. heimii*, in order to investigate their lateral and vertical distribution and the interaction of the species association with related environmental parameters, such as temperature, salinity and chlorophyll-*a*. This may lead to a better paleoceanographic interpretation of the fossil assemblages of dinoflagellates.

5.6.2.CTD profiling

A Seabird SBE-19 CTD profiler was deployed at 7 stations during cruise M78/3. Unfortunately, the CTD profile of station GeoB 13805-1, the first CTD station, is incomplete due to technical difficulties. The CTD profiler is equipped with sensors for conductivity, temperature, pressure and oxygen. In addition, it was used to determine the sampling depths for the dinoflagellates and thus had an additional WETLAB fluorometer attached. The fluorometer measures chlorophyll concentration and enables us to detect phytoplankton and the depth of the DCM. The CTD profiler is able to provide data during deployment via a cable connected to a PC on board. Afterwards the raw data of each downcast were converted into Excel spreadsheets with the program Seabird.

Figure 38 shows an example of a typical profile of the Brazil-Malvinas Confluence zone. Two different surface currents can be defined. The Brazil Current is subdivided by the Malvinas Current, which is characterized by lower temperatures and lower salinity. This was observed at station GeoB 13844-3 between 100-150 m and at GeoB 13866-2 between 50-100 m water depth.

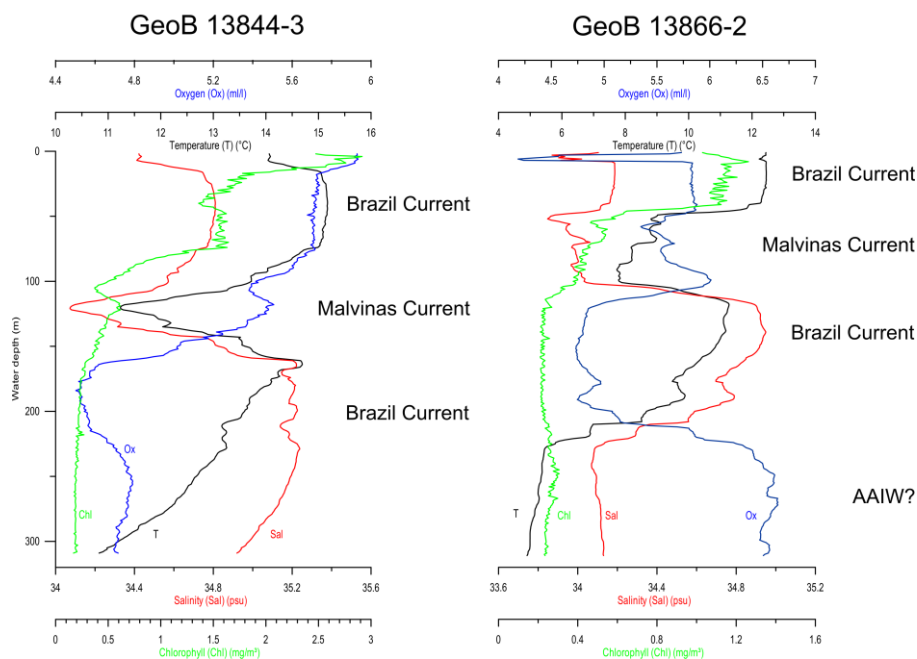


Figure 38: Typical CTD profile of the Malvinas confluence zone (stations GeoB 13844-3 and GeoB 13866-2) – AAIW = Antarctic Intermediate Water

Figure 39 gives an example of the different intermediate and deep water masses that could be identified in the western South Atlantic. At station GeoB 13850-2, 3 different water masses were well observed. Between 500 and 1250 m, a salinity minimum and oxygen maximum indicate the characteristics of AAIW. Below, the northward flowing, less oxygenated Circumpolar Deep Water (CDW) is subdivided by the thick layer of NADW into an upper and lower branch. In stations GeoB 13866-1 and GeoB 13866-2, there is the appearance of an intermediate water mass which has the characteristics of the AAIW. However, the depth at which this water mass appears is not in accordance with the AAIW. Some discussion remains for the identification of this water mass.

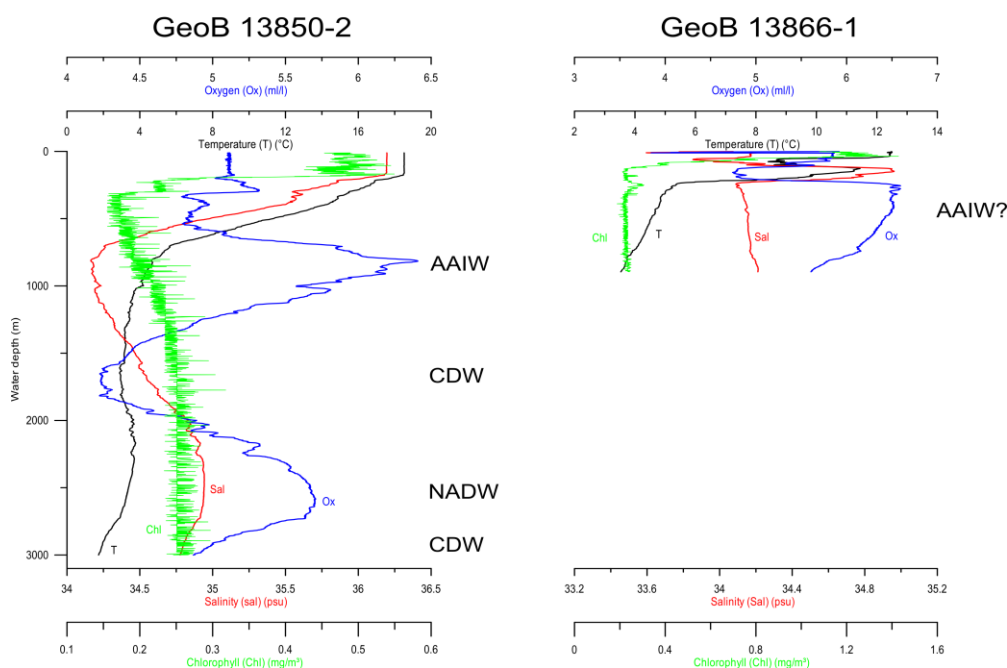


Figure 39: Typical CTD profile of the intermediate and deep water masses in the western South Atlantic (stations GeoB 13850-2 and GeoB 13866-1) – AAIW = Antarctic Intermediate Water, CDW = Circumpolar Deep Water, NADW = North Atlantic Deep Water

5.6.3. Water sampling

The CTD profiler was coupled to a rosette sampling system (HydroBios No. 436918A) equipped with 18 Niskin bottles (10 liters each). Rosette water samples were retrieved at 3 stations during cruise M78/3a and at 3 stations during cruise M78/3b (Table 11). During cruise M78/3a, the CTD-rosette system was deployed once at every station, except at station GeoB 13819, where it was deployed twice. During cruise M78/3b, the CTD-rosette system was deployed twice at every station. During the first CTD deployment at each station, parameters of the total water column were measured and water samples for geochemical purposes were taken at 18 different depths (10 liters water per depth). These samples will be used for trace element analysis at the Max Planck Institute for Marine Microbiology (MPI) in Bremen, Germany, as well as acantharian counts at the Alfred Wegener Institute for Polar and Marine Research (AWI) in Bremerhaven, Germany. Also during the first deployment, the depth of the DCM, based on the chlorophyll concentration, was determined. The second CTD deployment at each station investigated the upper 200 m of the water column. Here samples from 6 different water depths (30 liters water per depth) were taken for the analysis of stable carbon and oxygen isotopes, alkalinity, DIC, dinoflagellates and/or coccoliths.

Table 11: List of rosette water samples for dinoflagellates and geochemistry
(WD = water depth; DD = deployment depth)

GeoB Station	Date	Lat (S)	Long (W)	WD (m)	DD (m)	Samples for
M78/3a						
13805-1	24.05.2009	35° 53.02'	52° 06.78'		2300	no samples
13809-3	25.05.2009	36° 07.08'	52° 50.55'	1334	840	dinoflagellates, coccos
13819-1	31.05.2009	39° 29.44'	53° 42.56'	4275	4100	geochemistry
13819-3	31.05.2009	39° 29.28'	53° 42.49'	4275	100	dinoflagellates, coccos
13833-3	09.06.2009	37° 57.12'	53° 50.31'	3353	2700	dinoflagellates, coccos
M78/3b						
13844-1	21.06.2009	37° 25.06'	53° 43.32'	1150,2	1000	geochemistry
13844-3	21.06.2009	37° 25.06'	53° 43.32'	1150,9	200	dinoflagellates
13850-2	25.06.2009	36° 10.28'	51° 44.10'	3269,9	3000	geochemistry
13850-3	25.06.2009	36° 10.28'	51° 43.96'	3268,6	200	dinoflagellates
13866-1	02.07.2009	37° 55.38'	54° 30.97'	1013.4	900	geochemistry
13866-2	02.07.2009	37° 55.36'	54° 30.99'	1013.3	200	dinoflagellates

For stable carbon isotopes, 2 x 50 ml of water from two depths, within the DCM and 40 m above it, were filled into a brown glass bottle, carefully avoiding air bubbles to minimize the exchange of CO₂ between water and air. The stable isotope samples were always taken immediately after the rosette was brought on deck to avoid degassing of CO₂ from the water. The samples were poisoned with 0.05 ml of saturated HgCl₂ solution and then sealed with melted paraffin. The samples for stable oxygen isotope (2 x 50 ml) and DIC (1 x 50 ml) analyses were treated similarly, but were not poisoned. Immediately after sampling, these samples were sealed airtight with melted paraffin. Additionally, at each depth, 250 ml of water were taken for alkalinity measurements. Alkalinity was measured on board using a titration method with HCl; isotope and DIC analysis will be performed at the University of Bremen. The remainder of water was filtered twice through 75 µm and 20 µm sieves and then vacuum filtered through 10 µm gauze, oven dried and stored at 4°C. These samples will be examined at the University of Bremen for calcareous dinoflagellates cysts. The vertical distribution patterns of these cysts in relation to environmental characteristics of the upper water column are of interest for further research.

For the coccolith assemblage analysis, 5 liters of seawater from each depth was filtered through a glass fiber filter with 0.4 µm pore size.

5.6.4. In-situ pumps

To retrieve additional plankton samples, 2 *in-situ* pumps were attached to the CTD-rosette wire during the second CTD-rosette deployment at stations GeoB 13809-3, GeoB 13819-3 and GeoB 13833-3 during cruise M78/3a and at station GeoB 13866-2 during cruise M78/3b (Table 12). Over 2.5 hours, 300 l of seawater was pumped through an 8 µm cellulose nitrate filter at 2 different depths. The deepest *in-situ* pump was situated within the DCM and the second pump above. At stations GeoB 13819-3 and GeoB 13844-3 only 1 *in-situ* pump could be deployed.

After sampling, the filters were removed and oven dried for 24 hrs, then stored at 4°C. The samples will also be examined at the University of Bremen for regional distribution patterns of calcareous dinoflagellate cysts in and above the DCM.

Table 12 : *In-situ* pump plankton samples for dinoflagellates

GeoB Station	Date	Lat (S)	Long (W)	Water depth (m)	Deployment depth (m)
M78/3a					
13809-3	25.05.2009	36° 07.08'	52° 50.55'	1334	20 & 40
13819-3	31.05.2009	39 °29.28'	53° 42.49'	4275	15
13833-3	09.06.2009	37° 57.12'	53° 50.31'	3353	10 & 15
M78/3b					
13844-3	21.06.2009	37° 25.10'	53° 43.02'	1150,9	110
13866-2	02.07.2009	37° 55.36'	54° 30.99'	1013.3	100 & 60

5.6.5.Sediment samples

At 10 stations during cruise M78/3a and 2 stations during cruise M78/3b, sediment samples were taken from one large tube (10 cm diameter) of the multicorer and from the Giant Box Corer (Table 13). The upper 3 cm was cut into 1 cm sections and stored at 4 °C. The samples will be examined at the University of Bremen in order to describe distribution patterns of calcareous dinoflagellate cysts in surface sediments in relation to environmental characteristics.

Table 13: MUC sediment samples for dinoflagellates (WD = water depth; DD = deployment depth)

GeoB Station	Date	Lat (S)	Lon (W)	WD (m)	Device	DD (cm)
M78/3a						
13802-1	20.05.2009	35° 52.00'	52° 07.17'	142	GKG	surface sediment
13803-1	21.05.2009	35° 52.00'	52° 07.17'	142	MUC	0-1, 1-2, 2-3
13804-2	23.05.2009	35° 54.26'	52° 05.43'	2593	MUC	0-1, 1-2, 2-3
13809-2	25.05.2009	36° 07.67'	52° 49.90'	1398	MUC	0-1, 1-2, 2-3
13813-1	27.05.2009	34° 44.19'	53° 33.24'	58	GKG	surface sediment
13814-1	27.05.2009	34° 46.67'	53° 28.07'		GKG	surface sediment
13817-3	28.05.2009	34° 27.54'	53° 04.51'		GKG	surface sediment
13819-4	31.05.2009	39° 29.44'	53° 42.56'	4273	MUC	0-1, 1-2, 2-3
13829-2	07.06.2009	37° 42.79'	54° 19.19'	951	GKG	surface sediment
13833-1	08.06.2009	37° 57.46'	53° 50.21'	3408	GKG	surface sediment
M78/3b						
13845-2	22.06.2009	38° 10.42'	55° 7.07'	549,8	MUC	0-1, 1-2, 2-3
13846-1	23.06.2009	38° 7.18'	54° 57.48'	636,5	MUC	0-1, 1-2, 2-3

6. Ship's Meteorological Station

6.1. Weather conditions during Leg M78/3a (T. Truscheit)

Fair and weak northern winds predominated when R/V METEOR left the port of Montevideo in the afternoon of May 19th 2009. The synoptic situation looked as follows on these days: A high pressure system of 1025 hPa was analyzed over Uruguay. It was moving eastward very slowly. The first working area of this leg was located approximately 200 nautical miles north-east of the La Plata mouth. Weak differences of air pressure were responsible for moderate north-north-easterly winds of 5 to 6 Beaufort. However, the sea just reached 1.5 to 2 meters. Only in the morning of May 21st 2009, these ideal conditions were interrupted by heavy thunderstorms and shower with gusts of 7 Beaufort. These thunderstorms developed in the periphery of a low pressure system nearby south of Argentina and a high, which was located over the southern coast of Brazil. The Brazil current was responsible for increasing of water temperature up to 22°C. Low pressure systems moved eastward just south of 40°S and the sub tropical high eastward of Uruguay shifted only slightly; hence the conditions were stable for the next days. A water temperature, 3°C lower than air temperature and only weak winds resulted in occasional fog on May 25th in the afternoon.

Between a high pressure system west of Chile and a low south-east of the working area the differences of air pressure increased on May 26th. The cold air out of polar areas which was shifted by the low west of Chile was responsible for a decrease in air temperature to 14°C but contemporaneous for very good visibilities. The wind turned to south westerly directions but did not increase in opposite to the sea. The sea increased up to 3.5 meters in the evening of May 28th. On the following day the high was analyzed south-west of La Plata mouth and therefore the wind decreased to 2 Beaufort temporary.

Strong increasing differences of air pressure were caused by a low north of Falkland Islands and a high over Central Argentina on May 31st. The wind turned to north westerly directions, initially with 3 to 4 Beaufort but increasing up to 7 Beaufort very fast. Remarkable was a cooling of water temperature of 7°C within 15 minutes in the frontier zone of Brazil- and Falkland current.

The second working area (starting on May 31st) was located south-east of La Plata mouth. A high over Argentina and a low pressure system east of Argentina caused increasing wind speeds up to 8 Beaufort and a sea of 4 to 5 meters. The maximum wind speed (9 Beaufort) was reached on June 2nd with seas up to 6.5 meters at the same time. For a short time these uncomfortable conditions were interrupted in the morning of June 3rd by a high close to the working area of R/V METEOR. Temporary the conditions improved. The wind speed decreased as well as the sea to Beaufort 6 to 7 and 3 meters, respectively. On June 5th, however, the wind speed increased again up to Beaufort 8 to 9. This was caused by a strong cyclone, which was moving fast eastward on June 6th. It was replaced by a new sub tropical high pressure system, which developed over Argentina. It reached the working area on June 7th. High pressure prevailed for the last week of this leg in the second working area south east of La Plata mouth as well as in the third working area, which was the same as the first one. Wind speed decreased to 2 to 3 Beaufort already on June 7th temporarily to calm as well as the sea decreased to less than 1 meter. These conditions have been stable for the last week until R/V METEOR reached the port of Montevideo in the morning of June 13th 2009.

6.2. Weather conditions during Leg M78/3b

(A. Beck)

The working area of Leg M78/3b was located at the southern side of the subtropical high-pressure belt. During southern winter, dynamic low pressure zones with high wind speeds originating from the frontal zone extend to the north against the subtropical high-pressure belt resulting in quickly changing weather conditions with strong variations in wind speed as well as wave and swell height. In addition, small local deep pressure systems may develop at the mouth of the Rio de la Plata; from where they move eastward to the working area of cruise M78/3b.

This setting resulted in relatively long lasting bad weather conditions with high wind seas interrupted by short fair weather situations; hence sampling work was seriously hampered by the weather conditions. A low-pressure system with wind speeds between force 10-12 crossed the working area of RV Meteor in an easterly direction between 26.09 and 01.07.09.

19.06.2009 – 28.06.2009

RV Meteor left the port of Montevideo on June 20th at 00:30 UTC with a delay of more than two days. A subtropical high (1030 hPa) located at 35°S / 25°W dominated the working area of RV Meteor at the beginning of the cruise. Northwesterly winds of Bft 3 – 5 generated wind waves up to 1.0m height; the swell with 2.0m height was coming from SE.

Small branches of a low pressure system located south of Cape Horn moved from West to East resulting in varying wind- and wave fields until June 26th. The first half of the week was characterized by SSW- NNW winds of Bft 3 – 5 (gusts up Bft 6); wind waves reached a height of 1.0 – 1.5 m while a swell with 2.0 – 2.5 m height was observed from varying directions.

During the night of June 23rd, wind speed increased to Bft 5 – 6 with gusts up to Bft 7 -8; the significant wave height was temporarily 3.0 – 4.0 m with a swell height of 2.5 – 3.5 m from an easterly direction.

Following the development of a strong high pressure cell above Uruguay, wind speed decreased to Bft 2 – 3 with strong variations in direction. The swell remained at 3.0m mainly from a southerly direction.

29.06. – 06.07.2009

On June 28th a widespread low pressure system was located above Paraguay and northern Argentina including a prominent trough reaching to the SE. At this trough a low pressure system developed above Uruguay.

First effects of this intensifying low pressure system were already noted in the morning of June 29th. The wind significantly increased to NE 6 – 7 with gusts of Bft 8 – 9. The significant wave height quickly reached 3.0 – 4.0 m. Following a further drop in pressure down to 997 hPa, the low pressure system arrived at Montevideo at 18:00 UTC on June 29th. The low pressure system moved along the Rio de la Plata to the SW to 37°S / 49°W at 24:00 UTC on June 30th.

Based on predicted wind speeds of Bft 10 – 11 with gusts up to Bft 12, RV Meteor left the working area to the southwest. The decision to move to the south and not to the north was based on the fact, that the way back to the working area would have been much longer (24h) for the northern alternative.

On June 30th at 16:00 UTC RV Meteor moved back to the position 37°37'S / 53°35'W. During the transit the wind changed from SE 7 -8 with gusts of Bft 9 to SW 8 with gusts of Bft 9-10. Wind waves were 2.5m to 3.5m high, the swell was initially 3.0m from a SW and changed later to 5.0m from NE.

The stormy conditions continued on July 1st with strong southwesterly winds (Bft 8, gust up to Bft 9). The wind waves stayed at 3.0 – 3.5m, while the swell was still 5.0m from NE. In the following night the subtropical high pressure belt finally moved back to the south. A high pressure wedge above Brazil and Uruguay led to significantly reduced wind speeds.

Early morning of July 5th, wind direction changed to NNE and wind speed increased to Bft 6 -7 (gusts up to Bft 8). For a short time a significant wave height of 2.5 – 3.0m was observed.

RV Meteor arrived in the port of Montevideo with sheet lightning at the morning of July 6th

7. Station List M78/3

Abbreviations:

GC: Gravity Corer

MUC: Multicorer

GS: Grab Sampler

RO: Rosette water sampler

VC: Vibro-Corer

GBC: Giant Box Corer

MeBo: sea floor drill

ISP: In-situ Pumps

EPC: Experimental Piston Corer

SVP: Sound Velocity Profiler

CPT: Cone Penetration Testing

List of sampling stations during Leg M78/3a

Ship's #	GeoB #	Date	Time (UTC)	PositionLat	PositionLon	Depth [m]	Device	Recovery Remarks
346	13801-1	20.05.09	15:25	36° 8.50' S	53° 16.98' W	243	MUC-12	7xL, 3xS, 35 cm
347	13801-2	20.05.09	16:10	36° 8.49' S	53° 17.16' W	240	GC-12	955 cm
348	13802-1	20.05.09	17:23	36° 5.30' S	53° 20.72' W	142	GBC	4xsurface, 2xL, 28 cm
349	13802-2	20.05.09	18:59	36° 5.30' S	53° 20.72' W	141	VC-5	345 cm
351	13803-1	22.05.09	15:30	35° 52.67' S	52° 7.17' W	2465	MUC-12	7xL, 3xS, 21 cm
352	13803-2	22.05.09	18:00	35° 52.65' S	52° 7.19' W	2462	GC-12	321 cm
353	13804-1	22.05.09	20:08	35° 54.30' S	52° 5.42' W	2593	GC-12	608 cm
362	13804-2	24.05.09	01:19	35° 54.26' S	52° 5.43' W	2593	MUC-12	7xL, 2xS, 23 cm
354	13805-1	22.05.09	22:19	35° 53.02' S	52° 6.78' W	2523	CTD/RO	failure at 2000 m WD
355	13805-2	23.05.09	00:05	35° 53.02' S	52° 6.79' W	2522	GC-6	196 cm
357	13806-1	23.05.09	14:52	35° 52.82' S	52° 4.61' W	2586	GC-12	944 cm
358	13807-1	23.05.09	17:00	35° 52.29' S	52° 5.15' W	2540	GC-12	476 cm
359	13808-1	23.05.09	18:58	35° 49.85' S	52° 7.76' W	2300	GC-12	467 cm
360	13808-2	23.05.09	20:44	35° 49.85' S	52° 7.76' W	2295	GC-12	
361	13808-3	23.05.09	22:37	35° 49.85' S	52° 7.76' W	2296	GC-12	182 cm
365	13809-1	25.05.09	19:38	36° 7.67' S	52° 49.90' W	1400	GC-12	942 cm
368	13809-2	26.05.09	00:22	36° 7.67' S	52° 49.90' W	1397	MUC-12	7xL, 1xS, 36 cm
369	13809-3	26.05.09	02:25	36° 7.29' S	52° 50.64' W	1335	CTD/RO	100 m WD
366	13810-1	25.05.09	21:20	36° 6.04' S	52° 52.49' W	1149	GC-12	124 cm, core bent
367	13811-1	25.05.09	22:39	36° 6.61' S	52° 51.56' W	1210	GC-12	216 cm, core bent
373	13812-1	27.05.09	15:29	34° 41.61' S	53° 38.97' W	32	GS	25 cm
374	13812-2	27.05.09	15:52	34° 41.61' S	53° 38.97' W	32	GBC	empty
375	13812-3	27.05.09	16:04	34° 41.61' S	53° 38.97' W	33	GBC	16 cm
376	13813-1	27.05.09	17:02	34° 44.21' S	53° 33.29' W	58	GBC	3xsurface, 2xL, 40 cm
377	13813-2	27.05.09	17:23	34° 44.21' S	53° 33.29' W	57	SVP	
383	13813-3	27.05.09	22:00	34° 44.22' S	53° 33.28' W	56	GC-6	565 cm, overpenetrated
384	13813-4	27.05.09	22:44	34° 44.22' S	53° 33.27' W	57	GC-12	1028 cm
378	13814-1	27.05.09	18:09	34° 46.68' S	53° 28.11' W	40	GBC	3xsurface, 3xL, 32 cm
382	13814-2	27.05.09	21:05	34° 46.68' S	53° 28.10' W	39	GC-6	64 cm, core bent
430	13814-3	09.06.09	18:20	34° 46.68' S	53° 28.19' W	39	VC-5	507 cm

Ship's #	GeoB #	Date	Time (UTC)	PositionLat	PositionLon	Depth [m]	Device	Recovery Remarks
379	13815-1	27.05.09	18:58	34° 49.04' S	53° 23.08' W	47	GBC	3xsurface, 4xL, 40 cm
431	13815-2	09.06.09	19:22	34° 49.05' S	53° 23.10' W	46	VC-5	507 cm
380	13816-1	27.05.08	19:35	34° 50.04' S	53° 20.92' W	44	GS	empty
380	13816-2	27.05.09	19:38	34° 50.04' S	53° 20.92' W	44	GS	
381	13816-3	27.05.09	19:55	34° 50.04' S	53° 20.92' W	44	GBC	1xsurface, 3xL, 41 cm
432	13816-4	09.06.09	20:05	34° 50.06' S	53° 20.93' W	44	VC-5	508 cm
386	13817-1	28.05.09	12:32	34° 27.54' S	53° 4.52' W	63	GC-6	556 cm, overpenetrated
387	13817-2	28.05.09	13:23	34° 27.55' S	53° 4.52' W	61	GC-12	1111 cm
388	13817-3	28.05.09	14:01	34° 27.54' S	53° 4.51' W	62	GBC	3xsurface, 4xL, 49 cm
390	13818-1	28.05.09	18:05	34° 39.41' S	53° 29.36' W	40	GBC	1xsurface, 2xL, 17 cm
428	13818-2	09.06.09	16:13	34° 39.41' S	53° 29.36' W	40	VC-5	108 cm
429	13818-3	09.06.09	17:11	34° 39.41' S	53° 29.36' W	40	VC-5	271 cm
451	13818-4	12.06.09	15:27	34° 39.41' S	53° 29.36' W	40	VC-5	
393	13819-1	31.05.09	12:52	39° 29.45' S	53° 42.54' W	4278	CTD/RO	4100 m WD
394	13819-2	31.05.09	15:42	39° 29.44' S	53° 42.56' W	4274	GC-12	792 cm
395	13819-3	31.05.09	17:07	39° 29.28' S	53° 42.49' W	4275	CTD/RO	100 m WD
396	13819-4	31.05.09	21:40	39° 29.44' S	53° 42.56' W	4273	MUC-12	5xL, 2xS, 31 cm
397	13820-1	01.06.09	03:12	39° 18.06' S	53° 58.03' W	3613	GC-15	966 cm
399	13821-1	01.06.09	14:59	38° 6.58' S	53° 31.07' W	3749	GC-6	565 cm, overpenetrated
406	13821-2	03.06.09	19:55	38° 6.57' S	53° 31.02' W	3761	GC-12	737 cm
401	13822-1	02.06.09	16:03	37° 53.70' S	54° 14.63' W	1384	GC-6	core bent
403	13823-1	03.06.09	10:06	38° 8.69' S	53° 20.65' W	3783	GC-6	570 cm, overpenetrated
404	13823-2	03.06.09	12:47	38° 8.68' S	53° 20.64' W	3780	GC-12	938 cm
405	13824-1	03.06.09	15:36	38° 13.14' S	53° 21.29' W	3821	GC-12	1066 cm
409	13825-1	06.06.09	10:36	37° 16.72' S	53° 40.80' W	1230	GC-6	573 cm, overpenetrated
410	13825-2	06.06.09	11:42	37° 16.72' S	53° 40.80' W	1233	GC-12	749 cm
412	13826-1	06.06.09	14:33	37° 14.44' S	53° 43.83' W	1223	GC-6	475 cm
413	13827-1	06.06.09	17:16	37° 24.92' S	53° 43.32' W	1154	GC-12	581 cm
414	13827-2	06.06.09	18:24	37° 24.93' S	53° 43.33' W	1154	GC-12	631 cm
415	13828-1	06.06.09	21:20	37° 32.39' S	53° 33.54' W	1730	GC-12	494 cm
417	13829-1	07.06.09	11:10	37° 42.79' S	54° 19.19' W	949	GC-6	empty
418	13829-2	07.06.09	12:11	37° 42.79' S	54° 19.19' W	950	GBC	3xsurface, 3xL, 27 cm
419	13830-1	07.06.09	13:49	37° 46.66' S	54° 19.83' W	1261	GBC	1xsurface, 2xL, 22-25cm
420	13831-1	07.06.09	15:15	37° 47.83' S	54° 20.76' W	1087	GBC	1xsurface, 2xL, 20 cm
421	13832-1	07.06.09	18:54	37° 54.14' S	54° 8.47' W	2229	GBC	1xsurface, 2xL, 30 cm
422	13832-2	07.06.09	20:54	37° 54.15' S	54° 8.44' W	2204	GC-6	560 cm
423	13833-1	08.06.09	01:11	37° 57.45' S	53° 50.21' W	3369	GBC	3xsurface, 4xL, 41 cm
424	13833-2	08.06.09	03:46	37° 57.45' S	53° 50.21' W	3404	GC-12	805 cm
425	13833-3	08.06.09	06:34	37° 57.10' S	53° 50.17' W	3358	CTD/RO	75m WD
426	13834-1	09.06.09	09:05	35° 3.27' S	53° 41.74' W	16	GBC	1xsurface, 2xL, 12-16 cm
427	13834-2	09.06.09	10:00	35° 3.29' S	53° 41.74' W	16	VC-5	486 cm
434	13835-1	10.06.09	11:52	35° 43.10' S	53° 5.13' W	131	GBC	1xsurface, 2xL, 28 cm
441	13835-2	10.06.09	17:21	35° 43.10' S	53° 5.13' W	131	VC-5	506 cm
445	13835-3	11.06.09	09:49	35° 43.11' S	53° 5.14' W	131	GC-12	435 cm
435	13836-1	10.06.09	12:33	35° 44.72' S	53° 3.66' W	134	GBC	1xsurface, 3xL, 32 cm
440	13836-2	10.06.09	16:28	35° 44.72' S	53° 3.66' W	134	VC-5	507 cm

Ship's #	GeoB #	Date	Time (UTC)	PositionLat	PositionLon	Depth [m]	Device	Recovery Remarks
436	13837-1	10.06.09	13:06	35° 46.18' S	53° 2.31' W	167	GBC	1xsurface, 3xL, 30 cm
439	13837-2	10.06.09	15:38	35° 46.18' S	53° 2.29' W	140	VC-5	314 cm
437	13838-1	10.06.09	13:50	35° 48.69' S	52° 59.97' W	148	GBC	1xsurface, 3xL, 16 cm
438	13838-2	10.06.09	14:32	35° 48.69' S	52° 59.97' W	150	VC-5	508 cm
442	13839-1	10.06.09	19:20	35° 30.87' S	53° 16.43' W	66	VC-5	492 cm
443	13939-2	10.06.09	20:12	35° 30.87' S	53° 16.43' W	67	GKC	1xsurface, 2xL, 18 cm
446	13840-1	11.06.09	11:13	35° 49.21' S	52° 54.56' W	232	GC-6	387 cm
447	13841-1	11.06.09	11:55	35° 49.53' S	52° 53.88' W	285	GC-6	568 cm, overpenetrated
448	13841-2	11.06.09	12:45	35° 49.53' S	52° 53.87' W	285	GC-12	817 cm
449	13842-1	11.06.09	15:35	35° 57.57' S	52° 36.30' W	1555	GC-12	1002 cm
452	13843-1	12.06.09	17:54	34° 45.88' S	53° 48.51' W	37	VC-5	389 cm

List of sampling stations during Leg M78/3b

Ship's #	GeoB #	Date	Time (UTC)	PositionLat	PositionLon	Depth [m]	Device	Recovery Remarks
454	13844-1	20.06.09	18:36	37°25.06' S	53°43.32' W	1150	CTD/RO	
455	13844-2	20.06.09	20:16	37°24.98' S	53°43.29' W	1150	EPC	30
455	13844-3	20.06.09	20:58	37°24.97' S	53°43.18' W	1151	CTD-ISP	
458	13844-4	21.06.09	09:30	37°25.07' S	53°43.56' W	1150	MeBo	240
459	13845-1	22.06.09	03:23	38°10.42' S	55°07.07' W	555	EPC	190
461	13845-2	22.06.09	10:34	38°10.42' S	55°07.07' W	550	MUC	6xL, 4xS, 30
462	13845-3	22.06.09	11:37	38°10.42' S	55°07.07' W	550	GC-12	Bag sample, core bent
463_1	13845-4	22.06.09	13:30	38°10.42' S	55°07.07' W	550	CPT	
463_2	13845-5	22.06.09	14:11	38°10.45' S	55°06.93' W	550	CPT	
463_3	13845-6	22.06.09	14:44	38°10.46' S	55°06.80' W	550	CPT	
463_4	13845-7	22.06.09	15:23	38°10.49' S	55°06.67' W	550	CPT	
464	13845-8	22.06.09	18:20	38°10.40' S	55°07.11' W	548	MeBo	2150
465	13845-9	23.06.09	-	38°10.42' S	55°07.08' W	550	GC-6	empty
466	13845-10	23.06.09	13:30	38°10.43' S	55°07.07' W	549	EPC	83
507	13845-11	02.07.09	22:09	38°10.44' S	55°07.11' W	547	MeBo	2900
467	13846-1	23.06.09	15:15	38°07.21' S	54°57.442' W	637	MUC	6xL, 4xS, 20
468	13846-2	23.06.09	16:16	38°07.19' S	54°57.46' W	637	GC-6	520
469	13847-1	23.06.09	01:18	38°00.50' S	53°45.48' W	3560	GC-12	empty
471_1	13848-1	24.06.09	17:02	38°05.85' S	52°52.74' W	1111	CPT	
471_2	13848-2	24.06.09	18:20	38°05.98' S	52°52.59' W	1126	CPT	
472	13849-1	25.06.09	04:10	36°10.41' S	51°43.96' W	3278	GC-12	1129
473	13850-1	25.06.09	07:35	36°10.28' S	51°44.15' W	3267	GC-12	820
475	13850-2	25.06.09	09:57	36°10.29' S	51°44.11' W	3000	CTD/RO	
476	13850-3	25.06.09	12:51	36°10.30' S	51°44.06' W	400	CTD/RO	
477	13851-1	25.06.09	17:28	35°46.00' S	52°07.20' W	2213	GC-12	72
480	13852-1	26.06.09	00:28	36°05.70' S	52°48.984' W	1320	GC-6	560
481	13853-1	26.06.09	03:33	36°07.18' S	52°57.51' W	973	EPC	-
483	13854-1	26.06.09	09:46	35°45.54' S	52°07.89' W	2109	GC-6	552
484	13855-1	26.06.09	12:32	35°47.30' S	52°05.48' W	2277	GC-6	479
486	13856-1	26.06.09	17:29	36°03.94' S	51°52.25' W	3059	GC-12	779
487	13857-1	26.06.09	20:27	36°04.31' S	51°51.79' W	3077	GC-12	802

Ship's #	GeoB #	Date	Time (UTC)	PositionLat	PositionLon	Depth [m]	Device	Recovery Remarks
489	13858-1	27.06.09	02:40	35°38.06' S	52°28.73' W	1103	EPC	150
491_1	13859-1	27.06.09	08:24	36°06.70' S	52°51.29' W	1197	CPT	
491_2	13859-2	27.06.09	09:57	36°06.96' S	52°50.92' W	1227	CPT	
492	13860-1	27.06.09	11:49	36°06.65' S	52°51.58' W	1190	MeBo	3560
494	13861-1	28.06.09	00:51	38°05.51' S	53°36.59' W	3715	GC-12	668
496	13862-1	29.06.09	04:44	38°01.11' S	53°44.70' W	3588	GC-12	1026
498	13863-1	29.06.09	14:38	39°18.70' S	53°57.16' W	3687	GC-12	856
499	13864-1	02.07.09	00:25	37°37.43' S	53°35.29' W	2776	GC-12	748
500	13864-2	02.07.09	02:59	37°37.47' S	53°35.33' W	2757	GC-12	792
501	13865-1	02.07.09	05:25	37°35.19' S	53°43.10' W	1634	GC-12	530
503	13866-1	02.07.09	11:08	37°55.37' S	54°30.98' W	1013	CTD/RO	-
504	13866-2	02.07.09	12:06	37°55.36' S	54°30.99' W	1013	CTD-ISP	
506	13867-1	02.07.09	18:48	38°10.40' S	55°07.01' W	548	EPC	-
509	13868-1	04.07.09	10:40	37°24.87' S	53°43.32' W	1146	MeBo	727
512	13869-1	05.07.09	01:23	37°36.67' S	53°37.22' W	2503	CPT	-
513	13869-2	05.07.09	01:37	37°36.85' S	53°37.35' W	2467	CPT	-

List of seismic lines during Leg M78/3a

Ship's #	Profil-Nr.	Date	Time Start	Time End	Latitude Start	Longitude Start	Latitude End	Longitude End
					[S] xx° xx.x'	[W] xx° xx.x'	[S] xx° xx.x'	[W] xx° xx.x'
350	09-069	21.05.2009	00:05	20:22	35°47,94	52°57,36	35°47,94	52°57,36
350	09-070	21.-22.05.2009	22:31	02:59	35°47,94	52°57,36	35°47,94	52°57,36
350	09-071	22.05.2009	03:08	11:27	35°47,94	52°57,36	35°47,94	52°57,36
356	09-072	23.05.2009	03:00	04:13	35°47,94	52°57,36	35°47,94	52°57,36
356	09-073	23.05.2009	04:27	05:02	35°47,94	52°57,36	35°47,94	52°57,36
356	09-074	23.05.2009	05:12	08:00	35°47,94	52°57,36	35°47,94	52°57,36
356	09-075	23.05.2009	08:02	10:23	35°47,94	52°57,36	35°47,94	52°57,36
356	09-076	23.05.2009	10:23	11:29	35°47,94	52°57,36	35°47,94	52°57,36
356	09-077	23.05.2009	11:38	13:00	35°47,94	52°57,36	35°47,94	52°57,36
363	09-078	24.05.2009	04:00	04:36	35°47,94	52°57,36	35°47,94	52°57,36
363	09-079	24.05.2009	05:02	05:40	35°47,94	52°57,36	35°47,94	52°57,36
363	09-080	24.05.2009	08:16	10:16	35°47,94	52°57,36	35°47,94	52°57,36
363	09-081	24.05.2009	10:19	15:29	35°47,94	52°57,36	35°47,94	52°57,36
363	09-082	24.05.2009	15:40	22:00	35°47,94	52°57,36	35°47,94	52°57,36
363	09-083	24.-25.05.2009	22:11	04:17	35°47,94	52°57,36	35°47,94	52°57,36
363	09-084	25.05.2009	04:26	09:30	35°48,43	52°57,90	36°12,17	52°40,70
363	09-085	25.05.2009	09:41	12:02	36°12,89	52°41,61	36°05,99	52°52,57
363	09-086	25.05.2009	12:14	12:31	36°05,44	52°52,46	36°04,18	52°52,46
363	09-087	25.05.2009	12:32	13:40	36°04,38	52°51,52	36°08,77	52°45,16
363	09-088	25.05.2009	13:46	14:26	36°09,36	52°45,50	36°11,62	52°49,16
363	09-089	25.05.2009	14:27	16:01	36°11,60	52°49,20	36°08,21	52°54,97
385	09-090	28.05.2009	00:07	01:14	34°44,50	53°33,88	34°38,87	53°32,89
385	09-091	28.05.2009	01:21	05:10	34°38,75	53°32,32	34°43,60	53°10,04
385	09-092	28.05.2009	05:14	08:50	34°43,33	53°9,85	34°25,53	53°14,68
385	09-093	28.05.2009	09:04	11:19	34°25,90	53°14,12	34°28,47	53°01,09
391	09-094	29.05.2009	09:58	13:17	36°14,30	54°09,62	36°19,80	54°23,71
391	09-095	29.-30.05.2009	13:22	05:08	36°20,14	54°23,86	37°20,19	55°20,69
391	09-096	30.05.2009	05:17	12:55	37°20,92	55°20,56	37°50,02	54°50,00

Ship's #	Profil-Nr.	Date	Time Start	Time End	Latitude Start [S]	Longitude Start [W]	Latitude End [S]	Longitude End [W]
			UTC		xx° xx.x'	xx° xx.x'	xx° xx.x'	xx° xx.x'
391	09-097	30.05.2009	13:05	18:20	37°49,92	54°48,83	37°27,42	54°23,91
408	09-098	04.06.2009	12:11	12:21	37°54,77	54°17,36	37°54,36	54°18,05
408	09-098b	04.06.2009	12:23	19:47	37°54,16	54°18,08	37°23,52	53°47,91
408	09-099	04.06.2009	19:58	21:34	37°23,38	53°46,83	37°27,32	53°39,91
408	09-100	04.-05.06.2009	21:43	04:41	37°28,04	53°36,61	38°3,91	53°51,50
408	09-101	05.06.2009	06:22	08:42	38°6,29	53°55,33	38°09,45	53°39,79
408	09-102	05.06.2009	08:51	11:12	38°08,97	53°39,06	37°56,72	53°35,15
408	09-103	05.06.2009	11:20	18:15	37°56,07	53°35,56	37°38,77	54°14,04
408	09-104	05.06.2009	18:39	20:22	37°36,76	54°13,54	37°28,00	54°09,14
408	09-105	05-06.06.2009	20:32	01:38	37°27,77	54°08,23	37°41,09	53°37,57
408	09-106	06.06.2009	01:54	05:36	37°40,56	53°36,38	37°22,64	53°30,14
408	09-107	06.06.2009	05:45	08:30	37°21,99	53°30,36	37°13,92	53,44,80
416	09-108	07.06.2009	02:20	05:30	37°41,23	54°11,51	37°30,807	54°24,53
416	09-109	07.06.2009	05:39	07:16	37°53,86	54°25,45	37°48,40	54°33,63
416	09-110	07.06.2009	07:25	09:15	37°47,83	54°33,60	37°39,07	54°27,83
433	09-111	09.-10.06.2009	22:27	09:12	34°42,64	53°10,72	35°33,76	52°41,70
444	09-112	10.-11.06.2009	21:39	02:37	35°27,84	53°16,84	35°78,40	52°57,59
444	09-113	11.06.2009	02:41	03:13	35°45,57	52°57,72	35°50,61	53°00,17
444	09-114	11.06.2009	03:19	04:58	35°50,51	53°00,64	35°43,57	53°07,24
444	09-115	11.06.2009	05:02	06:05	35°43,27	53°07,11	35°39,35	53°02,38
444	09-116	11.06.2009	06:20	07:36	35°40,10	53°01,77	35°45,17	53°07,15
444	09-117	11.06.2009	07:42	07:58	35°45,33	53°07,02	35°46,40	53°06,00
444	09-118	11.06.2009	08:04	08:58	35°46,29	53°05,41	35°42,75	53°01,56
450	09-119	11.06.2009	17:31	21:06	36°3,39	52°34,13	35°46,07	52°40,63
450	09-120	11.06.2009	21:10	22:24	35°45,97	52°40,356	35°45,95	53°32,67
450	09-121	11.06.2009	22:27	22:40	35°46,14	52°32,45	35°47,24	52°31,65
450	09-122	11.-12.06.2009	22:46	02:42	35°47,60	52°31,85	36°02,88	52°48,30
450	09-123	12.06.2009	02:51	04:13	36°03,32	52°47,86	36°3,9*4	52°39,39
450	09-124	12.06.2009	04:20	06:20	36°3,4	52°39,21	35°55,72	52°47,45

8. Data and Sample Storage and Availability

All cores are stored and archived in the Bremen core repository. All data measured at the cores during the and post cruise are included in the PANGAEA data base in Bremerhaven which will then provide long-term archival and access to the data within WDC-MARE.

The seismic, bathymetric and hydro-acoustic raw data as well as processed seismic data will be archived on a dedicated server at Bremen University and IFM-GEOMAR. The IFM-GEOMAR server is daily backed up and holds all data since the founding days of IFM-GEOMAR.

9. Acknowledgements

The scientific party of both legs of Meteor Cruise M78/3 gratefully acknowledges the purposive and effective cooperation with Captain Baschek and his crew. The remarkably reliable short- and long-term weather forecast by the DWD was extremely helpful for the station planning. We thank Celeste Saulo and her colleagues from the Centro de Investigaciones de Mar y la Atmosfera at the University of Buenos Aires for their support of the forecast with daily updates of CIMA regional atmospheric model. The compensation of at least some of the delay due to the late container arrival could be compensated thanks to the extraordinary support by Humberto Heins organizing the harbor logistics in Montevideo. We also appreciate the professional support by the Leitstelle Meteor/Merian. This expedition was funded by the Deutsche Forschungsgemeinschaft.

10. References

- Arnold, G.L., Weyer, S. and Anbar, A.D., 2004. Fe isotope variations in natural materials measured using high mass resolution multiple collector ICPMS. *Analytical Chemistry* 76(2), 322-327.
- Blum, P., 1997. *Physical Properties Handbook: A guide to the shipboard measurement of physical properties of deep-sea cores*. ODP Technical Notes 26.
- Boyce, R.E., 1977. Deep Sea Drilling Project procedures for shear strength measurement of clayey sediment using modified Wykeham Farrance laboratory vane apparatus. In Barker, P.F., Dalziel, I.W.D. and shipboard scientific party. (eds), *Initial Reports DSDP*. U.S. Govt. Printing Office, Washington, 1059–1068.
- Cline, J.D., 1969. Spectrophotometric determination of hydrogen sulfide in natural waters. *Limnol. Oceanogr.* 14, 454-458.
- Cowie, G.L., Hedges, J.I., 1992. Sources and reactivities of amino acids in a coastal marine environment. *Limnol. Oceanogr.* 37(4), 703-724.
- Dale, B. 1986. Life strategies of oceanic dinoflagellates. UNESCO technical papers in marine science.
- Evitt, W.R., 1985. Sporopollenin dinoflagellate cysts: their morphology and interpretation. American Association of Stratigraphic Palynologists Foundation, Dallas, 333.
- Gordon, A.L. 1989. Brazil-Malvinas Confluence – 1984. *Deep-Sea Research* 36 (3), 359-384.
- Grasshoff, K., Kremling, K., Ehrhardt, M. (eds), 1999. *Methods of seawater analysis*, 3rd edition. Wiley-VCH, Weinheim, New York.
- Haeckel, M., Suess, E., Wallman, K., and Rickert, D., 2004. Rising methane gas bubbles form massive hydrate layers at the seafloor. *Geochimica et Cosmochimica Acta* 68, 4335-4345.

- Hansbo, S., 1957. A new approach to the determination of the shear strength of clay by the fall-cone test, Stockholm.
- Hensen, C., Zabel, M., Pfeifer, K., Schwenk, T., Kasten, S., Riedinger, N., Schulz, H.D. and Boetius, A., 2003. Control of sulfate pore-water profiles by sedimentary events and the significance of anaerobic oxidation of methane for the burial of sulfur in marine sediments. *Geochimica et Cosmochimica Acta* 67, 2631-2647.
- Hernández-Molina, F.J., Paterlini, M., Violante, R., Marshall, P., de Isasi, M., Somoza, L. and Rebesco, M., 2009. Contourite depositional system on the Argentine Slope: An exceptional record of the influence of Antarctic water masses. *Geology* 37, 507-510.
- Jørgensen, B.B., 1978. A comparison of methods for the quantification of bacterial sulfate reduction in coastal marine sediments. I. Measurement with radiotracer techniques. *Geomicrobiol. J.* 1, 29-47.
- Kallmeyer, J., Ferdelman, T.G., Weber, A., Fossing, H. and Jørgensen, B.B., 2004. A cold chromium distillation procedure for radiolabeled sulfide applied to sulfate reduction measurements. *Limnol. Oceanogr. Methods* 2, 171-180.
- Kamyshny, Jr., A., Borkenstein, C. and Ferdelman, T.G., (submitted)
- Lee, H.J., Edwards, B.D. and Field, M.E., 1979. Offshore soil sampling and geotechnical parameter determination, 11th offshore Technology Conference, Houston, Texas, 1449-1453.
- Lu, T.S. and Bryant, W.R., 1997. Comparison of vane shear and fall cone strengths of soft marine clay. *Marine Georesources & Geotechnology* 15(1), 67-82.
- McDonagh, EL; Arhan, M; Heywood, KJ. 2002. On the circulation of bottom water in the region of the Vema Channel. *Deep-Sea Research I*, 49, 1119-1139.
- Peterson, RG. 1992. The boundary currents in the western Argentine Basin. *Deep-Sea Research Part A: Oceanographic Research Papers* 39 (3-4), 623-644.
- Piola, AR; Gordon, AL. 1989. Intermediate waters in the southwest South Atlantic. *Deep-Sea Research* 6 (1), 1-16.
- Riedinger, N., Pfeifer, K., Kasten, S., Garming, J.F.L., Vogt, C. and Hensen, C., 2005. Diagenetic alteration of magnetic signals by anaerobic oxidation of methane related to a change in sedimentation rate. *Geochimica et Cosmochimica Acta* 69, 4117-4126.
- Schubert, C.J., Ferdelman, T.G., Strotmann, B., 2000. Organic matter composition and sulfate reduction rates in sediments off Chile. *Org. Geochem.* 31, 351-361.
- Seeberg-Elverfeldt, J., Schlüter, M., Feseker, T., and Kölling, M. 2005. Rhizon sampling of porewaters near the sediment-water interface of aquatic systems. *Limnology and Oceanography: Methods* 3, 361-371.
- Spieß, V., and cruise participants 2002. Report and preliminary results of Meteor Cruise M 49/2, Montevideo (Uruguay) - Montevideo, 13.02. - 07.03.2001., Berichte, Fachbereich Geowissenschaften, Universität Bremen. pp 84.
- Torres, M.E., Wallman, K., Tréhu, A.M., Bohrmann, G., Borowski, W.S. and Tomaru, H., 2004. Gas hydrate growth, methane transport, and chloride enrichment at the southern summit of Hydrate Ridge Cascadia margin off Oregon. *Earth and Planetary Science Letters* 226, 225-241.
- Ussler III, W. and Paull, C., 2001. Ion exclusion associated with marine gas hydrate deposits. In Paull, C. and Dillon, W.P. (eds.), *Natural gas hydrates-occurrence, distribution and detection*. Geophysical Monograph 124, Washington, AGU, 41-51.




















- Wood, D.M., 1982. Cone penetrometer and liquid limit. *Géotechnique* 32(2), 152-157.
- Wood, D.M., 1985. Some fall-cone tests. *Géotechnique* 38, 64-68.
- Zonneveld, K.A.F. 2004. Potential use of stable oxygen isotope composition of *Thoracosphaera heimii* (Dinophyceae) for upper water column (thermocline) temperature reconstruction. *Marine Micropaleontology* 50 (3-4), 307-317.

Argentine Margin Core Plot Summary Legend

Colour Legend

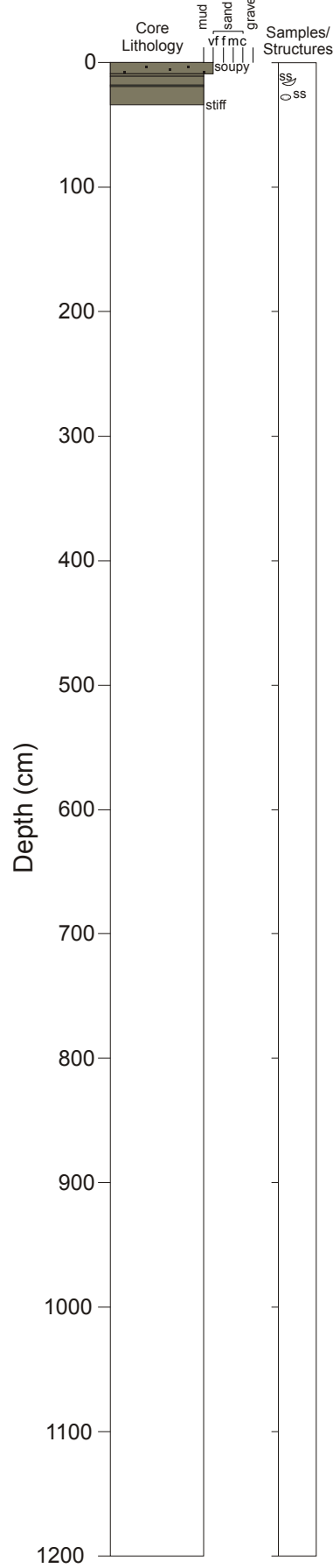
	Foram Ooze
	Olive Grey Mud (Ogm)
	Olive Grey Sandy Mud (Ogm1)
	Olive Grey Mud with Ice-Rafted Detritus (Ogm2)
	Brick Red Mud (Brm)
	Red Brown Mud (Rbm)
	Red Brown Sandy Mud (Rbm1)
	Red Brown Mud with Ice-Rafted Detritus (Rbm2)
	Brown Mud (Bm)
	Brown Sandy Mud (Bm1)
	Brown Mud with Ice-Rafted Detritus (Bm2)
	Grey Mud (Gm)
	Grey Sandy Mud (Gm1)
	Grey Mud with Ice-Rafted Detritus (Gm2)
	volcanic ash
	Sand
	Gravel
	dusk yellow silty mud
	yellow brown silty mud
	olive yellow mud
	mud clast conglomerate

Symbol Legend

Sharp Contact	
Lamination/Thin Beds	
Piston Core Disturbance	
Subsampled Core	
Granule	
Pebble	
Bivalve	
Gastropod	
Shell fragment	
Mudclast	
Sand bleb	
Forams	
Abundant sponge spicules	
Bioturbation	SS
Gradation	
coral fragment	
plant remains	
volcanic shards	
diatoms	
white specs	

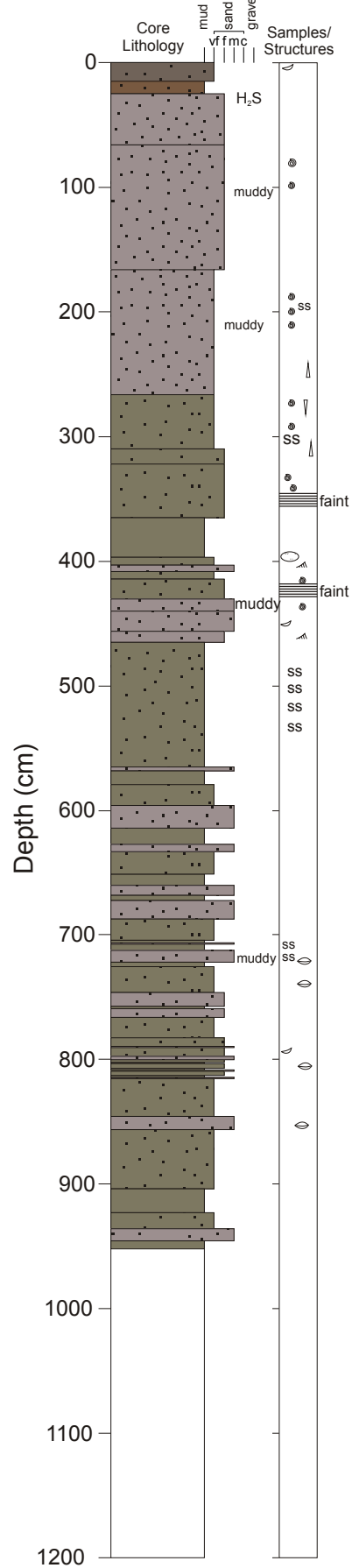
Meteor 78/3a GeoB 13801-1 MUC

TD 33.5 cm Water depth 244 m



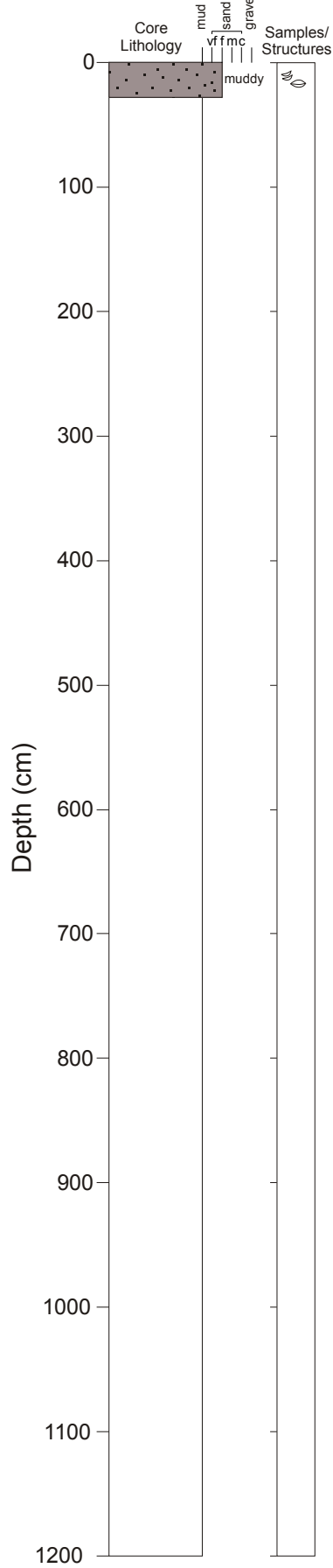
Meteor 78/3a GeoB 13801-2 GC

TD 953 cm Water depth 241 m



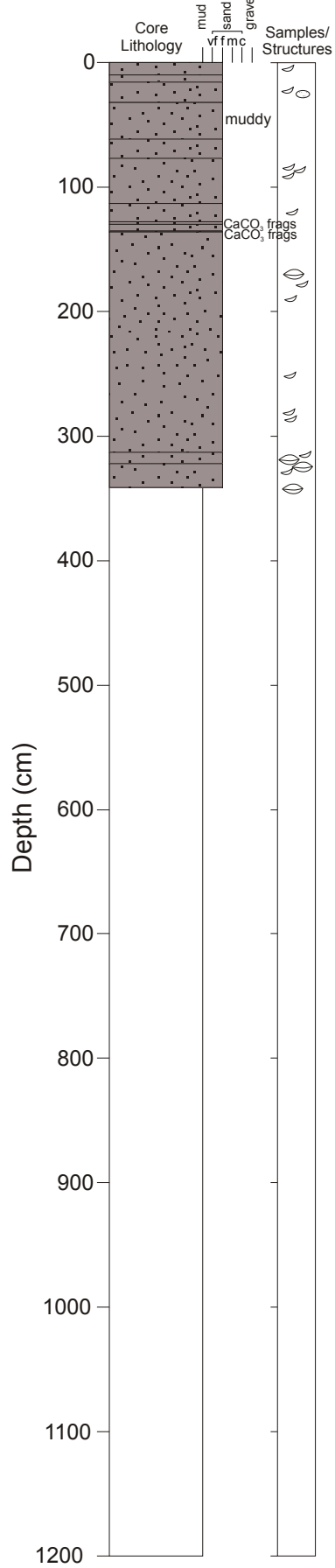
Meteor 78/3a GeoB 13802-1 Pushcore in Grab

TD 28 cm Water depth 141 m



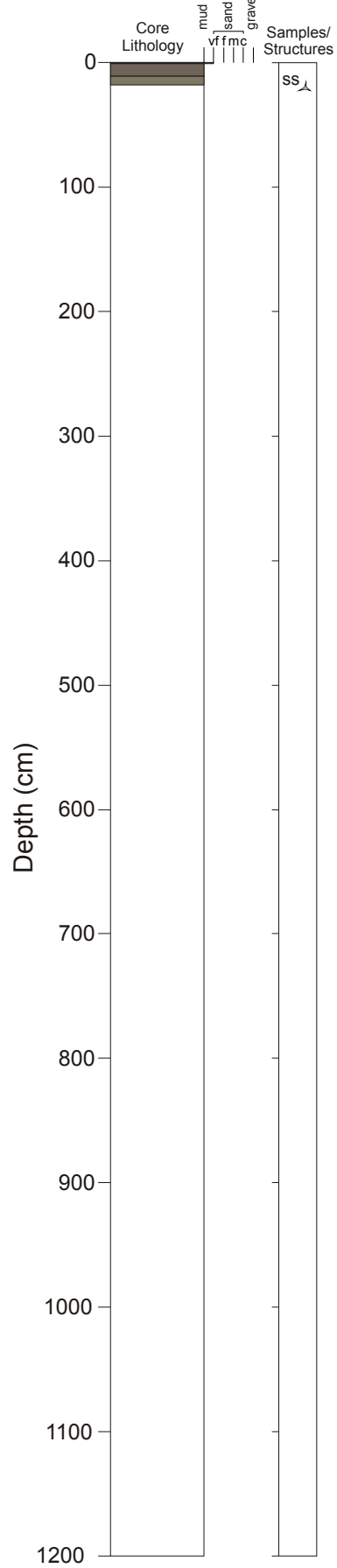
Meteor 78/3a GeoB 13802-2 VC

TD 341 cm Water depth 141 m



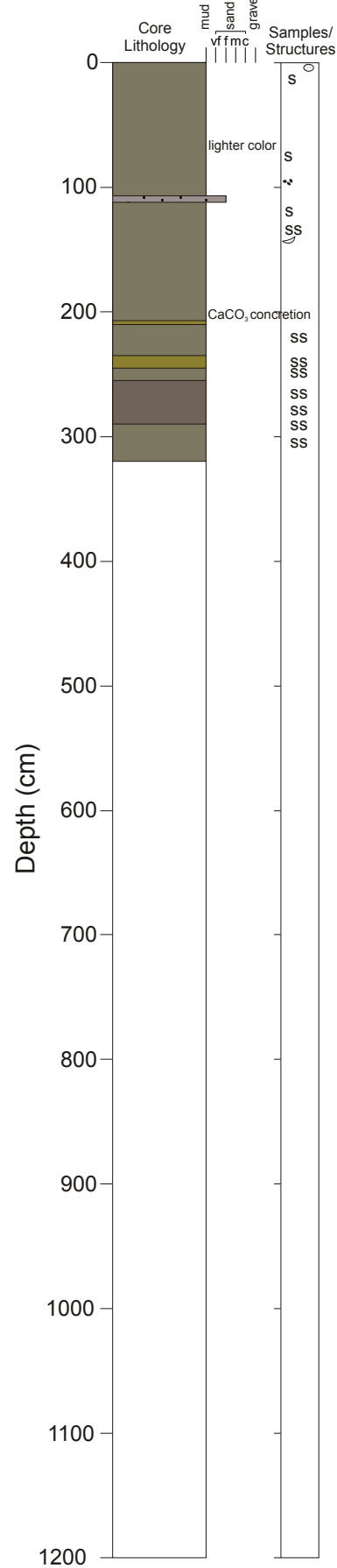
Meteor 78/3a GeoB 13803-1 MUC

TD 18 cm Water depth 2468 m



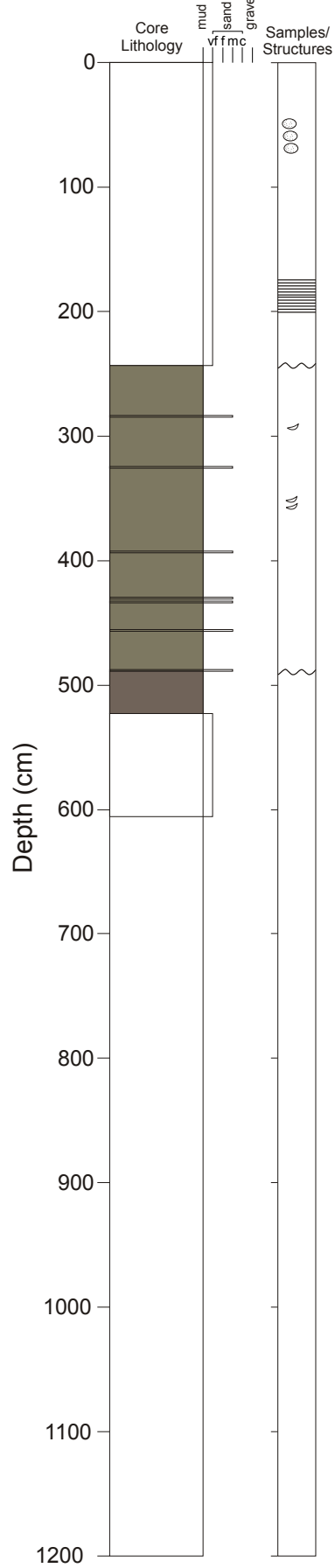
Meteor 78/3a GeoB 13803-2 GC

TD 321 cm Water depth 4482 m



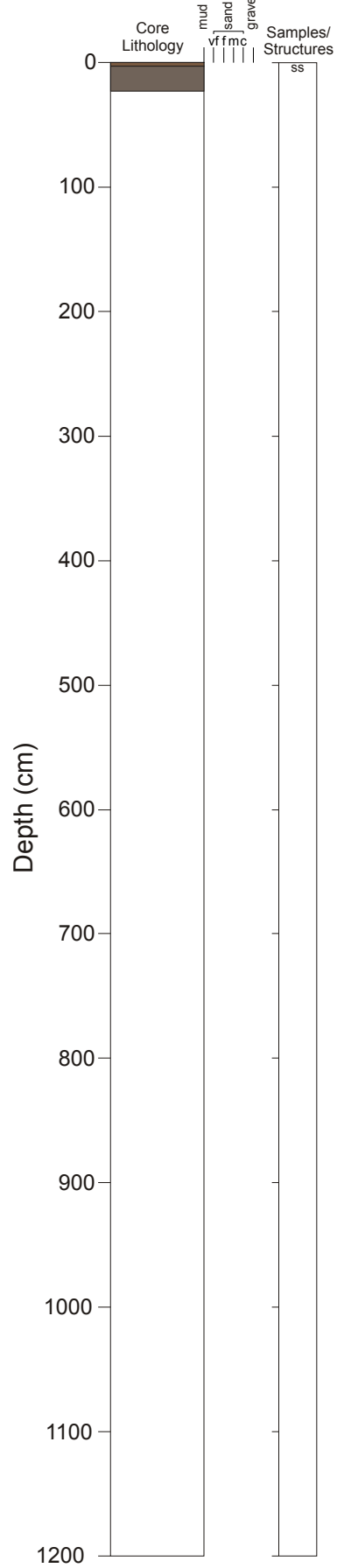
Meteor 78/3a GeoB core 13804-1 GC

TD 608 cm Water depth 2579 m



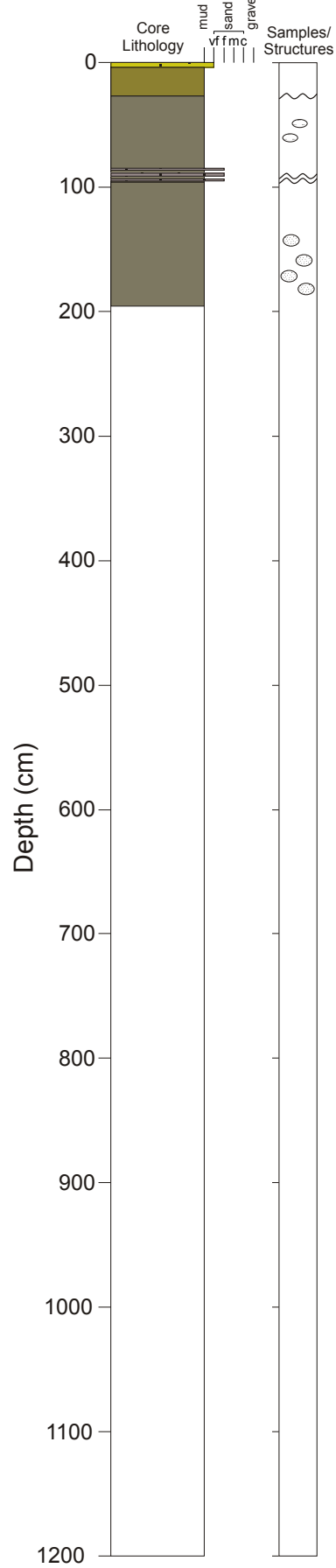
Meteor 78/3a GeoB 13804-2 MUC

TD 23 cm Water depth 2593 m



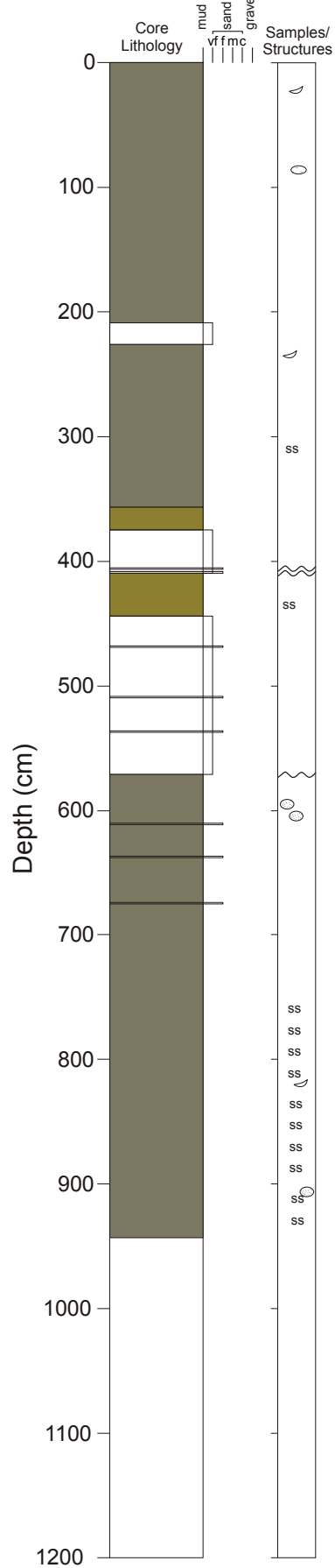
Meteor 78/3a GeoB 13805-2 GC

TD 196 cm Water depth 2503 m



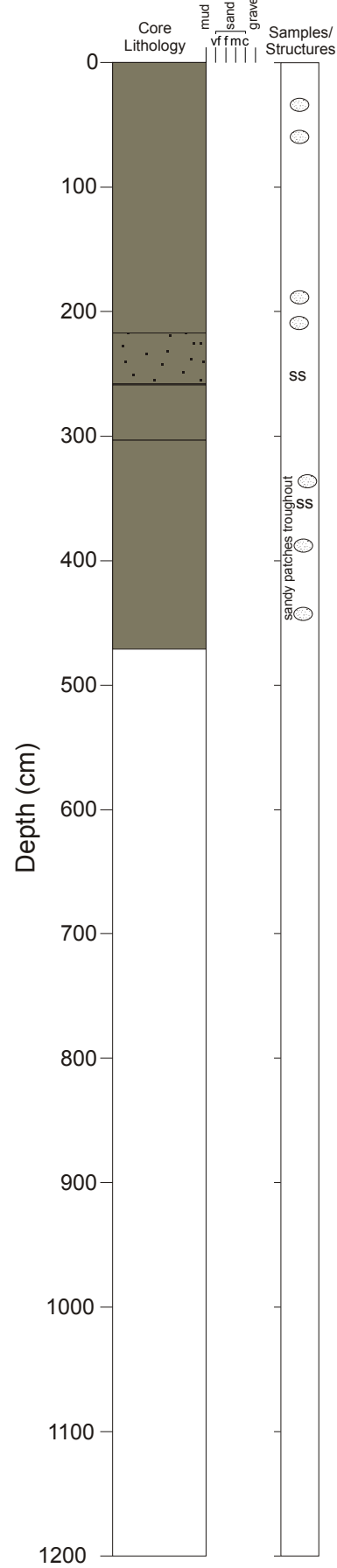
Meteor 78/3a GeoB core 13806-1 GC

TD 944 cm Water depth 2575 m



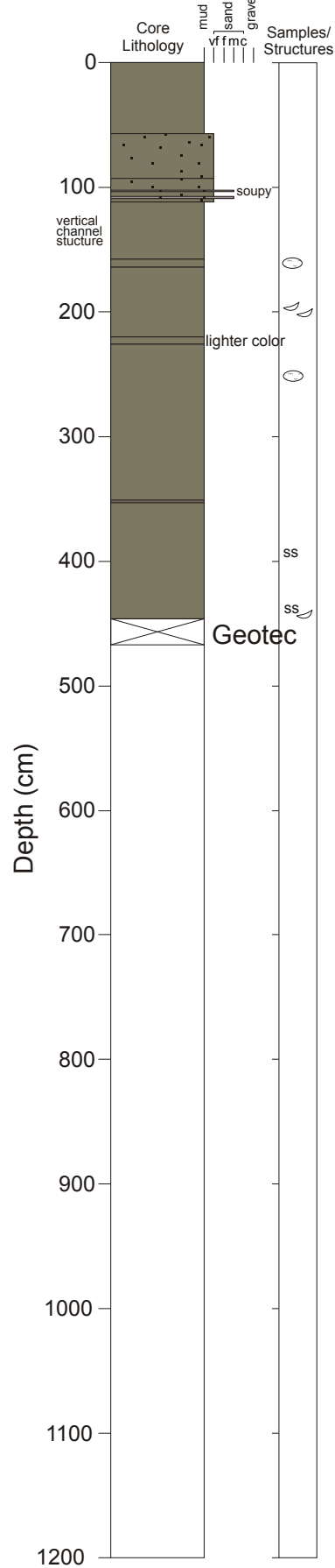
Meteor 78/3a GeoB 13807-1 GC

TD 476 cm Water depth 2547 m



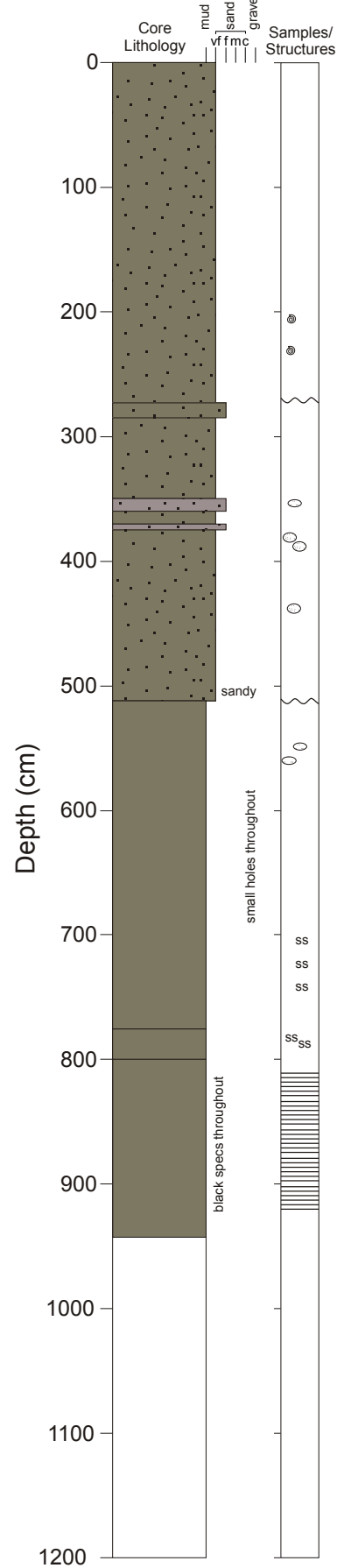
Meteor 78/3a GeoB 13808-1 GC

TD 467 cm Water depth 2293 m



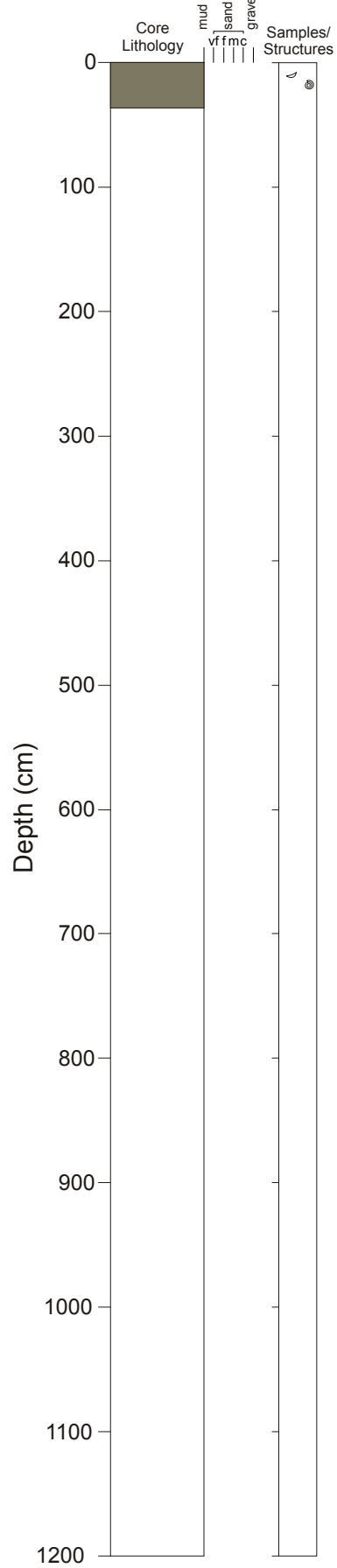
Meteor 78/3a GeoB 13809-1 GC

TD 942 cm Water depth 1402 m



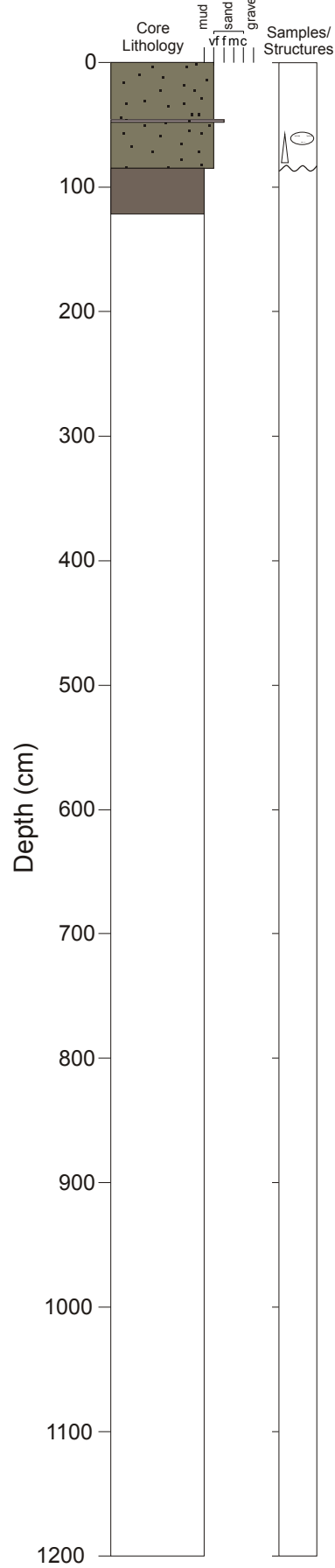
Meteor 78/3a GeoB 13809-2 MUC

TD 36.5 cm Water depth 1400 m



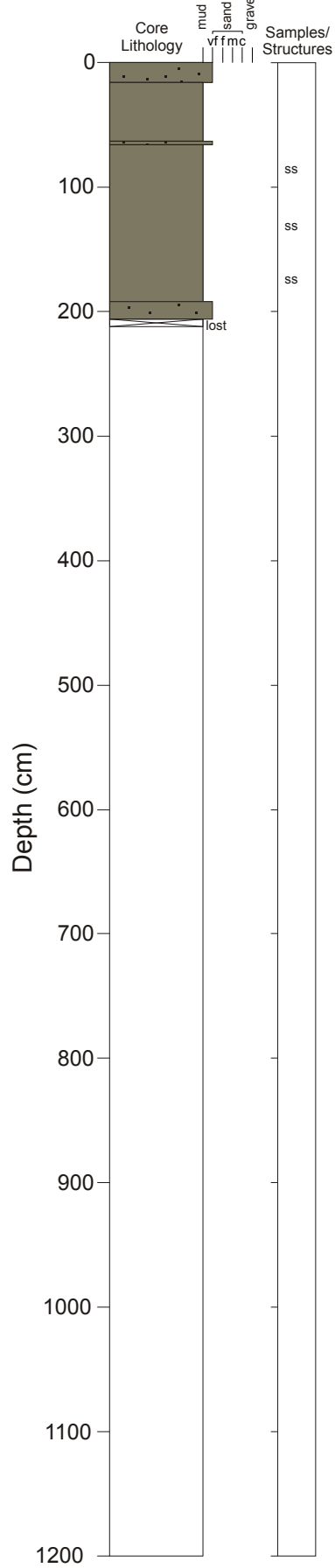
Meteor 78/3a GeoB 13810-1 GC

TD 124 cm Water depth 1150 m



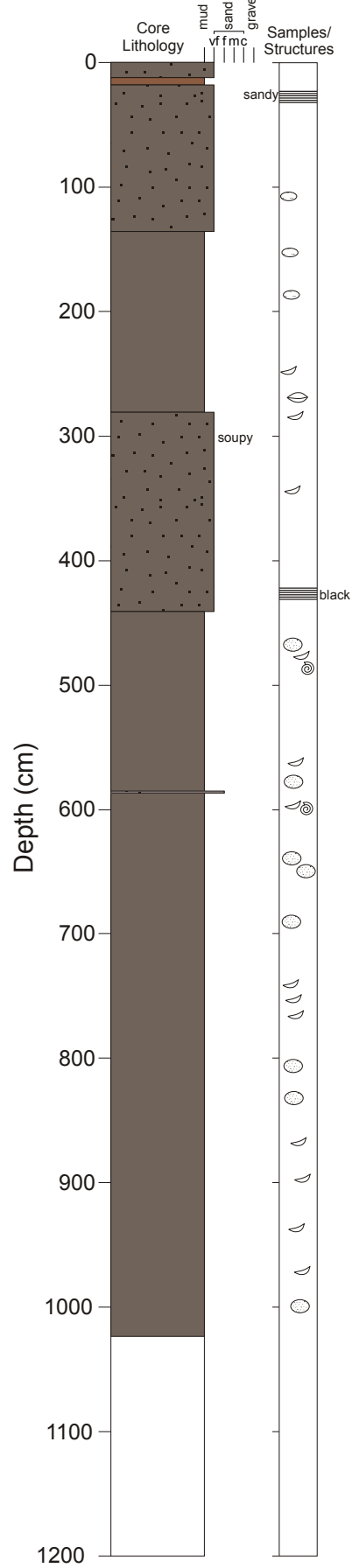
Meteor 78/3a GeoB 13811-1 GC

TD 216 cm Water depth 1210 m



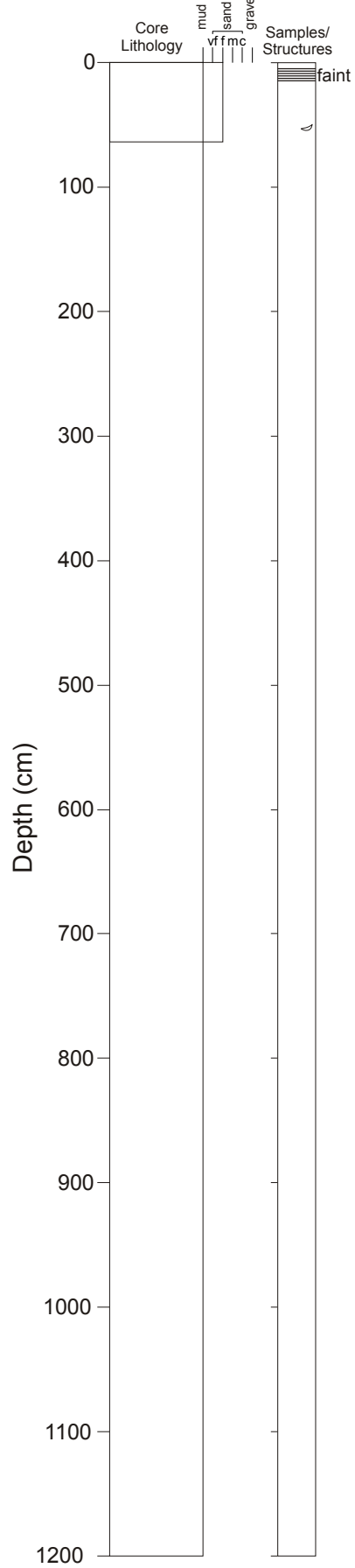
Meteor 78/3a GeoB 13813-4 GC

TD 1024 cm Water depth 57 m



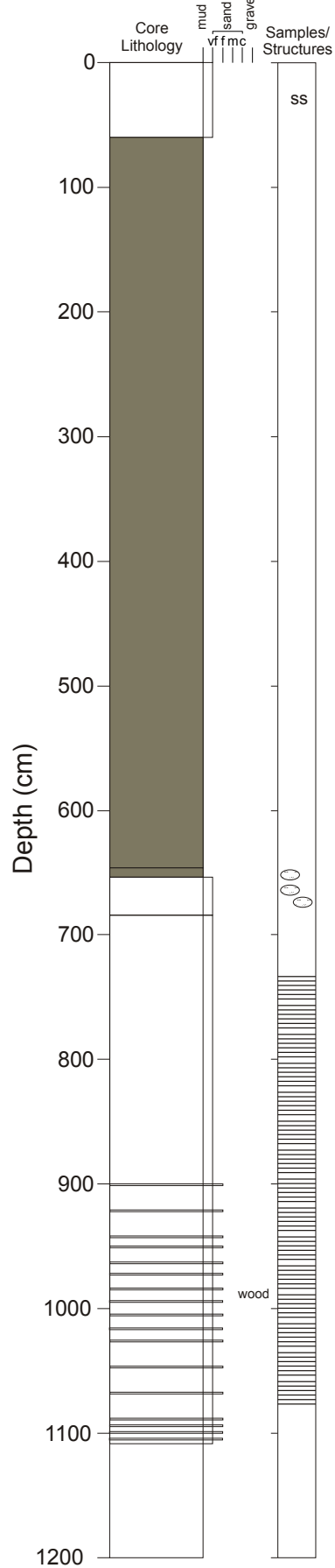
Meteor 78/3a GeoB core 13814-2 GC

TD 64 cm Water depth 40 m



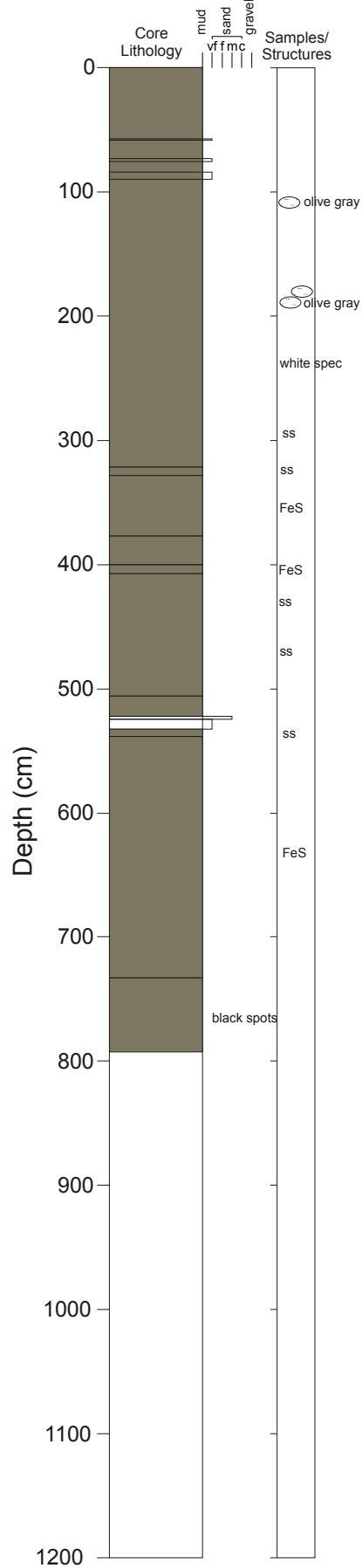
Meteor 78/3a GeoB core 13817-2 GC

TD 1111 cm Water depth 62 m



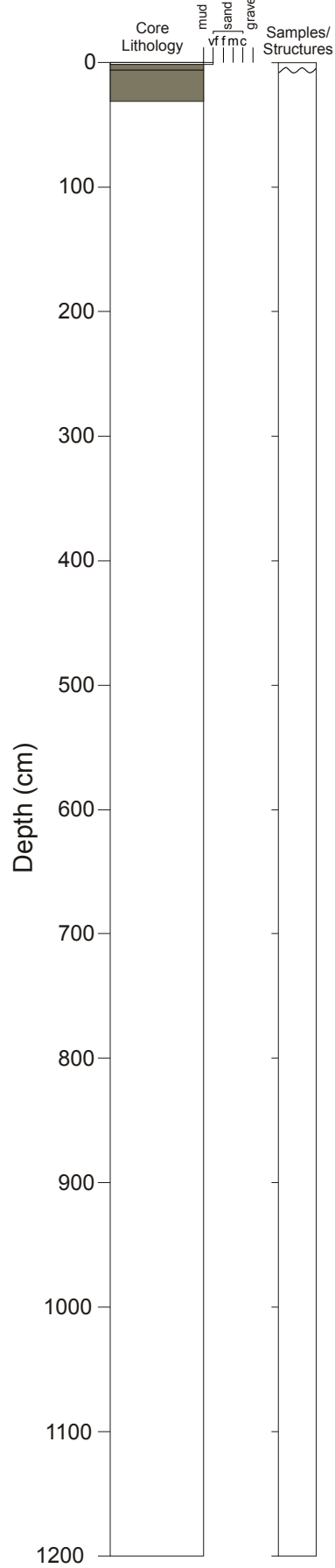
Meteor 78/3a GeoB core 13819-2 GC

TD 792 cm Water depth 4274 m



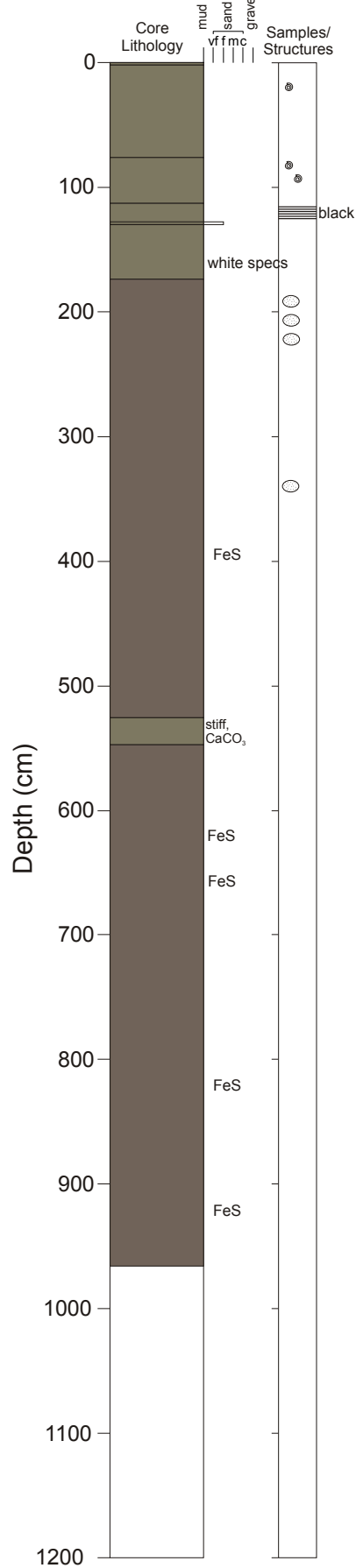
Meteor 78/3a GeoB core 13819-4 MUC

TD 31 cm Water depth 4273 m



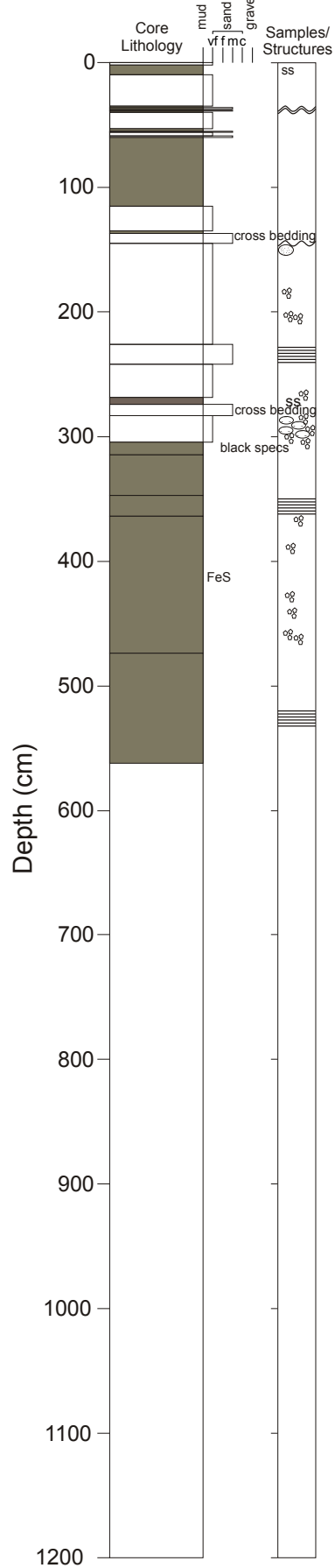
Meteor 78/3a GeoB core 13820-1 GC

TD 966 cm Water depth 3614 m



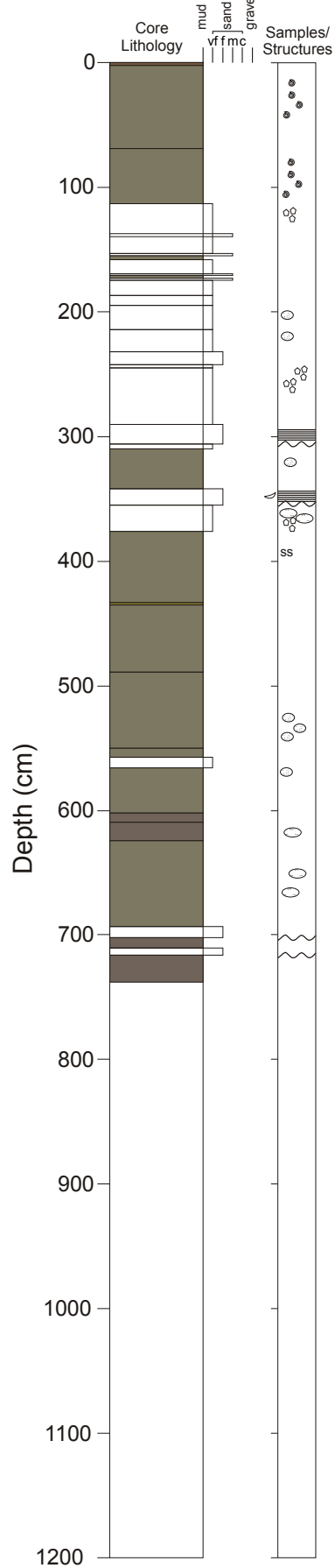
Meteor 78/3a GeoB core 13821-1 GC

TD 565 cm Water depth 3749 m, top missing: shot through



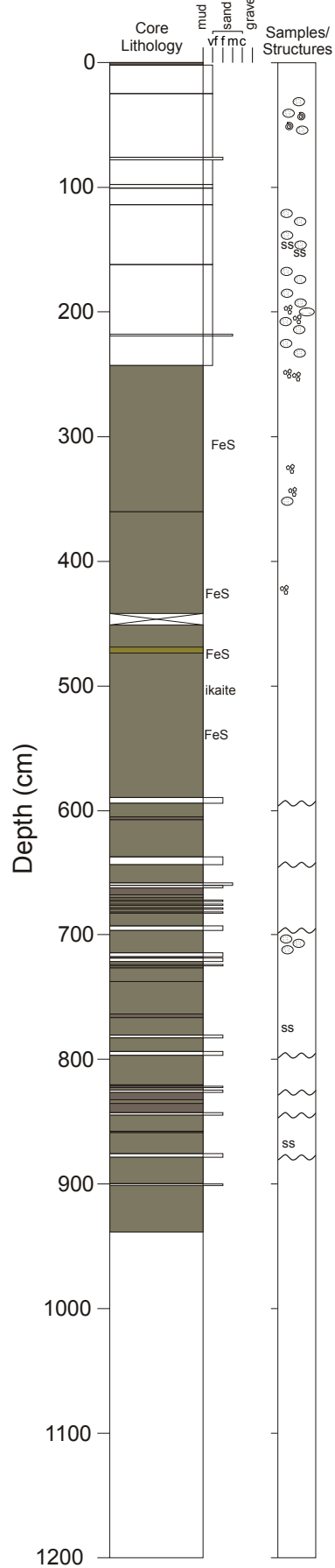
Meteor 78/3a GeoB core 13821-2 GC

TD 737 cm Water depth 3762 m



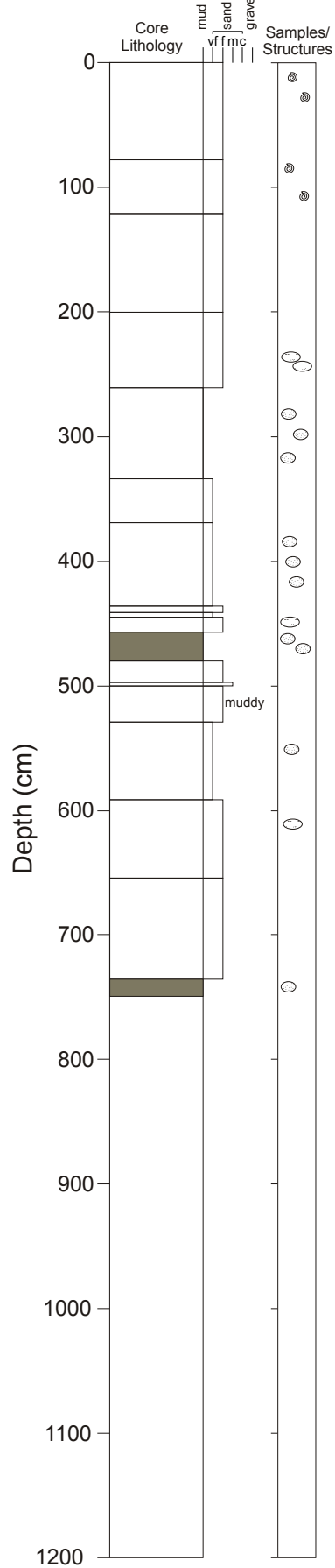
Meteor 78/3a GeoB core 13823-2 GC

TD 938 cm Water depth 3780 m



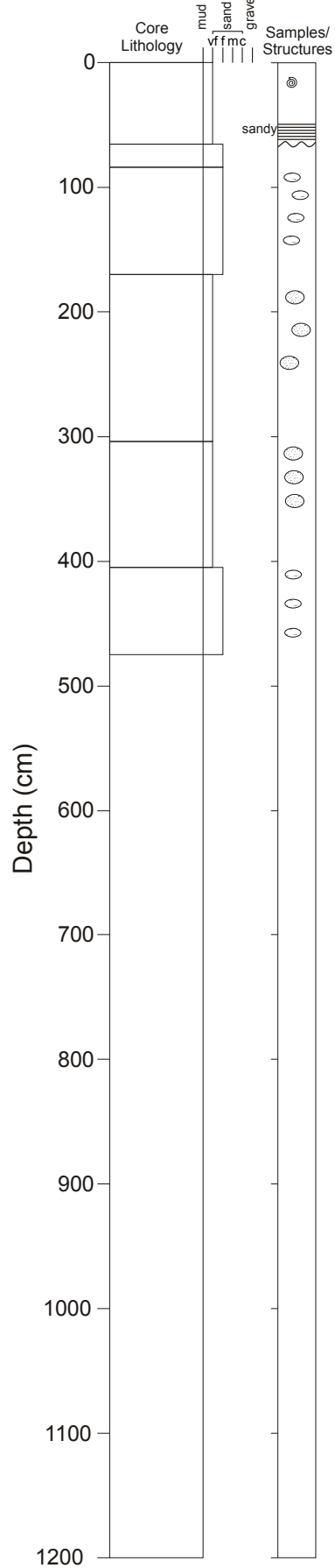
Meteor 78/3a GeoB core 13825-2 GC

TD 749 cm Water depth 1228 m



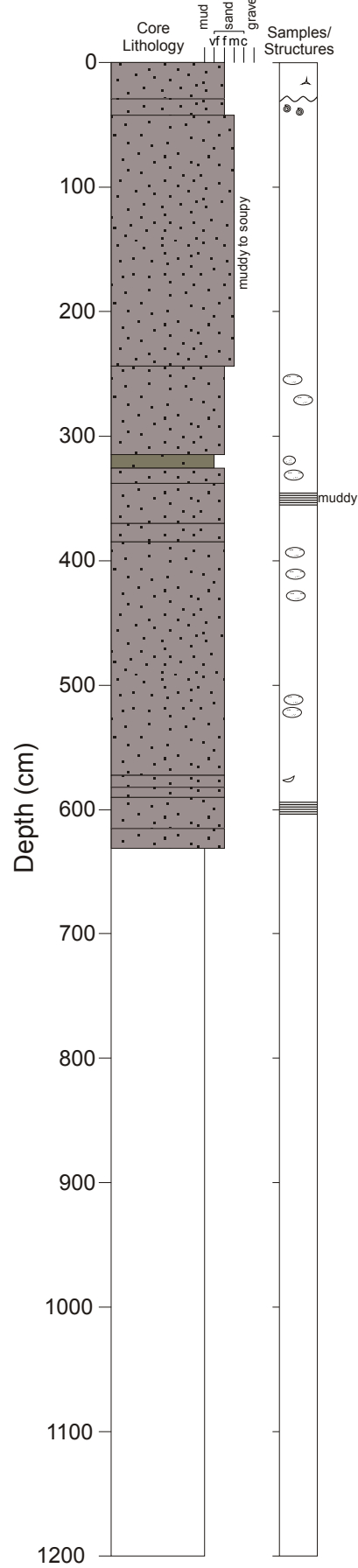
Meteor 78/3a GeoB core 13826-1 GC

TD 475 cm Water depth 1224 m



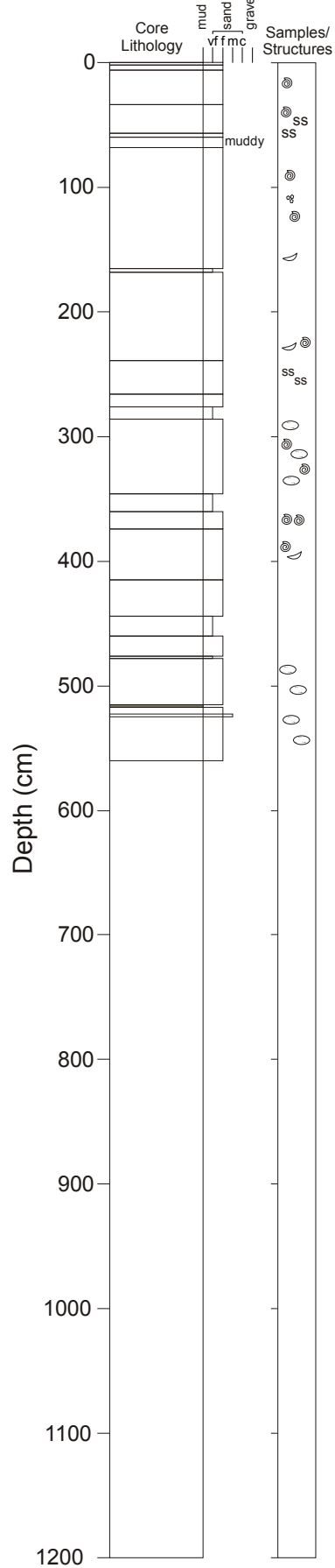
Meteor 78/3a GeoB core 13827-2

TD 631 cm Water depth 1155 m



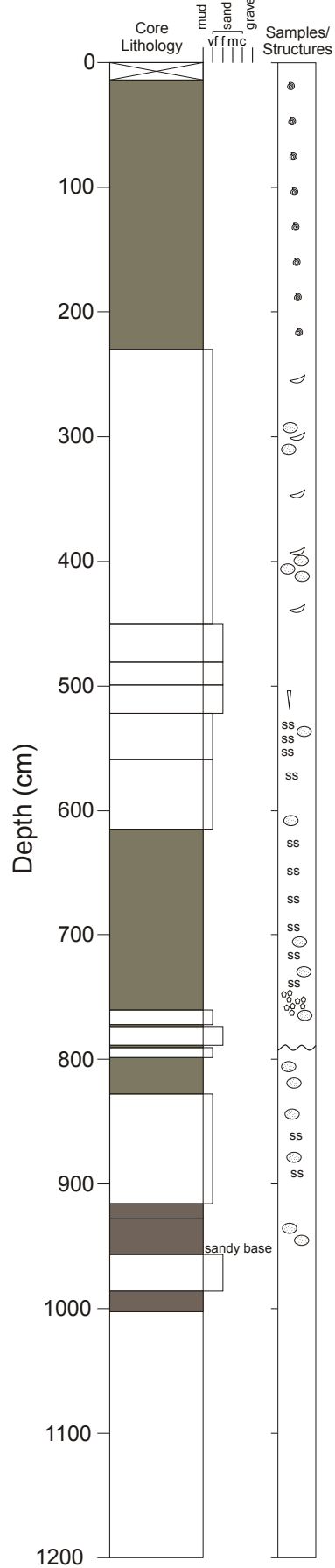
Meteor 78/3a GeoB core 13832-2 GC

TD 560 cm Water depth 2205 m



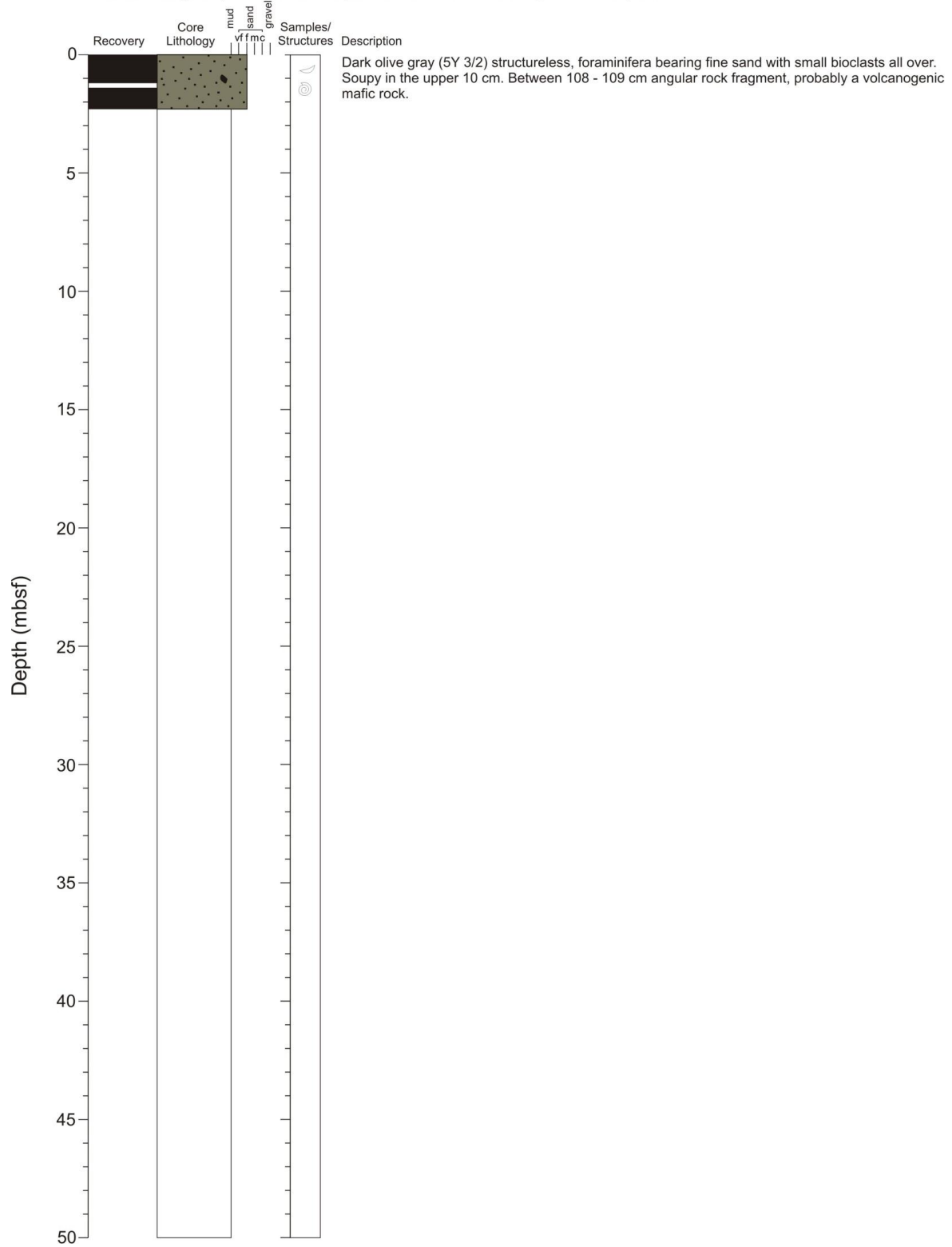
Meteor 78/3a GeoB core 13842-1 GC

TD 1002 cm Water depth 1555 m



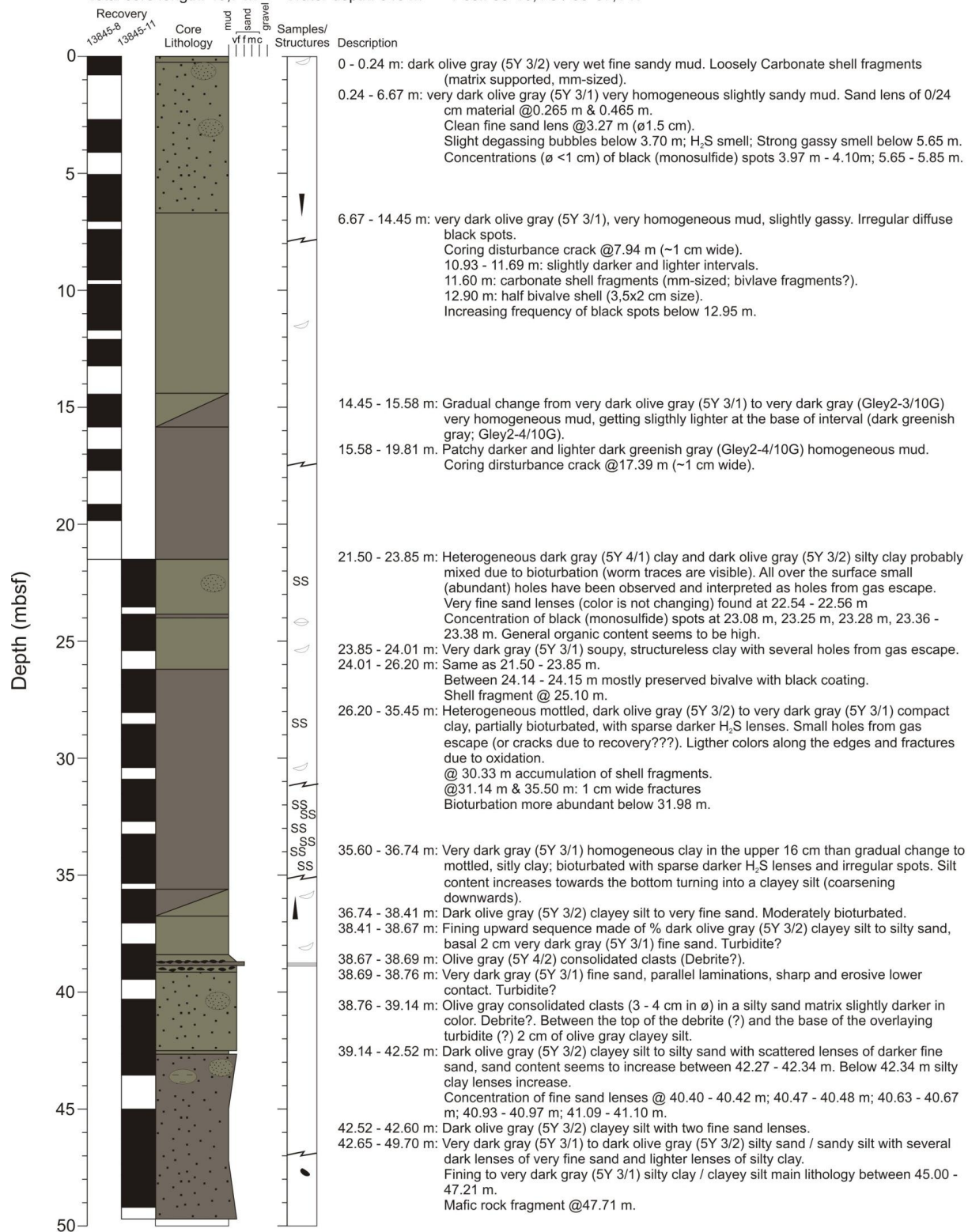
Meteor 78/3b GeoB 13844-4 (MeBo)

Total core length: 2,4 m Water depth: 1150 m Pos.: 37°25,07'S / 53°43,56'W



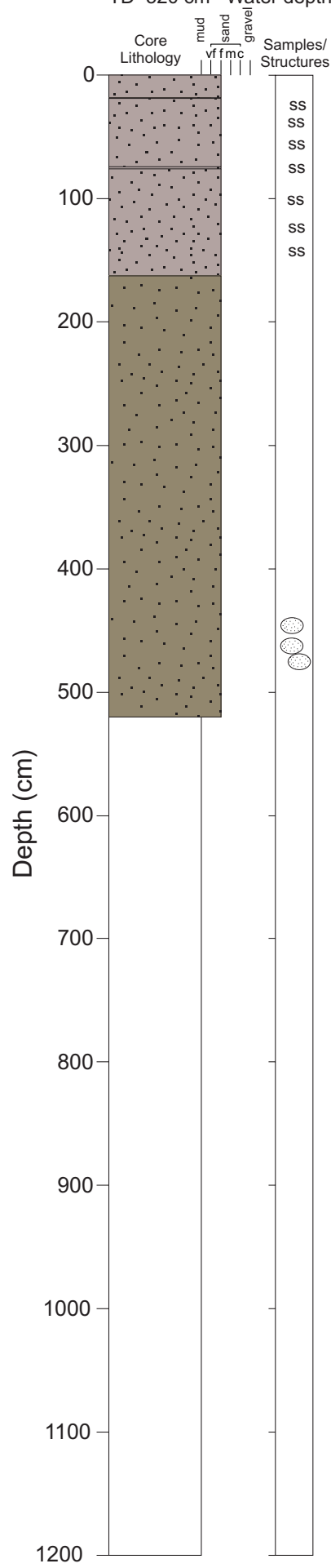
Meteor 78/3b GeoB 13845-8 & -11 (MeBo)

Total core length: 49,7 m Water depth: 548 m Pos.: 38°10,4'S / 55°07,1'W



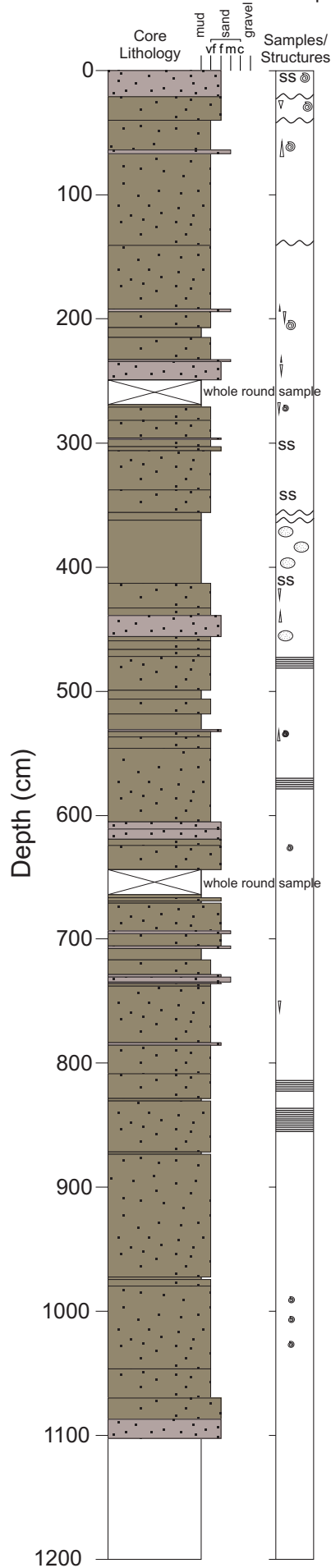
Meteor 78/3b GeoB core 13846-2

TD 520 cm Water depth 637 m



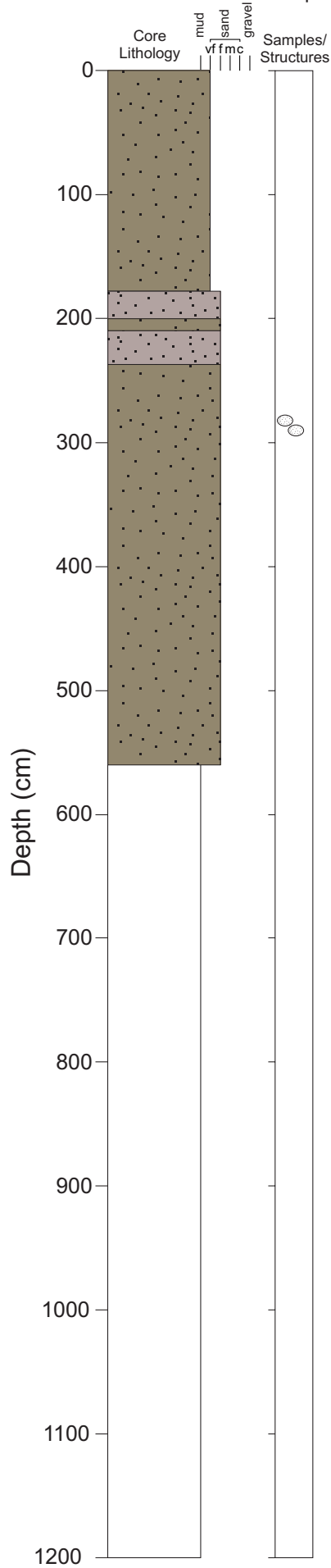
Meteor 78/3b GeoB core 13849-1

TD 1129 cm Water depth 3278 m



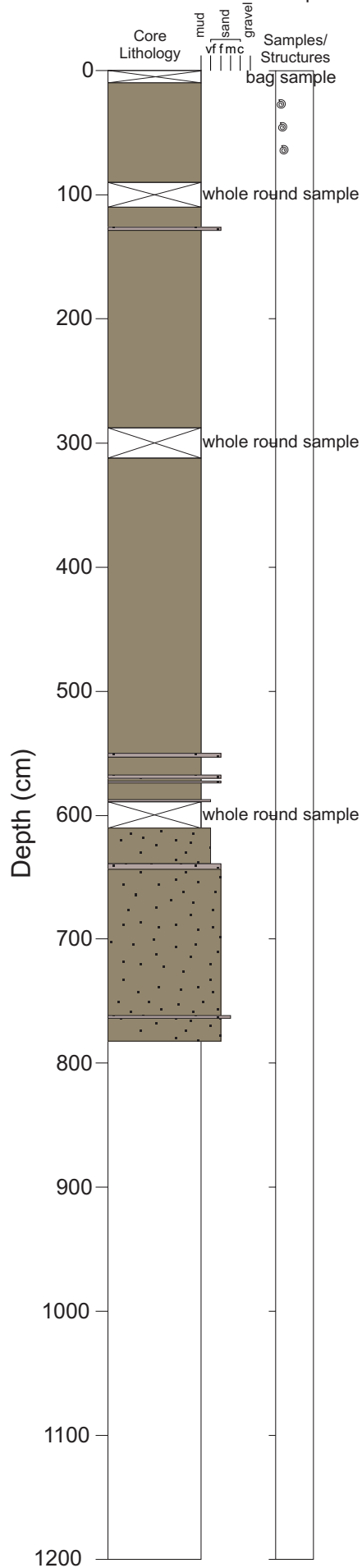
Meteor 78/3b GeoB core 13852-1

TD 560 cm Water depth 1320 m



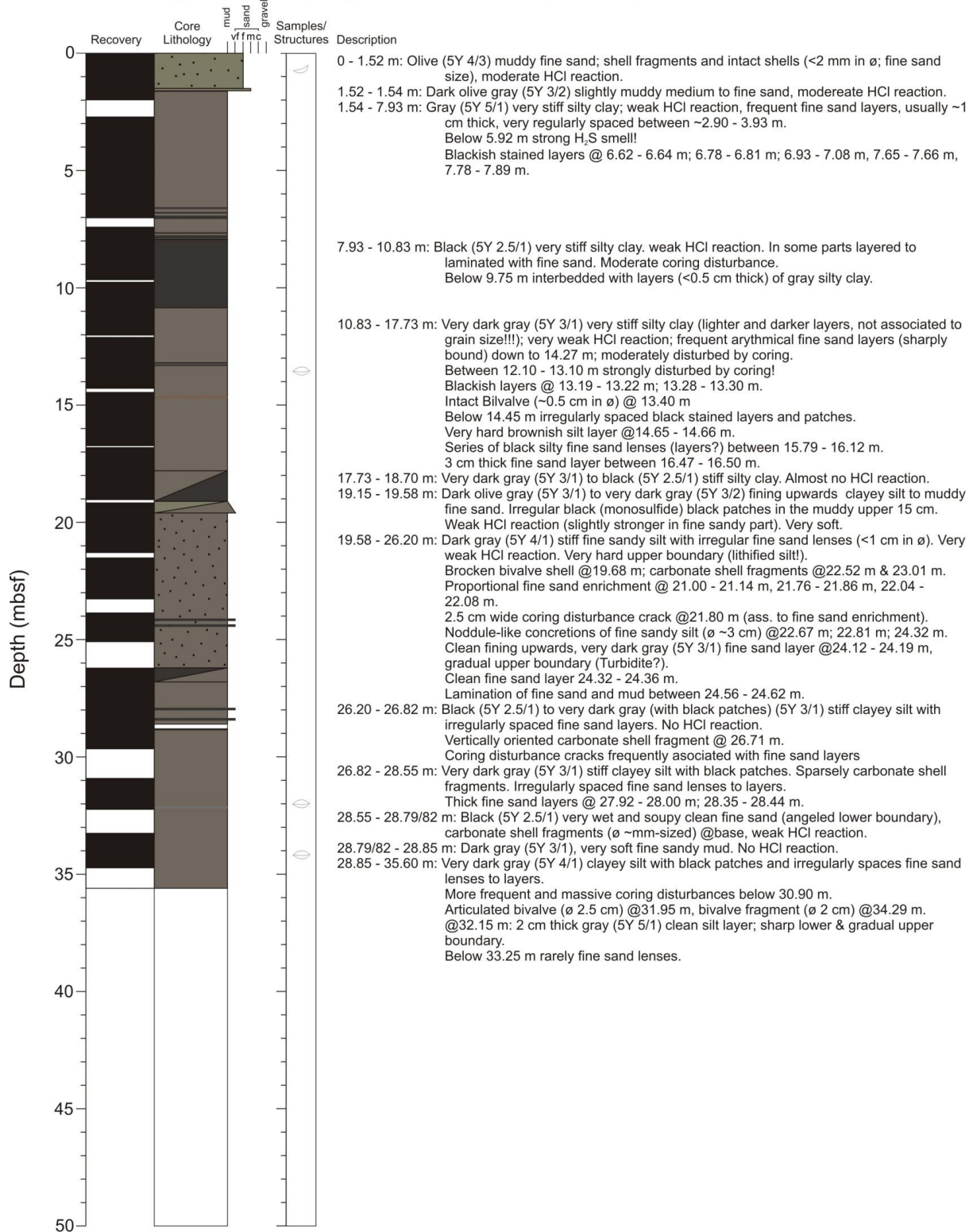
Meteor 78/3b GeoB core 13857-1

TD 802 cm Water depth 3076 m



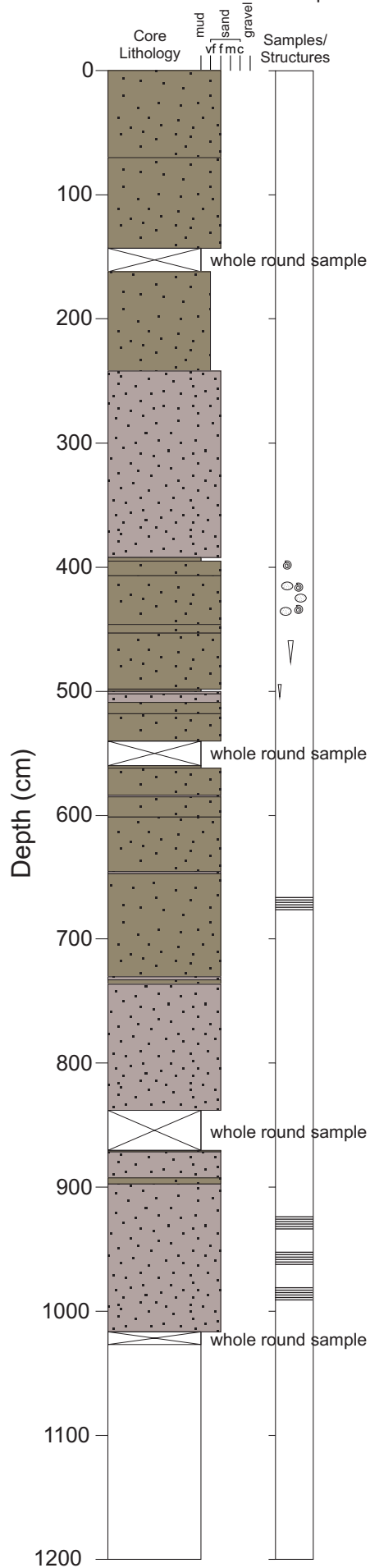
Meteor 78/3b GeoB 13860-1 (MeBo)

Total core length: 35,6 m Water depth: 1190 m Pos.: 36°06,65'S / 52°51,58'W



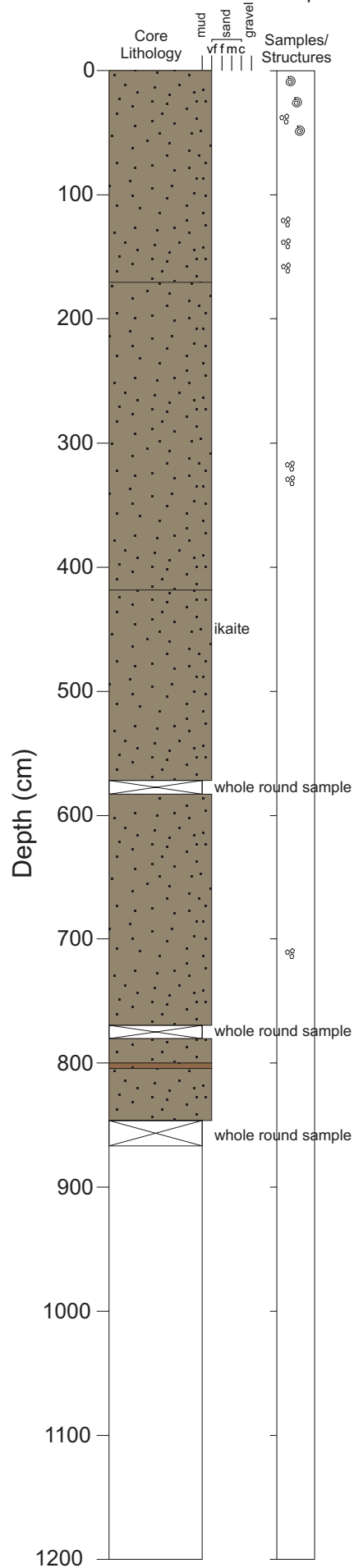
Meteor 78/3b GeoB core 13862-1

TD 1026 cm Water depth 3587 m



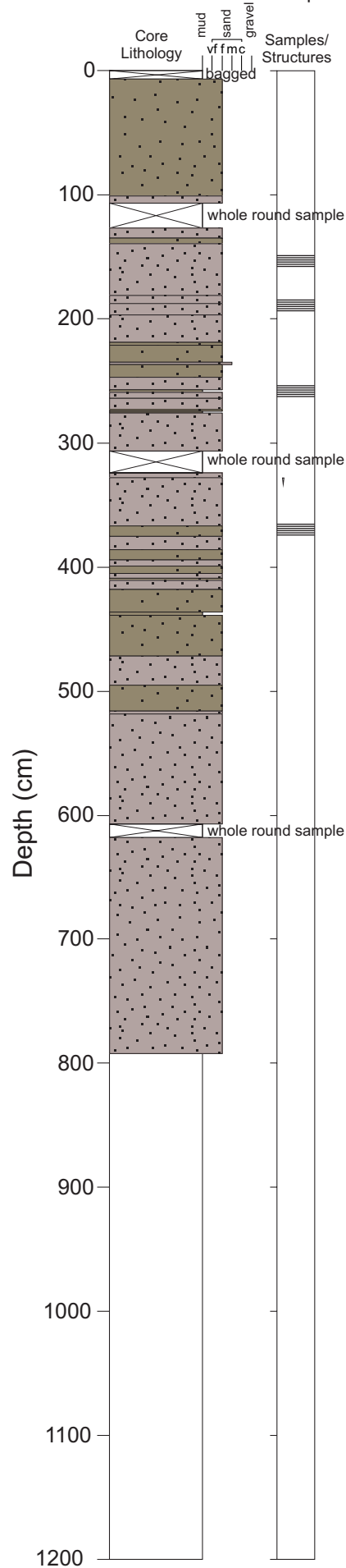
Meteor 78/3a GeoB core 13863

TD 856 cm Water depth 3687 m



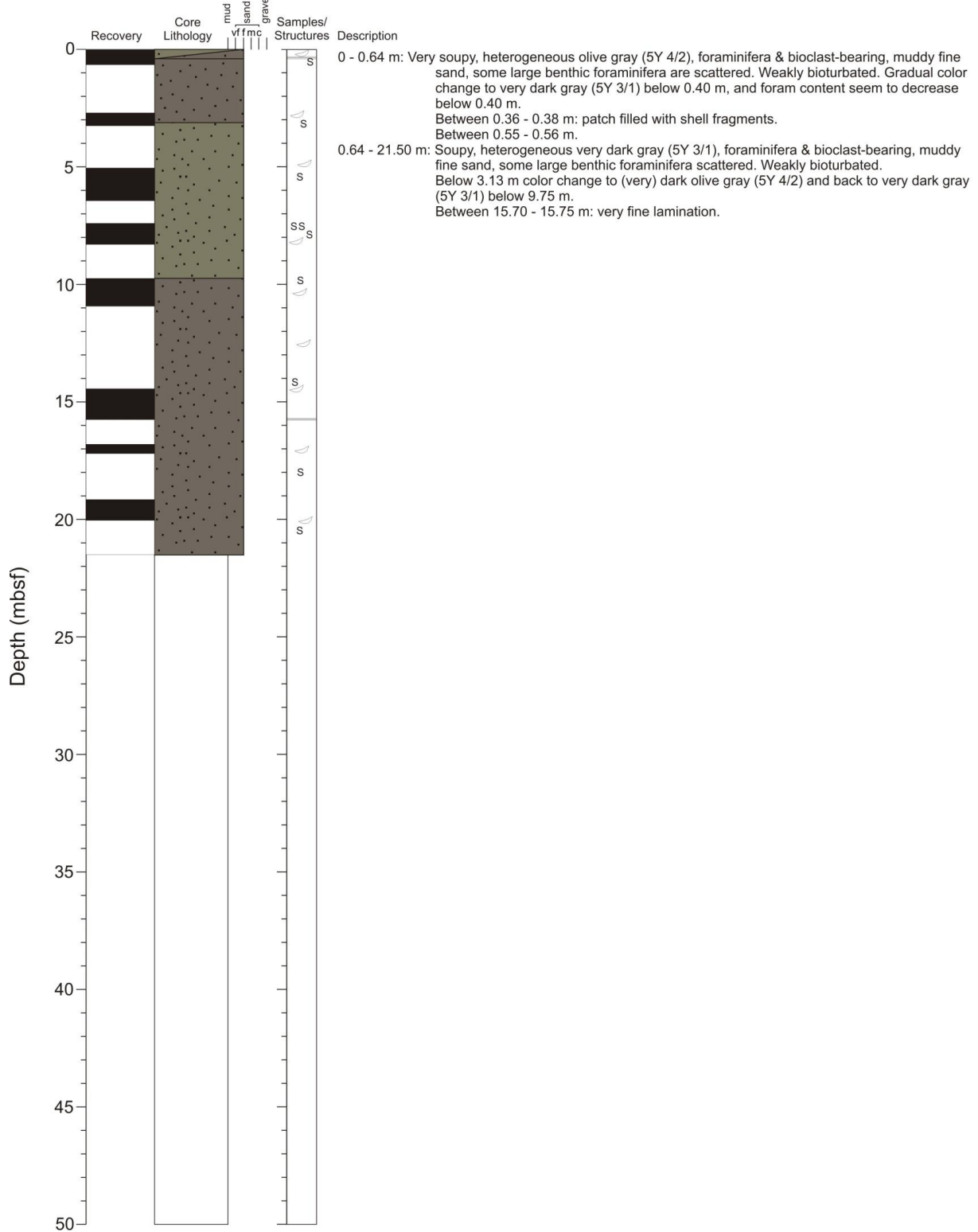
Meteor 78/3b GeoB core 13864-2

TD 792 cm Water depth 2757 m



Meteor 78/3b GeoB 13868-1 (MeBo)

Total core length: 7,27 m Water depth: 1145 m Pos.: 37°24,87'S / 53°43,32'W



Sign key



Magnetic susceptibility [10^{-6} SI] (not verified)



Water content [] (fraction relative to dry weight)



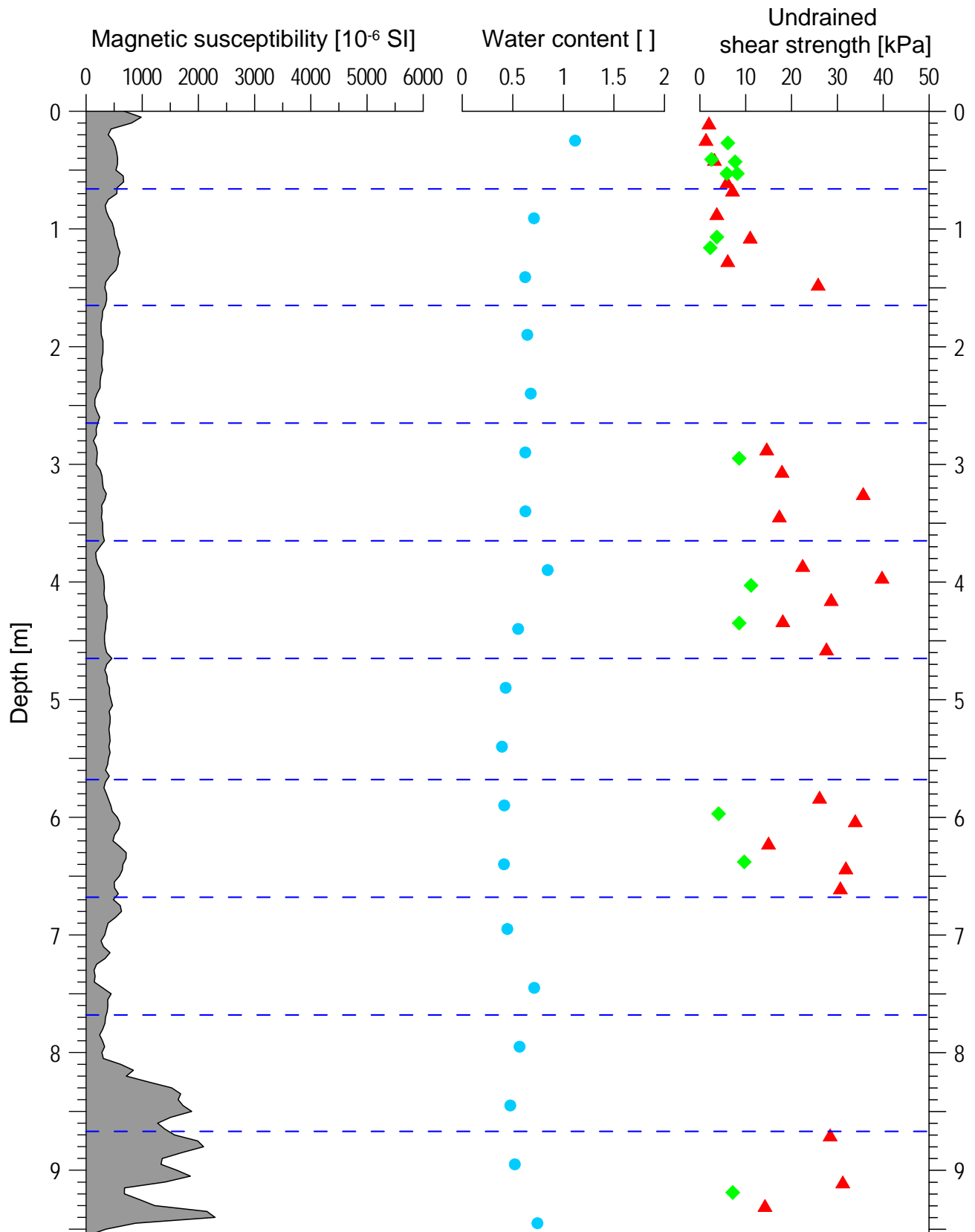
Undrained shear strength [kPa] (vane shear)



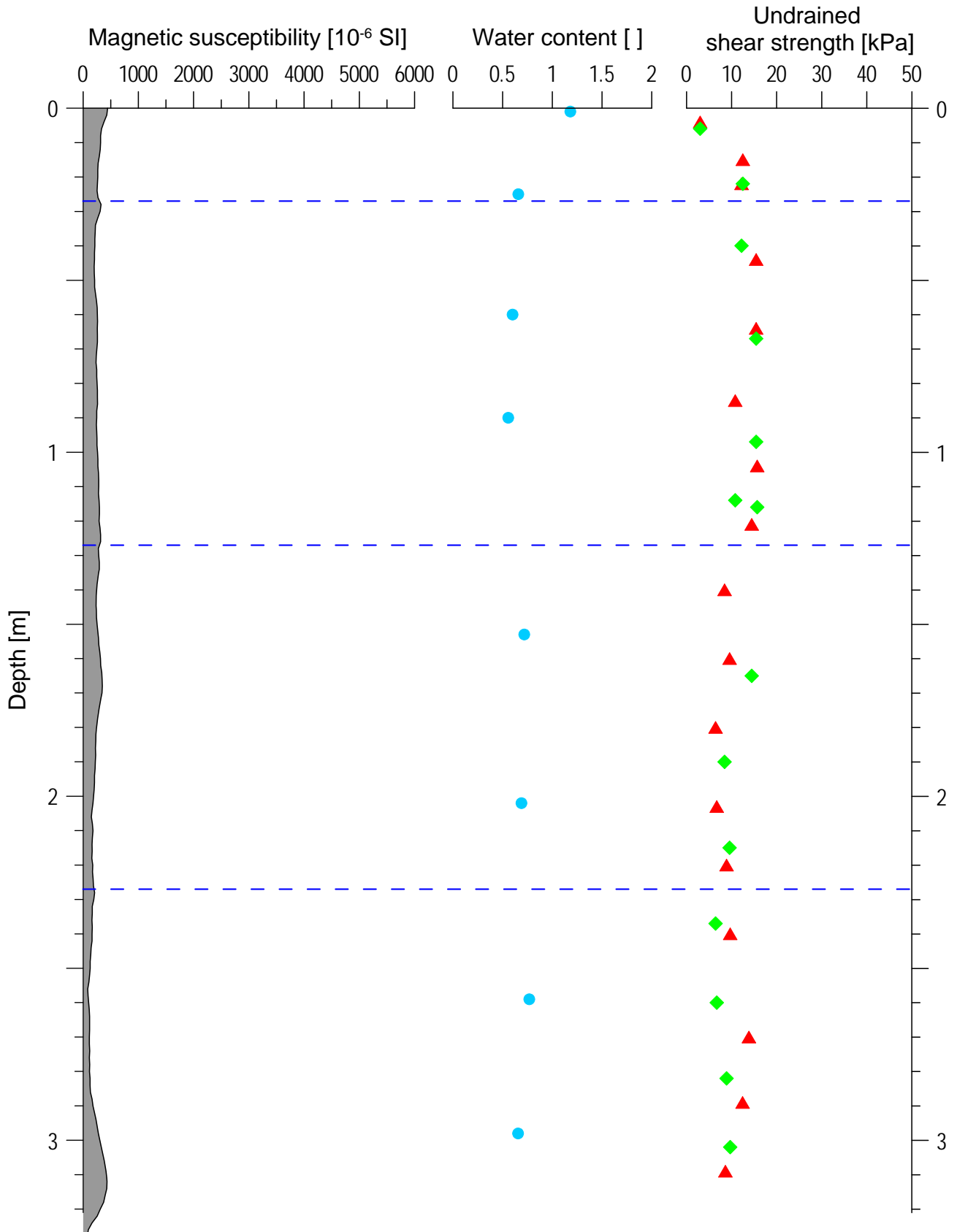
Undrained shear strength [kPa] (fall-cone penetrometer)

If blank plot existent, parameter not measured yet.

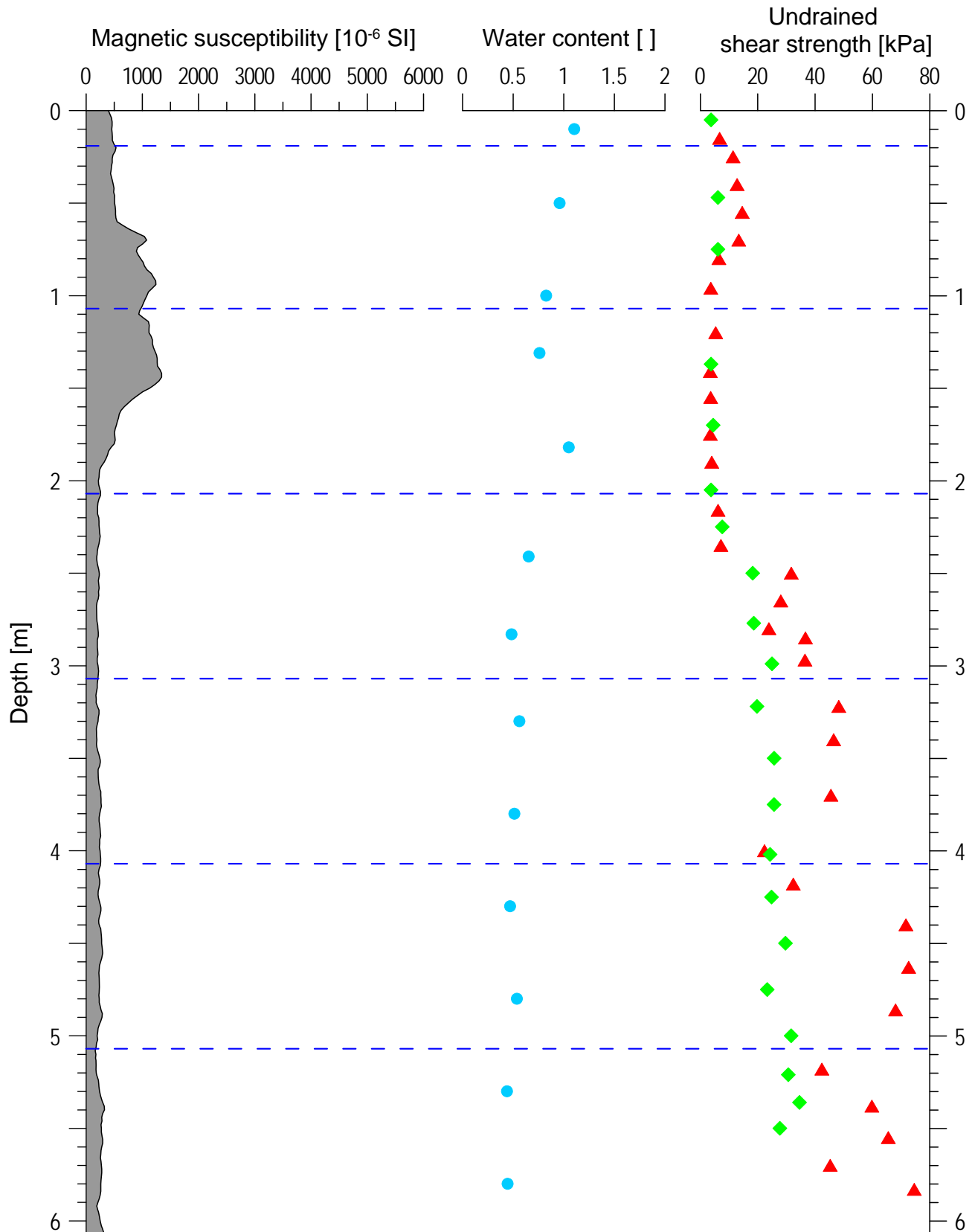
GeoB 13801-02 Date: 20.05.09 Position: 36° 08.49' S 53° 17.16' W
Water depth: 241.1 m Core length: 9.55 m



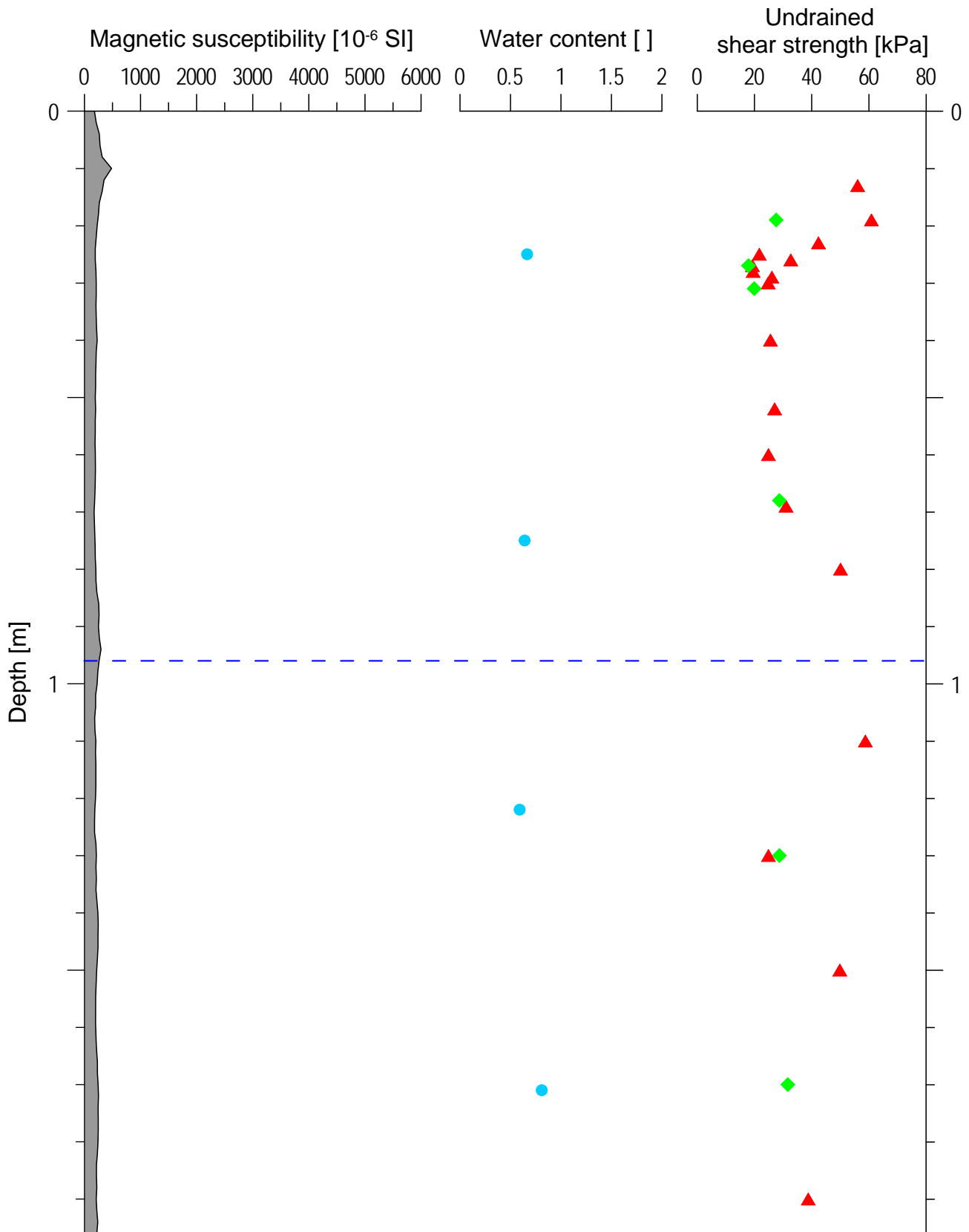
GeoB 13803-02 Date: 22.05.09 Position: 35° 52.65' S 52° 07.19' W
 Water depth: 2463.3 m Core length: 3.21 m



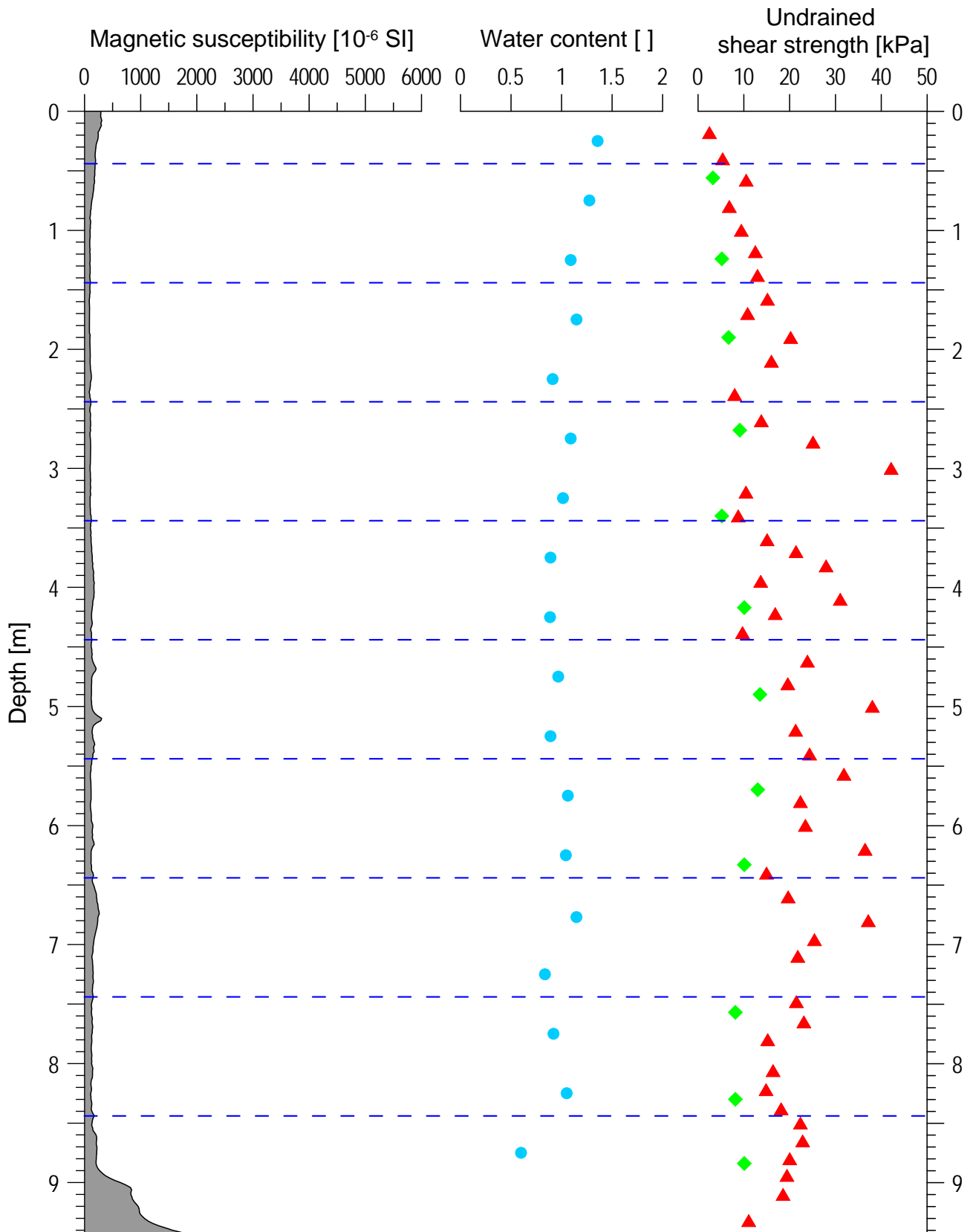
GeoB 13804-01 Date: 22.05.09 Position: 35° 54.30' S 52° 05.42' W
Water depth: 2578.6 m Core length: 6.08 m



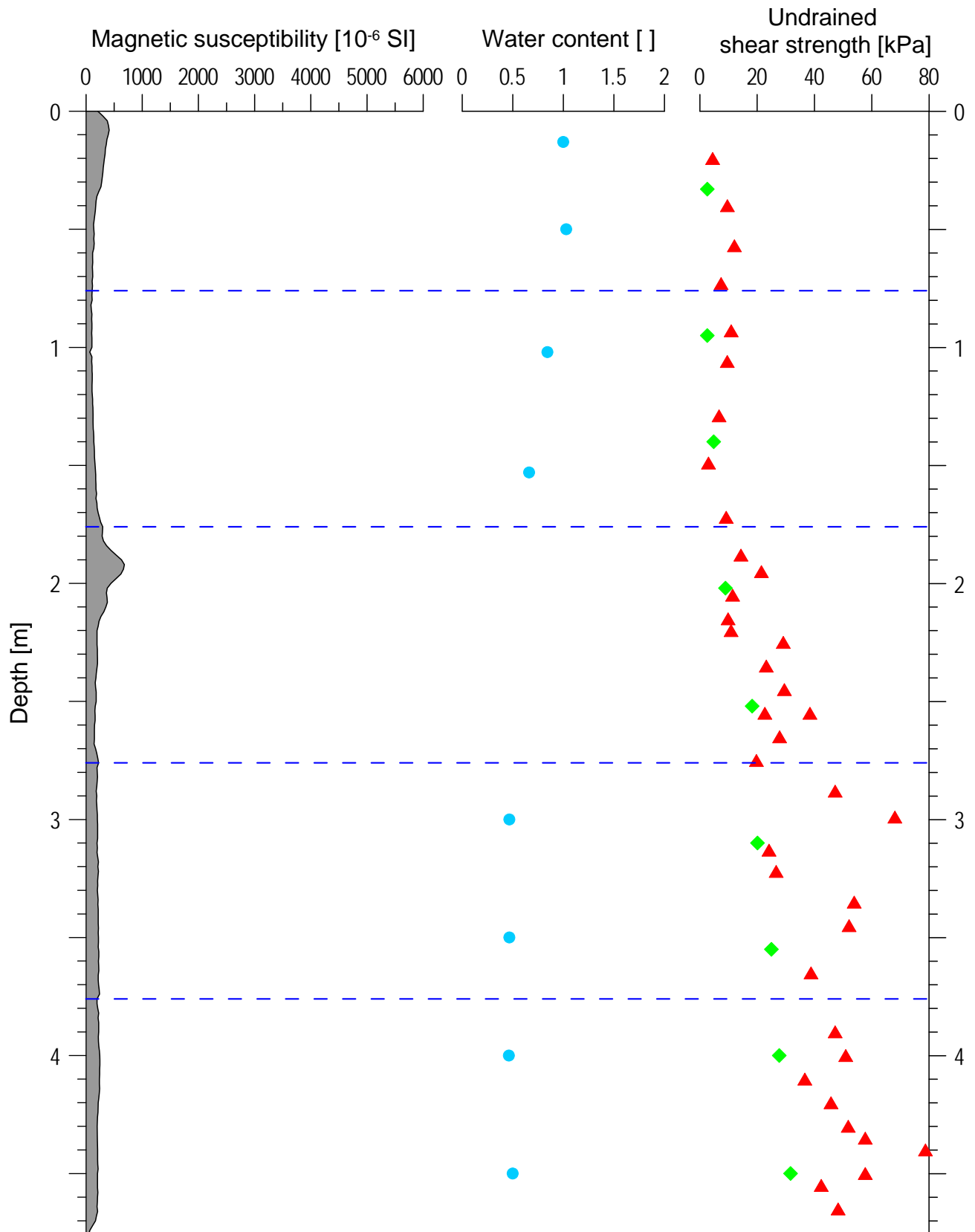
GeoB 13805-02 Date: 22.05.09 Position: 35° 53.02' S 52° 06.79' W
Water depth: 2522 m Core length: 1.96 m



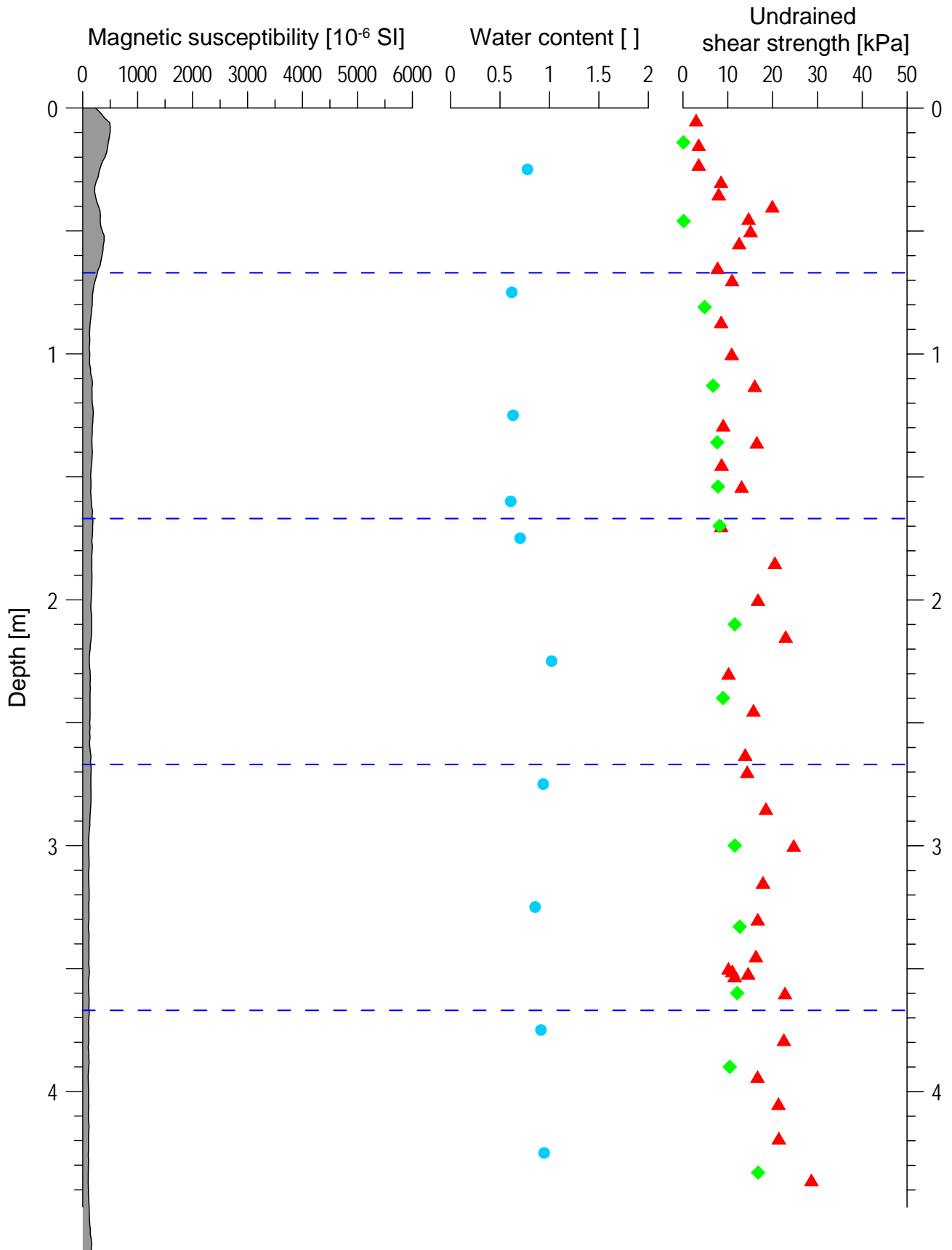
GeoB 13806-01 Date: 23.05.09 Position: 35° 52.82' S 52° 04.61' W
Water depth: 2575 m Core length: 9.44 m



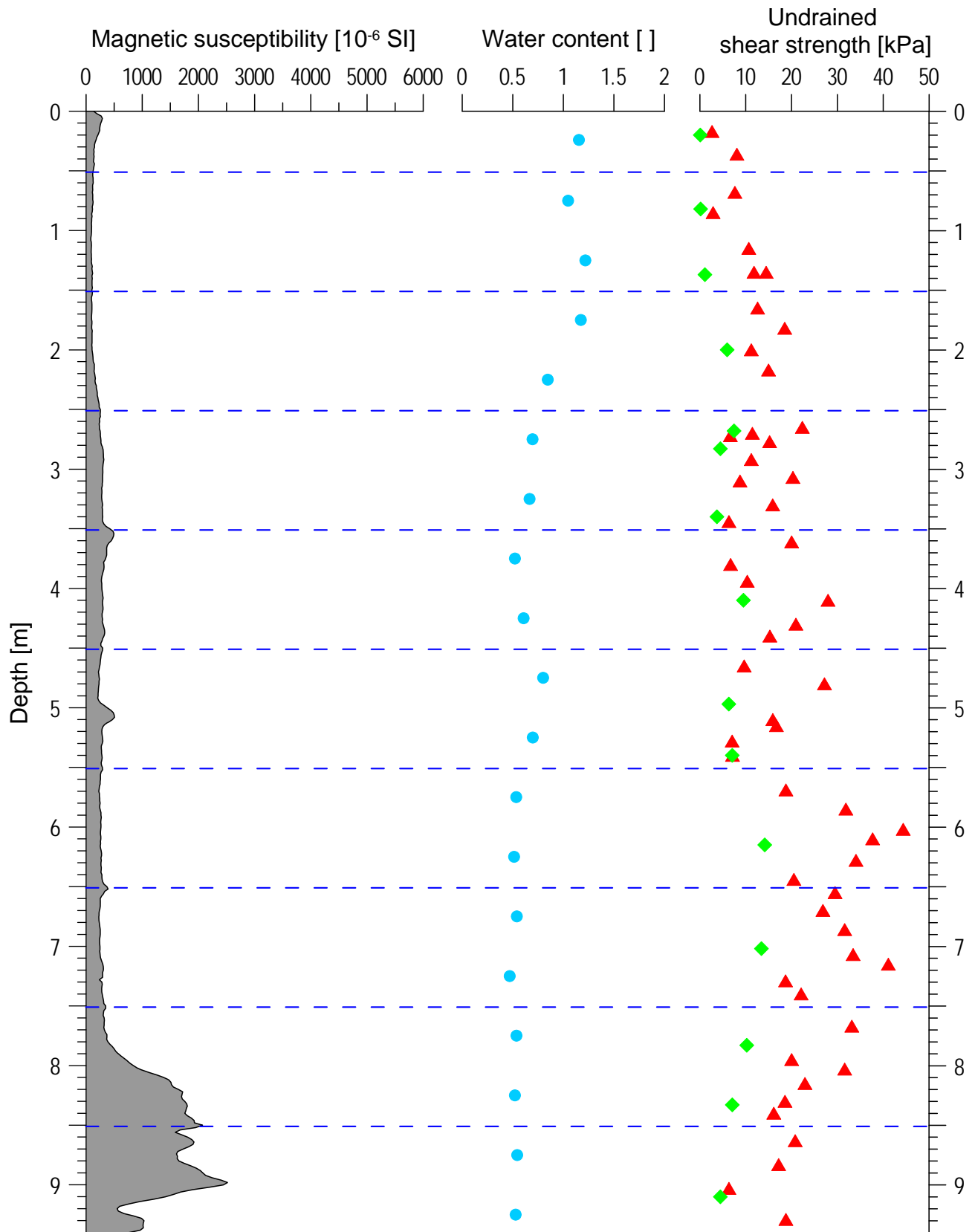
GeoB 13807-01 Date: 23.05.09 Position: 35° 52.29' S 52° 05.15' W
Water depth: 2557 m Core length: 4.76 m



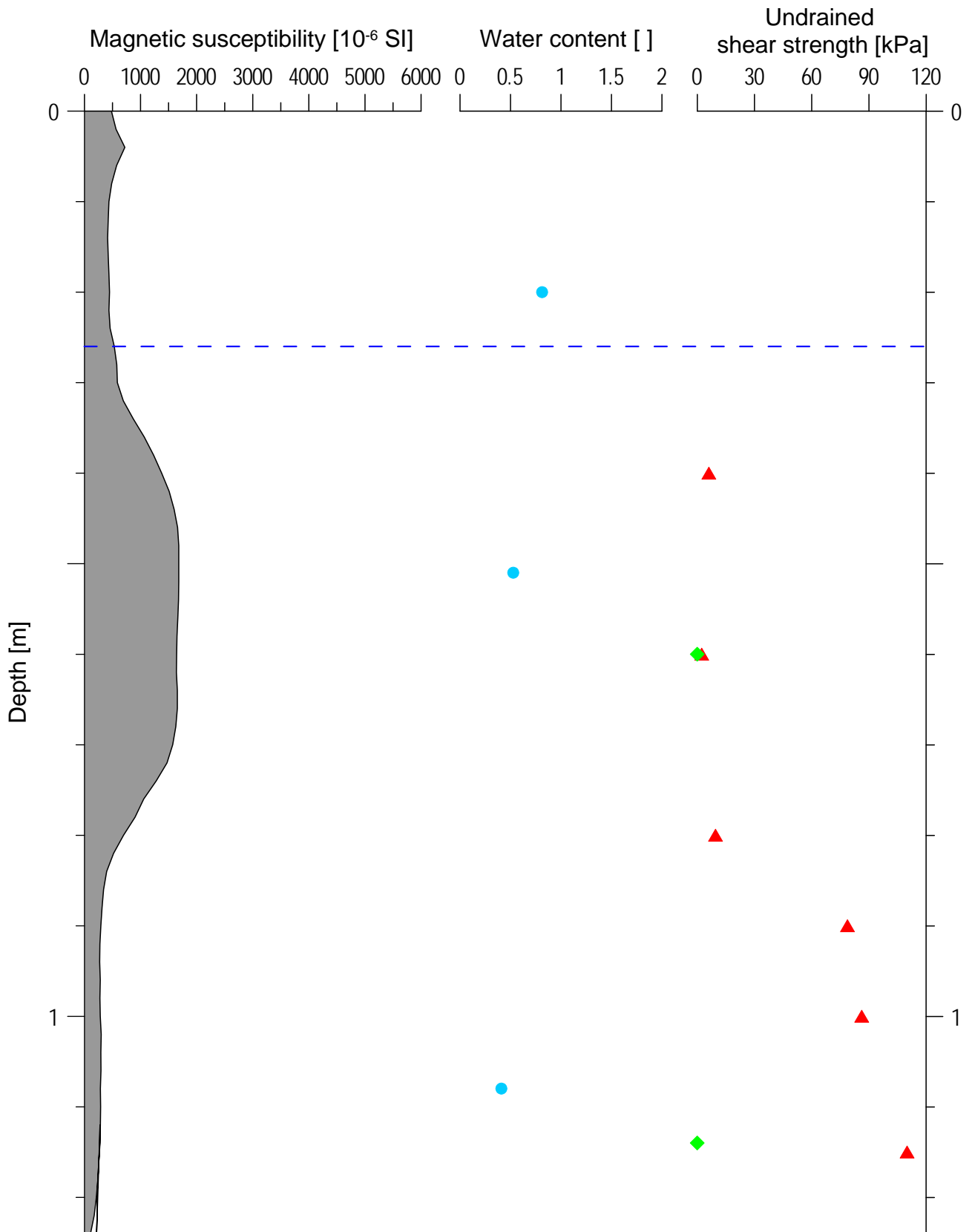
GeoB 13808-01 Date: 23.05.09 Position: 35° 49.85' S 52° 07.76' W
 Water depth: 2312 m Core length: 4.47 m



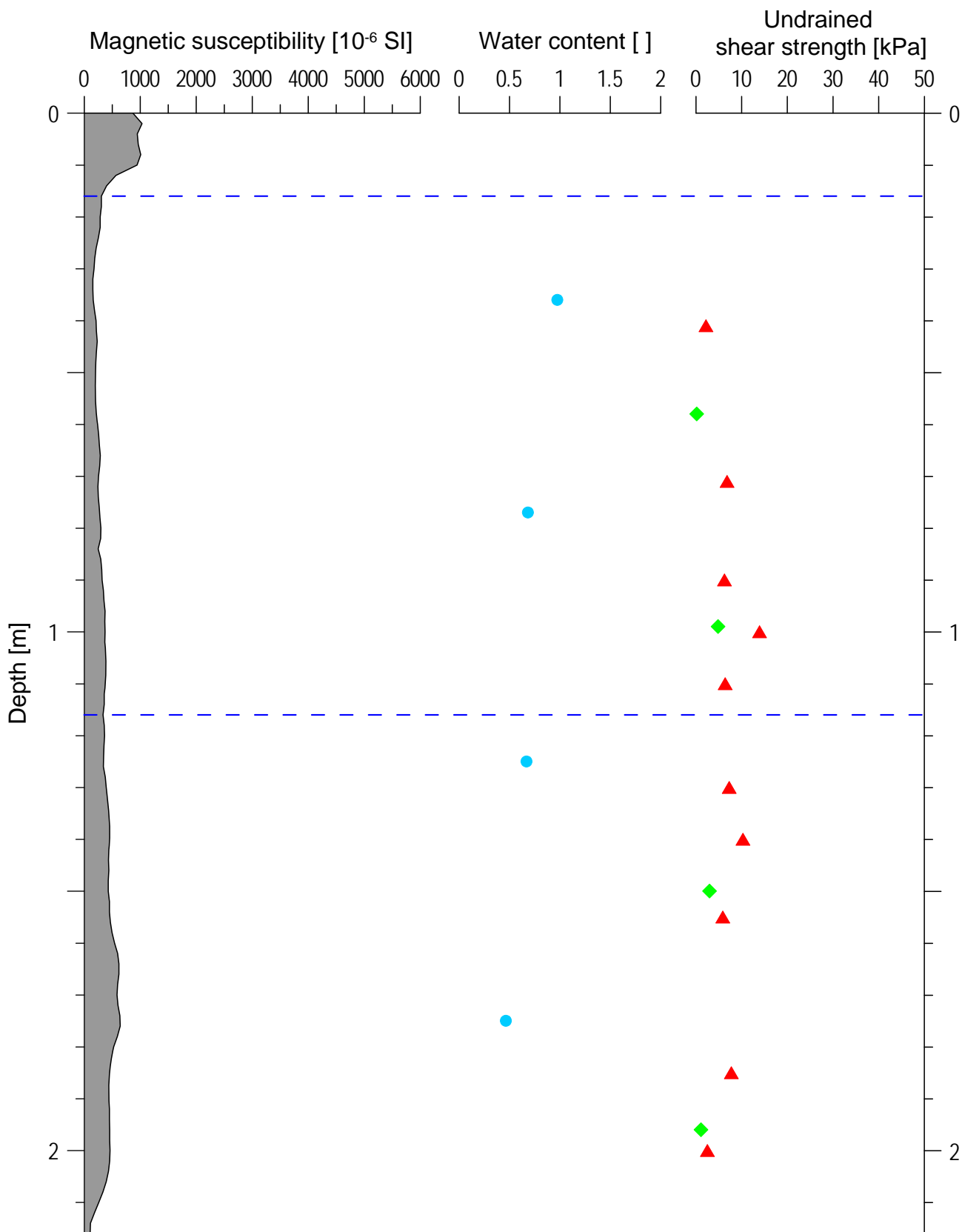
GeoB 13809-01 Date: 25.05.09 Position: 36° 07.67' S 52° 49.90' W
Water depth: 1402.5 m Core length: 9.42 m



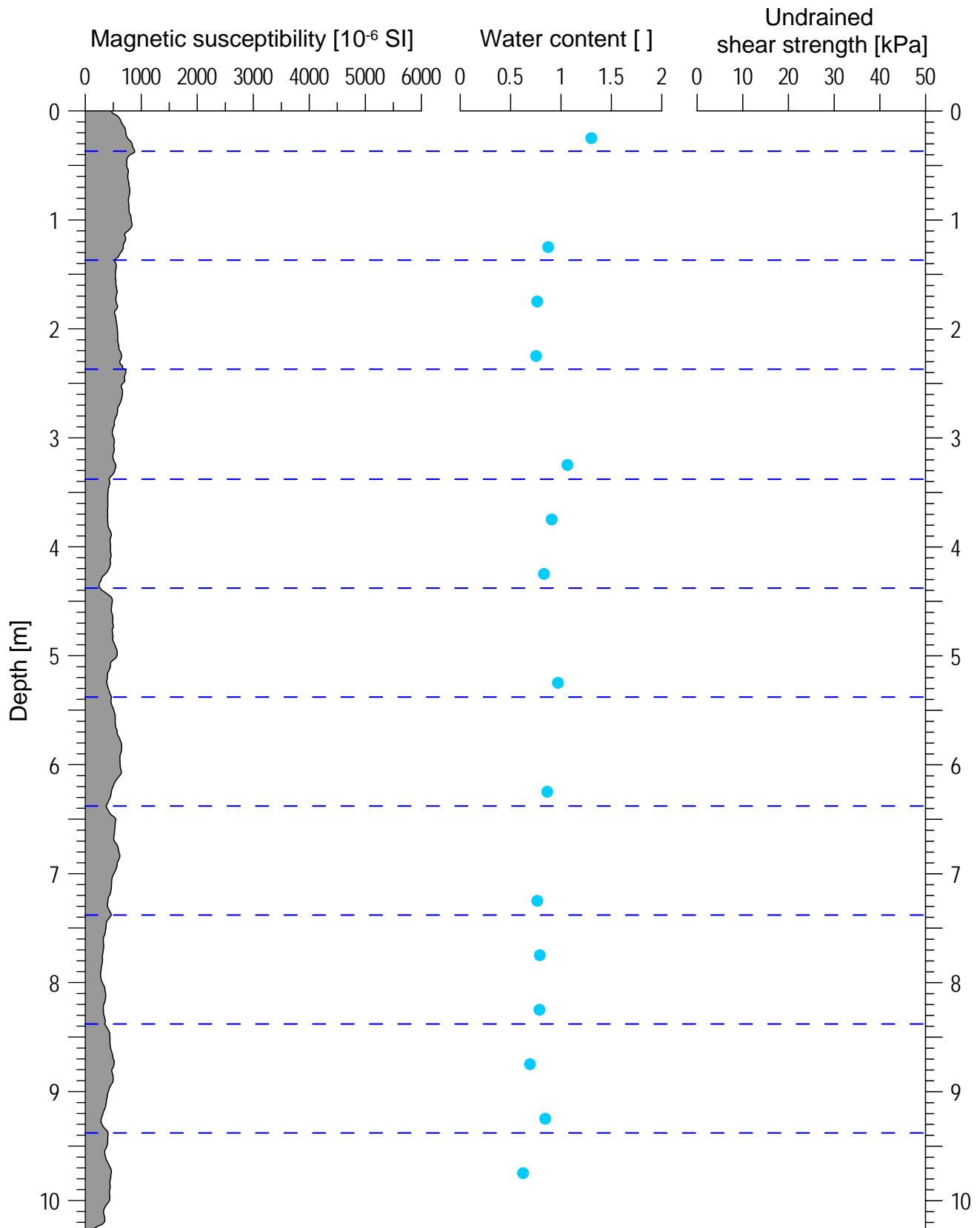
GeoB 13810-01 Date: 25.05.09 Position: 36° 06.04' S 52° 52.49' W
Water depth: 1150 m Core length: 1.24 m



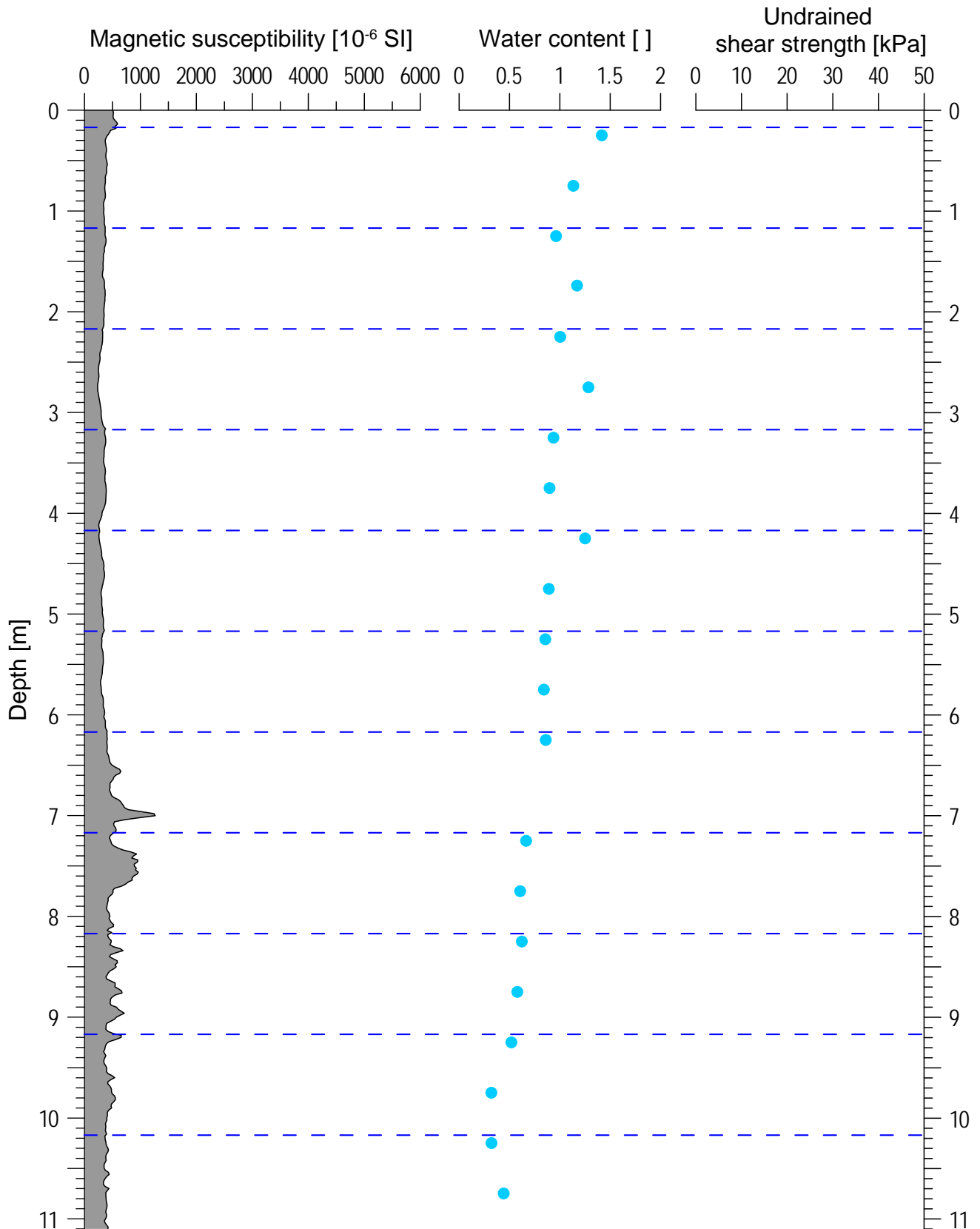
GeoB 13811-01 Date: 25.05.09 Position: 36° 06.61' S 52° 51.56' W
 Water depth: 1210.6 m Core length: 2.16 m



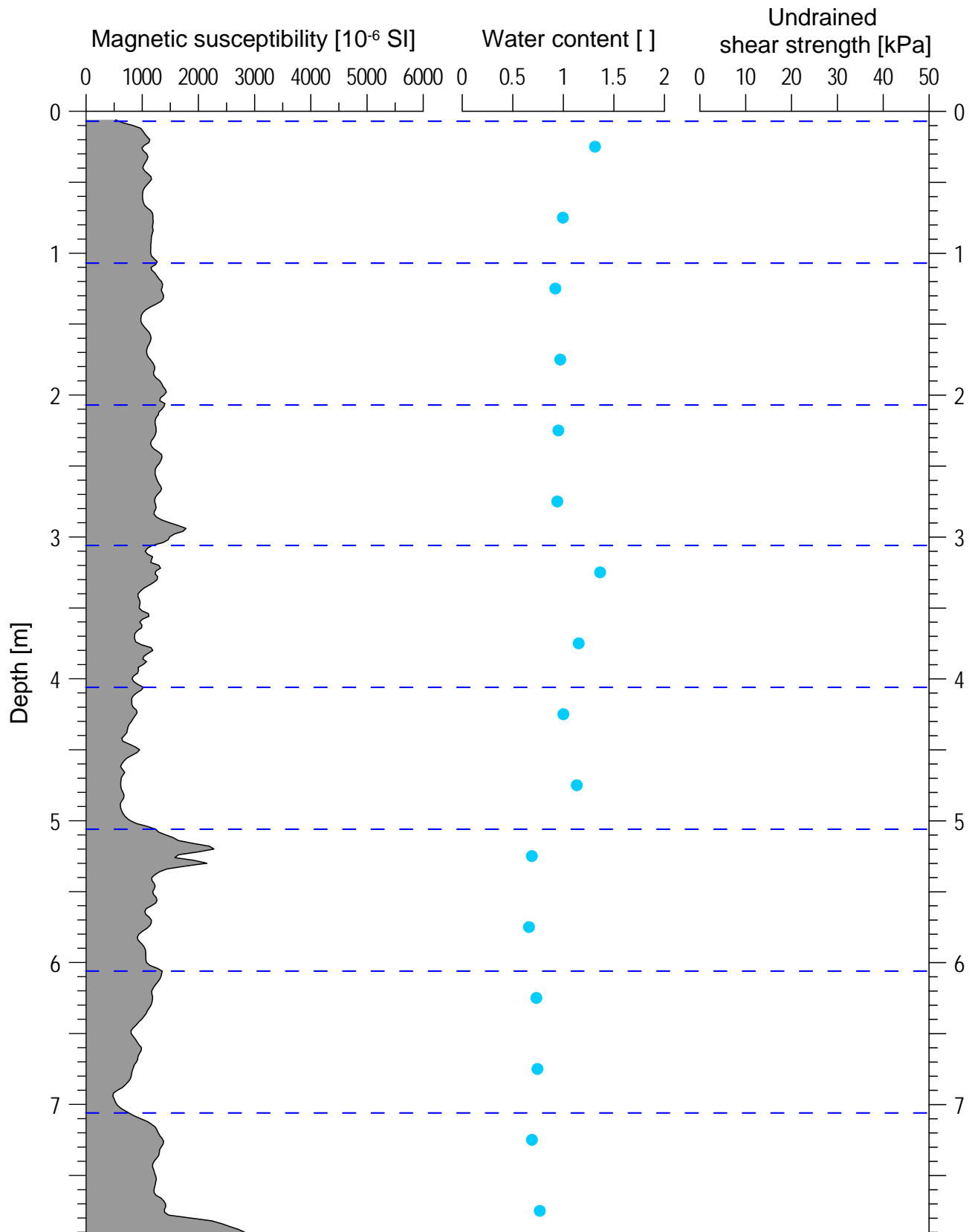
GeoB 13813-04 Date: 27.05.09 Position: 34° 44.22' S 53° 33.27' W
Water depth: 57.1 m Core length: 10.28 m



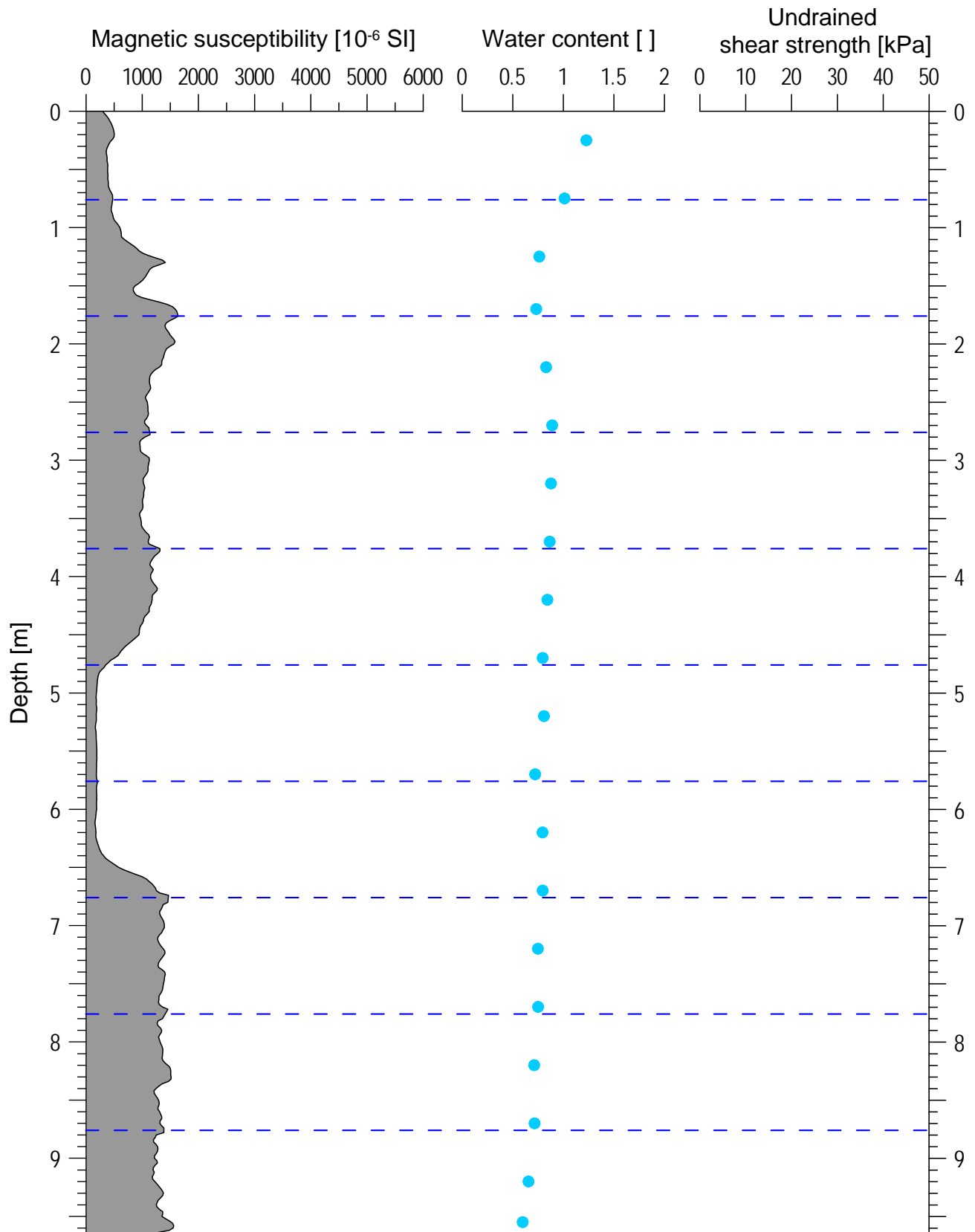
GeoB 13817-02 Date: 28.05.09 Position: 34° 27.55' S 53° 04.52' W
Water depth: 61.9 m Core length: 11.11 m



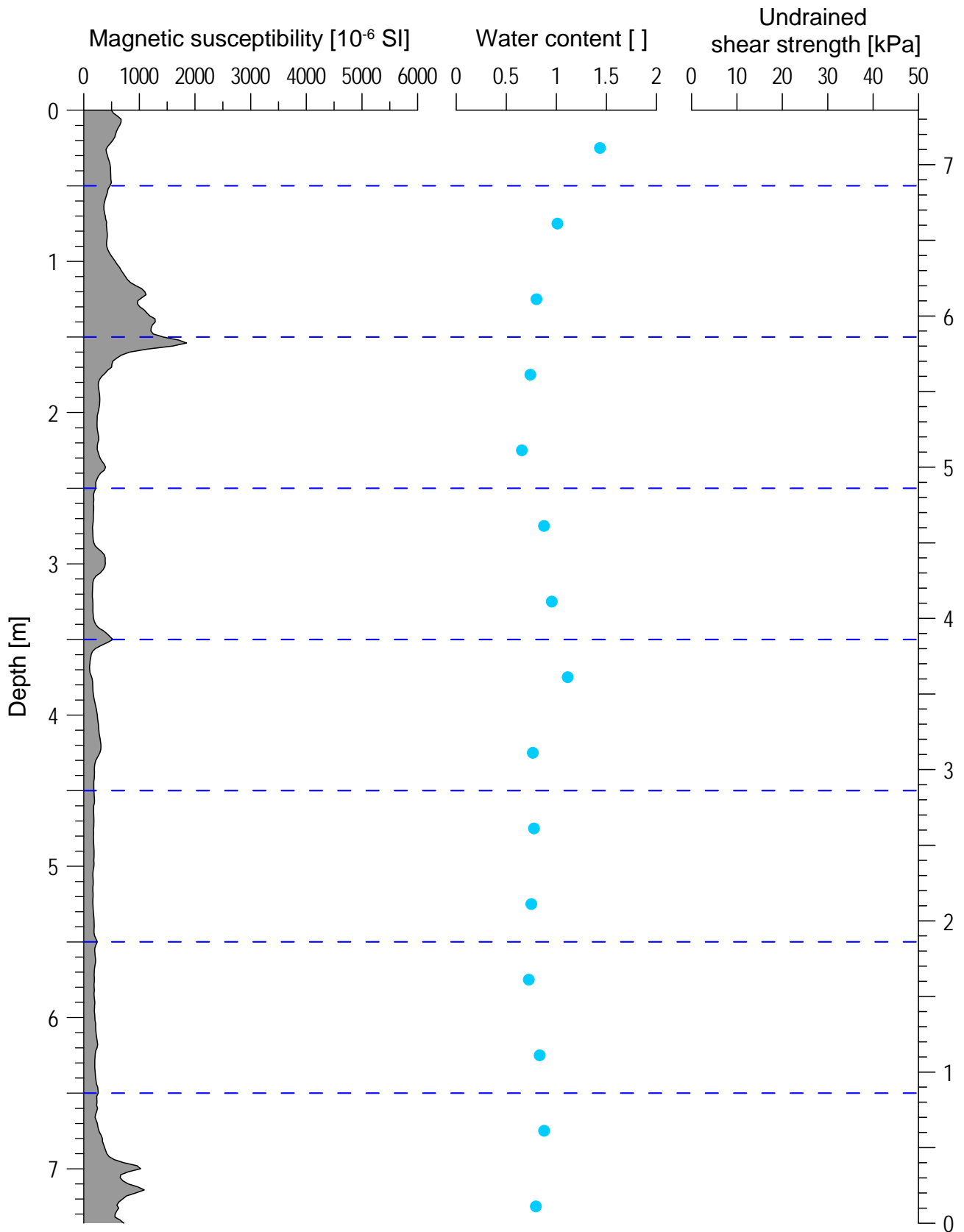
GeoB 13819-02 Date: 31.05.09 Position: 39° 29.44' S 53° 42.56' W
Water depth: 4274 m Core length: 7.92 m



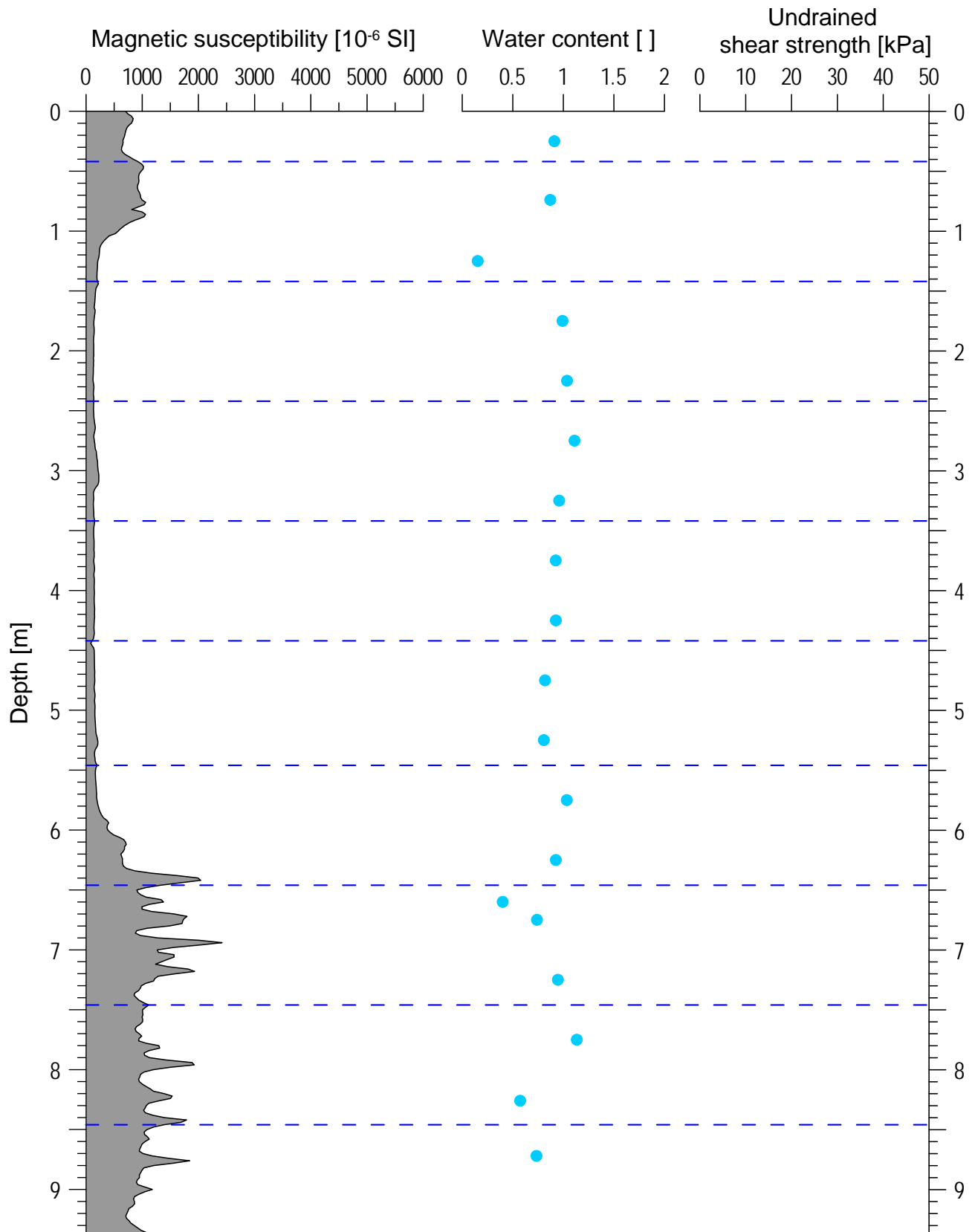
GeoB 13820-01 Date: 31.05.09 Position: 39° 18.06' S 53° 58.03' W
Water depth: 3613.8 m Core length: 9.66 m



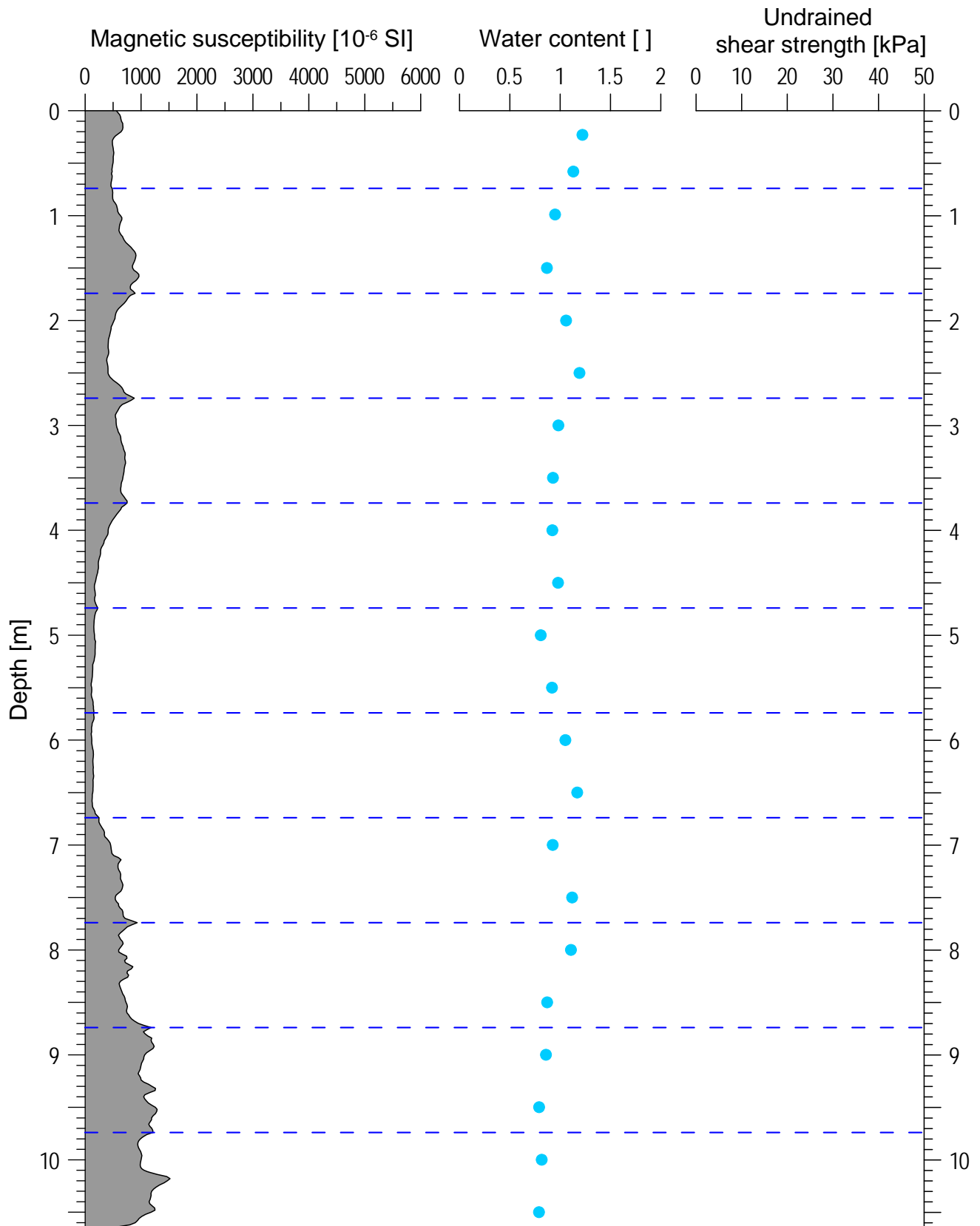
GeoB 13821-02 Date: 01.06.09 Position: 38° 06.57' S 53° 31.02' W
 Water depth: 3555.5 m Core length: 7.36 m



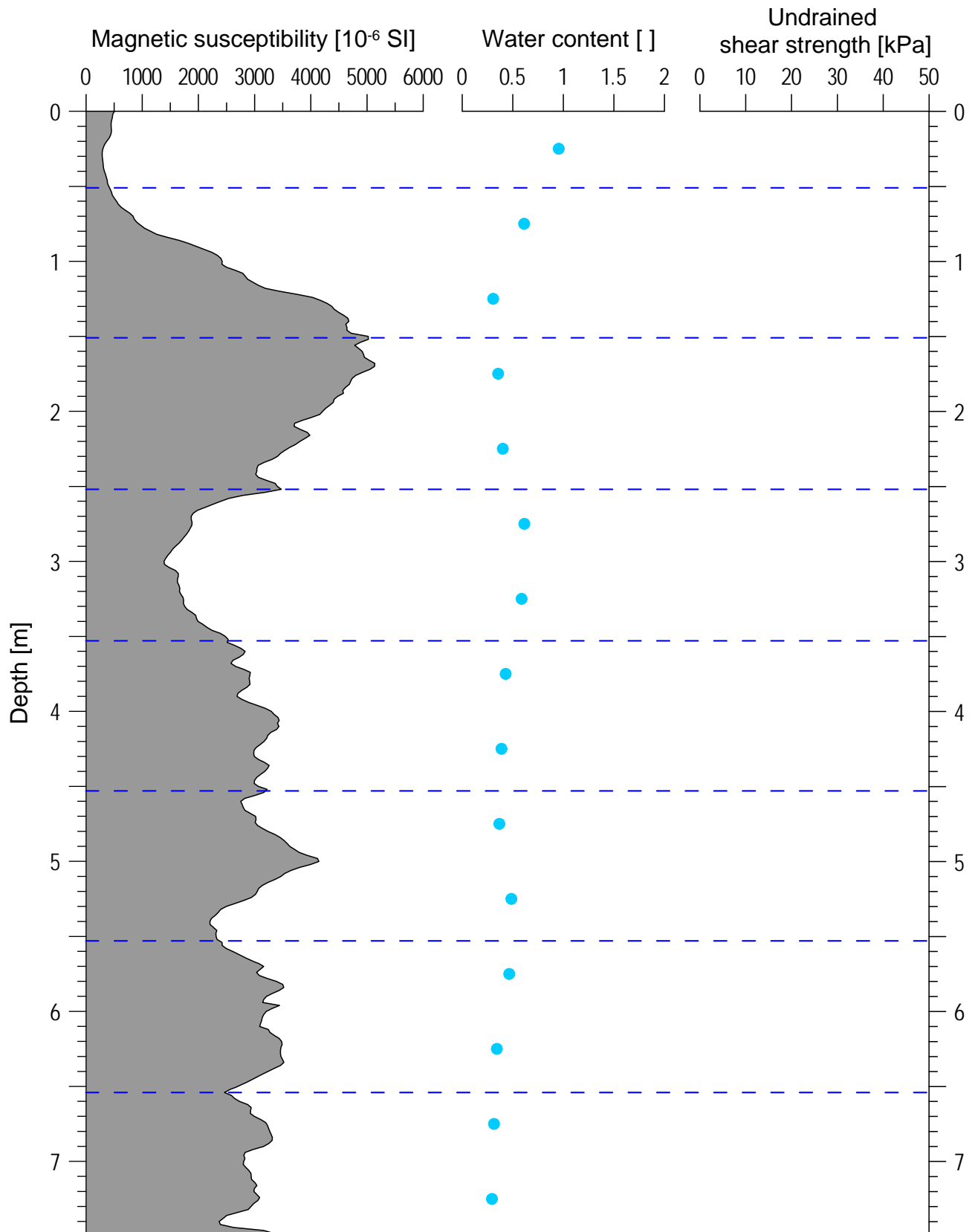
GeoB 13823-02 Date: 03.06.09 Position: 38° 08.68' S 53° 20.64' W
Water depth: 3780 m Core length: 9.38 m



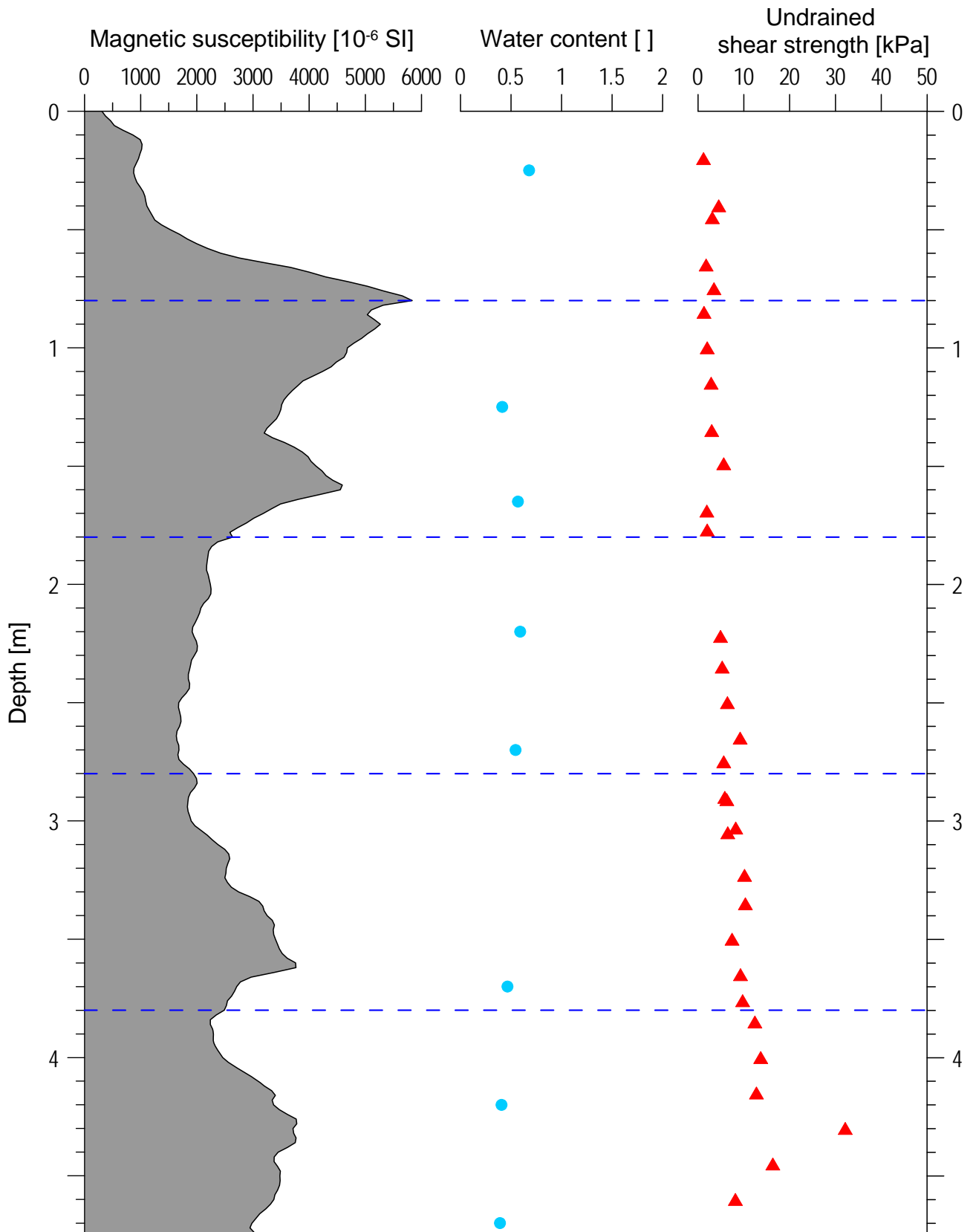
GeoB 13824-01 Date: 03.06.09 Position: 38° 13.14' S 53° 21.29' W
Water depth: 3819 m Core length: 10.66 m



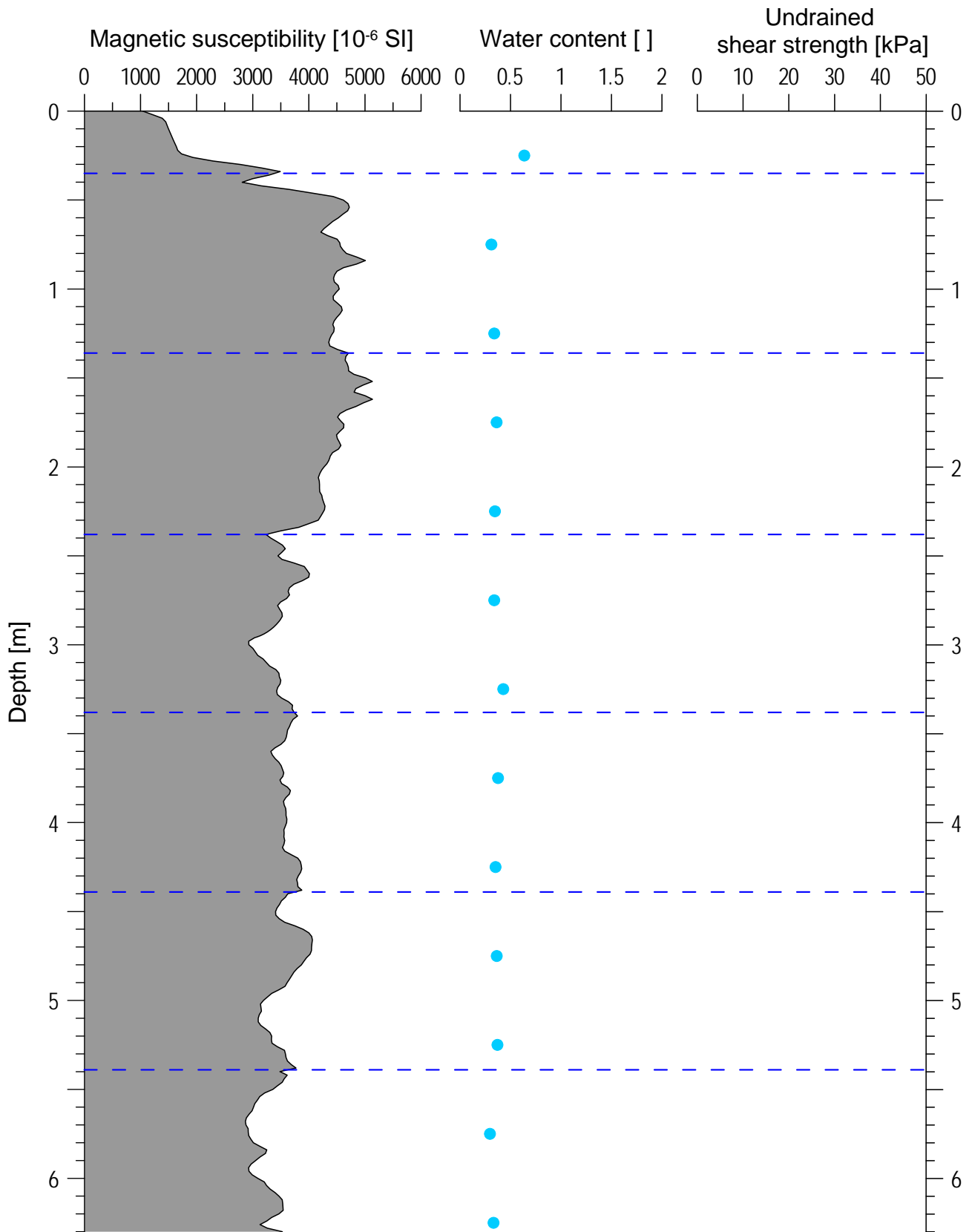
GeoB 13825-02 Date: 06.06.09 Position: 37° 16.72' S 53° 40.80' W
Water depth: 1228 m Core length: 7.49 m



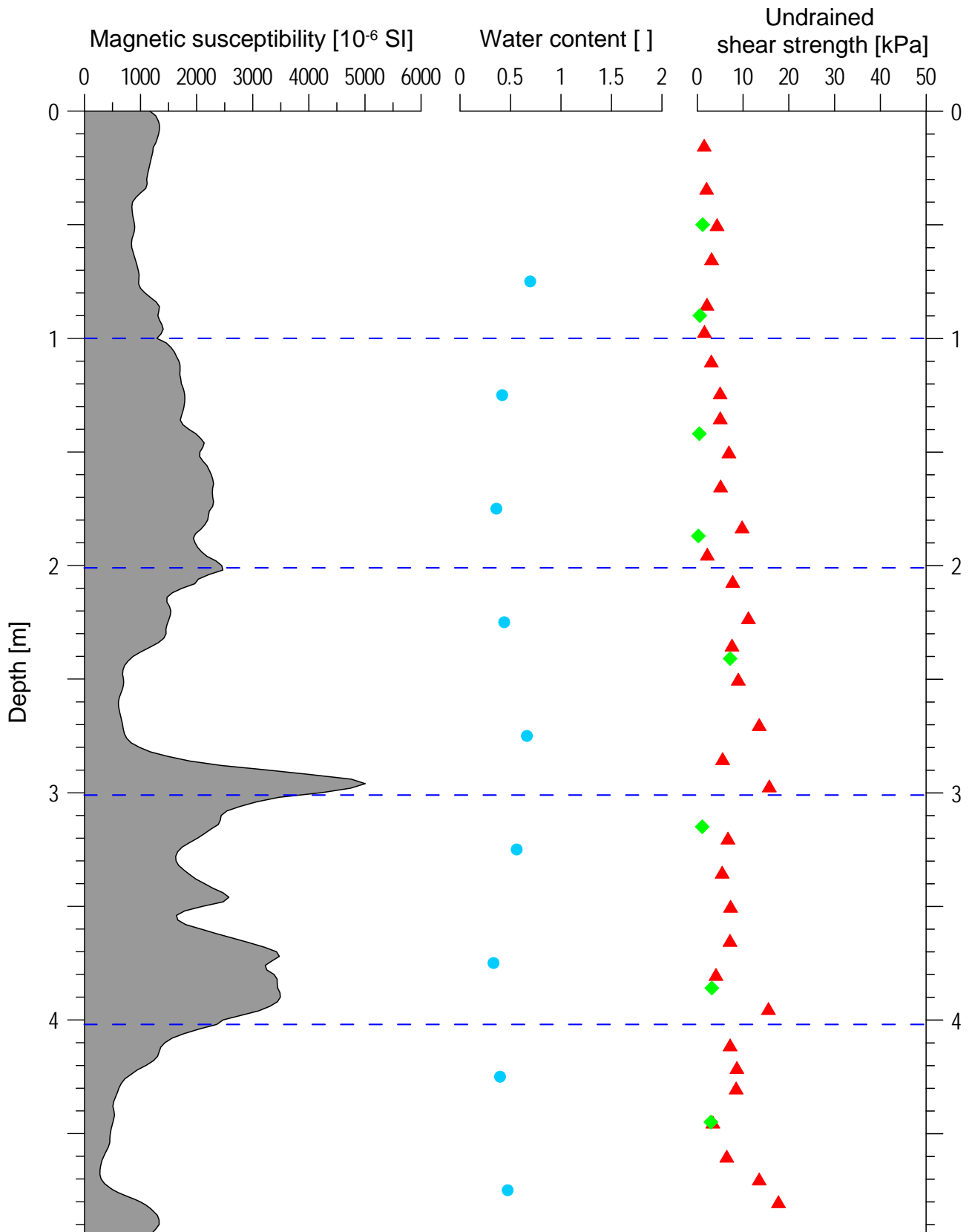
GeoB 13826-01 Date: 06.06.09 Position: 37° 14.44' S 53° 43.83' W
 Water depth: 1224 m Core length: 4.75 m



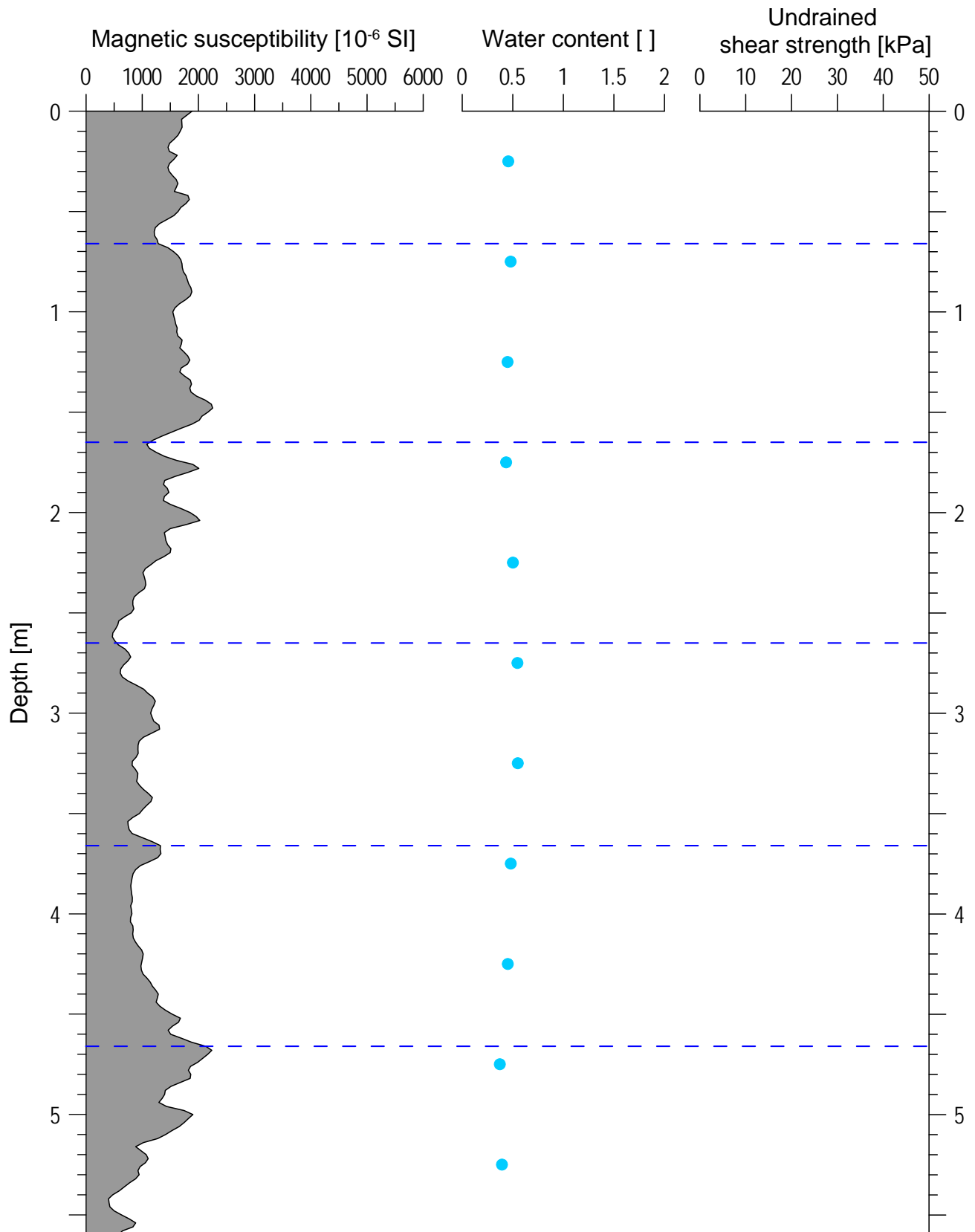
GeoB 13827-02 Date: 06.06.09 Position: 37° 24.93' S 53° 43.33' W
 Water depth: 1155 m Core length: 6.31 m



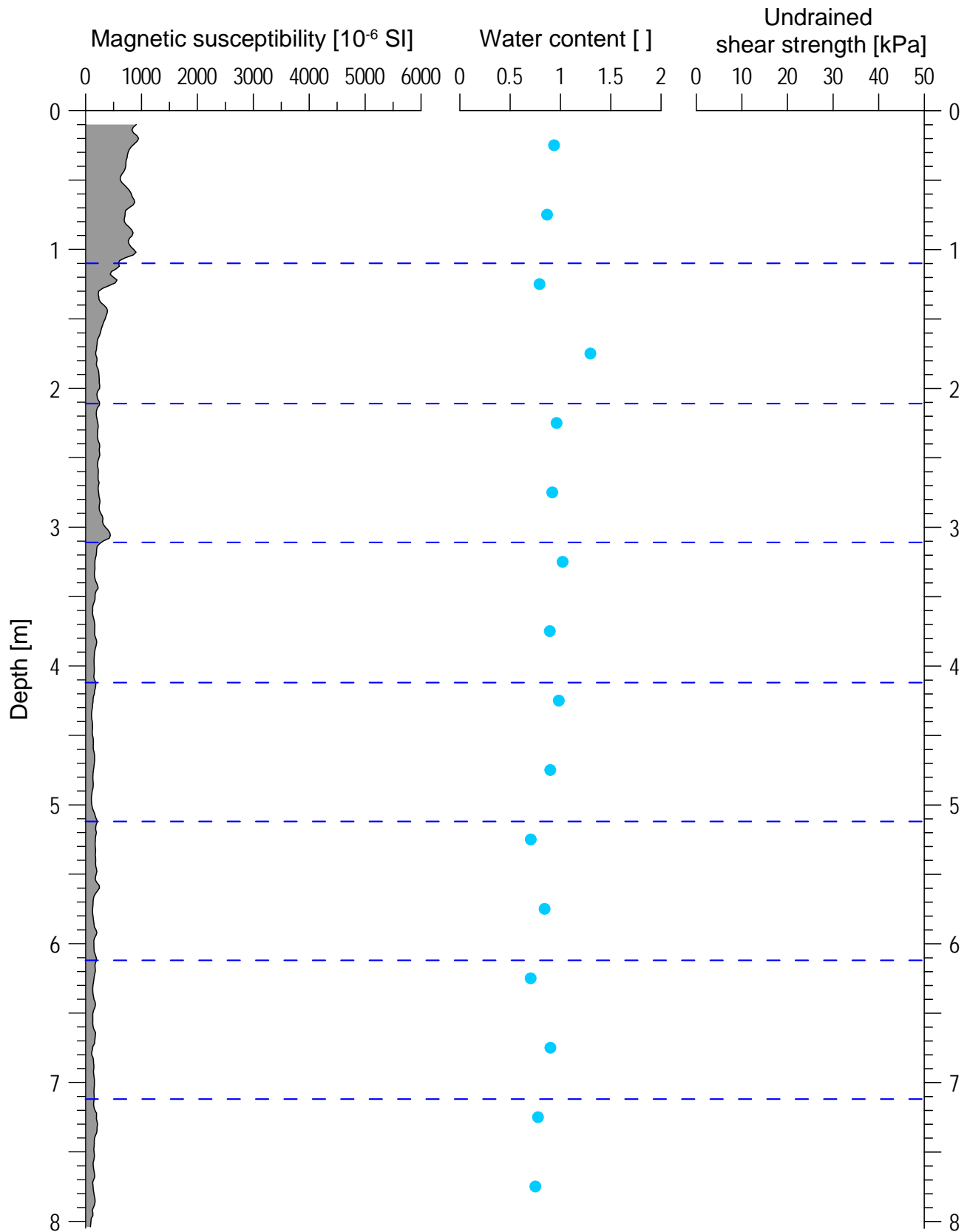
GeoB 13828-01 Date: 06.06.09 Position: 37° 32.39' S 53° 33.54' W
 Water depth: 1730 m Core length: 4.94 m



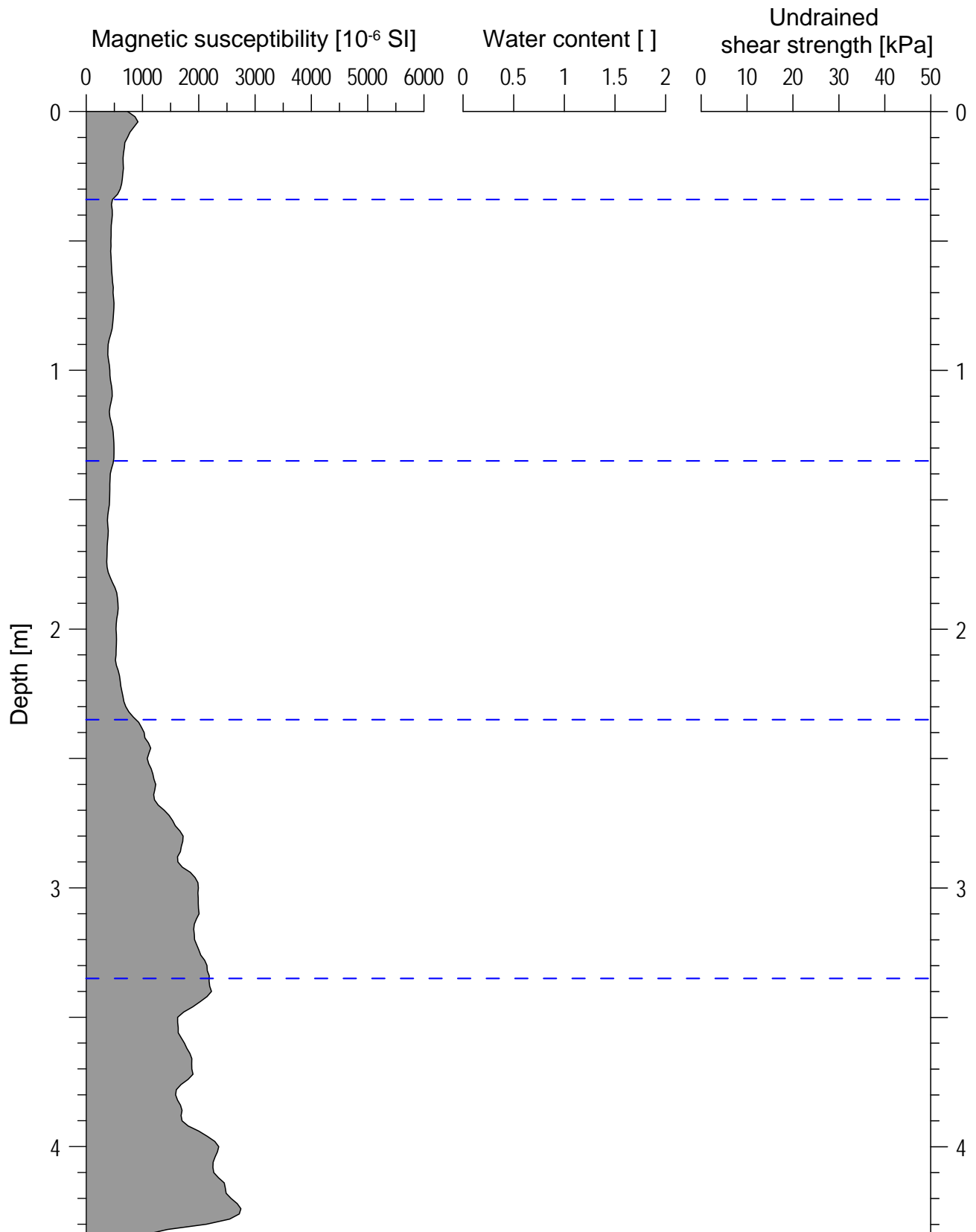
GeoB 13832-02 Date: 07.06.09 Position: 37° 54.15' S 54° 08.44' W
Water depth: 2205 m Core length: 5.60 m



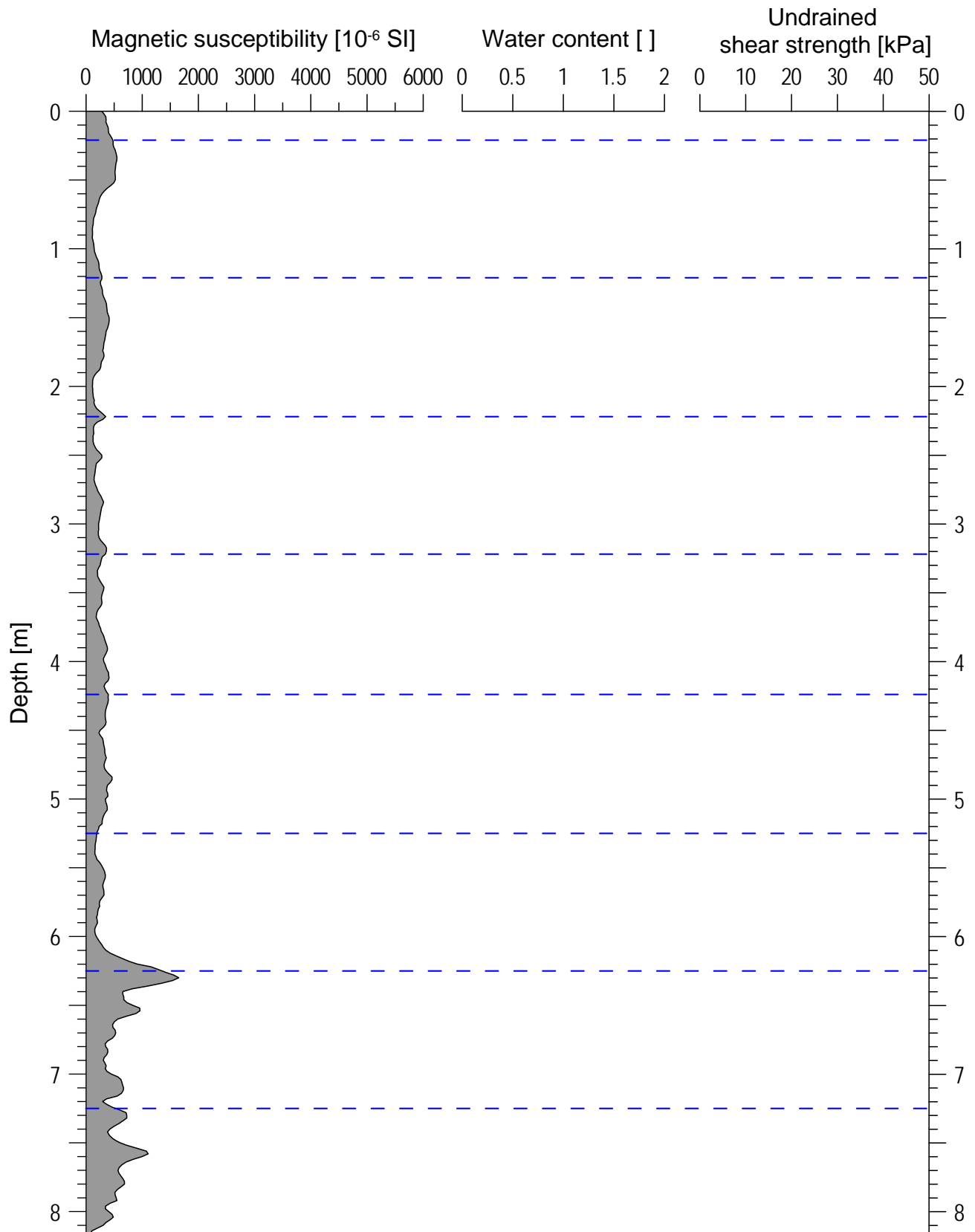
GeoB 13833-02 Date: 07.06.09 Position: 37° 57.45' S 53° 50.21' W
Water depth: 3362 m Core length: 8.05 m



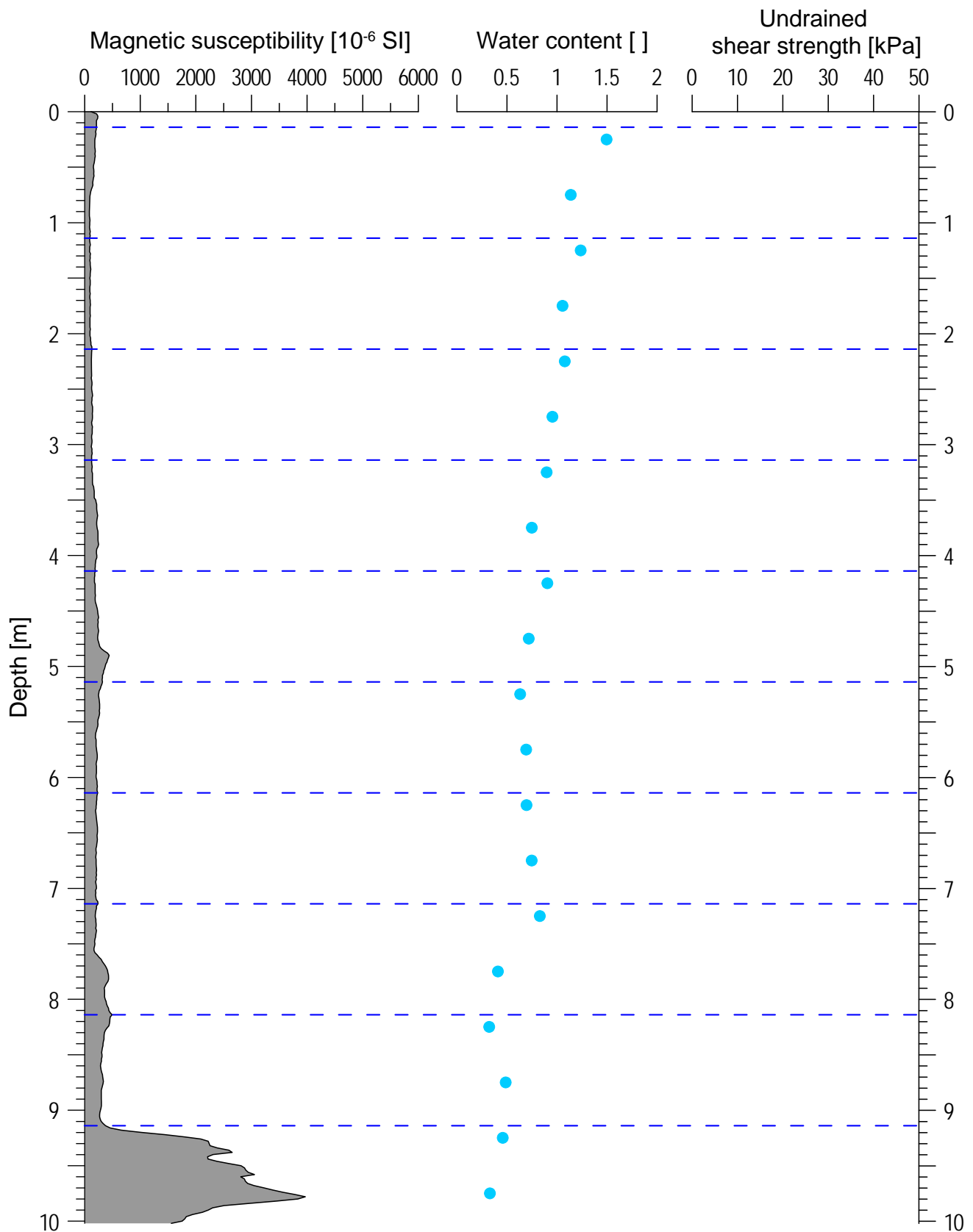
GeoB 13835-03 Date: 11.06.09 Position: 35° 43.11' S 53° 05.14' W
Water depth: 131 m Core length: 4.35 m



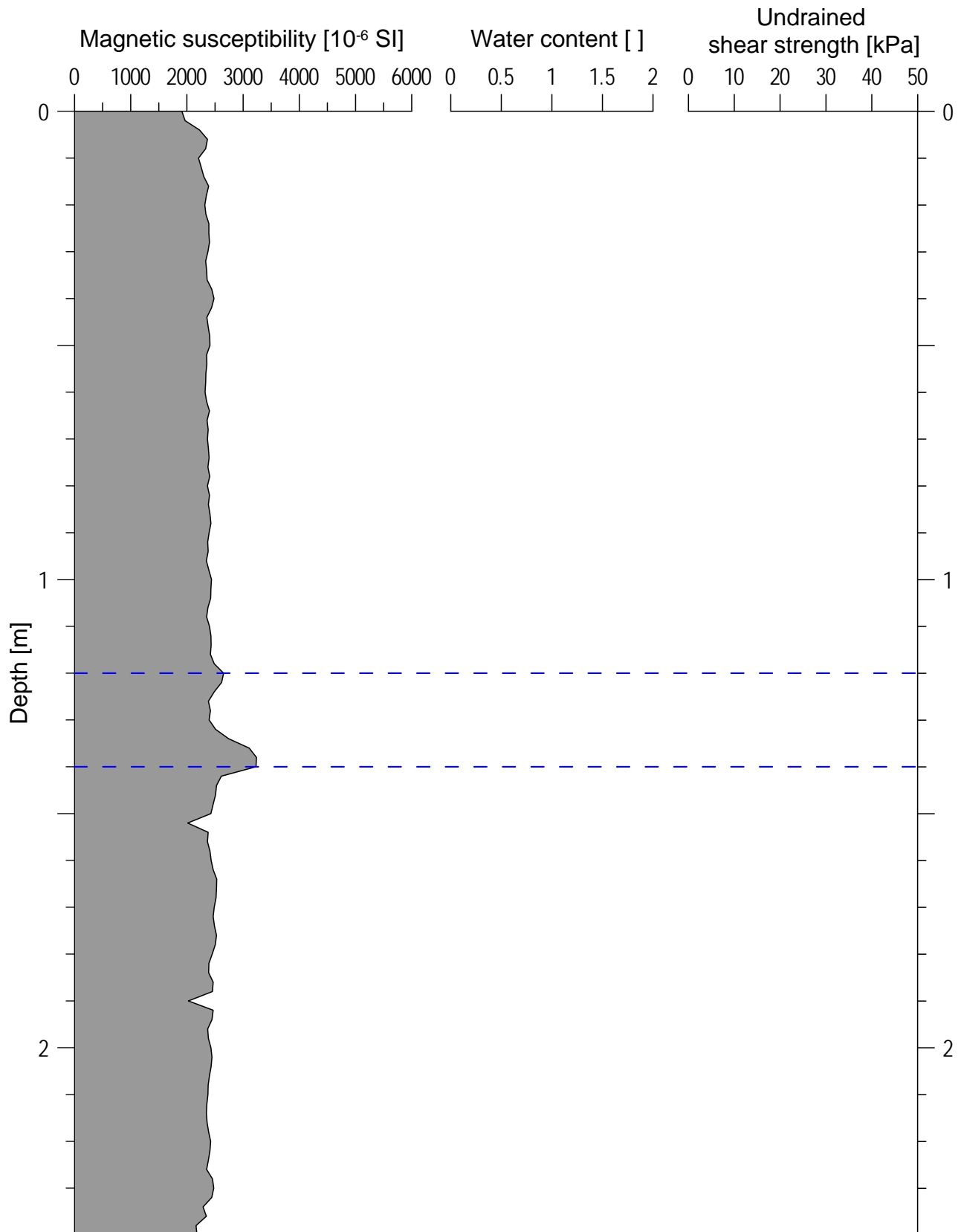
GeoB 13841-02 Date: 10.06.09 Position: 35° 49.53' S 52° 53.87' W
Water depth: 285 m Core length: 8.17 m



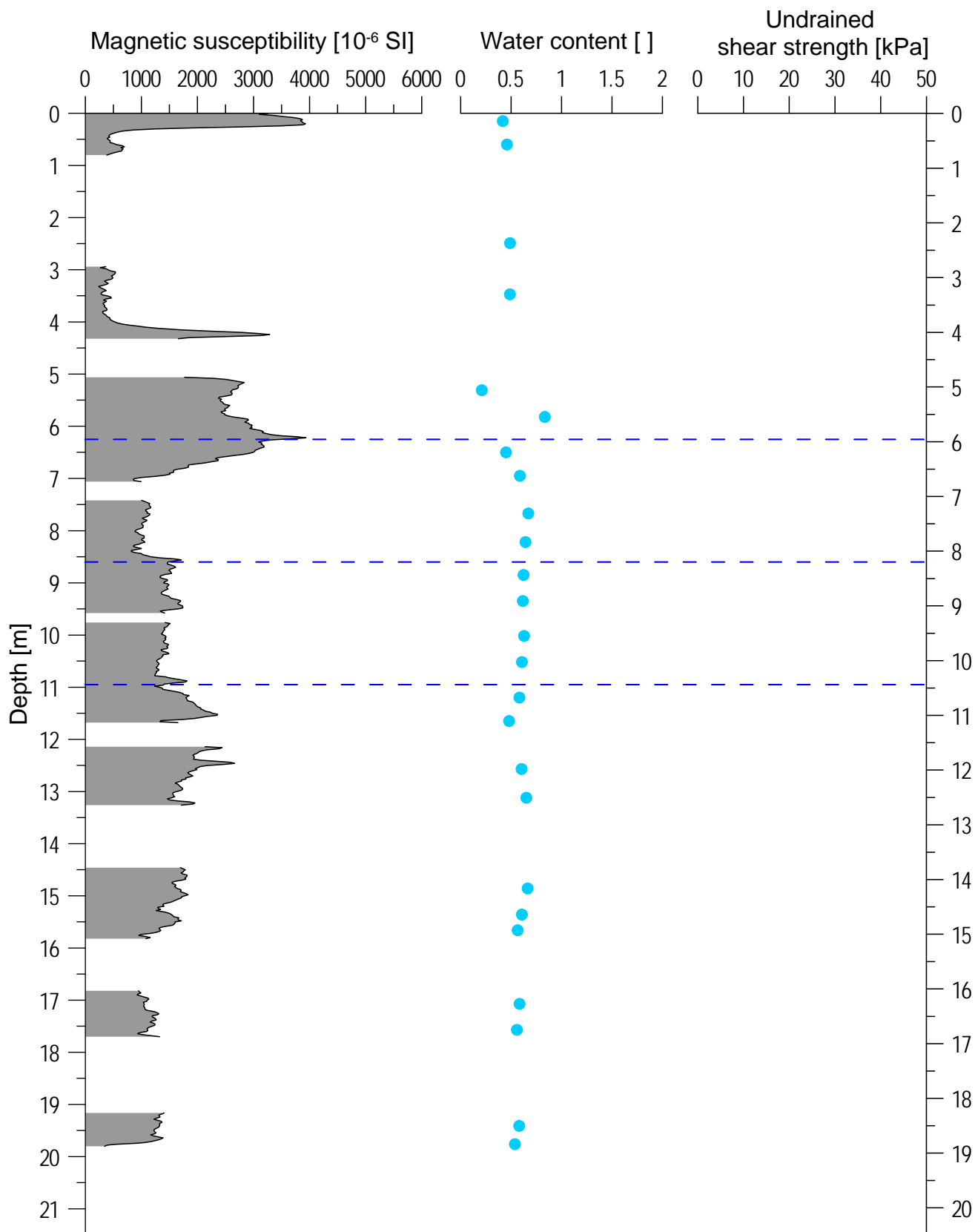
GeoB 13842-01 Date: 10.06.09 Position: 35° 57.57' S 52° 36.30' W
Water depth: 1555 m Core length: 10.02 m



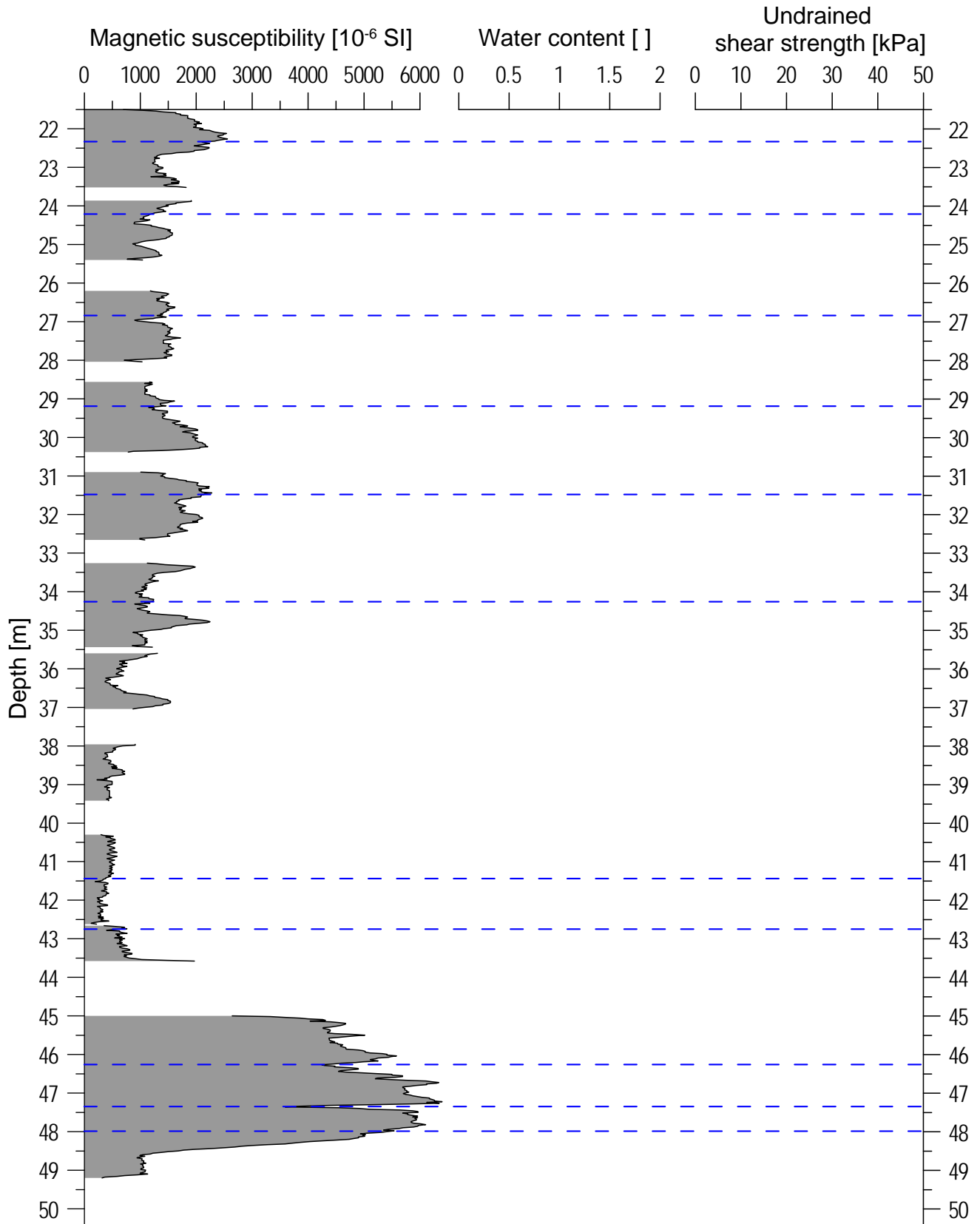
GeoB 13844-04 Date: 20.06.09 Position: 37° 25.07' S 53° 43.56' W
Water depth: 1150 m Core length: 2.4 m



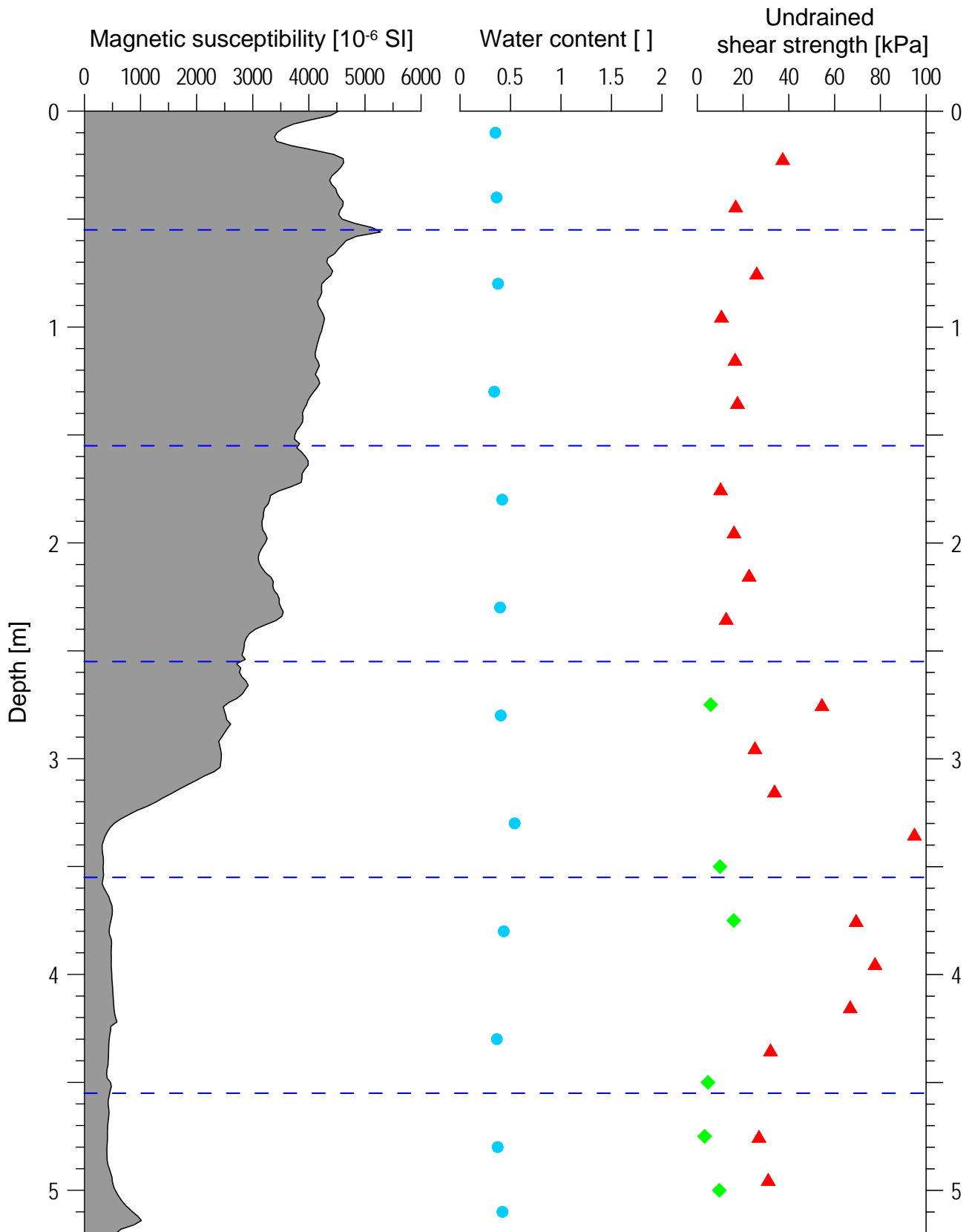
GeoB 13845-08 Date: 22.06.09 Position: 38° 10.40' S 55° 07.11' W
Water depth: 548.2 m Core length: 21.50 m



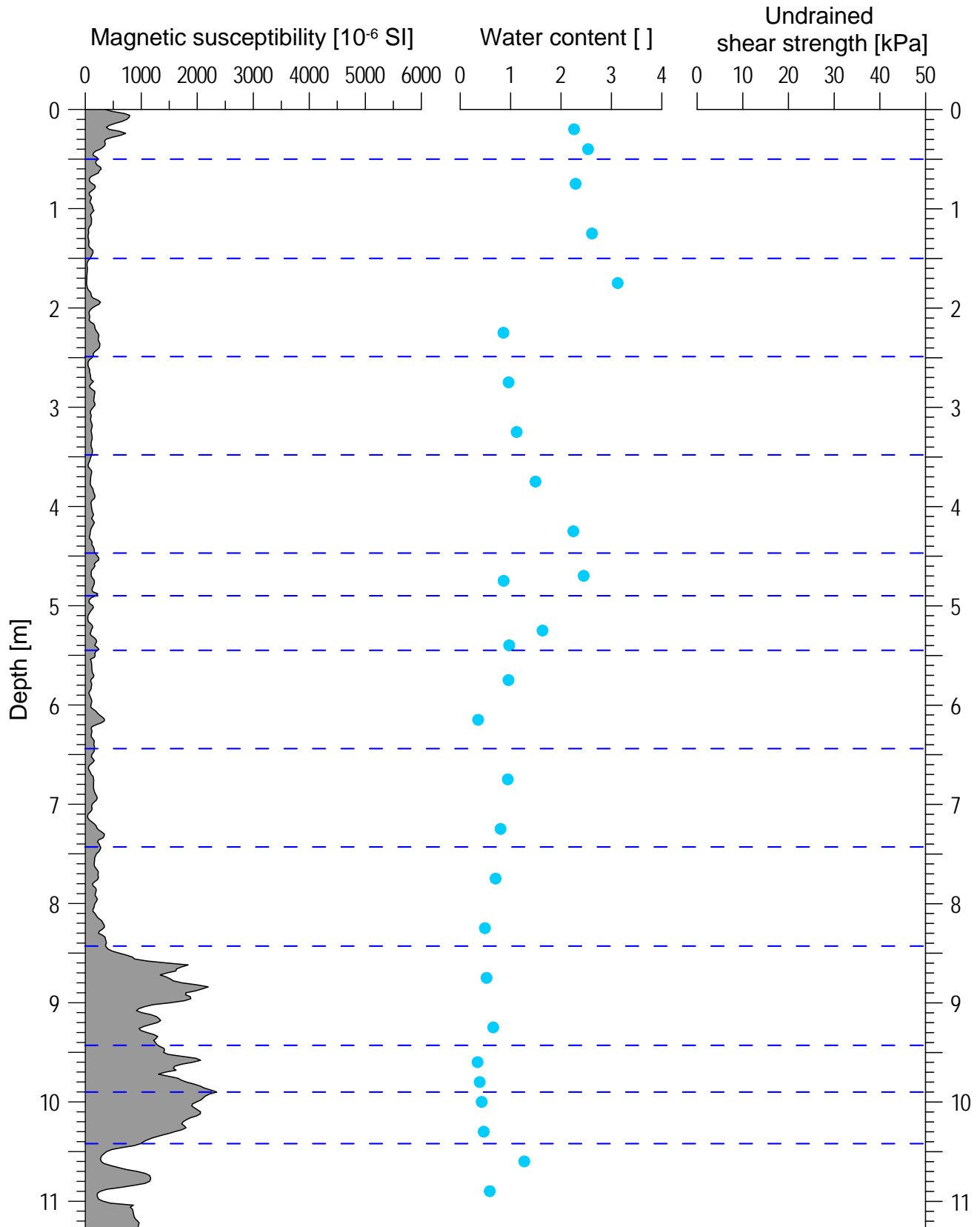
GeoB 13845-11 Date: 22.06.09 Position: 38° 10.436' S 55° 07.11' W
Water depth: 547 m Core length: 29 m



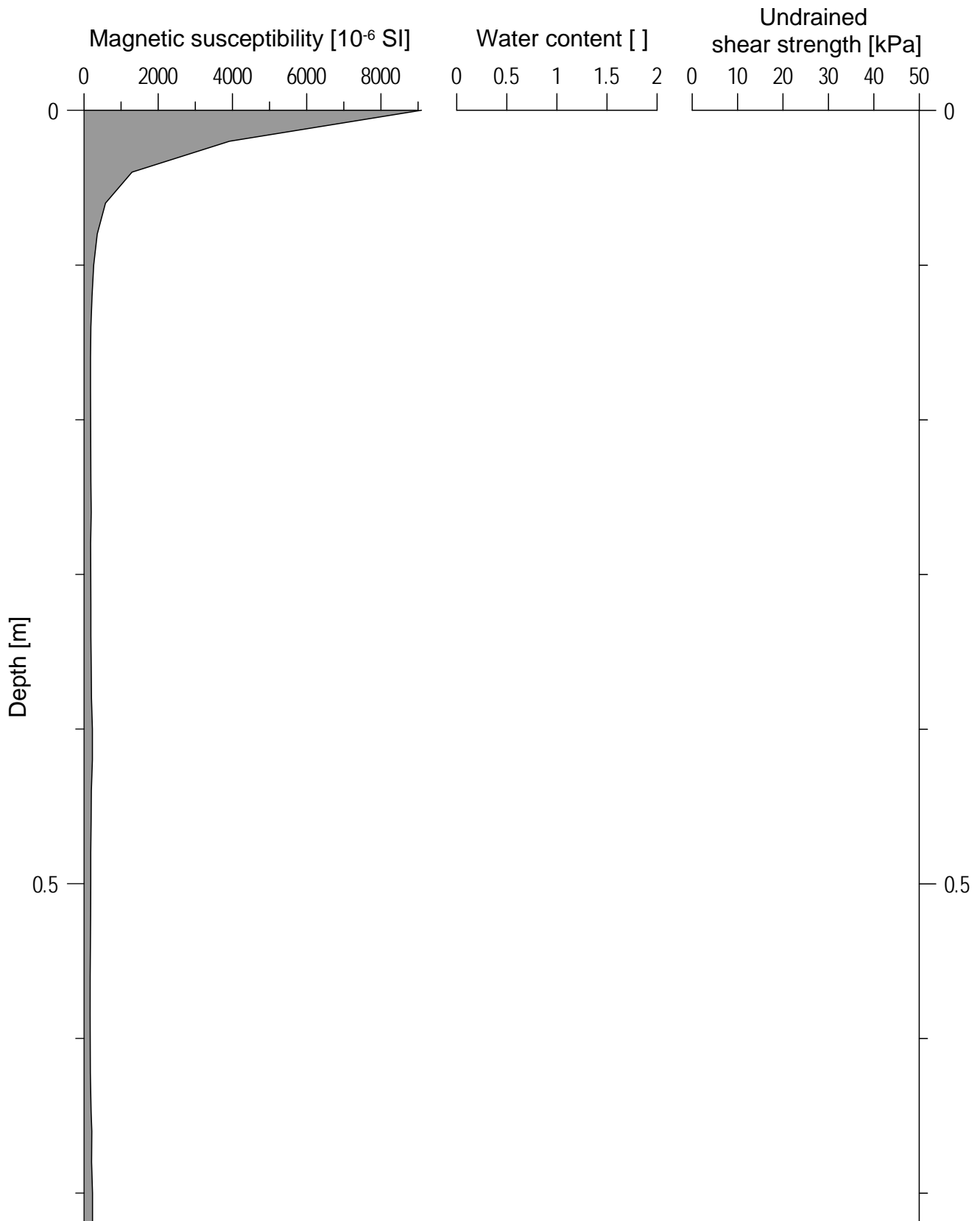
GeoB 13846-02 Date: 23.06.09 Position: 38° 07.19' S 54° 57.46' W
 Water depth: 637 m Core length: 5.20 m



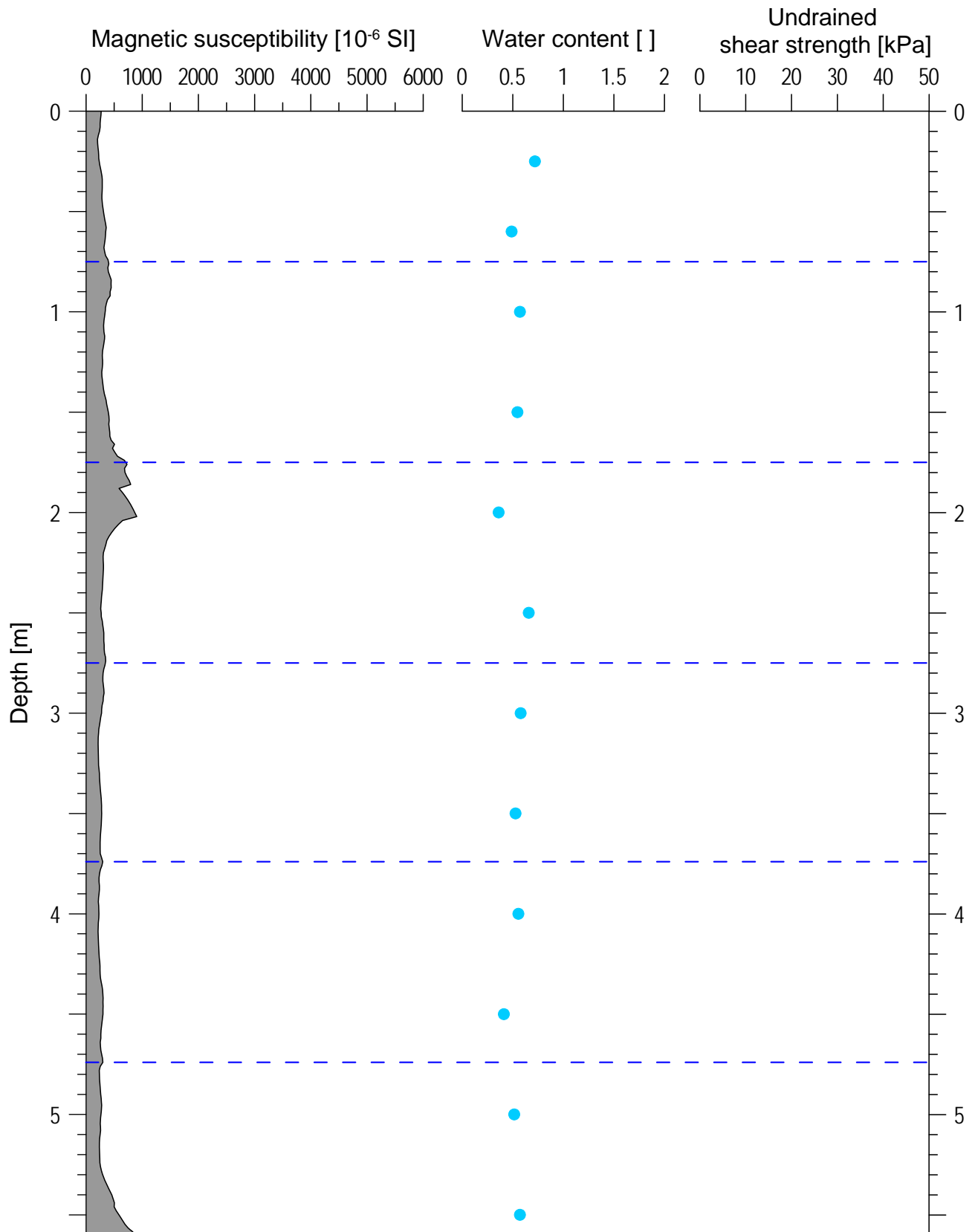
GeoB 13849-01 Date: 23.06.09 Position: 36° 10.41' S 51° 43.96' W
Water depth: 3278 m Core length: 11.29 m



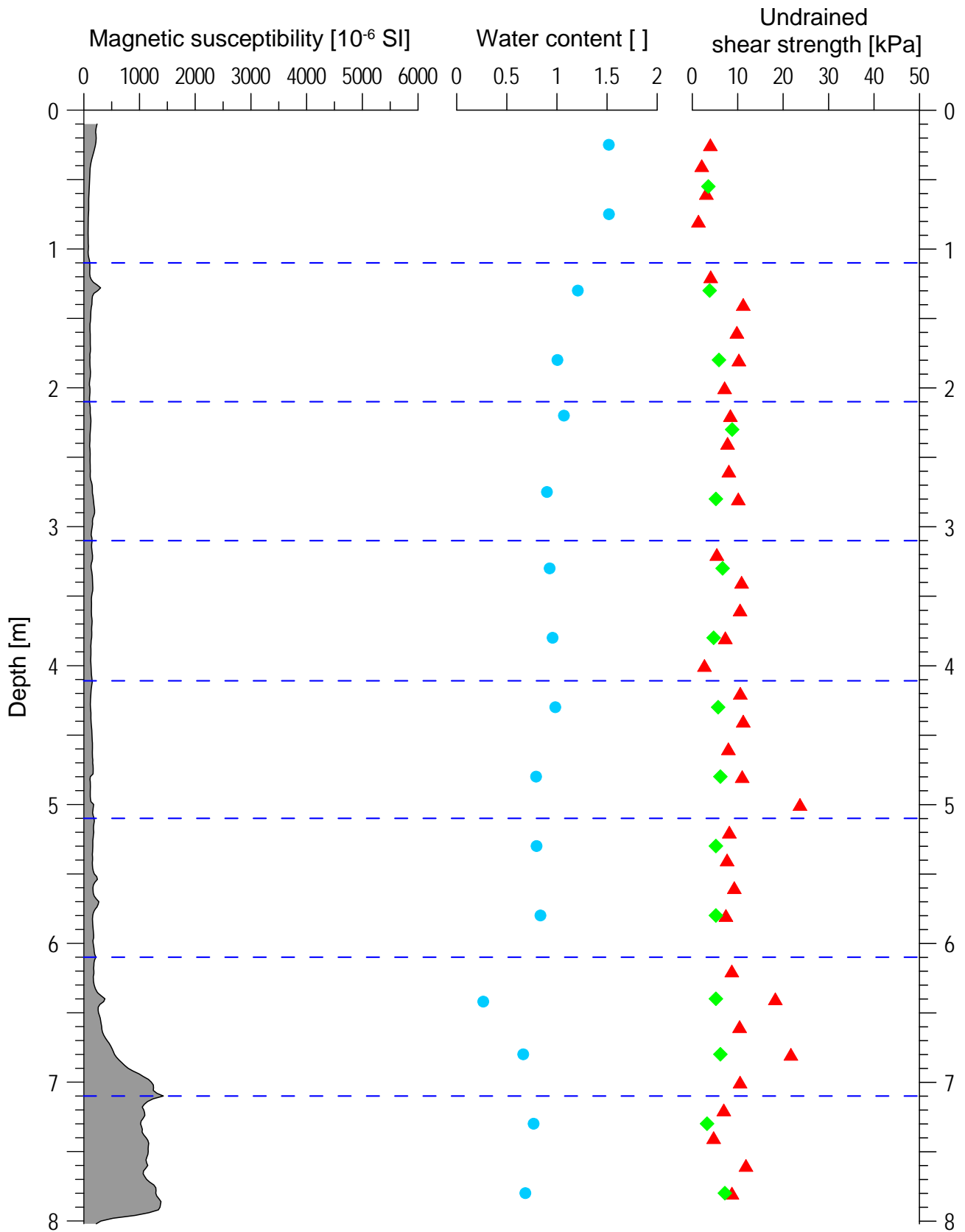
GeoB 13851-01 Date: 25.06.09 Position: 35° 46.00' S 52° 07.20' W
Water depth: 2213 m Core length: 0.72 m



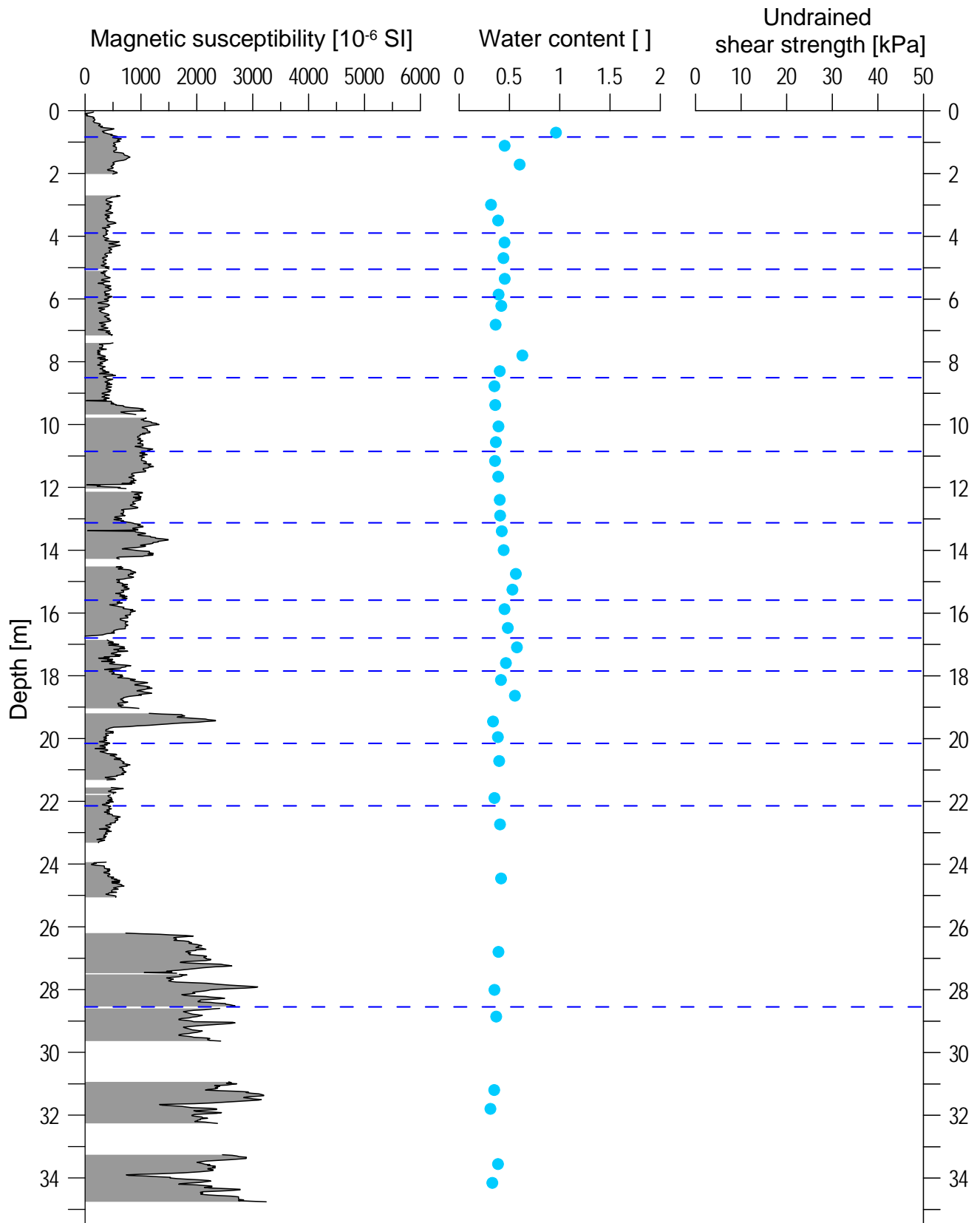
GeoB 13852-01 Date: 26.06.09 Position: 36° 05.70' S 52° 48.984' W
Water depth: 1320.1 m Core length: 5.6 m



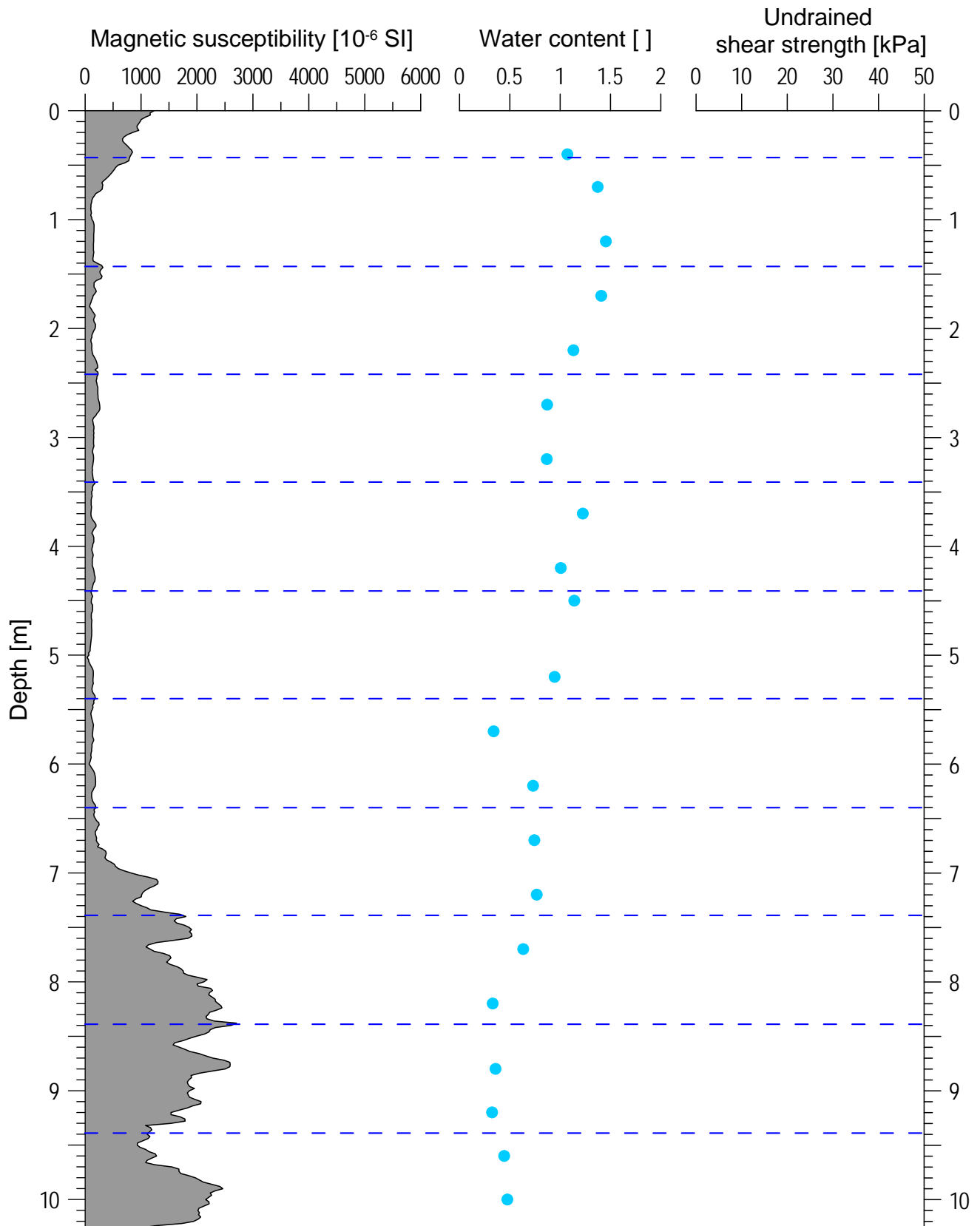
GeoB 13857-01 Date: 26.06.09 Position: 36° 04.31' S 51° 51.79' W
 Water depth: 3076.9 m Core length: 8.02 m



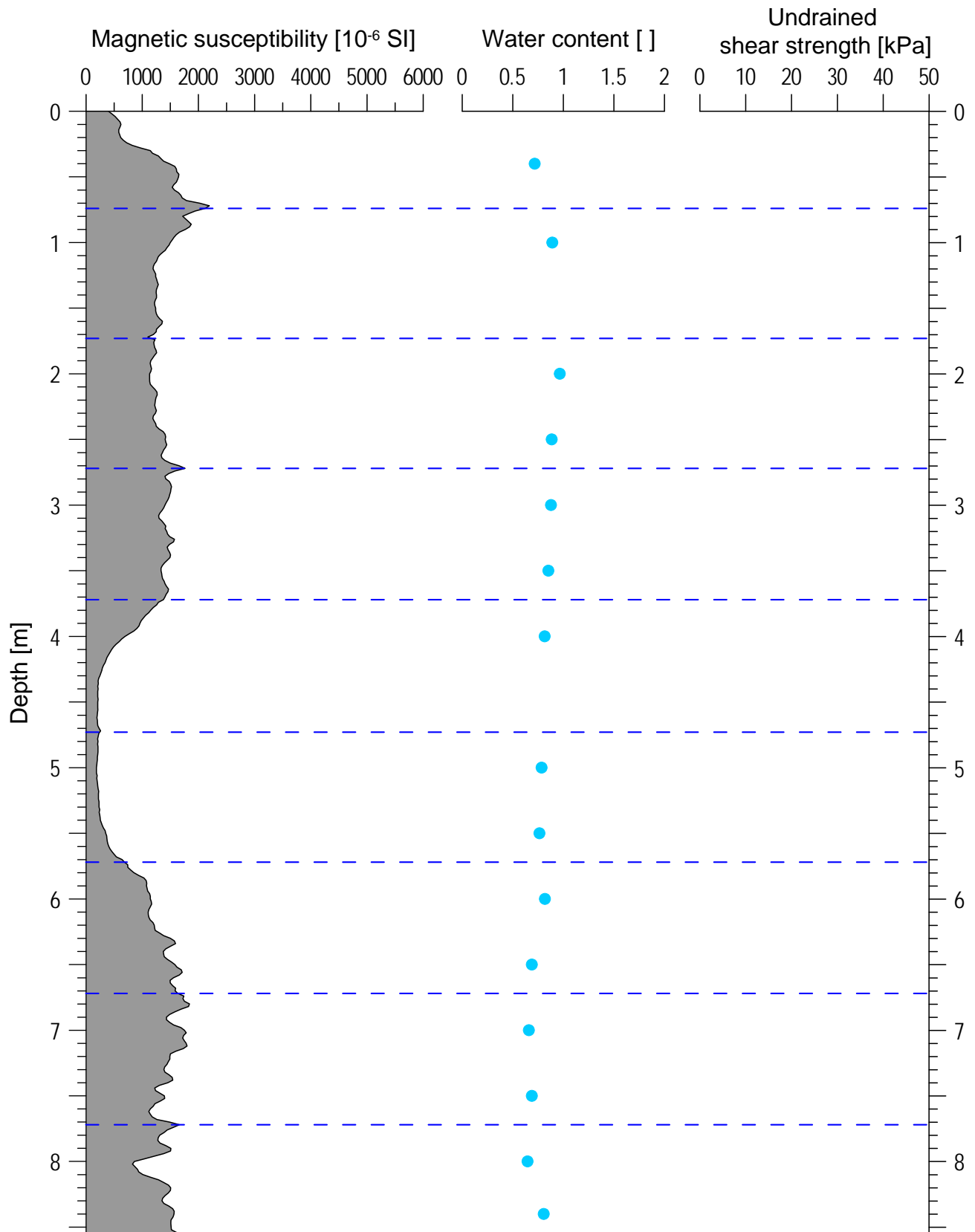
GeoB 13860-01 Date: 27.06.09 Position: 36° 06.65' S 52° 51.58' W
Water depth: 1190 m Core length: 35.60 m



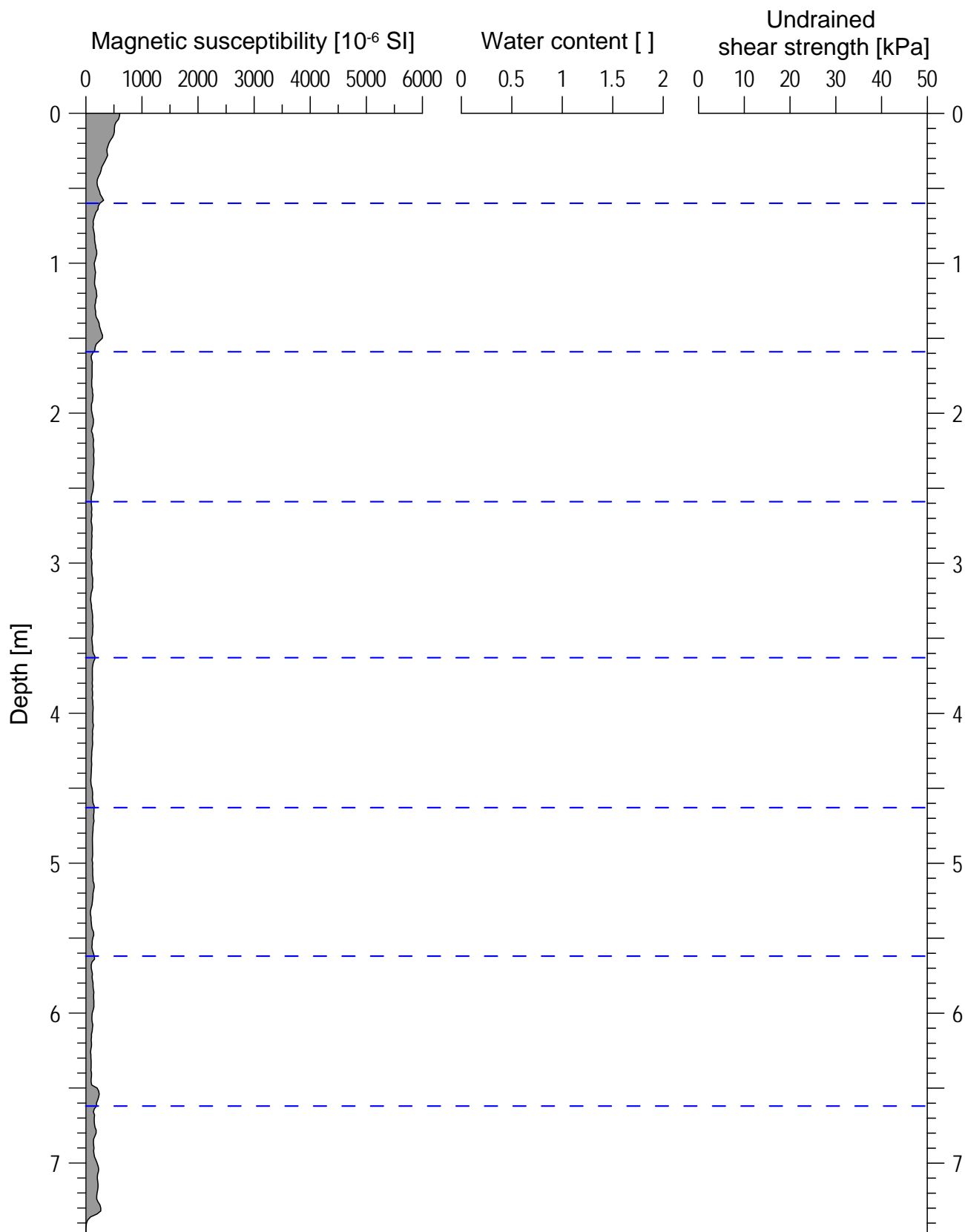
GeoB 13862-01 Date: 29.06.09 Position: 38° 01.11' S 53° 44.70' W
Water depth: 3587.5 m Core length: 10.26 m



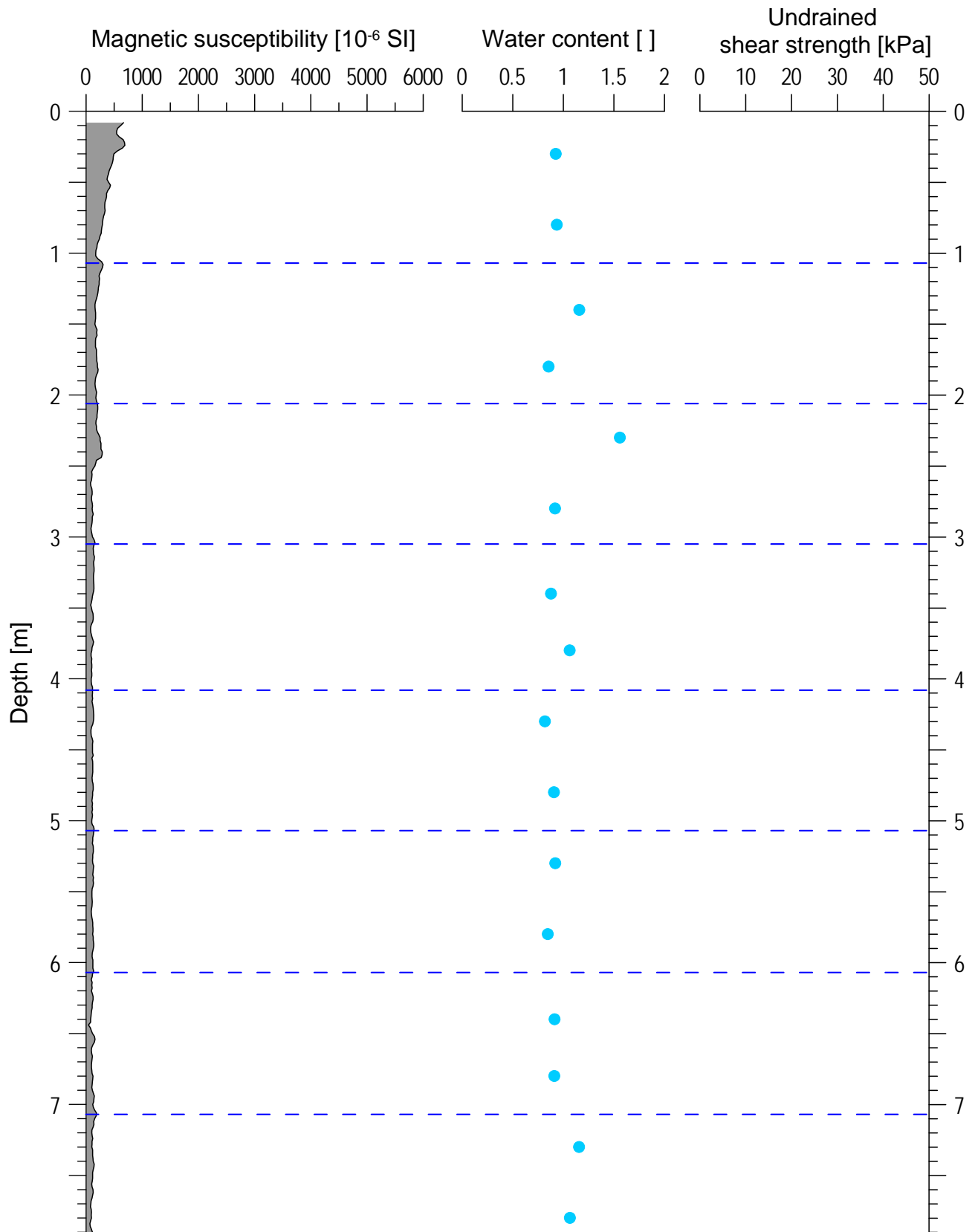
GeoB 13863-01 Date: 29.06.09 Position: 39° 18.70' S 53° 57.16' W
Water depth: 3687 m Core length: 8.56 m



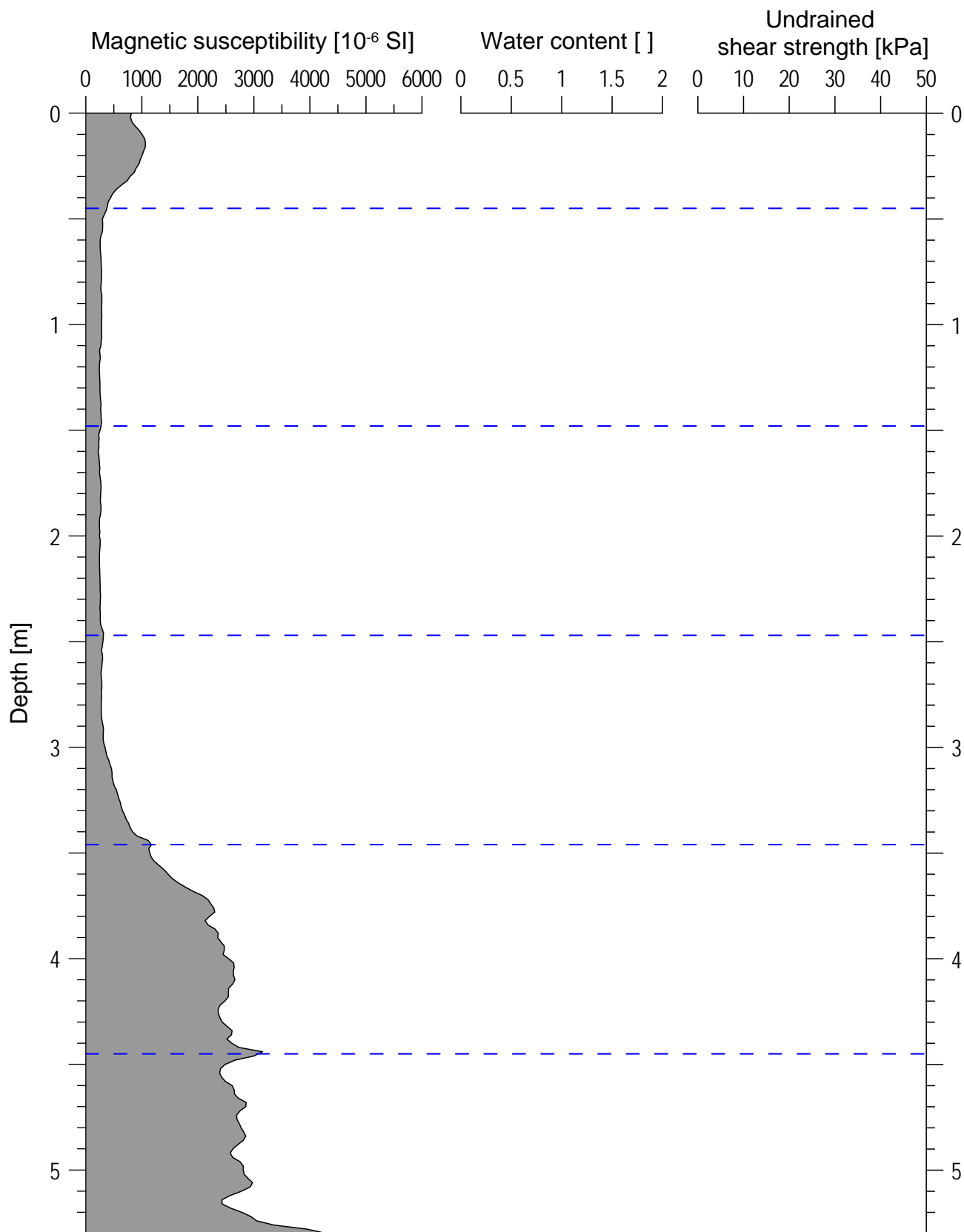
GeoB 13864-01 Date: 01.07.09 Position: 37° 37.43' S 53° 35.289' W
Water depth: 2776 m Core length: 7.48 m



GeoB 13864-02 Date: 01.07.09 Position: 37° 37.475' S 53° 35.33' W
Water depth: 2757 m Core length: 7.92 m



GeoB 13865-01 Date: 02.07.09 Position: 37° 35.12' S 53° 43.10' W
Water depth: 1634 m Core length: 5.3 m



Publications of this series:

- No. 1** **Wefer, G., E. Suess and cruise participants**
Bericht über die POLARSTERN-Fahrt ANT IV/2, Rio de Janeiro - Punta Arenas, 6.11. - 1.12.1985.
60 pages, Bremen, 1986.
- No. 2** **Hoffmann, G.**
Holozänstratigraphie und Küstenlinienverlagerung an der andalusischen Mittelmeerküste.
173 pages, Bremen, 1988. (out of print)
- No. 3** **Wefer, G. and cruise participants**
Bericht über die METEOR-Fahrt M 6/6, Libreville - Las Palmas, 18.2. - 23.3.1988.
97 pages, Bremen, 1988.
- No. 4** **Wefer, G., G.F. Lutze, T.J. Müller, O. Pfannkuche, W. Schenke, G. Siedler, W. Zenk**
Kurzbericht über die METEOR-Expedition No. 6, Hamburg - Hamburg, 28.10.1987 - 19.5.1988.
29 pages, Bremen, 1988. (out of print)
- No. 5** **Fischer, G.**
Stabile Kohlenstoff-Isotope in partikulärer organischer Substanz aus dem Südpolarmeer
(Atlantischer Sektor). 161 pages, Bremen, 1989.
- No. 6** **Berger, W.H. and G. Wefer**
Partikelfluß und Kohlenstoffkreislauf im Ozean.
Bericht und Kurzfassungen über den Workshop vom 3.-4. Juli 1989 in Bremen.
57 pages, Bremen, 1989.
- No. 7** **Wefer, G. and cruise participants**
Bericht über die METEOR - Fahrt M 9/4, Dakar - Santa Cruz, 19.2. - 16.3.1989.
103 pages, Bremen, 1989.
- No. 8** **Kölling, M.**
Modellierung geochemischer Prozesse im Sickerwasser und Grundwasser.
135 pages, Bremen, 1990.
- No. 9** **Heinze, P.-M.**
Das Auftriebsgeschehen vor Peru im Spätquartär. 204 pages, Bremen, 1990. (out of print)
- No. 10** **Willems, H., G. Wefer, M. Rinski, B. Donner, H.-J. Bellmann, L. Eißmann, A. Müller,
B.W. Flemming, H.-C. Höfle, J. Merkt, H. Streif, G. Hertweck, H. Kuntze, J. Schwaar,
W. Schäfer, M.-G. Schulz, F. Grube, B. Menke**
Beiträge zur Geologie und Paläontologie Norddeutschlands: Exkursionsführer.
202 pages, Bremen, 1990.
- No. 11** **Wefer, G. and cruise participants**
Bericht über die METEOR-Fahrt M 12/1, Kapstadt - Funchal, 13.3.1990 - 14.4.1990.
66 pages, Bremen, 1990.
- No. 12** **Dahmke, A., H.D. Schulz, A. Kölling, F. Kracht, A. Lücke**
Schwermetallspuren und geochemische Gleichgewichte zwischen Porenlösung und Sediment
im Wesermündungsgebiet. BMFT-Projekt MFU 0562, Abschlußbericht. 121 pages, Bremen, 1991.
- No. 13** **Rostek, F.**
Physikalische Strukturen von Tiefseesedimenten des Südatlantiks und ihre Erfassung in
Echolotregistrierungen. 209 pages, Bremen, 1991.
- No. 14** **Baumann, M.**
Die Ablagerung von Tschernobyl-Radiocäsium in der Norwegischen See und in der Nordsee.
133 pages, Bremen, 1991. (out of print)
- No. 15** **Kölling, A.**
Frühdiaagenetische Prozesse und Stoff-Flüsse in marinen und ästuarinen Sedimenten.
140 pages, Bremen, 1991.
- No. 16** **SFB 261 (ed.)**
1. Kolloquium des Sonderforschungsbereichs 261 der Universität Bremen (14.Juni 1991):
Der Südatlantik im Spätquartär: Rekonstruktion von Stoffhaushalt und Stromsystemen.
Kurzfassungen der Vorträge und Poster. 66 pages, Bremen, 1991.
- No. 17** **Pätzold, J. and cruise participants**
Bericht und erste Ergebnisse über die METEOR-Fahrt M 15/2, Rio de Janeiro - Vitoria,
18.1. - 7.2.1991. 46 pages, Bremen, 1993.
- No. 18** **Wefer, G. and cruise participants**
Bericht und erste Ergebnisse über die METEOR-Fahrt M 16/1, Pointe Noire - Recife,
27.3. - 25.4.1991. 120 pages, Bremen, 1991.
- No. 19** **Schulz, H.D. and cruise participants**
Bericht und erste Ergebnisse über die METEOR-Fahrt M 16/2, Recife - Belem, 28.4. - 20.5.1991.
149 pages, Bremen, 1991.

- No. 20 Berner, H.**
Mechanismen der Sedimentbildung in der Fram-Straße, im Arktischen Ozean und in der Norwegischen See. 167 pages, Bremen, 1991.
- No. 21 Schneider, R.**
Spätquartäre Produktivitätsänderungen im östlichen Angola-Becken: Reaktion auf Variationen im Passat-Monsun-Windsystem und in der Advektion des Benguela-Küstenstroms. 198 pages, Bremen, 1991. (out of print)
- No. 22 Hebbeln, D.**
Spätquartäre Stratigraphie und Paläozoo- und Paläobotanographie in der Fram-Straße. 174 pages, Bremen, 1991.
- No. 23 Lücke, A.**
Umsetzungsprozesse organischer Substanz während der Frühdiagenese in ästuarinen Sedimenten. 137 pages, Bremen, 1991.
- No. 24 Wefer, G. and cruise participants**
Bericht und erste Ergebnisse der METEOR-Fahrt M 20/1, Bremen - Abidjan, 18.11.- 22.12.1991. 74 pages, Bremen, 1992.
- No. 25 Schulz, H.D. and cruise participants**
Bericht und erste Ergebnisse der METEOR-Fahrt M 20/2, Abidjan - Dakar, 27.12.1991 - 3.2.1992. 173 pages, Bremen, 1992.
- No. 26 Gingele, F.**
Zur klimaabhängigen Bildung biogener und terrigener Sedimente und ihrer Veränderung durch die Frühdiagenese im zentralen und östlichen Südatlantik. 202 pages, Bremen, 1992.
- No. 27 Bickert, T.**
Rekonstruktion der spätquartären Bodenwasserzirkulation im östlichen Südatlantik über stabile Isotope benthischer Foraminiferen. 205 pages, Bremen, 1992. (out of print)
- No. 28 Schmidt, H.**
Der Benguela-Strom im Bereich des Walfisch-Rückens im Spätquartär. 172 pages, Bremen, 1992.
- No. 29 Meinecke, G.**
Spätquartäre Oberflächenwassertemperaturen im östlichen äquatorialen Atlantik. 181 pages, Bremen, 1992.
- No. 30 Bathmann, U., U. Bleil, A. Dahmke, P. Müller, A. Nehr Korn, E.-M. Nöthig, M. Olesch, J. Pätzold, H.D. Schulz, V. Smetacek, V. Spieß, G. Wefer, H. Willems**
Bericht des Graduierten Kollegs. Stoff-Flüsse in marinen Geosystemen. Berichtszeitraum Oktober 1990 - Dezember 1992. 396 pages, Bremen, 1992.
- No. 31 Damm, E.**
Frühdiagenetische Verteilung von Schwermetallen in Schlicksedimenten der westlichen Ostsee. 115 pages, Bremen, 1992.
- No. 32 Antia, E.E.**
Sedimentology, Morphodynamics and Facies Association of a mesotidal Barrier Island Shoreface (Spiekeroog, Southern North Sea). 370 pages, Bremen, 1993.
- No. 33 Duinker, J. and G. Wefer (ed.)**
Bericht über den 1. JGOFS-Workshop. 1./2. Dezember 1992 in Bremen. 83 pages, Bremen, 1993.
- No. 34 Kasten, S.**
Die Verteilung von Schwermetallen in den Sedimenten eines stadtbremischen Hafenbeckens. 103 pages, Bremen, 1993.
- No. 35 Spieß, V.**
Digitale Sedimentographie. Neue Wege zu einer hochauflösenden Akustostratigraphie. 199 pages, Bremen, 1993.
- No. 36 Schinzel, U.**
Laborversuche zu frühdiagenetischen Reaktionen von Eisen (III) - Oxidhydraten in marinen Sedimenten. 189 pages, Bremen, 1993.
- No. 37 Sieger, R.**
CoTAM - ein Modell zur Modellierung des Schwermetalltransports in Grundwasserleitern. 56 pages, Bremen, 1993. (out of print)
- No. 38 Willems, H. (ed.)**
Geoscientific Investigations in the Tethyan Himalayas. 183 pages, Bremen, 1993.
- No. 39 Hamer, K.**
Entwicklung von Laborversuchen als Grundlage für die Modellierung des Transportverhaltens von Arsenat, Blei, Cadmium und Kupfer in wassergesättigten Säulen. 147 pages, Bremen, 1993.
- No. 40 Sieger, R.**
Modellierung des Stofftransports in porösen Medien unter Ankopplung kinetisch gesteuerter Sorptions- und Redoxprozesse sowie thermischer Gleichgewichte. 158 pages, Bremen, 1993.

- No. 41** **Thießen, W.**
Magnetische Eigenschaften von Sedimenten des östlichen Südatlantiks und ihre paläozeanographische Relevanz. 170 pages, Bremen, 1993.
- No. 42** **Spieß, V. and cruise participants**
Report and preliminary results of METEOR-Cruise M 23/1, Kapstadt - Rio de Janeiro, 4.-25.2.1993. 139 pages, Bremen, 1994.
- No. 43** **Bleil, U. and cruise participants**
Report and preliminary results of METEOR-Cruise M 23/2, Rio de Janeiro - Recife, 27.2.-19.3.1993. 133 pages, Bremen, 1994.
- No. 44** **Wefer, G. and cruise participants**
Report and preliminary results of METEOR-Cruise M 23/3, Recife - Las Palmas, 21.3. - 12.4.1993. 71 pages, Bremen, 1994.
- No. 45** **Giese, M. and G. Wefer (ed.)**
Bericht über den 2. JGOFS-Workshop. 18./19. November 1993 in Bremen. 93 pages, Bremen, 1994.
- No. 46** **Balzer, W. and cruise participants**
Report and preliminary results of METEOR-Cruise M 22/1, Hamburg - Recife, 22.9. - 21.10.1992. 24 pages, Bremen, 1994.
- No. 47** **Stax, R.**
Zyklische Sedimentation von organischem Kohlenstoff in der Japan See: Anzeiger für Änderungen von Paläozeanographie und Paläoklima im Spätkänozoikum. 150 pages, Bremen, 1994.
- No. 48** **Skowronek, F.**
Frühdigenetische Stoff-Flüsse gelöster Schwermetalle an der Oberfläche von Sedimenten des Weser Ästuares. 107 pages, Bremen, 1994.
- No. 49** **Dersch-Hansmann, M.**
Zur Klimaentwicklung in Ostasien während der letzten 5 Millionen Jahre: Terrigener Sedimenteintrag in die Japan See (ODP Ausfahrt 128). 149 pages, Bremen, 1994.
- No. 50** **Zabel, M.**
Frühdigenetische Stoff-Flüsse in Oberflächen-Sedimenten des äquatorialen und östlichen Südatlantik. 129 pages, Bremen, 1994.
- No. 51** **Bleil, U. and cruise participants**
Report and preliminary results of SONNE-Cruise SO 86, Buenos Aires - Capetown, 22.4. - 31.5.93. 116 pages, Bremen, 1994.
- No. 52** **Symposium: The South Atlantic: Present and Past Circulation.**
Bremen, Germany, 15 - 19 August 1994. Abstracts. 167 pages, Bremen, 1994.
- No. 53** **Kretzmann, U.B.**
57Fe-Mössbauer-Spektroskopie an Sedimenten - Möglichkeiten und Grenzen. 183 pages, Bremen, 1994.
- No. 54** **Bachmann, M.**
Die Karbonatrampe von Organyà im oberen Oberapt und unteren Unteralt (NE-Spanien, Prov. Lerida): Fazies, Zylo- und Sequenzstratigraphie. 147 pages, Bremen, 1994. (out of print)
- No. 55** **Kemle-von Mücke, S.**
Oberflächenwasserstruktur und -zirkulation des Südostatlantiks im Spätquartär. 151 pages, Bremen, 1994.
- No. 56** **Petermann, H.**
Magnetotaktische Bakterien und ihre Magnetosome in Oberflächensedimenten des Südatlantiks. 134 pages, Bremen, 1994.
- No. 57** **Mulitza, S.**
Spätquartäre Variationen der oberflächennahen Hydrographie im westlichen äquatorialen Atlantik. 97 pages, Bremen, 1994.
- No. 58** **Segl, M. and cruise participants**
Report and preliminary results of METEOR-Cruise M 29/1, Buenos-Aires - Montevideo, 17.6. - 13.7.1994. 94 pages, Bremen, 1994.
- No. 59** **Bleil, U. and cruise participants**
Report and preliminary results of METEOR-Cruise M 29/2, Montevideo - Rio de Janeiro 15.7. - 8.8.1994. 153 pages, Bremen, 1994.
- No. 60** **Henrich, R. and cruise participants**
Report and preliminary results of METEOR-Cruise M 29/3, Rio de Janeiro - Las Palmas 11.8. - 5.9.1994. Bremen, 1994. (out of print)

- No. 61** **Sagemann, J.**
Saisonale Variationen von Porenwasserprofilen, Nährstoff-Flüssen und Reaktionen in intertidalen Sedimenten des Weser-Ästuars. 110 pages, Bremen, 1994. (out of print)
- No. 62** **Giese, M. and G. Wefer**
Bericht über den 3. JGOFs-Workshop. 5./6. Dezember 1994 in Bremen. 84 pages, Bremen, 1995.
- No. 63** **Mann, U.**
Genese kretazischer Schwarzschiefer in Kolumbien: Globale vs. regionale/lokale Prozesse. 153 pages, Bremen, 1995. (out of print)
- No. 64** **Willems, H., Wan X., Yin J., Dongdui L., Liu G., S. Dürr, K.-U. Gräfe**
The Mesozoic development of the N-Indian passive margin and of the Xigaze Forearc Basin in southern Tibet, China. – Excursion Guide to IGCP 362 Working-Group Meeting "Integrated Stratigraphy". 113 pages, Bremen, 1995. (out of print)
- No. 65** **Hünken, U.**
Liefergebiets - Charakterisierung proterozoischer Goldseifen in Ghana anhand von Fluideinschluß - Untersuchungen. 270 pages, Bremen, 1995.
- No. 66** **Nyandwi, N.**
The Nature of the Sediment Distribution Patterns in the Spiekeroog Backbarrier Area, the East Frisian Islands. 162 pages, Bremen, 1995.
- No. 67** **Isenbeck-Schröter, M.**
Transportverhalten von Schwermetallkationen und Oxoanionen in wassergesättigten Sanden. - Laborversuche in Säulen und ihre Modellierung -. 182 pages, Bremen, 1995.
- No. 68** **Hebbeln, D. and cruise participants**
Report and preliminary results of SONNE-Cruise SO 102, Valparaiso - Valparaiso, 95. 134 pages, Bremen, 1995.
- No. 69** **Willems, H. (Sprecher), U. Bathmann, U. Bleil, T. v. Dobeneck, K. Herterich, B.B. Jorgensen, E.-M. Nöthig, M. Olesch, J. Pätzold, H.D. Schulz, V. Smetacek, V. Speiß, G. Wefer**
Bericht des Graduierten-Kollegs Stoff-Flüsse in marine Geosystemen. Berichtszeitraum Januar 1993 - Dezember 1995. 45 & 468 pages, Bremen, 1995.
- No. 70** **Giese, M. and G. Wefer**
Bericht über den 4. JGOFs-Workshop. 20./21. November 1995 in Bremen. 60 pages, Bremen, 1996. (out of print)
- No. 71** **Meggers, H.**
Pliozän-quartäre Karbonatsedimentation und Paläozoogeographie des Nordatlantiks und des Europäischen Nordmeeres - Hinweise aus planktischen Foraminiferengemeinschaften. 143 pages, Bremen, 1996. (out of print)
- No. 72** **Teske, A.**
Phylogenetische und ökologische Untersuchungen an Bakterien des oxidativen und reduktiven marinen Schwefelkreislaufs mittels ribosomaler RNA. 220 pages, Bremen, 1996. (out of print)
- No. 73** **Andersen, N.**
Biogeochemische Charakterisierung von Sinkstoffen und Sedimenten aus ostatlantischen Produktions-Systemen mit Hilfe von Biomarkern. 215 pages, Bremen, 1996.
- No. 74** **Treppke, U.**
Saisonalität im Diatomeen- und Silikoflagellatenfluß im östlichen tropischen und subtropischen Atlantik. 200 pages, Bremen, 1996.
- No. 75** **Schüring, J.**
Die Verwendung von Steinkohlebergematerialien im Deponiebau im Hinblick auf die Pyritverwitterung und die Eignung als geochemische Barriere. 110 pages, Bremen, 1996.
- No. 76** **Pätzold, J. and cruise participants**
Report and preliminary results of VICTOR HENSEN cruise JOPS II, Leg 6, Fortaleza - Recife, 10.3. - 26.3. 1995 and Leg 8, Vitoria - Vitoria, 10.4. - 23.4.1995. 87 pages, Bremen, 1996.
- No. 77** **Bleil, U. and cruise participants**
Report and preliminary results of METEOR-Cruise M 34/1, Cape Town - Walvis Bay, 3.-26.1.1996. 129 pages, Bremen, 1996.
- No. 78** **Schulz, H.D. and cruise participants**
Report and preliminary results of METEOR-Cruise M 34/2, Walvis Bay - Walvis Bay, 29.1.-18.2.96. 133 pages, Bremen, 1996.
- No. 79** **Wefer, G. and cruise participants**
Report and preliminary results of METEOR-Cruise M 34/3, Walvis Bay - Recife, 21.2.-17.3.1996. 168 pages, Bremen, 1996.

- No. 80** **Fischer, G. and cruise participants**
Report and preliminary results of METEOR-Cruise M 34/4, Recife - Bridgetown, 19.3.-15.4.1996. 105 pages, Bremen, 1996.
- No. 81** **Kulbrok, F.**
Biostratigraphie, Fazies und Sequenzstratigraphie einer Karbonatrampe in den Schichten der Oberkreide und des Alttertiärs Nordost-Ägyptens (Eastern Desert, N'Golf von Suez, Sinai). 153 pages, Bremen, 1996.
- No. 82** **Kasten, S.**
Early Diagenetic Metal Enrichments in Marine Sediments as Documents of Nonsteady-State Depositional Conditions. Bremen, 1996.
- No. 83** **Holmes, M.E.**
Reconstruction of Surface Ocean Nitrate Utilization in the Southeast Atlantic Ocean Based on Stable Nitrogen Isotopes. 113 pages, Bremen, 1996.
- No. 84** **Rühlemann, C.**
Akkumulation von Carbonat und organischem Kohlenstoff im tropischen Atlantik: Spätquartäre Produktivitäts-Variationen und ihre Steuerungsmechanismen. 139 pages, Bremen, 1996.
- No. 85** **Ratmeyer, V.**
Untersuchungen zum Eintrag und Transport lithogener und organischer partikulärer Substanz im östlichen subtropischen Nordatlantik. 154 pages, Bremen, 1996.
- No. 86** **Cepek, M.**
Zeitliche und räumliche Variationen von Coccolithophoriden-Gemeinschaften im subtropischen Ost-Atlantik: Untersuchungen an Plankton, Sinkstoffen und Sedimenten. 156 pages, Bremen, 1996.
- No. 87** **Otto, S.**
Die Bedeutung von gelöstem organischen Kohlenstoff (DOC) für den Kohlenstofffluß im Ozean. 150 pages, Bremen, 1996.
- No. 88** **Hensen, C.**
Frühdiaagenetische Prozesse und Quantifizierung benthischer Stoff-Flüsse in Oberflächensedimenten des Südatlantiks. 132 pages, Bremen, 1996.
- No. 89** **Giese, M. and G. Wefer**
Bericht über den 5. JGOFS-Workshop. 27./28. November 1996 in Bremen. 73 pages, Bremen, 1997.
- No. 90** **Wefer, G. and cruise participants**
Report and preliminary results of METEOR-Cruise M 37/1, Lisbon - Las Palmas, 4.-23.12.1996. 79 pages, Bremen, 1997.
- No. 91** **Isenbeck-Schröter, M., E. Bedbur, M. Kofod, B. König, T. Schramm & G. Mattheß**
Occurrence of Pesticide Residues in Water - Assessment of the Current Situation in Selected EU Countries. 65 pages, Bremen 1997.
- No. 92** **Kühn, M.**
Geochemische Folgereaktionen bei der hydrogeothermalen Energiegewinnung. 129 pages, Bremen 1997.
- No. 93** **Determann, S. & K. Herterich**
JGOFS-A6 "Daten und Modelle": Sammlung JGOFS-relevanter Modelle in Deutschland. 26 pages, Bremen, 1997.
- No. 94** **Fischer, G. and cruise participants**
Report and preliminary results of METEOR-Cruise M 38/1, Las Palmas - Recife, 25.1.-1.3.1997, with Appendix: Core Descriptions from METEOR Cruise M 37/1. Bremen, 1997.
- No. 95** **Bleil, U. and cruise participants**
Report and preliminary results of METEOR-Cruise M 38/2, Recife - Las Palmas, 4.3.-14.4.1997. 126 pages, Bremen, 1997.
- No. 96** **Neuer, S. and cruise participants**
Report and preliminary results of VICTOR HENSEN-Cruise 96/1. Bremen, 1997.
- No. 97** **Villinger, H. and cruise participants**
Fahrtbericht SO 111, 20.8. - 16.9.1996. 115 pages, Bremen, 1997.
- No. 98** **Lüning, S.**
Late Cretaceous - Early Tertiary sequence stratigraphy, paleoecology and geodynamics of Eastern Sinai, Egypt. 218 pages, Bremen, 1997.
- No. 99** **Haese, R.R.**
Beschreibung und Quantifizierung frühdiaagenetischer Reaktionen des Eisens in Sedimenten des Südatlantiks. 118 pages, Bremen, 1997.

- No. 100** **Lührte, R. von**
Verwertung von Bremer Baggergut als Material zur Oberflächenabdichtung von Deponien - Geochemisches Langzeitverhalten und Schwermetall-Mobilität (Cd, Cu, Ni, Pb, Zn). Bremen, 1997.
- No. 101** **Ebert, M.**
Der Einfluß des Redoxmilieus auf die Mobilität von Chrom im durchströmten Aquifer. 135 pages, Bremen, 1997.
- No. 102** **Krögel, F.**
Einfluß von Viskosität und Dichte des Seewassers auf Transport und Ablagerung von Wattsedimenten (Langeooger Rückseitenwatt, südliche Nordsee). 168 pages, Bremen, 1997.
- No. 103** **Kerntopf, B.**
Dinoflagellate Distribution Patterns and Preservation in the Equatorial Atlantic and Offshore North-West Africa. 137 pages, Bremen, 1997.
- No. 104** **Breitzke, M.**
Elastische Wellenausbreitung in marinen Sedimenten - Neue Entwicklungen der Ultraschall Sedimentphysik und Sedimentechographie. 298 pages, Bremen, 1997.
- No. 105** **Marchant, M.**
Rezente und spätquartäre Sedimentation planktischer Foraminiferen im Peru-Chile Strom. 115 pages, Bremen, 1997.
- No. 106** **Habicht, K.S.**
Sulfur isotope fractionation in marine sediments and bacterial cultures. 125 pages, Bremen, 1997.
- No. 107** **Hamer, K., R.v. Lührte, G. Becker, T. Felis, S. Keffel, B. Strotmann, C. Waschowitz, M. Kölling, M. Isenbeck-Schröter, H.D. Schulz**
Endbericht zum Forschungsvorhaben 060 des Landes Bremen: Baggergut der Hafengruppe Bremen-Stadt: Modelluntersuchungen zur Schwermetallmobilität und Möglichkeiten der Verwertung von Hafenschlick aus Bremischen Häfen. 98 pages, Bremen, 1997.
- No. 108** **Greeff, O.W.**
Entwicklung und Erprobung eines benthischen Landersystemes zur in situ-Bestimmung von Sulfatreduktionsraten mariner Sedimente. 121 pages, Bremen, 1997.
- No. 109** **Pätzold, M. und G. Wefer**
Bericht über den 6. JGOFS-Workshop am 4./5.12.1997 in Bremen. Im Anhang: Publikationen zum deutschen Beitrag zur Joint Global Ocean Flux Study (JGOFS), Stand 1/1998. 122 pages, Bremen, 1998.
- No. 110** **Landenberger, H.**
CoTRem, ein Multi-Komponenten Transport- und Reaktions-Modell. 142 pages, Bremen, 1998.
- No. 111** **Villinger, H. und Fahrtteilnehmer**
Fahrtbericht SO 124, 4.10. - 16.10.199. 90 pages, Bremen, 1997.
- No. 112** **Gietl, R.**
Biostratigraphie und Sedimentationsmuster einer nordostägyptischen Karbonatrampe unter Berücksichtigung der Alveolinen-Faunen. 142 pages, Bremen, 1998.
- No. 113** **Ziebis, W.**
The Impact of the Thalassinidean Shrimp *Callinassa truncata* on the Geochemistry of permeable, coastal Sediments. 158 pages, Bremen 1998.
- No. 114** **Schulz, H.D. and cruise participants**
Report and preliminary results of METEOR-Cruise M 41/1, Málaga - Libreville, 13.2.-15.3.1998. Bremen, 1998.
- No. 115** **Völker, D.J.**
Untersuchungen an strömungsbeeinflussten Sedimentationsmustern im Südozean. Interpretation sedimentechographischer Daten und numerische Modellierung. 152 pages, Bremen, 1998.
- No. 116** **Schlünz, B.**
Riverine Organic Carbon Input into the Ocean in Relation to Late Quaternary Climate Change. 136 pages, Bremen, 1998.
- No. 117** **Kuhnert, H.**
Aufzeichnung des Klimas vor Westaustralien in stabilen Isotopen in Korallenskeletten. 109 pages, Bremen, 1998.
- No. 118** **Kirst, G.**
Rekonstruktion von Oberflächenwassertemperaturen im östlichen Südatlantik anhand von Alkenonen. 130 pages, Bremen, 1998.
- No. 119** **Dürkoop, A.**
Der Brasil-Strom im Spätquartär: Rekonstruktion der oberflächennahen Hydrographie während der letzten 400 000 Jahre. 121 pages, Bremen, 1998.

- No. 120** **Lamy, F.**
Spätquartäre Variationen des terrigenen Sedimenteintrags entlang des chilenischen Kontinentalhangs als Abbild von Klimavariabilität im Milanković- und Sub-Milanković-Zeitbereich. 141 pages, Bremen, 1998.
- No. 121** **Neuer, S. and cruise participants**
Report and preliminary results of POSEIDON-Cruise Pos 237/2, Vigo – Las Palmas, 18.3.-31.3.1998. 39 pages, Bremen, 1998
- No. 122** **Romero, O.E.**
Marine planktonic diatoms from the tropical and equatorial Atlantic: temporal flux patterns and the sediment record. 205 pages, Bremen, 1998.
- No. 123** **Spiess, V. und Fahrtteilnehmer**
Report and preliminary results of RV SONNE Cruise 125, Cochín – Chittagong, 17.10.-17.11.1997. 128 pages, Bremen, 1998.
- No. 124** **Arz, H.W.**
Dokumentation von kurzfristigen Klimaschwankungen des Spätquartärs in Sedimenten des westlichen äquatorialen Atlantiks. 96 pages, Bremen, 1998.
- No. 125** **Wolff, T.**
Mixed layer characteristics in the equatorial Atlantic during the late Quaternary as deduced from planktonic foraminifera. 132 pages, Bremen, 1998.
- No. 126** **Dittert, N.**
Late Quaternary Planktic Foraminifera Assemblages in the South Atlantic Ocean: Quantitative Determination and Preservational Aspects. 165 pages, Bremen, 1998.
- No. 127** **Höll, C.**
Kalkige und organisch-wandige Dinoflagellaten-Zysten in Spätquartären Sedimenten des tropischen Atlantiks und ihre palökologische Auswertbarkeit. 121 pages, Bremen, 1998.
- No. 128** **Hencke, J.**
Redoxreaktionen im Grundwasser: Etablierung und Verlagerung von Reaktionsfronten und ihre Bedeutung für die Spurenelement-Mobilität. 122 pages, Bremen 1998.
- No. 129** **Pätzold, J. and cruise participants**
Report and preliminary results of METEOR-Cruise M 41/3, Vitória, Brasil – Salvador de Bahia, Brasil, 18.4. - 15.5.1998. Bremen, 1999.
- No. 130** **Fischer, G. and cruise participants**
Report and preliminary results of METEOR-Cruise M 41/4, Salvador de Bahia, Brasil – Las Palmas, Spain, 18.5. – 13.6.1998. Bremen, 1999.
- No. 131** **Schlünz, B. and G. Wefer**
Bericht über den 7. JGOFS-Workshop am 3. und 4.12.1998 in Bremen. Im Anhang: Publikationen zum deutschen Beitrag zur Joint Global Ocean Flux Study (JGOFS), Stand 1/ 1999. 100 pages, Bremen, 1999.
- No. 132** **Wefer, G. and cruise participants**
Report and preliminary results of METEOR-Cruise M 42/4, Las Palmas - Las Palmas - Viena do Castelo; 26.09.1998 - 26.10.1998. 104 pages, Bremen, 1999.
- No. 133** **Felis, T.**
Climate and ocean variability reconstructed from stable isotope records of modern subtropical corals (Northern Red Sea). 111 pages, Bremen, 1999.
- No. 134** **Draschba, S.**
North Atlantic climate variability recorded in reef corals from Bermuda. 108 pages, Bremen, 1999.
- No. 135** **Schmieder, F.**
Magnetic Cyclostratigraphy of South Atlantic Sediments. 82 pages, Bremen, 1999.
- No. 136** **Rieß, W.**
In situ measurements of respiration and mineralisation processes – Interaction between fauna and geochemical fluxes at active interfaces. 68 pages, Bremen, 1999.
- No. 137** **Devey, C.W. and cruise participants**
Report and shipboard results from METEOR-cruise M 41/2, Libreville – Vitoria, 18.3. – 15.4.98. 59 pages, Bremen, 1999.
- No. 138** **Wenzhöfer, F.**
Biogeochemical processes at the sediment water interface and quantification of metabolically driven calcite dissolution in deep sea sediments. 103 pages, Bremen, 1999.
- No. 139** **Klump, J.**
Biogenic barite as a proxy of paleoproductivity variations in the Southern Peru-Chile Current. 107 pages, Bremen, 1999.

- No. 140** **Huber, R.**
Carbonate sedimentation in the northern Northatlantic since the late pliocene. 103 pages, Bremen, 1999.
- No. 141** **Schulz, H.**
Nitrate-storing sulfur bacteria in sediments of coastal upwelling. 94 pages, Bremen, 1999.
- No. 142** **Mai, S.**
Die Sedimentverteilung im Wattenmeer: ein Simulationsmodell. 114 pages, Bremen, 1999.
- No. 143** **Neuer, S. and cruise participants**
Report and preliminary results of Poseidon Cruise 248, Las Palmas - Las Palmas, 15.2.-26.2.1999. 45 pages, Bremen, 1999.
- No. 144** **Weber, A.**
Schwefelkreislauf in marinen Sedimenten und Messung von in situ Sulfatreduktionsraten. 122 pages, Bremen, 1999.
- No. 145** **Hadeler, A.**
Sorptionreaktionen im Grundwasser: Unterschiedliche Aspekte bei der Modellierung des Transportverhaltens von Zink. 122 pages, 1999.
- No. 146** **Dierßen, H.**
Zum Kreislauf ausgewählter Spurenmetalle im Südatlantik: Vertikaltransport und Wechselwirkung zwischen Partikeln und Lösung. 167 pages, Bremen, 1999.
- No. 147** **Zühlsdorff, L.**
High resolution multi-frequency seismic surveys at the Eastern Juan de Fuca Ridge Flank and the Cascadia Margin – Evidence for thermally and tectonically driven fluid upflow in marine sediments. 118 pages, Bremen 1999.
- No. 148** **Kinkel, H.**
Living and late Quaternary Coccolithophores in the equatorial Atlantic Ocean: response of distribution and productivity patterns to changing surface water circulation. 183 pages, Bremen, 2000.
- No. 149** **Pätzold, J. and cruise participants**
Report and preliminary results of METEOR Cruise M 44/3, Aqaba (Jordan) - Safaga (Egypt) – Dubá (Saudi Arabia) – Suez (Egypt) - Haifa (Israel), 12.3.-26.3.-2.4.-4.4.1999. 135 pages, Bremen, 2000.
- No. 150** **Schlünz, B. and G. Wefer**
Bericht über den 8. JGOFS-Workshop am 2. und 3.12.1999 in Bremen. Im Anhang: Publikationen zum deutschen Beitrag zur Joint Global Ocean Flux Study (JGOFS), Stand 1/ 2000. 95 pages, Bremen, 2000.
- No. 151** **Schnack, K.**
Biostratigraphie und fazielle Entwicklung in der Oberkreide und im Alttertiär im Bereich der Kharga Schwelle, Westliche Wüste, SW-Ägypten. 142 pages, Bremen, 2000.
- No. 152** **Karwath, B.**
Ecological studies on living and fossil calcareous dinoflagellates of the equatorial and tropical Atlantic Ocean. 175 pages, Bremen, 2000.
- No. 153** **Moustafa, Y.**
Paleoclimatic reconstructions of the Northern Red Sea during the Holocene inferred from stable isotope records of modern and fossil corals and molluscs. 102 pages, Bremen, 2000.
- No. 154** **Villinger, H. and cruise participants**
Report and preliminary results of SONNE-cruise 145-1 Balboa – Talcahuana, 21.12.1999 – 28.01.2000. 147 pages, Bremen, 2000.
- No. 155** **Rusch, A.**
Dynamik der Feinfraktion im Oberflächenhorizont permeabler Schelfsedimente. 102 pages, Bremen, 2000.
- No. 156** **Moos, C.**
Reconstruction of upwelling intensity and paleo-nutrient gradients in the northwest Arabian Sea derived from stable carbon and oxygen isotopes of planktic foraminifera. 103 pages, Bremen, 2000.
- No. 157** **Xu, W.**
Mass physical sediment properties and trends in a Wadden Sea tidal basin. 127 pages, Bremen, 2000.
- No. 158** **Meinecke, G. and cruise participants**
Report and preliminary results of METEOR Cruise M 45/1, Malaga (Spain) - Lissabon (Portugal), 19.05. - 08.06.1999. 39 pages, Bremen, 2000.
- No. 159** **Vink, A.**
Reconstruction of recent and late Quaternary surface water masses of the western subtropical Atlantic Ocean based on calcareous and organic-walled dinoflagellate cysts. 160 pages, Bremen, 2000.
- No. 160** **Willems, H. (Sprecher), U. Bleil, R. Henrich, K. Herterich, B.B. Jørgensen, H.-J. Kuß, M. Olesch, H.D. Schulz, V. Spieß, G. Wefer**
Abschlußbericht des Graduierten-Kollegs Stoff-Flüsse in marine Geosystemen. Zusammenfassung und Berichtszeitraum Januar 1996 - Dezember 2000. 340 pages, Bremen, 2000.

- No. 161** **Sprenkel, C.**
Untersuchungen zur Sedimentation und Ökologie von Coccolithophoriden im Bereich der Kanarischen Inseln: Saisonale Flussmuster und Karbonatexport. 165 pages, Bremen, 2000.
- No. 162** **Donner, B. and G. Wefer**
Bericht über den JGOFS-Workshop am 18.-21.9.2000 in Bremen: Biogeochemical Cycles: German Contributions to the International Joint Global Ocean Flux Study. 87 pages, Bremen, 2000.
- No. 163** **Neuer, S. and cruise participants**
Report and preliminary results of Meteor Cruise M 45/5, Bremen – Las Palmas, October 1 – November 3, 1999. 93 pages, Bremen, 2000.
- No. 164** **Devey, C. and cruise participants**
Report and preliminary results of Sonne Cruise SO 145/2, Talcahuano (Chile) - Arica (Chile), February 4 – February 29, 2000. 63 pages, Bremen, 2000.
- No. 165** **Freudenthal, T.**
Reconstruction of productivity gradients in the Canary Islands region off Morocco by means of sinking particles and sediments. 147 pages, Bremen, 2000.
- No. 166** **Adler, M.**
Modeling of one-dimensional transport in porous media with respect to simultaneous geochemical reactions in CoTRem. 147 pages, Bremen, 2000.
- No. 167** **Santamarina Cuneo, P.**
Fluxes of suspended particulate matter through a tidal inlet of the East Frisian Wadden Sea (southern North Sea). 91 pages, Bremen, 2000.
- No. 168** **Benthien, A.**
Effects of CO₂ and nutrient concentration on the stable carbon isotope composition of C_{37:2} alkenones in sediments of the South Atlantic Ocean. 104 pages, Bremen, 2001.
- No. 169** **Lavik, G.**
Nitrogen isotopes of sinking matter and sediments in the South Atlantic. 140 pages, Bremen, 2001.
- No. 170** **Budziak, D.**
Late Quaternary monsoonal climate and related variations in paleoproductivity and alkenone-derived sea-surface temperatures in the western Arabian Sea. 114 pages, Bremen, 2001.
- No. 171** **Gerhardt, S.**
Late Quaternary water mass variability derived from the pteropod preservation state in sediments of the western South Atlantic Ocean and the Caribbean Sea. 109 pages, Bremen, 2001.
- No. 172** **Bleil, U. and cruise participants**
Report and preliminary results of Meteor Cruise M 46/3, Montevideo (Uruguay) – Mar del Plata (Argentina), January 4 – February 7, 2000. Bremen, 2001.
- No. 173** **Wefer, G. and cruise participants**
Report and preliminary results of Meteor Cruise M 46/4, Mar del Plata (Argentina) – Salvador da Bahia (Brazil), February 10 – March 13, 2000. With partial results of METEOR cruise M 46/2. 136 pages, Bremen, 2001.
- No. 174** **Schulz, H.D. and cruise participants**
Report and preliminary results of Meteor Cruise M 46/2, Recife (Brazil) – Montevideo (Uruguay), December 2 – December 29, 1999. 107 pages, Bremen, 2001.
- No. 175** **Schmidt, A.**
Magnetic mineral fluxes in the Quaternary South Atlantic: Implications for the paleoenvironment. 97 pages, Bremen, 2001.
- No. 176** **Bruhns, P.**
Crystal chemical characterization of heavy metal incorporation in brick burning processes. 93 pages, Bremen, 2001.
- No. 177** **Karius, V.**
Baggergut der Hafengruppe Bremen-Stadt in der Ziegelherstellung. 131 pages, Bremen, 2001.
- No. 178** **Adegbe, A. T.**
Reconstruction of paleoenvironmental conditions in Equatorial Atlantic and the Gulf of Guinea Basins for the last 245,000 years. 113 pages, Bremen, 2001.
- No. 179** **Spieß, V. and cruise participants**
Report and preliminary results of R/V Sonne Cruise SO 149, Victoria - Victoria, 16.8. - 16.9.2000. 100 pages, Bremen, 2001.
- No. 180** **Kim, J.-H.**
Reconstruction of past sea-surface temperatures in the eastern South Atlantic and the eastern South Pacific across Termination I based on the Alkenone Method. 114 pages, Bremen, 2001.

- No. 181** **von Lom-Keil, H.**
Sedimentary waves on the Namibian continental margin and in the Argentine Basin – Bottom flow reconstructions based on high resolution echosounder data. 126 pages, Bremen, 2001.
- No. 182** **Hebbeln, D. and cruise participants**
PUCK: Report and preliminary results of R/V Sonne Cruise SO 156, Valparaiso (Chile) - Talcahuano (Chile), March 29 - May 14, 2001. 195 pages, Bremen, 2001.
- No. 183** **Wendler, J.**
Reconstruction of astronomically-forced cyclic and abrupt paleoecological changes in the Upper Cretaceous Boreal Realm based on calcareous dinoflagellate cysts. 149 pages, Bremen, 2001.
- No. 184** **Volbers, A.**
Planktic foraminifera as paleoceanographic indicators: production, preservation, and reconstruction of upwelling intensity. Implications from late Quaternary South Atlantic sediments. 122 pages, Bremen, 2001.
- No. 185** **Bleil, U. and cruise participants**
Report and preliminary results of R/V METEOR Cruise M 49/3, Montevideo (Uruguay) - Salvador (Brasil), March 9 - April 1, 2001. 99 pages, Bremen, 2001.
- No. 186** **Scheibner, C.**
Architecture of a carbonate platform-to-basin transition on a structural high (Campanian-early Eocene, Eastern Desert, Egypt) – classical and modelling approaches combined. 173 pages, Bremen, 2001.
- No. 187** **Schneider, S.**
Quartäre Schwankungen in Strömungsintensität und Produktivität als Abbild der Wassermassen-Variabilität im äquatorialen Atlantik (ODP Sites 959 und 663): Ergebnisse aus Siltkorn-Analysen. 134 pages, Bremen, 2001.
- No. 188** **Uliana, E.**
Late Quaternary biogenic opal sedimentation in diatom assemblages in Kongo Fan sediments. 96 pages, Bremen, 2002.
- No. 189** **Esper, O.**
Reconstruction of Recent and Late Quaternary oceanographic conditions in the eastern South Atlantic Ocean based on calcareous- and organic-walled dinoflagellate cysts. 130 pages, Bremen, 2001.
- No. 190** **Wendler, I.**
Production and preservation of calcareous dinoflagellate cysts in the modern Arabian Sea. 117 pages, Bremen, 2002.
- No. 191** **Bauer, J.**
Late Cenomanian – Santonian carbonate platform evolution of Sinai (Egypt): stratigraphy, facies, and sequence architecture. 178 pages, Bremen, 2002.
- No. 192** **Hildebrand-Habel, T.**
Die Entwicklung kalkiger Dinoflagellaten im Südatlantik seit der höheren Oberkreide. 152 pages, Bremen, 2002.
- No. 193** **Hecht, H.**
Sauerstoff-Optopoden zur Quantifizierung von Pyritverwitterungsprozessen im Labor- und Langzeit-in-situ-Einsatz. Entwicklung - Anwendung – Modellierung. 130 pages, Bremen, 2002.
- No. 194** **Fischer, G. and cruise participants**
Report and Preliminary Results of RV METEOR-Cruise M49/4, Salvador da Bahia – Halifax, 4.4.-5.5.2001. 84 pages, Bremen, 2002.
- No. 195** **Gröger, M.**
Deep-water circulation in the western equatorial Atlantic: inferences from carbonate preservation studies and silt grain-size analysis. 95 pages, Bremen, 2002.
- No. 196** **Meinecke, G. and cruise participants**
Report of RV POSEIDON Cruise POS 271, Las Palmas - Las Palmas, 19.3.-29.3.2001. 19 pages, Bremen, 2002.
- No. 197** **Meggers, H. and cruise participants**
Report of RV POSEIDON Cruise POS 272, Las Palmas - Las Palmas, 1.4.-14.4.2001. 19 pages, Bremen, 2002.
- No. 198** **Gräfe, K.-U.**
Stratigraphische Korrelation und Steuerungsfaktoren Sedimentärer Zyklen in ausgewählten Borealen und Tethyalen Becken des Cenoman/Turon (Oberkreide) Europas und Nordwestafrikas. 197 pages, Bremen, 2002.
- No. 199** **Jahn, B.**
Mid to Late Pleistocene Variations of Marine Productivity in and Terrigenous Input to the Southeast Atlantic. 97 pages, Bremen, 2002.
- No. 200** **Al-Rousan, S.**
Ocean and climate history recorded in stable isotopes of coral and foraminifers from the northern Gulf of Aqaba. 116 pages, Bremen, 2002.

- No. 201** **Azouzi, B.**
Regionalisierung hydraulischer und hydrogeochemischer Daten mit geostatistischen Methoden. 108 pages, Bremen, 2002.
- No. 202** **Spieß, V. and cruise participants**
Report and preliminary results of METEOR Cruise M 47/3, Libreville (Gabun) - Walvis Bay (Namibia), 01.06 - 03.07.2000. 70 pages, Bremen 2002.
- No. 203** **Spieß, V. and cruise participants**
Report and preliminary results of METEOR Cruise M 49/2, Montevideo (Uruguay) - Montevideo, 13.02 - 07.03.2001. 84 pages, Bremen 2002.
- No. 204** **Mollenhauer, G.**
Organic carbon accumulation in the South Atlantic Ocean: Sedimentary processes and glacial/interglacial Budgets. 139 pages, Bremen 2002.
- No. 205** **Spieß, V. and cruise participants**
Report and preliminary results of METEOR Cruise M49/1, Cape Town (South Africa) - Montevideo (Uruguay), 04.01.2001 - 10.02.2001. 57 pages, Bremen, 2003.
- No. 206** **Meier, K.J.S.**
Calcareous dinoflagellates from the Mediterranean Sea: taxonomy, ecology and palaeoenvironmental application. 126 pages, Bremen, 2003.
- No. 207** **Rakic, S.**
Untersuchungen zur Polymorphie und Kristallchemie von Silikaten der Zusammensetzung $Me_2Si_2O_5$ (Me:Na, K). 139 pages, Bremen, 2003.
- No. 208** **Pfeifer, K.**
Auswirkungen frühdiagenetischer Prozesse auf Calcit- und Barytgehalte in marinen Oberflächen-sedimenten. 110 pages, Bremen, 2003.
- No. 209** **Heuer, V.**
Spurenelemente in Sedimenten des Südatlantik. Primärer Eintrag und frühdiagenetische Überprägung. 136 pages, Bremen, 2003.
- No. 210** **Streng, M.**
Phylogenetic Aspects and Taxonomy of Calcareous Dinoflagellates. 157 pages, Bremen 2003.
- No. 211** **Boeckel, B.**
Present and past coccolith assemblages in the South Atlantic: implications for species ecology, carbonate contribution and palaeoceanographic applicability. 157 pages, Bremen, 2003.
- No. 212** **Precht, E.**
Advective interfacial exchange in permeable sediments driven by surface gravity waves and its ecological consequences. 131 pages, Bremen, 2003.
- No. 213** **Frenz, M.**
Grain-size composition of Quaternary South Atlantic sediments and its paleoceanographic significance. 123 pages, Bremen, 2003.
- No. 214** **Meggers, H. and cruise participants**
Report and preliminary results of METEOR Cruise M 53/1, Limassol - Las Palmas – Mindelo, 30.03.2002 - 03.05.2002. 81 pages, Bremen, 2003.
- No. 215** **Schulz, H.D. and cruise participants**
Report and preliminary results of METEOR Cruise M 58/1, Dakar – Las Palmas, 15.04..2003 – 12.05.2003. Bremen, 2003.
- No. 216** **Schneider, R. and cruise participants**
Report and preliminary results of METEOR Cruise M 57/1, Cape Town – Walvis Bay, 20.01. – 08.02.2003. 123 pages, Bremen, 2003.
- No. 217** **Kallmeyer, J.**
Sulfate reduction in the deep Biosphere. 157 pages, Bremen, 2003.
- No. 218** **Røy, H.**
Dynamic Structure and Function of the Diffusive Boundary Layer at the Seafloor. 149 pages, Bremen, 2003.
- No. 219** **Pätzold, J., C. Hübscher and cruise participants**
Report and preliminary results of METEOR Cruise M 52/2&3, Istanbul – Limassol – Limassol, 04.02. – 27.03.2002. Bremen, 2003.
- No. 220** **Zabel, M. and cruise participants**
Report and preliminary results of METEOR Cruise M 57/2, Walvis Bay – Walvis Bay, 11.02. – 12.03.2003. 136 pages, Bremen 2003.
- No. 221** **Salem, M.**
Geophysical investigations of submarine prolongations of alluvial fans on the western side of the Gulf of Aqaba-Red Sea. 100 pages, Bremen, 2003.

- No. 222** **Tilch, E.**
Oszillation von Wattflächen und deren fossiles Erhaltungspotential (Spiekerooger Rückseitenwatt, südliche Nordsee). 137 pages, Bremen, 2003.
- No. 223** **Frisch, U. and F. Kockel**
Der Bremen-Knoten im Strukturnetz Nordwest-Deutschlands. Stratigraphie, Paläogeographie, Strukturgeologie. 379 pages, Bremen, 2004.
- No. 224** **Kolonic, S.**
Mechanisms and biogeochemical implications of Cenomanian/Turonian black shale formation in North Africa: An integrated geochemical, millennial-scale study from the Tarfaya-LaAyoune Basin in SW Morocco. 174 pages, Bremen, 2004. Report online available only.
- No. 225** **Panteleit, B.**
Geochemische Prozesse in der Salz- Süßwasser Übergangszone. 106 pages, Bremen, 2004.
- No. 226** **Seiter, K.**
Regionalisierung und Quantifizierung benthischer Mineralisationsprozesse. 135 pages, Bremen, 2004.
- No. 227** **Bleil, U. and cruise participants**
Report and preliminary results of METEOR Cruise M 58/2, Las Palmas – Las Palmas (Canary Islands, Spain), 15.05. – 08.06.2003. 123 pages, Bremen, 2004.
- No. 228** **Kopf, A. and cruise participants**
Report and preliminary results of SONNE Cruise SO175, Miami - Bremerhaven, 12.11 - 30.12.2003. 218 pages, Bremen, 2004.
- No. 229** **Fabian, M.**
Near Surface Tilt and Pore Pressure Changes Induced by Pumping in Multi-Layered Poroelastic Half-Spaces. 121 pages, Bremen, 2004.
- No. 230** **Segl, M. , and cruise participants**
Report and preliminary results of POSEIDON cruise 304 Galway – Lisbon, 5. – 22. Oct. 2004. 27 pages, Bremen 2004
- No. 231** **Meinecke, G. and cruise participants**
Report and preliminary results of POSEIDON Cruise 296, Las Palmas – Las Palmas, 04.04 – 14.04.2003. 42 pages, Bremen 2005.
- No. 232** **Meinecke, G. and cruise participants**
Report and preliminary results of POSEIDON Cruise 310, Las Palmas – Las Palmas, 12.04 – 26.04.2004. 49 pages, Bremen 2005.
- No. 233** **Meinecke, G. and cruise participants**
Report and preliminary results of METEOR Cruise 58/3, Las Palmas - Ponta Delgada, 11.06 - 24.06.2003. 50 pages, Bremen 2005.
- No. 234** **Feseker, T.**
Numerical Studies on Groundwater Flow in Coastal Aquifers. 219 pages. Bremen 2004.
- No. 235** **Sahling, H. and cruise participants**
Report and preliminary results of R/V POSEIDON Cruise P317/4, Istanbul-Istanbul , 16 October - 4 November 2004. 92 pages, Bremen 2004.
- No. 236** **Meinecke, G. und Fahrtteilnehmer**
Report and preliminary results of POSEIDON Cruise 305, Las Palmas (Spain) - Lisbon (Portugal), October 28th – November 6th, 2004. 43 pages, Bremen 2005.
- No. 237** **Ruhland, G. and cruise participants**
Report and preliminary results of POSEIDON Cruise 319, Las Palmas (Spain) - Las Palmas (Spain), December 6th – December 17th, 2004. 50 pages, Bremen 2005.
- No. 238** **Chang, T.S.**
Dynamics of fine-grained sediments and stratigraphic evolution of a back-barrier tidal basin of the German Wadden Sea (southern North Sea). 102 pages, Bremen 2005.
- No. 239** **Lager, T.**
Predicting the source strength of recycling materials within the scope of a seepage water prognosis by means of standardized laboratory methods. 141 pages, Bremen 2005.
- No. 240** **Meinecke, G.**
DOLAN - Operationelle Datenübertragung im Ozean und Laterales Akustisches Netzwerk in der Tiefsee. Abschlußbericht. 42 pages, Bremen 2005.
- No. 241** **Guasti, E.**
Early Paleogene environmental turnover in the southern Tethys as recorded by foraminiferal and organic-walled dinoflagellate cysts assemblages. 203 pages, Bremen 2005.
- No. 242** **Riedinger, N.**
Preservation and diagenetic overprint of geochemical and geophysical signals in ocean margin sediments related to depositional dynamics. 91 pages, Bremen 2005.

- No. 243** **Ruhland, G. and cruise participants**
Report and preliminary results of POSEIDON cruise 320, Las Palmas (Spain) - Las Palmas (Spain), March 08th - March 18th, 2005. 57 pages, Bremen 2005.
- No. 244** **Inthorn, M.**
Lateral particle transport in nepheloid layers – a key factor for organic matter distribution and quality in the Benguela high-productivity area. 127 pages, Bremen, 2006.
- No. 245** **Aspetsberger, F.**
Benthic carbon turnover in continental slope and deep sea sediments: importance of organic matter quality at different time scales. 136 pages, Bremen, 2006.
- No. 246** **Hebbeln, D. and cruise participants**
Report and preliminary results of RV SONNE Cruise SO-184, PABESIA, Durban (South Africa) – Cilacap (Indonesia) – Darwin (Australia), July 08th - September 13th, 2005. 142 pages, Bremen 2006.
- No. 247** **Ratmeyer, V. and cruise participants**
Report and preliminary results of RV METEOR Cruise M61/3. Development of Carbonate Mounds on the Celtic Continental Margin, Northeast Atlantic. Cork (Ireland) – Ponta Delgada (Portugal), 04.06. – 21.06.2004. 64 pages, Bremen 2006.
- No. 248** **Wien, K.**
Element Stratigraphy and Age Models for Pelagites and Gravity Mass Flow Deposits based on Shipboard XRF Analysis. 100 pages, Bremen 2006.
- No. 249** **Krastel, S. and cruise participants**
Report and preliminary results of RV METEOR Cruise M65/2, Dakar - Las Palmas, 04.07. – 26.07.2005. 185 pages, Bremen 2006.
- No. 250** **Heil, G.M.N.**
Abrupt Climate Shifts in the Western Tropical to Subtropical Atlantic Region during the Last Glacial. 121 pages, Bremen 2006.
- No. 251** **Ruhland, G. and cruise participants**
Report and preliminary results of POSEIDON Cruise 330, Las Palmas – Las Palmas, November 21th – December 03rd, 2005. 48 pages, Bremen 2006.
- No. 252** **Mulitza, S. and cruise participants**
Report and preliminary results of METEOR Cruise M65/1, Dakar – Dakar, 11.06.- 1.07.2005. 149 pages, Bremen 2006.
- No. 253** **Kopf, A. and cruise participants**
Report and preliminary results of POSEIDON Cruise P336, Heraklion - Heraklion, 28.04. – 17.05.2006. 127 pages, Bremen, 2006.
- No. 254** **Wefer, G. and cruise participants**
Report and preliminary results of R/V METEOR Cruise M65/3, Las Palmas - Las Palmas (Spain), July 31st - August 10th, 2005. 24 pages, Bremen 2006.
- No. 255** **Hanebuth, T.J.J. and cruise participants**
Report and first results of the POSEIDON Cruise P342 GALIOMAR, Vigo – Lisboa (Portugal), August 19th – September 06th, 2006. Distribution Pattern, Residence Times and Export of Sediments on the Pleistocene/Holocene Galician Shelf (NW Iberian Peninsula). 203 pages, Bremen, 2007.
- No. 256** **Ahke, A.**
Composition of molecular organic matter pools, pigments and proteins, in Benguela upwelling and Arctic Sediments. 192 pages, Bremen 2007.
- No. 257** **Becker, V.**
Seeper - Ein Modell für die Praxis der Sickerwasserprognose. 170 pages, Bremen 2007.
- No. 258** **Ruhland, G. and cruise participants**
Report and preliminary results of Poseidon cruise 333, Las Palmas (Spain) – Las Palmas (Spain), March 1st – March 10th, 2006. 32 pages, Bremen 2007.
- No. 259** **Fischer, G., G. Ruhland and cruise participants**
Report and preliminary results of Poseidon cruise 344, leg 1 and leg 2, Las Palmas (Spain) – Las Palmas (Spain), Oct. 20th – Nov 2nd & Nov. 4th – Nov 13th, 2006. 46 pages, Bremen 2007.
- No. 260** **Westphal, H. and cruise participants**
Report and preliminary results of Poseidon cruise 346, MACUMA. Las Palmas (Spain) – Las Palmas (Spain), 28.12.2006 – 15.1.2007. 49 pages, Bremen 2007.
- No. 261** **Bohrmann, G., T. Pape, and cruise participants**
Report and preliminary results of R/V METEOR Cruise M72/3, Istanbul – Trabzon – Istanbul, March 17th – April 23rd, 2007. Marine gas hydrates of the Eastern Black Sea. 130 pages, Bremen 2007.
- No. 262** **Bohrmann, G., and cruise participants**
Report and preliminary results of R/V METEOR Cruise M70/3, Iraklion – Iraklion, 21 November – 8 December 2006. Cold Seeps of the Anaximander Mountains / Eastern Mediterranean. 75 pages, Bremen 2008.

- No. 263** **Bohrmann, G., Spiess, V., and cruise participants**
Report and preliminary results of R/V Meteor Cruise M67/2a and 2b, Balboa -- Tampico -- Bridgetown, 15 March -- 24 April, 2006. Fluid seepage in the Gulf of Mexico. Bremen 2008.
- No. 264** **Kopf, A., and cruise participants**
Report and preliminary results of Meteor Cruise M73/1: LIMA-LAMO (Ligurian Margin Landslide Measurements & Observatory), Cadiz, 22.07.2007 – Genoa, 11.08.2007. 170 pages, Bremen 2008.
- No. 265** **Hebbeln, D., and cruise participants**
Report and preliminary results of RV Pelagia Cruise 64PE284. Cold-water Corals in the Gulf of Cádiz and on Coral Patch Seamount (NE Atlantic). Portimão - Portimão, 18.02. - 09.03.2008. 90 pages, Bremen 2008.
- No. 266** **Bohrmann, G. and cruise participants**
Report and preliminary results of R/V Meteor Cruise M74/3, Fujairah – Male, 30 October - 28 November, 2007. Cold Seeps of the Makran subduction zone (Continental margin of Pakistan). 161 pages, Bremen 2008.
- No. 267** **Sachs, O.**
Benthic organic carbon fluxes in the Southern Ocean: Regional differences and links to surface primary production and carbon export. 143 pages, Bremen, 2008.
- No. 268** **Zonneveld, K. and cruise participants**
Report and preliminary results of R/V POSEIDON Cruise P339, Piräus - Messina, 16 June - 2 July 2006. CAPPUCCINO - Calabrian and Adriatic palaeoproductivity and climatic variability in the last two millenia. 61 pages, Bremen, 2008.
- No. 269** **Ruhland, G. and cruise participants**
Report and preliminary results of R/V POSEIDON Cruise P360, Las Palmas (Spain) - Las Palmas (Spain), Oct. 29th - Nov. 6th, 2007. 27 pages, Bremen, 2008.
- No. 270** **Ruhland, G., G. Fischer and cruise participants**
Report and preliminary results of R/V POSEIDON Cruise 365 (Leg 1+2). Leg 1: Las Palmas - Las Palmas, 13.4. - 16.4.2008. Leg 2: Las Palmas - Las Palmas, 18.4. - 29.4.2008. 40 pages, Bremen, 2009.
- No. 271** **Kopf, A. and cruise participants**
Report and preliminary results of R/V POSEIDON Cruise P386: NAIL (Nice Airport Landslide), La Seyne sur Mer, 20.06.2009 – La Seyne sur Mer, 06.07.2009. 161 pages, Bremen, 2009.
- No. 272** **Freudenthal, T., G. Fischer and cruise participants**
Report and preliminary results of Maria S. Merian Cruise MSM04/4 a & b, Las Palmas (Spain) – Las Palmas (Spain), Feb 27th – Mar 16th & Mar 19th – Apr 1st, 2007. 117 pages, Bremen 2009.
- No. 273** **Hebbeln, D., C. Wienberg, L. Beuck, A. Freiwald, P. Wintersteller and cruise participants**
Report and preliminary results of R/V POSEIDON Cruise POS 385 "Cold-Water Corals of the Alboran Sea (western Mediterranean Sea)", Faro - Toulon, May 29 - June 16, 2009. 79 pages, Bremen 2009.
- No. 274** **Zonneveld, K. and cruise participants**
Report and preliminary results of R/V Poseidon Cruises P 366-1 and P 366-2, Las Palmas - Las Palmas - Vigo, 03 -19 May 2008 and 22 -30 May 2008. PERGAMOM Proxy Education and Research cruise off Galicai, Morocco and Mauretania. 47 pages, Bremen 2010.
- No. 275** **Wienberg, C. and cruise participants**
Report and preliminary results of RV POSEIDON cruise POS400 "CORICON - Cold-water corals along the Irish continental margin", Vigo - Cork, June 29 - July 15 2010. 46 pages, Bremen 2010.
- No. 276** **Villinger, H. and cruise participants**
Report and preliminary results of R/V Sonne Cruise SO 207, Caldera-Caldera, 21 June -13 July, 2010. SeamountFlux: Efficient cooling in young oceanic crust caused by circulation of seawater through seamounts (Guatemala Basin, East Pacific Ocean). 161 pages, Bremen 2010.
- No. 277** **Fischer, G. and cruise participants**
Report and preliminary results of RV POSEIDON Cruise POS 396, Las Palmas - Las Palmas (Spain), 24 February - 8 March 2010. 22 pages, Bremen 2011.
- No. 278** **Bohrmann, G. and cruise participants**
Report and preliminary results of RV MARIA S. MERIAN Cruise MSM 15/2, Istanbul (Turkey) – Piraeus (Greece), 10 May - 2 June 2010. Origin and structure of methane, gas hydrates and fluid flows in the Black Sea. 130 pages, Bremen 2011.
- No. 279** **Hebbeln, D. and cruise participants**
Report and preliminary results of RV SONNE Cruise SO-211, Valparaíso - Valparaíso, 2 November – 29 November 2010. ChiMeBo. Bremen 2011.
- No. 280** **Bach, W. and cruise participants**
Report and preliminary results of RV SONNE Cruise SO 216, Townsville (Australia) - Makassar (Indonesia), June 14 – July 23, 2011. BAMBUS, Back-Arc Manus Basin Underwater Solfataras. 87 pages, Bremen 2011.

- No. 281** **Bohrmann, G. and cruise participants**
Report and preliminary results of RV METEOR Cruise M84/2, Istanbul – Istanbul, 26 February – 02 April, 2011. Origin and Distribution of Methane and Methane Hydrates in the Black Sea. 164 pages, Bremen 2011.
- No. 282** **Zonneveld, K. and cruise participants**
Report and preliminary results of R/V POSEIDON Cruise P398, Las Palmas – Lissabon, 1 – 16 April 2010. PAPOCA, Production and preservation of organic carbon in relationship to dust input and nepheloid layers in the upwelling area off NW Africa. 33 pages, Bremen 2011.
- No. 283** **Hanebuth, T. J. J. and cruise participants**
Report and preliminary results of RV METEOR Cruise M84/4, GALIOMAR III, Vigo – Vigo, 1st – 28th May, 2011. 139 pages, Bremen 2012.
- No. 284** **Kopf, A. and cruise participants**
Report and preliminary results of RV POSEIDON Cruise P410: MUDFLOW (Mud volcanism, Faulting and Fluid Flow on the Mediterranean Ridge Accretionary Complex), Heraklion / Greece, 12.03.2011 – Taranto / Italy, 01.04.2011. 128 pages, Bremen 2012.
- No. 285** **Krastel, S., G. Wefer and cruise participants**
Report and preliminary results of RV METEOR Cruise M78/3. Sediment transport off Uruguay and Argentina: From the shelf to the deep sea. 19.05.2009 – 06.07.2009, Montevideo (Uruguay) – Montevideo (Uruguay). 79 pages, Bremen 2012.